STUDIES ON PROCESS DEVELOPMENT FOR PRODUCTION OF SYNTHETIC LUBES FROM LOW VALUE FEED STOCKS

A thesis submitted to the
University of Petroleum and Energy Studies

For the Award of
Doctor of Philosophy
in
Chemical Engineering

BY
Ramachandra Rao B

June, 2021

SUPERVISOR (S)
Dr. Ashoutosh Panday
Dr. N.V. Choudhary

UNIVERSITY WITH A PURPOSE
Department of Chemical Engineering
School of Engineering
University of Petroleum & Energy Studies
Dehradun – 248007: Uttarakhand

STUDIES ON PROCESS DEVELOPMENT FOR PRODUCTION OF SYNTHETIC LUBES FROM LOW VALUE FEED STOCKS

A thesis submitted to the
University of Petroleum and Energy Studies

For the Award of
Doctor of Philosophy
in
Chemical Engineering

BY
Ramachandra Rao B
(SAP ID 500049752)

June, 2021

Internal Supervisor
Dr. Ashoutosh Panday
Professor
Department of Chemical Engineering
University of Petroleum & Energy Studies

External Supervisor
Dr. N.V. Choudhary, FNAE
Scientist Emeritus
HP Green R&D Centre
HPCL, Bengaluru

UPES
UNIVERSITY WITH A PURPOSE

Department of Chemical Engineering
School of Engineering
University of Petroleum & Energy Studies
Dehradun – 248007: Uttarakhand

SEPTEMBER 2021

DECLARATION

I declare that the thesis on "**STUDIES ON PROCESS DEVELOPMENT FOR PRODUCTION OF SYNTHETIC LUBES FROM LOW VALUE FEED STOCKS"** has been prepared by me under the joint guidance of **Dr. Ashoutosh Panday,** Professor, Dept. of Chemical Engineering UPES, Dehradun and **Dr. N. V. Choudary,** FNAE, Scientist Emeritus
HP Green R&D Centre, HPCL, Bengaluru.

No part of this thesis has formed the basis for the award of any degree or fellowship previously.

Ramachandra Rao Bojja
SAP ID 500049752
Dept. of Chemical Engineering
University of Petroleum & Energy Studies
Dehradun

Date: September 01, 2021

UPES
UNIVERSITY WITH A PURPOSE

Great Place To Work® Certified
INDIA

THESIS COMPLETION CERTIFICATE

This is to certify that the thesis on **“STUDIES ON PROCESS DEVELOPMENT FOR PRODUCTION OF SYNTHETIC LUBES FROM LOW VALUE FEED STOCKS”** submitted by **Mr. Ramachandra Rao Bojja** in partial completion of the requirements for the award of the Degree of Doctor of Philosophy (Engineering) is an original work carried out by him under my supervision and guidance.

It is certified that the work has not been submitted anywhere else for the award of any other diploma or degree of this or any other University.

A Panday

Internal Supervisor

Dr. Ashoutosh Panday

Professor, Dept. of Chemical Engineering

UPES, Dehradun

Date: September 01, 2021

THESIS COMPLETION CERTIFICATE

This is to certify that the thesis on **"STUDIES ON PROCESS DEVELOPMENT FOR PRODUCTION OF SYNTHETIC LUBES FROM LOW VALUE FEED STOCKS" submitted** by **Mr. Ramachandra Rao Bojja in** partial completion of the requirements for the award of the Degree of Doctor of Philosophy (Engineering) is an original work carried out by him under my supervision and guidance.

It is certified that the work has not been submitted anywhere else for the award of any other diploma or degree of this or any other University.

External Supervisor
Dr. N. V. Choudary, FNAE
Scientist Emeritus
HP Green R&D Centre,
HPCL Bengaluru

Date: September 01, 2021

ABSTRACT

The demand for synthetic lubricants has driven the search for low value feed stocks for production of synthetic base oils such as Poly Alpha Olefins (PAOs). This doctoral project work aims at screening of low value feed stocks rich in linear alpha olefins (LAO), synthesis & screening of catalysts and development of a novel process for production of high value PAO.

Various feed stocks, rich in Linear Alpha Olefins (LAOs), were identified which have potential for production of PAOs. These identified streams are currently being used for production of fuels such as petrol and diesel which fetch relatively lower value for petroleum refineries. As proposed under this thesis, these streams can be utilized more effectively by converting into synthetic base oils.

Model compound studies were carried to develop novel tuneable Lewis acid catalyst systems. Based on the identified feed stocks and the formulated catalyst blends, oligomerisation reactions were conducted at varying residence times and temperatures. Among the screened feed streams, wax cracked naphtha (WCN) and delayed coker naphtha (DCN) were determined to be the most prospective feed stocks for PAO production as oligomerisation of these feed stocks could produce PAOs that match the commercial specifications.

Based on the experimental data, a mathematical model was developed in MATLAB for determining the kinetic parameters associated with various oligomerisation reactions. These kinetic parameters were adopted to develop a process simulation model using ASPEN HYSYS. Flow Sheeting was carried out using the simulation model for production of PAOs from shortlisted low value feed stocks (WCN and DCN).

Economics of the developed process was analysed for 0.2 MMTPA plant with WCN as a feed stock which is currently routed to a FCC unit for production of fuel grade material. The study indicated that the wax thermal cracking process followed by oligomerization of cracked naphtha to produce PAOs is economically favourable with payback period of less than 2 years.

Sensitivity analysis was performed to determine the effect of cost parameters on the overall economics of the process. It was observed that the market price of PAO and other valuable products from wax cracking are two important parameters which govern the economics of the process.

ACKNOWLEDGEMENTS

During writing of this thesis and throughout the journey of my Ph.D work, I have received a great deal of support, guidance and assistance from all quarters.

First and foremost, I am extremely grateful to my supervisors **Prof. Ashoutosh Panday,** UPES and **Dr. N. V. Choudary**, FNAE for their invaluable advice and continuous support. Their immense knowledge and plentiful experience have helped me a lot in my academic pursuit.

I would like to sincerely express my gratitude to the management of Hindustan Petroleum Corporation Limited (HPCL) for having allowed me to pursue the doctoral work. Also, I would like to convey my appreciation to the scientific community at HP Green R&D Centre, Bengaluru, for facilitating continuous assistance and support during my research work.

I would like to express my deep sense of gratitude to the management and staff of University of Petroleum and Energy Studies (UPES), Dehradun, for providing me with requisite resources and support for carrying out the research work.

I would like to also thank my family members, especially my wife, Mrs. Rajya Lakshmi, for supporting me throughout the research tenure. Without their understanding and encouragement in the past few years, it would have been impossible for me to complete this study.

Finally, I would like to dedicate this thesis work to my late parents, who had developed the quest for knowledge in me.

LIST OF ABBREVIATIONS

API:	American Petroleum Institute
ASTM:	American Society for Testing of Materials
AW:	Anti Wear
CAGR:	Compounded Annual Growth Rate
CAPEX:	Capital Expenditure
cSt:	Centistoke
DAO:	De-Asphalted Oil
DCN:	Delayed Cocker Naphtha
DI:	Detergent Inhibitor
EP:	Extreme pressure
FCC:	Fluid Catalytic Cracking
GC-MS:	Gas Chromatography–Mass Spectrometry
GRM:	Gross Refinery Margin
HCGO:	Heavy Cracked Gas Oil
HCN:	Heavy Cracked Naphtha
HDA:	Hydro-De-Aromatization
HDN:	Hydro-De-Nitrification
HDPE:	High-Density Poly-Ethylene
HDS:	Hydro-De-Sulfurization
H-NMR	Hydrogen Nuclear Magnetic Resonance Spectrometer
HPLC:	High Pressure Liquid Chromatography

HVGO:	Heavy Vacuum Gas Oil
IOH:	Industrial Oil Hydrogenation Unit
KT:	Kilo Ton
LAO:	Linear Alpha Olefins
LCGO:	Light Cracked Gas Oil
LCO:	Light Cycle Oil
LCN:	Light Cracked Naphtha
LDPE:	Low-Density Poly Ethylene
LLDPE:	Linear Low-Density Poly Ethylene
LOUP:	Lube Oil Upgradation Project
LPG:	Liquified Petroleum Gas
LVGO:	Light Vacuum Gas Oil
MEK:	Methyl Ethyl Ketone
MMTPA:	Million Metric Tons Per Annum
MPS:	Mini Pot Still
MT:	Metric Ton
OPEX:	Operating Expenditure
PAG:	Poly Alkylene Glycol
PAO:	Poly Alpha Olefin
PDA:	Propane De-Asphalting Unit
PDU:	Propane De-waxing Unit
PE:	Poly Ethylene
POE:	Polyol Esters

PIONA:	Paraffins, Iso-paraffins, Olefins, Naphthenes, Aromatics
PONA:	Paraffins, Olefins, Naphthenes , Aromatics
RTP:	Refinery Transfer Price
SEU:	Solvent Extraction Unit
SHOP:	Shell Higher Olefin Process
SUS:	Saybolt Universal Seconds
VBN:	Viscosity Breaking Unit Naphtha
VDU:	Vacuum Distillation Unit
VI:	Viscosity Index
VLV:	Very Low Value
WCN:	Wax Cracked Naphtha

TABLE OF CONTENTS

Chapter 4: Development of Catalyst using Model Compounds

Chapter 5: Synthesis of PAOs from low value Feeds Stocks

Chapter 6: Process Modelling and Design

Chapter 7: Process Economics and Sensitivity Analysis

LIST OF FIGURES

LIST OF TABLES

CHAPTER 1

INTRODUCTION

1.1 Overview

Lubricants, in the form of thin liquid film, reduce friction and wear between moving surfaces [1, 2]. They also play a critical role in removal of generated frictional heat, can also prevent corrosion development, and are largely used in gasoline and diesel engines, machines, turbines, refrigeration systems, transformers, etc.

Some of the important properties of lubricants are [3] density, API, viscosity at 40 & 100^{o}C, viscosity index, pour point, cloud point, appearance, distillation, volatility, flash point, aniline point, refractive index, sulphur content, nitrogen content, aromatics content etc. These compounds (lubricants) contain various chemical constituents such as n-paraffins, iso-paraffins, cyclo-paraffins, aromatics, sulphur containing compounds, oxygen containing compounds, nitrogen containing compounds etc.

Lubricants consist of hydrocarbon base oils which constitute 80% to 98% by volume, the remaining 2% to 20% comprise of additives for improving performance of lubricants

1.2 Classification of Lubricants

The API created a system [4] to describe lubricants; Groups I-III, known as conventional lubricants, are derived from petroleum crude oil. Group IV describes the rapidly growing class of polyalphaolefin (PAO) based synthetic lubricants and Group V includes all other synthetics (mostly esters and glycols) not included in the other four group descriptions. Groups IV-V are generally marketed as synthetics.

Lubricants are also graded based on Viscosity, Viscosity Index, level of sulphur and degree of refining process.

1.3 Conventional process for PAO synthesis

The conventional PAO synthesis is achieved in two major steps involving (i) Oligomerization of ethylene [5, 6, 7, 8] to make linear alpha olefins (ii) Oligomerization / polymerisation of linear alpha olefins to PAOs as depicted in Figure 1.3. In the first step, ethylene is subjected to controlled polymerization to obtain the mixture of higher alkenes. The mixture of alkenes on further upon separation yields the desired linear alpha olefins, which are starting materials for PAO synthesis. In the second step, the linear alpha olefins are subjected to oligomerization / polymerisation to obtain the polymers of low molecular weight. The catalysts used for these two oligomerization processes are slightly different and mostly product driven.

Figure 1.1 Conventional process for PAO synthesis

1.4 Research Motivation

1.4.1 Current market demand for Group IV lubricants (PAO based)

The market [9, 10] for Poly Alpha Olefins (PAO) based lubricants has witnessed substantial growth with a CAGR of 31% (market demand of 1.8 KT in 2019) over the last 5 years, compared to its market demand of only 0.5 KT in 2014.

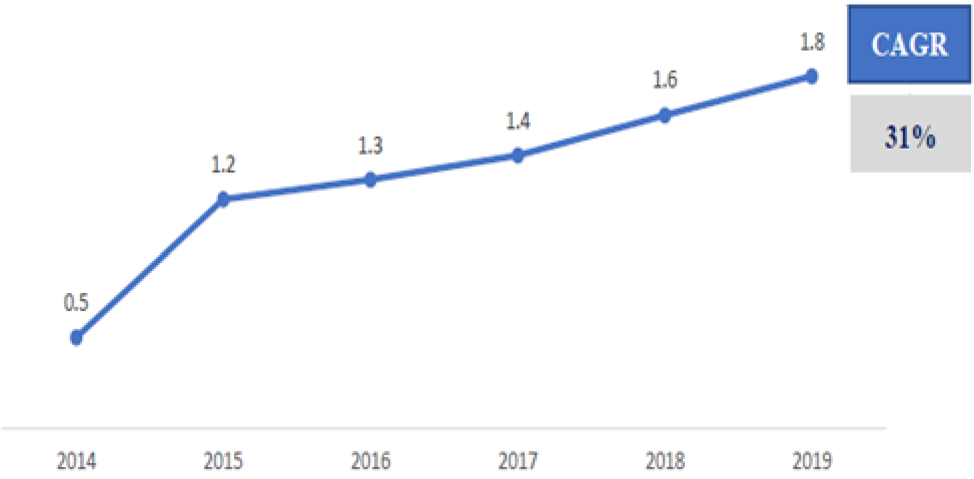

Figure 1.2: Demand for PAO based Lubricants

1.4.2 Market Forecast for PAOs

Market of PAO based lubricants is expected to grow [9, 10] substantially in the coming years, attributed to demand growth in products such as synthetic oil-based lubricants, greases, industrial oils, hydraulic fluids etc. This can also be attributed to the benefits obtained by the usage of PAOs in wear & tear protection, higher load carrying capacity and improved thermal stability as compared to those of conventional lubricants.

Even though, there are other synthetic lubricants available in the market based on Polyol Esters (POE), Polyalkylene glycol (PAG), other ester based base oils, PAO still holds better market segment and future growth owing to its better physical & chemical properties like higher viscosity index, lower pour point values, lower volatility, and better thermal stability.

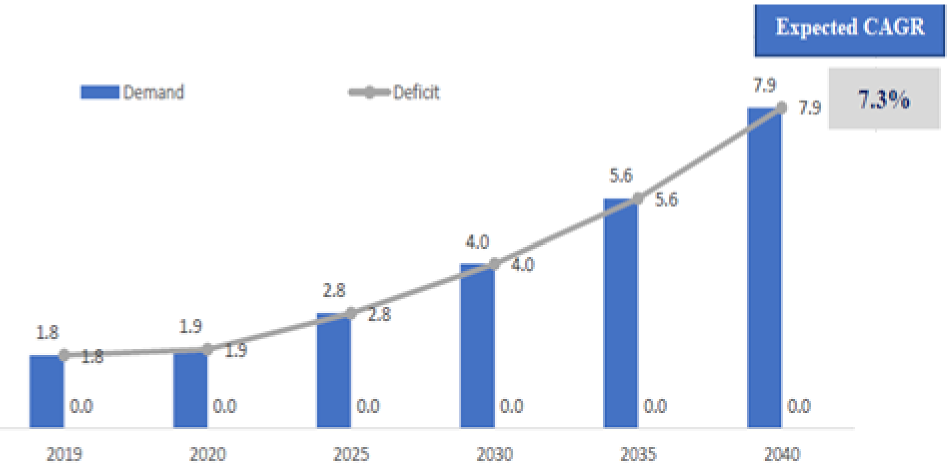

Figure 1.3: Market forecast for PAO based lubricants

As per market research reports, demand for PAO is expected to grow from 1.8 KT in 2019 to about 7.9 KT in 2040 with a CAGR of 7.3%, again attributed to positive growth in the application segments such as synthetic oil-based lubricants, greases, industrial oils, hydraulic fluids etc. However, the major drawback for the growth of PAO, especially in India, is its higher price compared to other base oils (Group I, II and III).

1.5 Research Questions

In spite of the various advantages and the higher market demand and growth potential of the PAOs, their application as synthetic base oils is yet limited due to its higher cost and limited feedstock availability [11], which creates favourable market for the competitive products. The conventional methodology of PAO synthesis suffers from high product cost, as it is based on ethylene product, which a very costly petrochemical feedstock. Hence there is a requirement to develop an alternative cost effective technique [12] for PAO preparation for lubricants application.

i. Can low value feed stocks be identified from crude oil refinery streams and non-refinery streams to bring down the cost of synthetic lubes ?
ii. Can a novel catalyst system be developed which will not only be producing PAOs of required commercial properties but also be resistant to sulphur impurities in the newly feed stocks identified?
iii. Can an alternate process be developed for production of PAOs that is economically viable ?

1.6 Research Gaps

From preliminary literature search, some of the findings are:

i. Not much research work was found [13, 14] in identifying the alternate feed stocks. Convention feed stock is ethylene. Few literatures were found on using wax as alternate feed stock. However, they report less linear alpha olefin yield or no data was provided on potential olefin yield.
ii. Most of the research was carried using model compounds like 1-hexene, 1-octene and 1-decene [15] or mixture of model compounds and little information is available using actual (industrial) feed stocks. Hence, the consequences of impurities in actual feed stocks on the catalysts are less known.
iii. No literature was found on direct synthesis process for oligomerization of refinery streams. Literature recommends to separate the linear alpha olefins from the mixture of hydrocarbon.

iv. Different catalysts studied in the literature are metellocene based catalysts, Ziegler Natta based catalysts, Zr based catalysts, Lewis acid based catalysts and ionic liquid based catalysts

v. Kinetics of the oligomerization reactions was also not much discussed in the literature

1.7 Research Approach

As evident from the above, the production cost can be reduced by either developing a low value feedstock which has the potential to produce PAO or selecting a process which can be cost effective with less number of steps. Thus, the focus in this particular research has been to select a low value feedstock and develop a novel process for production of PAOs.

Petroleum Refineries being complex and integrated with various unit operations [16 - 23] processes like distillation, catalytic cracking, thermal cracking, coking, solvent extraction, solvent dewaxing, reforming, hydrogenation, etc., for handling of different feed stocks and meeting the desired fuel specifications, numerous options will be available for selecting the right feed stock for production of PAOs. However, selecting the appropriate feeds stock from the options available is the most critical task.

Literature indicates that the olefin rich streams with high linear alpha olefins (LAOs) or the streams with potential to transform into high LAOs are good building blocks for PAO production [24 - 26]. Preliminary review of feedstocks suggests that the best suitable feed stocks for PAO production are as follows:

(i) Products streams derived from thermal cracking units like Vis-breaker and Delayed Coker

(ii) Streams derived from cracking of wax which is produced from Solvent Dewaxing unit in process of production of Group-I lube base oils.

Currently the above streams are routed to fuel pools and fetch low margins. Hence, by converting these streams into high value products such as PAOs, refineries would be able to enhance gross refinery margins (GRM).

1.8 Outline of Thesis Chapters

1.8.1 Literature Review (Chapter 2)

Various applications of lubricants, their important definitions as per American Petroleum Institute, important properties, classifications based on composition, synthesis methods and various recent research works in the area were studied in detail.

1.8.2 Identification of suitable olefin rich low value feed stocks (Chapter-3)

Identification of suitable olefin rich low value feedstocks and carrying out the physio/chemical characterization is one of the key steps. Various refinery streams like products from catalytic cracking units, thermal cracking units, wax samples, etc. were selected for studying their suitability for PAO production.

i. Cracked naphtha and LCO from FCC unit
ii. VB Naphtha and VB Gasoil streams from Visbreaker unit
iii. Coker naphtha and Coker gas oil samples from Delayed coker unit
iv. Slack wax produced from solvent dewaxing unit

Utilization of feedstock not based on refinery stream i.e. waste polyethylene (PE), and its conversion to LAO was also exploited. This would not only provide benefit of easy availability of this material but also can provide cost benefit compared to other feedstocks. The material can prove to be a very useful material in reducing carbon footprint and also could be a route of better valorization of the waste polymer.

1.8.3 Development of catalyst system using model compounds (Chapter 4)

To further produce PAOs from the screened low value feedstock, improved catalysts formulations were developed (homogeneous and heterogeneous) for oligomerization of linear alpha olefins. A novel cost effective tuneable Lewis acid systems, comprising of various ratios of group 13 stronger Lewis acid $AlCl_3$ and transition metal weak Lewis acid $FeCl_3$, were developed for oligomerization of alpha olefins to form polyalphaolefins (PAOs). The residence time and temperature dependent oligomer ratio of 1-decene is studied in the presence of Lewis acid catalysts containing various ratios of $AlCl_3/FeCl_3$. The transition metal based weak Lewis acid $FeCl_3$ yielded ready-to-use PAOs. The process involved following steps:

i. Catalyst preparation
ii. Performance evaluation of the catalyst in bench scale unit
iii. Screening of various catalyst formulations
iv. Shortlisting of best formulations

1.8.4 Synthesis of PAOs from low value feed stocks (Chapter 5)

In addition to the linear alpha olefin enrichment process, novel process of direct synthesis of PAOs from the low value feedstocks is also investigated. Conventionally, the enriched linear olefin rich stream will be subjected to further LAO enrichment by selectively separating the olefins using Diels –Alder based extraction process. However, in this work a novel catalyst is proposed which can sustain in different environment and help in direct synthesis of LAOs by eliminating expensive separation step.

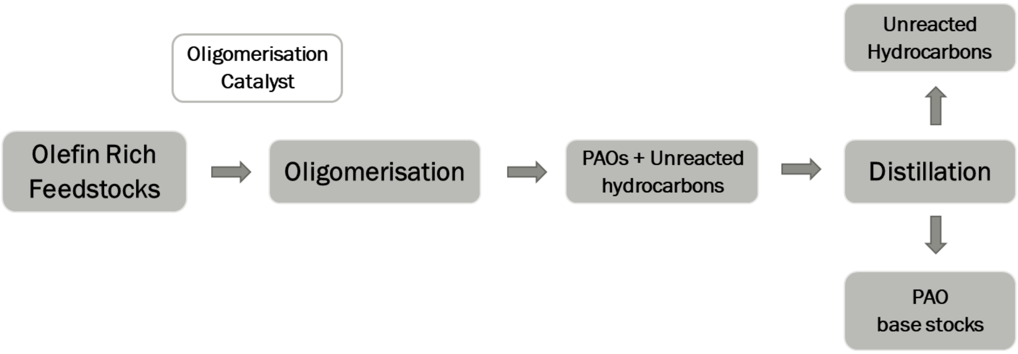

Figure 1.4: Block diagram for PAO production process

1.8.5 Process Flow Sheet Development for PAO production (Chapter 6)

Based on the experimental results, it is aimed to develop a kinetic model that predicts the reaction kinetics for different feed stocks with the formulated catalyst systems. These kinetic parameters will be used to develop a process simulation model for continuous production of PAOs from low value feed stocks in ASspen HYSYS.

1.8.6 Economics and Sensitivity Analysis (Chapter 7)

Further it is aimed to carryout economic evaluation and preliminary sizing calculations for the major equipment for continuous production. Figure 1.5 provides complete flow chart of the study intended in the current thesis work. It can be observed that every next step is dependent on the previous step. Thus, the work provides complete end to end product development and its subsequent analysis.

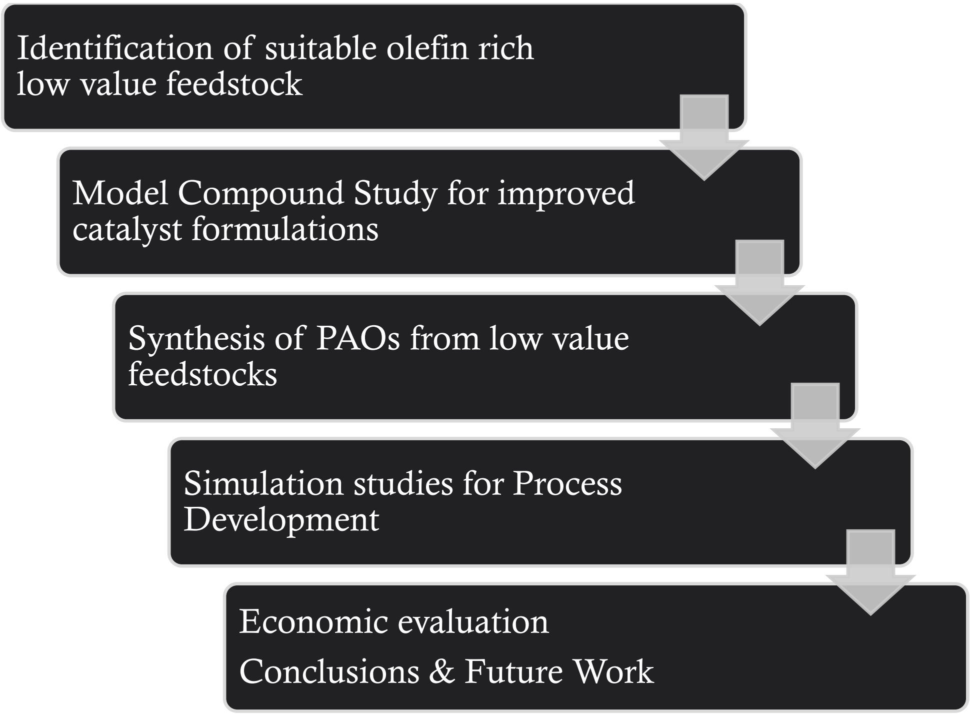

Figure 1.5 Complete flow chart of the thesis work

CHAPTER 2

LITERATURE REVIEW

2.1 Overview

This chapter provides details on various applications of lubricants, their important definitions as per American Petroleum Institute, important properties, classifications based on composition, synthesis methods and various recent research works in the area.

2.2 Lubricant Chemistry

From initial days of human civilization lubricants have helped to reduce loss in energy due to frictional forces of sliding objects. Animal fats, including whale oil, are known to be the first used lubricants. Lubricants, in the form of thin liquid film, reduces friction and wear between moving surfaces as depicted in Figure 2.1. They also play a critical role in removal generated frictional heat, and also prevents corrosion development [27 - 33].

Lubricants are used in some of the following applications [4]:

- Gasoline and diesel engine oils
- Machine lubrication
- Turbines
- Refrigeration systems
- Oils and greases used in transformer

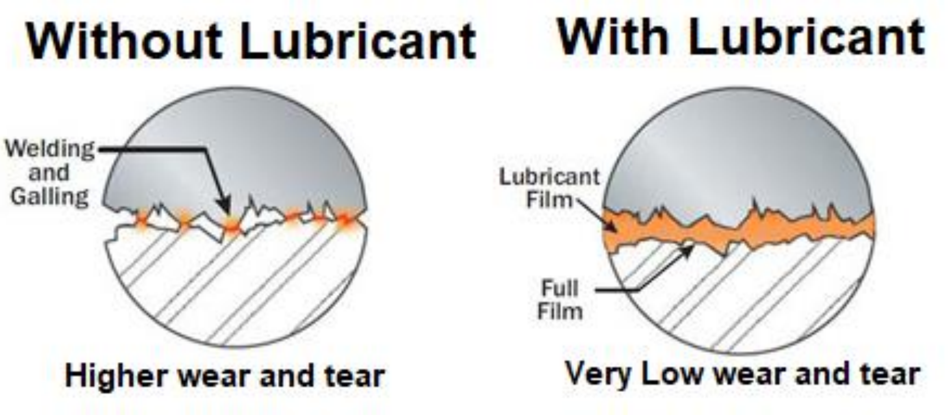

Figure 2.1: Illustration demonstrating lubrication action

Lubricants consist of hydrocarbon base stocks which constitute 80% to 98% by volume of finished products, the remaining 2% to 20% comprise of additives for improving performance of lubricants. Base stocks usually have boiling ranges between 315°C and 540°C. Lube feed stocks therefore come from the high-boiling region (except minute fraction from atmospheric distillation) which are vacuum gas oil fractions and the crude oil residue [5].

The petroleum refinery built by Samuel Weir in Pittsburgh was the first refinery in the world to produce base stocks in the 1850s. Current lubricant production across the world is well dispersed.

Some important definitions as per the American Petroleum Institute (API) [4] are:

i. Base stock: A lubricant component that is produced by a single manufacturer to the same specifications (independent of feeed source or manufacturer's location); that meets the same manufacturer's specification; and that is identified by a unique formula, product identification number or both".
ii. Base oil: The base stock or blend of base stocks used in an API licensed oil.
iii. Base stock slate: A product line of base stocks that have different viscosities but are in the same base stock grouping and from the same manufacturer.

Base stocks are generally of two types (a) naphthenic and (b) paraffinic, depending on the source of crude it is obtained from. Structure of these molecules are depicted in Figure 2.2 below.

Naphthenic crudes have nil or very low amounts of wax and are mostly cyclo-paraffinic and aromatic, and the naphthenic lube fractions are liquid at low temperatures.

Paraffinic crudes have n- and iso-paraffins having higher melting point, therefore these paraffins are removed by dewaxing process or are converted into iso-paraffins. They are useful for most lubricant applications constituting about 85% of the world lubricant supply.

Naphthenic and paraffinic base stocks are differentiated on the basis of viscosities; which is related to their molecular weights.

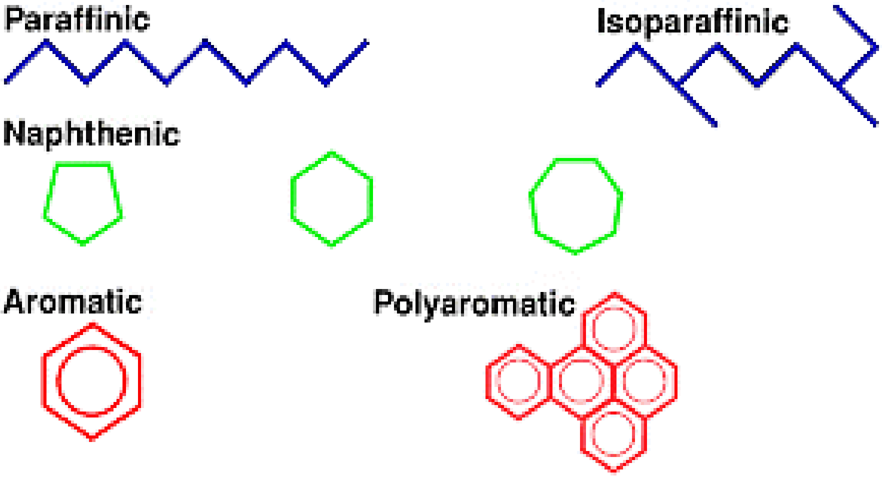

Figure 2.2: Shape of molecules – paraffinic, iso-paraffinic, naphthenic, aromatic and poly-aromatic [

2.3 Categorization based on Base Lubricant

Chemically, the lubricants consist of the base lubricant stock and array of additives. The various additives help [34] to enhance the performance of the lubricant as well as improve handling and storage stability [35 - 41]. Certain performance properties that additives impart upon the lubricant formulation include Viscosity Index (VI), Pour Point depression, Oxidation Stability improvement, anti-wear (AW), extreme pressure (EP), detergent inhibitor (DI) and dispersant.

Nonetheless, it is the base fluid that determines the basic properties of a lubricant and typically consist of anywhere from 80 to 98 percent of the total formulation. Obviously, the categorization stems from the physical and chemical nature of the base fluid. The lubricants, based on the method of manufacturing can broadly be categorized into two groups, Mineral oil based and Synthetic Oils. Synthetic lubricants can be further classified into different sub-categories, depending on their chemical origin and structure. The American Petroleum Institute has published a document named 1509 Engine Oil Licensing and Certification System to standardize and categorize the system .

The API originally created a system [4] to describe engine oil base fluids; But since then the system has found widespread acceptance as more general description of entire lubricant spectrum. Groups I-III are derived from petroleum crude oil and are mainly classified based on Viscosity Index, level of sulphur and degree of refinery processing. Group IV describes the rapidly growing class of polyalphaolefin(PAO) synthetic lubricants and Group V includes all other synthetics (mostly esters and glycols) [42, 43] not included in the other four group descriptions. Groups IV-V are generally marketed as synthetics. Basic details of Group I to Group V base oils is listed in Table 2.1.

Table 2.1: API base oil categories and properties

	BASE OIL CATEGORY		**SULFUR (%)**	**SATURATES (%)**	**VISCOSITY INDEX**
MINERAL	Group I	Solvent Refined	> 0.03	< 90	80 to 120
	Group II	Hydro-treated	< 0.03	> 90	80 to 120
	Group III	Hydro-cracked	< 0.03	> 95	120 to 140
SYNTHETIC	Group IV	PAO / Ester based	< 0.03	> 90	120 to 150
	Group V	All others not in Group I-IV	-*	-*	-*

*Under this group, synthetic lubes of varied properties are included.

2.4 Base Oil: Important Properties

Base stocks obtained in various refineries will never be identical; however, all these base stocks are characterized or analyzed for properties ranging from density to volatility and even flash point. Most important of which are mentioned in Figure 2.3 below:

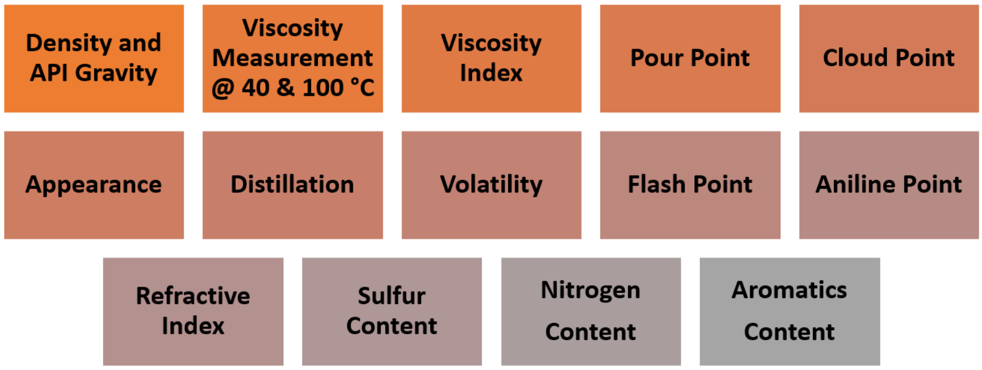

Figure 2.3: Important properties for base oil characterization

2.4.1 Density and API gravity

- Is an important property when managing different base stock types
- Values of density are directly proportional to viscosity, boiling range, and aromatic and naphthenic content
- Values of density are inversely proportional to iso-paraffin content
- $API\ gravity = \frac{141.5}{Specific\ gravity} - 131.5$; where, specific gravity is derived from density value

2.4.2 Viscosity Measurement at 40 & 100 °C

- Manufacturing and selling of Base Stock is in accordance with its viscosity measured at 40 or 100 °C
- Unit used for viscosity measurement is centistokes (cSt) at 40 °C; instead of Saybolt universal seconds (SUS) scale at 100 °F used earlier.

- Higher viscosity base stocks can only be prepared from heavy feed stocks such as High Vacuum Gas oil due to the molecular precursor requirement
- Distillation midpoint increases with increase in viscosity increases

2.4.3 Viscosity index (VI)

- Measures the extent of change in viscosity with respect to temperature
- Viscosity change will be minimal w.r.t. temperature when the base stock has higher VI, and is preferable
- It is also measured at 40 and 100 °C
- VI for a paraffinic base stock: 80
- VI after conventional solvent extraction/solvent dewaxing route: 95 to 140
- For VI greater than 140, feedstock must be either petroleum wax or Fischer-Tropsch wax based

2.4.4 Pour point

- It determines the temperature below which a base stock ceases to flow
- Paraffinic base stocks: −12 to −15 ° C
- Naphthenic base stocks: −30 to −50 °C

2.4.5 Cloud point

- It is the temperature at which initial wax crystals are formed.
- Visible as a cloud of microcrystals
- Values of cloud point are higher than those of pour point, and can be about 3 to 15 °C above the materials pour point

2.4.6 Distillation

- Performed using an actual distillation unit.

  - ASTM D86 @ atmospheric pressure
  - ASTM D1160 under vacuum for heavier ones
- Nowadays these tests are not performed much due higher time and manpower requirements
- These days it is determined using either a simulated distillation or gas chromatographic distillation technique as per ASTM D2887

2.4.7 Appearance

- Either clear or bright; or
- With or without sediments or haze

2.4.8 Flash point

- It determines the temperature at which the vapour above a liquid sample ignites, due to build-up of sufficient vapour pressure
- Is an important safety specification
- Increases with increase in viscosity of the grade. Higher flash points are always the requirement
- Determined using Cleveland Open Cup method (ASTM D92) methods

2.4.9 Volatility

- Very important test in automotive lubricant products
- Low volatility: lower emissions
  - Decreases consumption of oil
  - Avoids changes in engine oil viscosity changes
- Measurement methods:
  - ASTM D5800: Noack method
  - ASTM D6375: Thermogravimetric analysis
  - ASTM D6417: Gas chromatography technique

2.4.10 Aniline point

- Determines the ability of the base stock to behave as a solvent
- It is the temperature at which aniline and base stock are soluble, when taken in equal volumes.
- Determined as per ASTM D611
- Paraffinic base stock: ≥ 100 °C
- Naphthenic or aromatic base stock: < 100 °C

2.4.11 Refractive index

- One of the important parameters to characterize base stocks
- Values of refractive index increase with molecular weight
- Aromatic base stocks have higher refractive index values than paraffinic base stocks

2.4.12 Sulfur

- Sulfur is observed in all lube feed stocks refined from crude oil
- May be present in quantities ranging from ppm to even several %
- Process of refining cannot remove much sulfur from the base stock
- Treatment of base stock by technique such as ‘Hydrofinishing’ can substantially reduce its sulfur content; which can be lowered to values as low as parts per million (ppm)

2.4.13 Nitrogen

- Similar to sulfur, nitrogen-based compounds are also present in all lube feed stocks
- Approximate quantity: 500 to 2000 ppm
- Most of the nitrogen-based compounds are removed by the process of solvent extraction; whereas, about complete removal is possible by the utilization of process called as hydrocracking

2.4.14 Aromatics

- These are mostly monoaromatic compounds; however, substantial amounts of di- and triaromatic compounds are also observed in the feedstock
- Polyaromatic compounds adversely affects the oxidation stability of the base stock; however, these compounds can be completed removed by the conversion processes
- Feed stocks containing higher quantity of aromatic compounds demonstrates lower values of viscosity index (VI)
- Following are some of the techniques through which it is measured:
    - ASTM D5186: Supercritical fluid chromatography
    - ASTM D6379: High-pressure liquid chromatography (HPLC)
    - ASTM D2549: Chromatography over alumina/silica gel
    - ASTM D2007: Preparative chromatography

2.5 Compositional classification of base sock and feed stock

Distillation and refining of crude oil leads to presence of complex hydrocarbons in both the petroleum distillates and residues; which can also contain certain sulfur and nitrogen-based compounds. Certain important compounds are listed and described below in Figure 2.4.

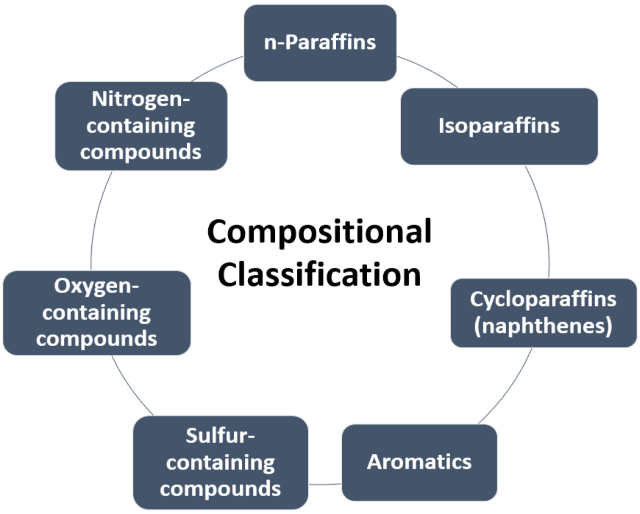

Figure 2.4: Illustration of compositional classification

2.5.1 n-Paraffins

These are hydrocarbon compounds having n-paraffin homologous series from C_{18} and above having boiling range from 315 to 450 °C; which again is based on the feeds wax content. n-paraffins having boiling point more than 450 °C are quite uncommon. These compounds can be easily characterized and quantified using the technique of gas chromatography. These hydrocarbon compounds have significant effect on the base stocks pour point, attributed to its higher melting point. Higher the n-paraffin content, higher will be the pour point of the base stock.

2.5.2 Iso-paraffins

These have n-paraffin backbones with alkyl branches; on an iso-paraffin chain there may well be several branches of methyl groups or higher. Those iso-paraffins most similar in structure to n-paraffins (single branches near a chain end) have higher pour points and will be removed by solvent dewaxing. Identification of individual members may be quite difficult. Iso-paraffins as a group have high VIs and low pour points, and confer good oxidation resistance. They are therefore a sought-after component in base stocks.

2.5.3 Cyclo-paraffins (naphthenes)

These are also hydrocarbon compounds having one or more cyclohexane or cyclo-pentane type of ring structures, which can be varied combination. Most favourable structure in the cyclo-paraffins is that of 1,4 substituted cyclo-paraffins; whereas, the most unfavourable compound are poly-naphthenes having 3+ rings, as it adversely affects the viscosity index and materials oxidation resistance.

2.5.4 Aromatics

These compounds have benzene rings which can be either single or combination of as more as six; wherein certain bonds of carbon–hydrogen are replaced with bonds of carbon–carbon. 1,4 alkyl-substituted benzenes having higher viscosity index values and better resistance to oxidation are the desired compounds; whereas, fused poly-aromatic structures are highly undesirable. Presence of aromatic compounds decreases the viscosity index of the stock.

2.5.5 Sulfur-containing compounds

Sulfur-containing compounds are generally based on thiol, sulfide, thiophene, benzo- and dibenzo-thiophene, moieties, and are highly complex structures. Sulfur content can be reduced by the process of solvent extraction; however, it cannot decrease them below a certain optimum level. However, intense processes such as lube hydrocracking can decrease sulfur content in the base stock to even lower than 10 ppm.

2.5.6 Nitrogen-containing compounds

These compounds are generally based on pyrrole, benzo- and dibenzo-carbazole, pyridine, and quinoline, structures, and can be reduced to few parts per million, again by the process of lube hydrocracking.

2.5.7 Oxygen-containing compounds

These compounds are structures having oxygen atom chemically bonded into the base molecule and are generally furans, carboxylic acids, and so on.; and are present in negligible amounts in the feedstock.

2.6 API based classification

In this method of classification base stocks are categorized for the purpose of base stock interchanges after the base stock categories developed by the American Petroleum Institute in the year 1993. API developed this classification based on the content of saturates, sulphur and VI of the material, and is as depicted in the Figure 2.5 below.

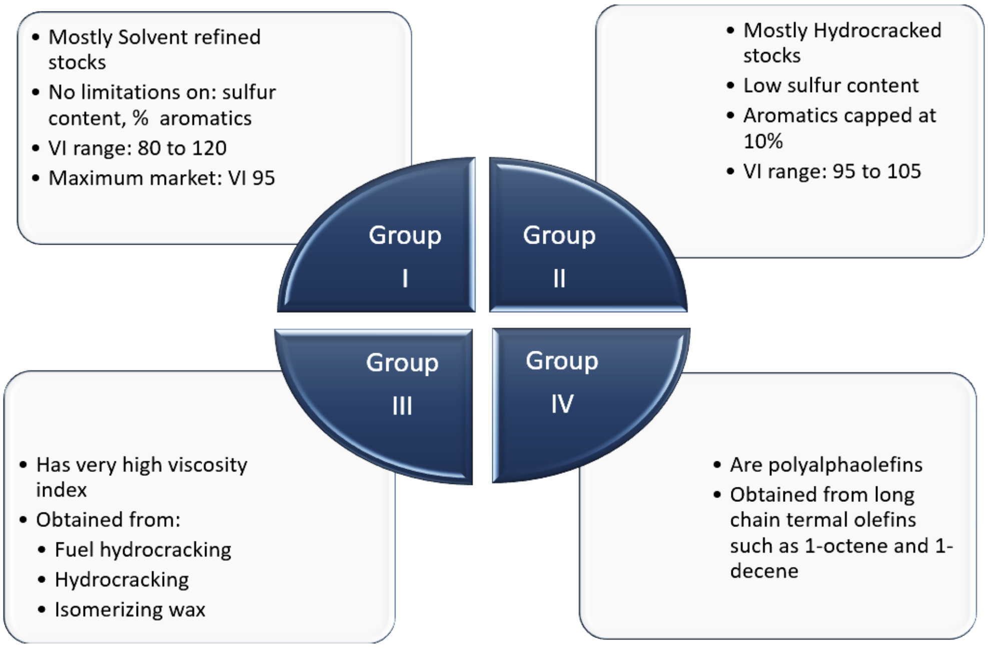

Figure 2.5: Basic properties of group I to group IV base stocks

Group V: Any base stocks not defined by groups I–IV

2.7 Viscosity grades

Base stocks are also differentiated based on their viscosity having measurement unit of mm2/s or cSt @ 40°C as per ASTM D2422. This system of classification covers base stock viscosity grades from of 2 to 3200 cSt.

Obsolete measurement of viscosity of the base stock was as per Saybolt Universal Seconds (SUS) determined at 100°F.

2.8 Conventional base stock production

Low boiling point refinery streams are not used for the production of lubricants [43]due to their lower viscosity and high volatility, and are blended to produce gasoline, kerosene, diesel etc. Vacuum distillation operation is performed on the high molecular weight fractions under lower pressures of 10 to 50 mmHg, producing light vacuum gas oil (LVGO) and heavy vacuum gas oil (HVGO); which are further subjected to solvent refining or hydrocracking.

High viscosity lube precursors, having boiling point of more than 500 °C, obtained as bottoms of the vacuum tower are subjected to deasphalting unit to remove asphaltenes giving deasphalted oil (DAO), a waxy lube feedstock; whereas, kits further refining produces valuable product named as bright stock. Representative boiling point and carbon number ranges for lube feed stocks are mentioned in the Table 2.2 below.

Table 2.2: Representative boiling and carbon number ranges for lube feed stocks

Fraction	Approximate Boiling Point Range (°C)	Carbon Number Range
LVGO	315 to 480	18–34
HVGO	425 to 590	28–53
DAO	110 +	38+

Two methods of refining waxy lube feed stocks are:

1. Chemical Separation Process

   Unrequired components such as poly-aromatics are separated with the solvent refining process. Molecular composition in the final base stock remains same as that of the feed stock.

2. Chemical Conversion Process

   Chemical components which are inappropriate lube manufacturing are completely or partially converted to appropriate base stock chemical by using a process called as catalytic hydro-processing.

   Processes involving conversion are usually lower costs process providing superior yields and high-quality base stock.

   In order to use the existing hardware in the refinery setup, they generally use combination of separation and conversion processes. Typical schematic process flow involving separation and conversion process is illustrated in the Figure 2.6 below.

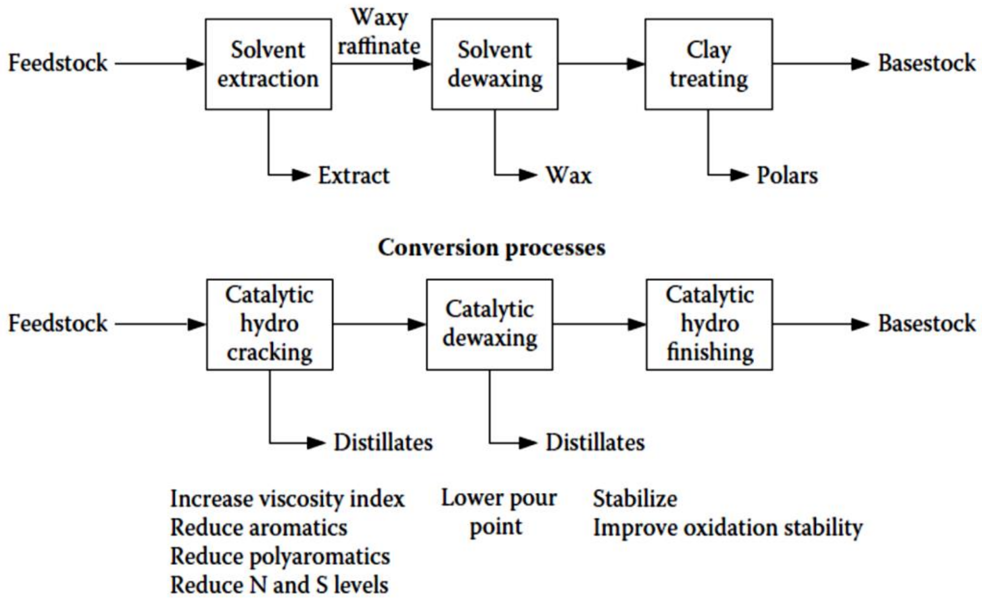

Figure 2.6: Comparison of process scheme for separation and conversion process routes for lubes

In the usual solvent-based refining process, a polar solvent is used to extract aromatic compounds (compounds having several aromatic rings in addition to polar functional groups) providing upgraded waxy raffinate having viscosity lower than that of the feed, and is less affected by the temperature change. Next, it is subjected to the dewaxing process to remove the residual wax content, which can leads to its freezing during winter. Obtained base stock is then determined to have all the required specifications. Modified base stock can then be subjected to advanced catalytic hydro-finishing step to improve its color and performance. This step primarily removes certain % of polyaromatics and nitrogen, sulfur, and any oxygen based compounds.

Steps involved in the conversion process are:

1. Catalytic hydrogenation: Feedstock aromatics hydrogenation to cycloparaffins (napthenes) and also certain molecular reorganization leads to improvement in VI. In addition, feed sulfur and nitrogen compounds are also removed completely

2. Solvent dewaxing or Catalytic hydroprocessing: Feedstock is boiled above about 370 °due to which wax gets cracked to gasoline or gets isomerized to low melting isoparaffins
3. Catalytic hydrogenation: Saturates most of the remaining aromatics improving its storage and performance

Advantages of the conversion process:

- Base stock obtained is water white
- Minimal dependence on procurement of high-cost and high-quality lube bearing crudes
- Higher yield of base stock and lubricants meeting the automotive lubricant requirement

Steps involved in the conventional lube manufacturing separation technology are:

a. Solvent refining

Adjusts the viscosity index and improves the response of base stock to oxidation. Involves usage of solvent extraction step to extract low viscosity index and easily oxidizable fractions from the highly desirable high viscosity index and oxidation-resistant components. Commonly used solvents are:

- Phenol
- Furfural
- N-methyl pyrrolidine

b. Solvent dewaxing

This process doesn’t involve use of any chemical reaction; thus, the composition of the dewaxed material depends solely on the feed composition. Initially developed process of dewaxing called as ‘cold-settling’ involved refrigeration and subsequent settling of the wax in the cold tanks or barrels. This process was then replaced by year-round refrigeration process involving wax removal by steps such as filtration or centrifugation using solvents or solvent mixtures such as sulfur dioxide-benzene, propane, benzene-acetone, toluene-methyl ethyl ketone (MEK) etc.

c. **Finishing to bring about final quality improvement**

Finishing step improves the color and performance of the material by removing the polar compounds (whatever remaining); although, most of it is removed in the extraction step. Process involved herein are:

- Clay-treating: For separation by adsorption, and
- Hydro-finishing: Involves hydrogenation to prepare acceptable lube components

Integrated lube processing is explained in Figure 2.7 below.

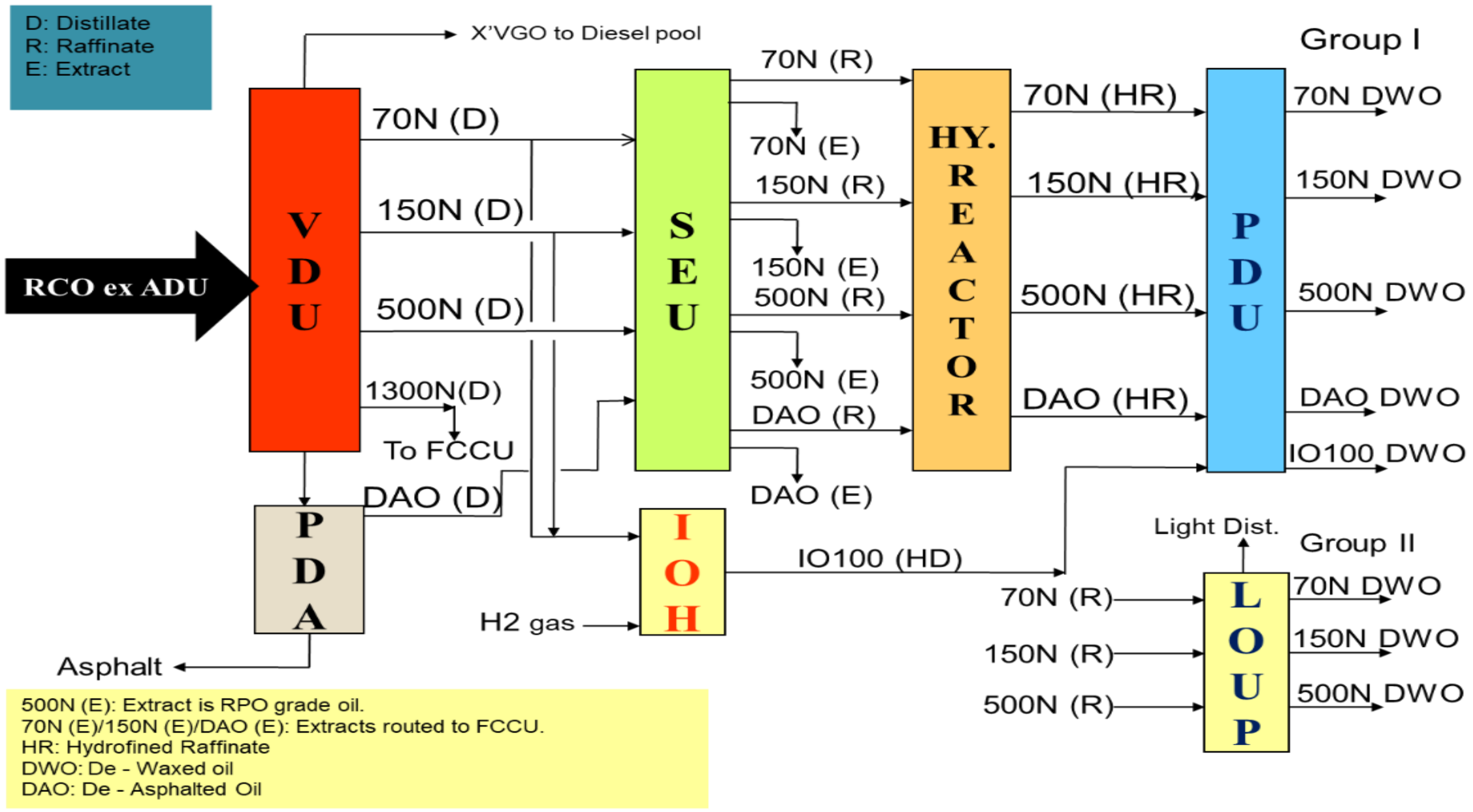

Figure 2.7: Flowchart for lube processing in refinery

2.9 Lubes hydrocracking

The process step involves reaction of the waxy feed (paraffinic distillate or deasphalted oil) and hydrogen using a catalyst to bring about molecular reorganization and its cracking. Some of the reactions types taking place are:

- Hydrodearomatization [HDA]
- Hydrodesulfurization [HDS]
- Hydrodenitrification [HDN])

Generic reaction parameters are: Reactor: Trickle bed downflow reactor, Hydrogen pressure: 100 to 275 bar, Temperature: >300 °C, Catalyst: “Dual functional” as it is involved in both cracking and hydrogenation steps, and is generally based on silica-alumina or Zeolite Y in combination of oxides from groups VI and VIII (nickel, cobalt, molybdenum, tungsten)

The process of hydrocracking produces Group II and Group III base oils.

2.10 Synthetic lubricants - History

These are mixture of chemical c compounds which are produced synthetically not involving direct usage of crude mineral oil. These materials can be produced from (a)Petrochemical components, (b) biomass feedstock and (c) any other suitable raw material. Operational advantages of the synthetics are explained in Figure 2.8.

Brief history of synthetic lubricants:

- 1877: Charles Friedel and James Mason Crafts designed a technique to produce alkyl benzene based lubricants; which were first of its kind
- 1929: Standard Oil Company of Indiana initiated commercialization of synthetic hydrocarbon oil
- 1931: Standard Oil, in a research paper explained a process for polymerization of olefinic compounds to oligomeric compounds
- 1931: I.G. Farben Industries also independently developed similar process
- 1950’s: Substantial developments initiated in synthetic lubricants attributed to the start and rapid growth of jet engine technology.

- 1960: Garwood of Socony-Mobil synthesized polymers of linear α-olefins using free radical initiators
- 1961: Southern et al. of Shell Research disclosed a patent, wherein, transition metal and organometallic catalysts(ethylaluminum sesquichloride/titanium tetrachloride) were used to synthesis polymers of linear α-olefins
- 1968: Brennan at Mobil Oil demonstrated production of polyalphaolefins by mixing two streams of olefins in the oligomerization process
- 1960's: First commercial breakthrough for PAOs
- 1973: Synthetic automotive engine oil developed by Mobil Corporation
- 1970's: Developed commercial high performance functional PAOs
- 1980's: Growth observed in the market for PAO
- 1998: Synthetic lubricant market accounted to about 200 million gallons/yr (2% of the total lubricant volume)

Figure 2.8: Operational advantages of synthetic oils
(source: www.efficientplantmag.com)

Type of synthetic lubricants, their applications, advantages and disadvantages are listed out in Table 2.3.

Table 2.3: Synthetic lubricant types

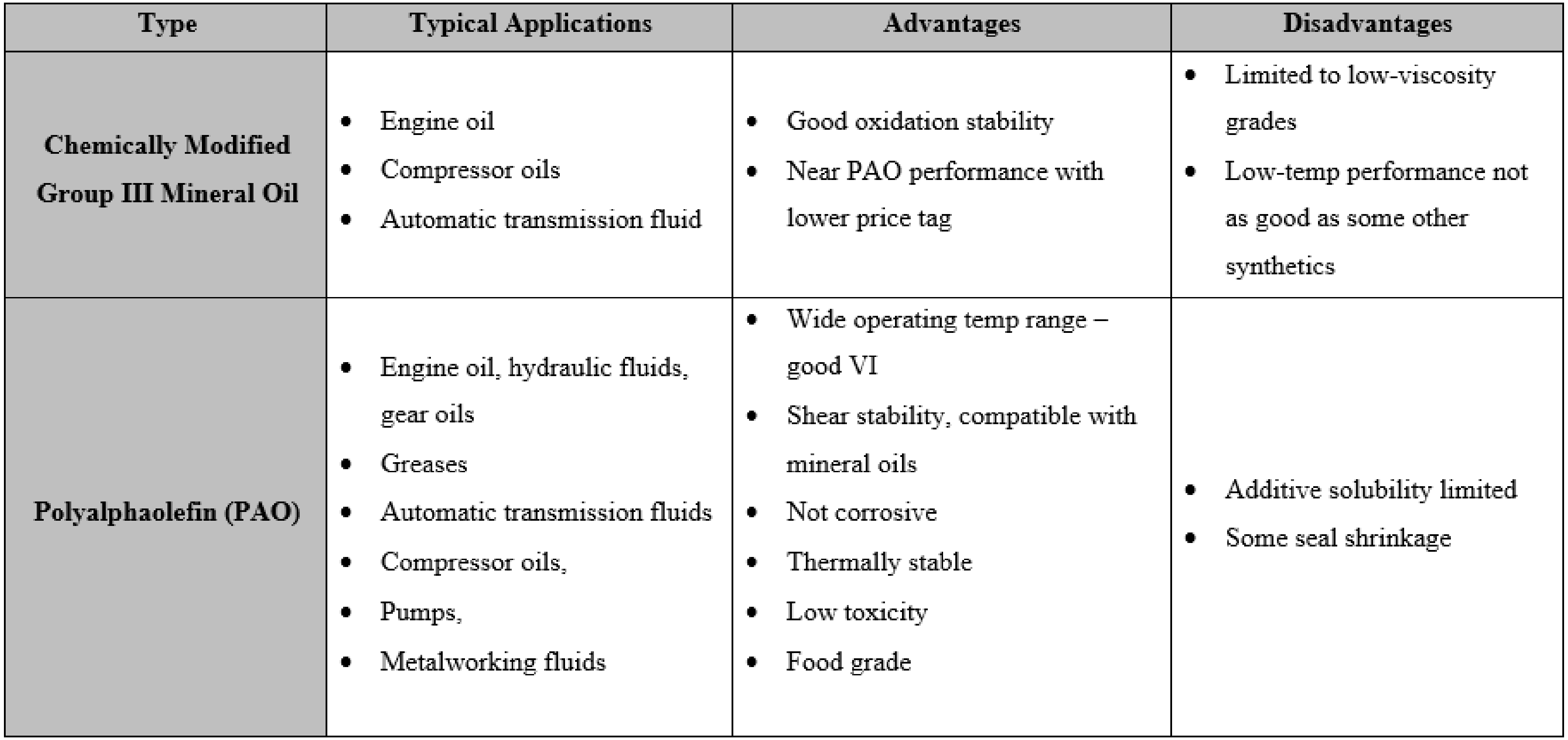

Type	Typical Applications	Advantages	Disadvantages
Chemically Modified Group III Mineral Oil	• Engine oil • Compressor oils • Automatic transmission fluid	• Good oxidation stability • Near PAO performance with lower price tag	• Limited to low-viscosity grades • Low-temp performance not as good as some other synthetics
Polyalphaolefin (PAO)	• Engine oil, hydraulic fluids, gear oils • Greases • Automatic transmission fluids • Compressor oils, • Pumps, • Metalworking fluids	• Wide operating temp range – good VI • Shear stability, compatible with mineral oils • Not corrosive • Thermally stable • Low toxicity • Food grade	• Additive solubility limited • Some seal shrinkage

Type	Typical Applications	Advantages	Disadvantages
Chemically Modified Group III Mineral Oil	• Engine oil • Compressor oils • Automatic transmission fluid	• Good oxidation stability • Near PAO performance with lower price tag	• Limited to low-viscosity grades • Low-temp performance not as good as some other synthetics
Polyalphaolefin (PAO)	• Engine oil, hydraulic fluids, gear oils • Greases • Automatic transmission fluids • Compressor oils, • Pumps, • Metalworking fluids	• Wide operating temp range – good VI • Shear stability, compatible with mineral oils • Not corrosive • Thermally stable • Low toxicity • Food grade	• Additive solubility limited • Some seal shrinkage

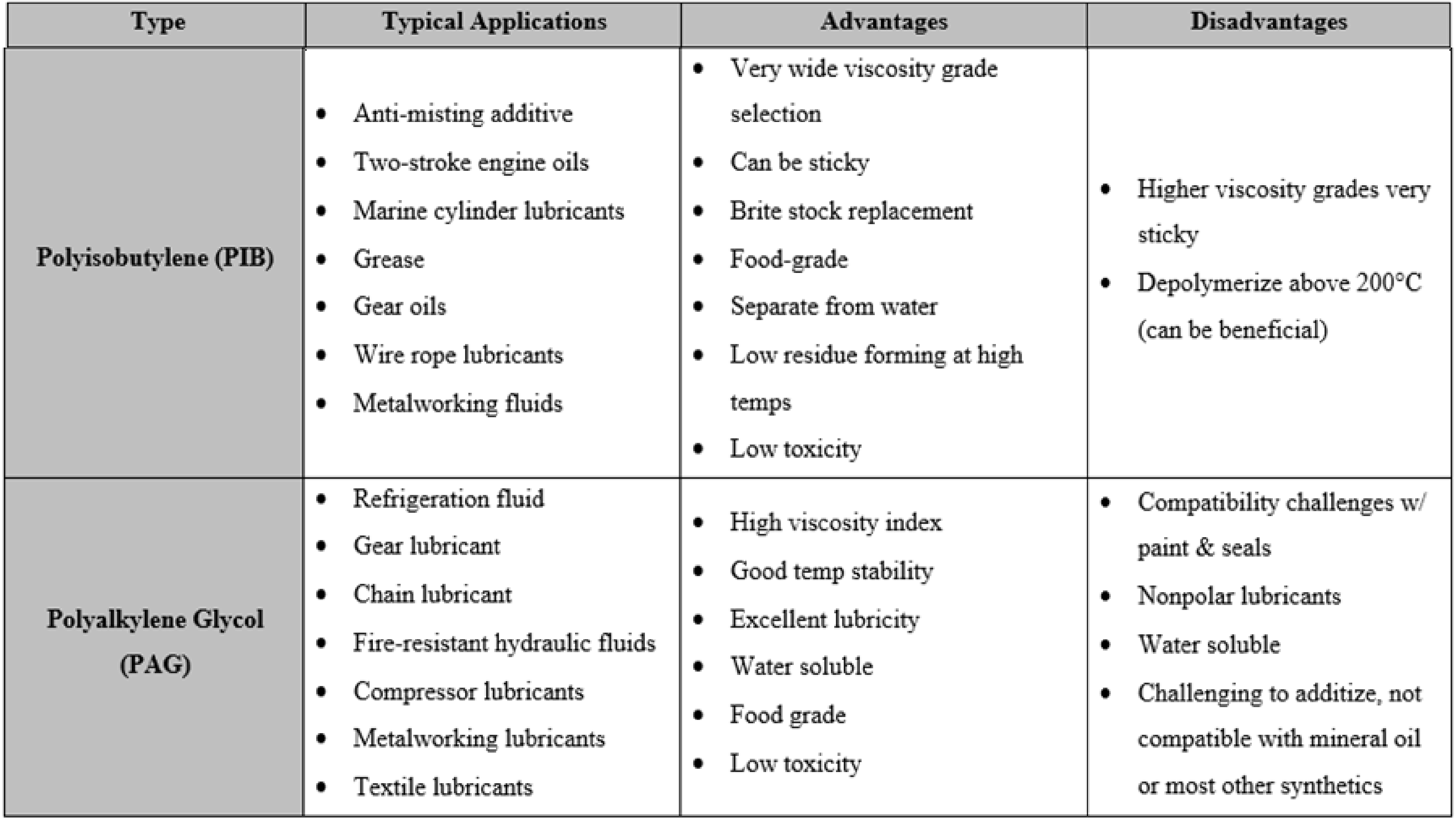

Type	Typical Applications	Advantages	Disadvantages
Polyisobutylene (PIB)	• Anti-misting additive • Two-stroke engine oils • Marine cylinder lubricants • Grease • Gear oils • Wire rope lubricants • Metalworking fluids	• Very wide viscosity grade selection • Can be sticky • Brite stock replacement • Food-grade • Separate from water • Low residue forming at high temps • Low toxicity	• Higher viscosity grades very sticky • Depolymerize above 200°C (can be beneficial)
Polyalkylene Glycol (PAG)	• Refrigeration fluid • Gear lubricant • Chain lubricant • Fire-resistant hydraulic fluids • Compressor lubricants • Metalworking lubricants • Textile lubricants	• High viscosity index • Good temp stability • Excellent lubricity • Water soluble • Food grade • Low toxicity	• Compatibility challenges w/ paint & seals • Nonpolar lubricants • Water soluble • Challenging to additize, not compatible with mineral oil or most other synthetics

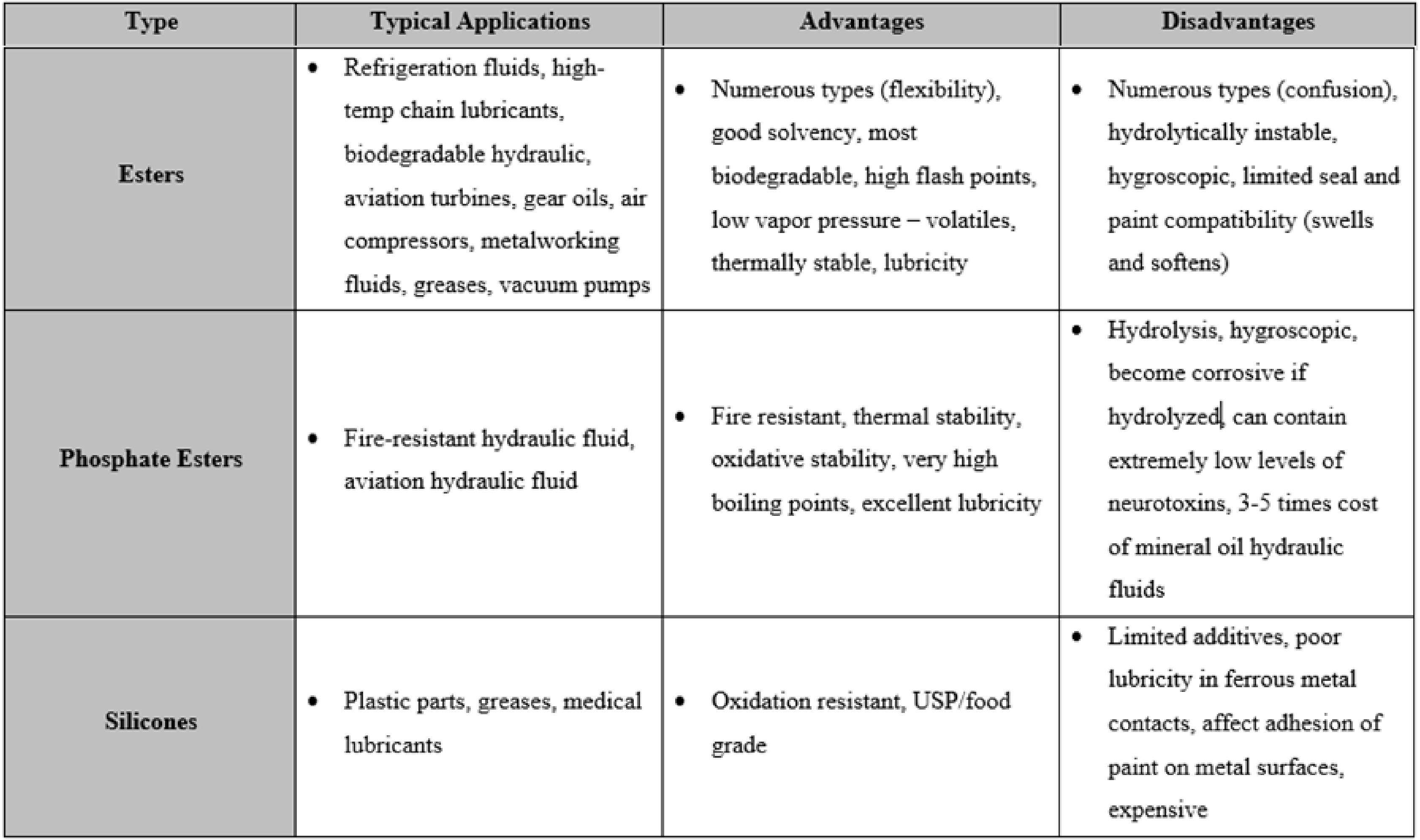

Type	Typical Applications	Advantages	Disadvantages
Esters	- Refrigeration fluids, high-temp chain lubricants, biodegradable hydraulic, aviation turbines, gear oils, air compressors, metalworking fluids, greases, vacuum pumps	- Numerous types (flexibility), good solvency, most biodegradable, high flash points, low vapor pressure – volatiles, thermally stable, lubricity	- Numerous types (confusion), hydrolytically instable, hygroscopic, limited seal and paint compatibility (swells and softens)
Phosphate Esters	- Fire-resistant hydraulic fluid, aviation hydraulic fluid	- Fire resistant, thermal stability, oxidative stability, very high boiling points, excellent lubricity	- Hydrolysis, hygroscopic, become corrosive if hydrolyzed, can contain extremely low levels of neurotoxins, 3-5 times cost of mineral oil hydraulic fluids
Silicones	- Plastic parts, greases, medical lubricants	- Oxidation resistant, USP/food grade	- Limited additives, poor lubricity in ferrous metal contacts, affect adhesion of paint on metal surfaces, expensive

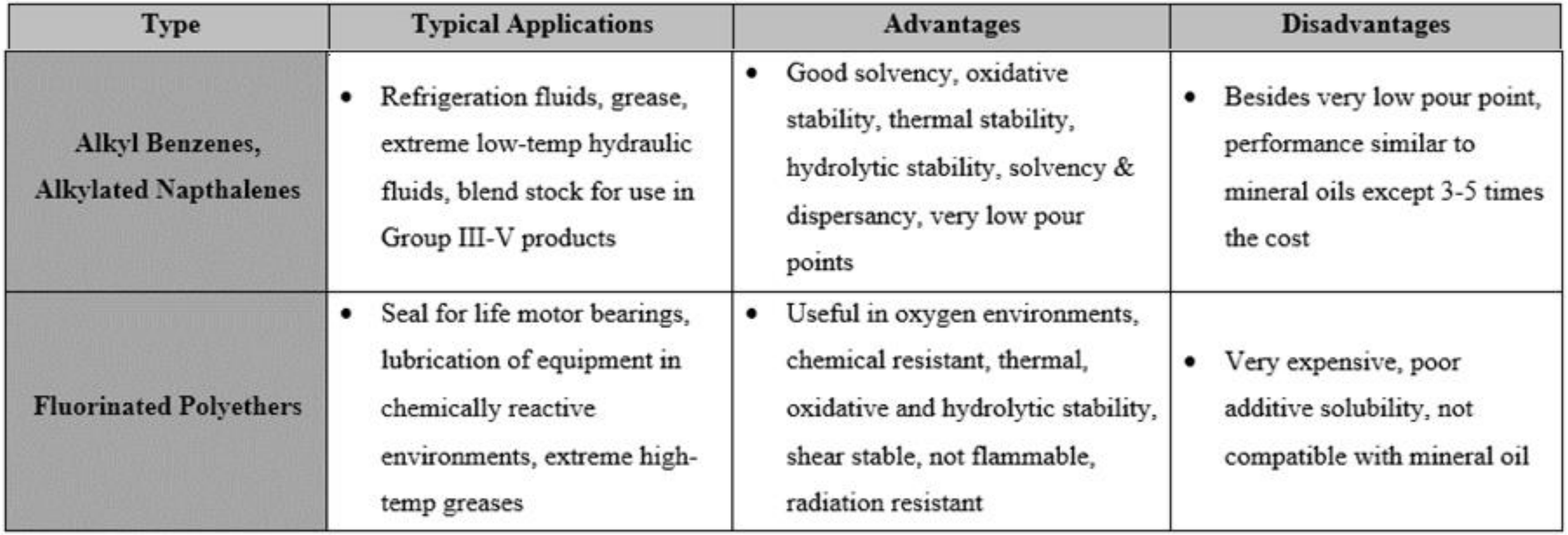

Type	Typical Applications	Advantages	Disadvantages
Alkyl Benzenes, Alkylated Napthalenes	• Refrigeration fluids, grease, extreme low-temp hydraulic fluids, blend stock for use in Group III-V products	• Good solvency, oxidative stability, thermal stability, hydrolytic stability, solvency & dispersancy, very low pour points	• Besides very low pour point, performance similar to mineral oils except 3-5 times the cost
Fluorinated Polyethers	• Seal for life motor bearings, lubrication of equipment in chemically reactive environments, extreme high-temp greases	• Useful in oxygen environments, chemical resistant, thermal, oxidative and hydrolytic stability, shear stable, not flammable, radiation resistant	• Very expensive, poor additive solubility, not compatible with mineral oil

2.11 Synthesis and production of PAOs

2.11.1 Catalyst systems used in PAO synthesis

As can be seen from the literature [20], [21], [22] synthesis of PAO is executed using the cationic polymerization technique. Some of the catalysts used in the cationic polymerization technique are generally Lewis acids namely aluminium chloride ($AlCl_3$) or boron trifluoride (BF_3); whereas some of the promoters used are water (H_2O), carboxylic acid (R-COOH), alkyl halides (RX), alcohols (R-OH) and ethers (R-O-R). Some research papers had reported synthesis of synthetic lubricants by oligomerization of α-olefins using a group IV metal oxide bed. Hamilton *et al.* reported synthesis of PAO oligomers from α-olefins using organic peroxide, Friedel-Crafts catalysts and also by thermal initiation polymerization method; stability of which is increased by further hydrogenation step. Details of some of the catalyst materials, other than Ziegler-Natta, is provided below.

2.11.1.1 Aluminium chloride

It is generally used in conjunction with a second compound such as alcohol or water; which act as co-activator producing active intermediate and formation of hydrogen chloride as by product. If used aluminium powder, instead of aluminium chloride, halogen free PAOs can be synthesized.

2.11.1.2 Boron trifluoride

It is one of the majorly used catalyst for PAO synthesis by 1-olefins oligomerization. This catalyst is specifically used for making low viscosity oils, appropriate for use in applications requiring lower temperatures.

2.11.1.3 Chromium-based catalyst systems

Various compounds containing chromium metal, in the reduced state mostly supported on inert carrier material such as silica, have been reported in literature for PAO synthesis. Synthesized PAOs have very high viscosity and viscosity index.

2.11.1.4 Titanium-based catalyst systems

It is used mainly in the chloride form.; wherein this particular moiety assists in controlling the molecular weight of the synthesized PAO, and thus its viscosity index.

2.11.1.5 Metallocenes catalysts

These are widely utilized in the synthesis of PAOs, as they are capable to produce very high viscosity base stocks similar in properties to that of supported chromium catalysts.

2.11.1.6 Ionic liquid catalysts

Ionic liquids are some of the recently developed catalysts for PAO synthesis, providing advantage of possibility of reaction dilution, and are commercially available at cheaper costs.

2.11.1.7 Synthetic zeolites

This catalyst systems are also extensively reported in literature for PAO synthesis, and works best in the atmosphere of minimum hydrogen, giving PAOs of acceptable qualities.

2.11.2 Co-catalyst system used in PAO synthesis

As found from the literature reports, utilization of a co-catalyst or promoter alongwith the catalyst system based on boron trifluoride or aluminum chloride imparts better control on the reaction kinetics synthesising oligomers with narrow molecular weight distribution. The co-catalyst or promoter used acts by forming a co-ordination complex with the catalyst improving its catalytic activity. Various co-catalyst systems are listed in Table 2.4.

Table 2.4: Different class of compounds used as co-catalysts

Sr. No.	Class	Compound
1	Aliphatic Esters	Dimethyl ether
2		Diethyl ether
3	Aliphatic alcohols	Methanol
4		Ethanol
5		n-Butanol
6		Decanol
7	Polyols	Ethylene glycol
8		Glycerol
9	Aliphatic Carboxylic Acids	Acetic acids
10		Propanoic Acid
11		Butyric acid
12	Esters	Ethyl Acetate
13		Methyl Propionate
14	Ketones	Acetone
15	Aldehydes	Acetaldehyde
16		Benzaldehyde
17	Acid Anhydrides	Acetic acid Anhydride
18		Succinic Anhydride

2.11.3 Linear alpha-olefins used in PAO synthesis

Following list of compounds are included in the list of linear alpha olefins:

- 1-butene
- 1-hexene
- 1-octene
- 1-decene
- 1-dodecene
- 1-tetradecene
- 1-hexadecene
- 1-octadecene, and
- higher olefin blends of C20-C24, C24-C30, and C20-C30 ranges.

Linear alpha olefin is produced by two of the known industrial processes: (a) oligomerization of ethylene and (b) by Fischer-Tropsch synthesis and subsequent purification; whereas prior to 1970s, these were manufactured by chlorination/dehydrochlorination of linear paraffins.

Major applications of alpha olefins include; (a) HDPE and LLDPE synthesis, (b) Synthesis of linear alcohols for plasticizer application, (c) aqueous detergent formulations; (d) paper sizing etc.

2.11.4 Poly alpha olefin

Oligomeric product obtained from various 1-olefins were determined to have properties appropriate for usage in some of the applications such as fluids for preparing: (a) lubricants, (b) hydraulic fluids, (c) transmission fluids, (d) transformer fluids, etc. The fluid used in the above-mentioned application is also called as functional fluid. 1-Decene is a majorly used and also a preferred monomer in the synthesis of oligomers suitable for the synthetic lubricant application. Literature search also describes synthesis of beneficial functional fluids by oligomerization of 1-decene with other α-olefins having carbon atoms from 6 to 12. Base oil prepared by oligomerization of α-olefins is usually a mixture of trimer, tetramer and its pentamer; % composition of which can vary depending on the application intended. Whereas, any dimers produced in the process, being volatile and low viscous in nature, are removed by the process of distillation as a reaction by-product.

2.12 Linear alpha olefins and its oligomeric products

In the recent past, various groups among the world focused on various aspects of synthetic PAO lubricants. The conventional PAO synthesis is achieved in two major steps involving (i) Oligomerization of ethylene to make linear alpha olefins (LAO) (ii) Oligomerization of LAOs to PAOs. Worldwide, lot of research is in progress in all the above-mentioned areas to optimize the existing processes and reduce the production cost. Therefore, a detailed literature review has been conducted to acknowledge the current status and identify the potential gaps in the PAO production processes and the detailed are summarized in Table 2.5.

Table 2.5: Compilation of research works in the synthesis of α-olefins and also its oligomers using various catalyst and co-catalyst systems

S. No.	Title & Publication	Author	Major Key Findings	Gaps
1	Recovery of hydrocarbon liquid from waste high density polyethylene by thermal pyrolysis	Kumar et al. *(NIT Rourkela, India)*	• Thermal cracking of polyethylene (concept is similar to wax cracking process) • Cracking is performed at 450 ^{o}C • Product composition was analyzed using GC-MS	Author didn't discuss about the potential of LAO production.
2	Process for preparing linear alpha olefins	Boer et al. *(Shell Oil Company, US)*	• Trialkyl aluminum catalyst for the linear alpha olefin synthesis .	This process talks about from pure alkene to alpha olefins. Authors did not talk about alpha olefins from refinery streams.
3	Processes for the production of higher linear α-olefins	Belov et al. *(Russian Academy of Sciences, Russia)*	• Discussed on various industrial processes and catalyst systems available for ethylene oligomerization to linear α-olefins for maximizing purity and selectivity	Review article

S. No.	Title & Publication	Author	Major Key Findings	Gaps
4	Oligomerization of ethylene to α-olefins: discovery and development of the shell higher olefin process (SHOP)	Keim et al. *(RWTH Aachen University, Germany)*	• The article discusses about the catalyst and process involved in the SHOP process for LAOS from ethylene • Details about metallocene catalyst is given	Ethylene based process
5	Alkylation of oligomers to make the superior lubricant or fuel blend stock	Elomari et al. *(Chevron USA Inc., US)*	• Mixtures of olefins an isoparafiins are subjected to produce the alkylated synthetic lubricants • 1-decene and isobutene are used as a feedstock to obtain the synthetic lubes with VI up to 140	The methodology did not mentioned about refinery feedstock
6	Synthesis of poly alpha olefins using alpha olefins obtained from the steam cracking process of coal liquefaction wax	Yu et al. *(East China University of Science and Technology, China)*	• Optimal operating conditions proposed for coal wax steam cracking are preheating T: 540 ^{o}C, rxn T: 670 ^{o}C, steam/wax: 0.16 and t: 2.5 sec	• No data is reported to increase alpha olefin percentage with additives • Study of the impurities on oligomerization process is not reported

S. No.	Title & Publication	Author	Major Key Findings	Gaps
			• (liq – 43.1% and gas – 19.5%) and α-olefin yield of 28.4%. • Compared the oligomer properties obtained from cracking product and 1-decene using Ziegler 3 wt% of $AlCl_3/TiCl_4$ catalyst	
7	Oligomerization of alpha olefins	Sarin et al. *(Indian Oil Corporation Ltd., India)*	• Proposed novel catalyst consisting of aluminium halide and group IVB transition metal alkoxide for selective oligomerization of α-olefins present in cracked refinery streams having carbon number of C8 – C20 to PAOs having viscosity of 7 – 30 cSt at 100 °C.	• Data on type of Cracked streams and type of olefins in the feed not mentioned. • Wax not considered as feed. • Process scheme not discussed

S. No.	Title & Publication	Author	• Major Key Findings	Gaps
8	Structurally uniform 1-hexene, 1-octene, and 1-decene oligomers: Zirconocene/MAO-catalyzed preparation, characterization, and prospects of their use as low-viscosity low-temperature oil base stocks	Nifant'ev et al. *(A. V. Topchiev Institute of Petrochemical Synthesis RAS, Russia Federation)*	• Oligomerization catalysts based on Metallocene were developed. • Studied the effects of catalyst on model compounds like 1-hexene, 1-octene, 1-decene. • produced the oligomer mixtures with oligomerization grades $P_n = 2–5$ with yields of up to 90%	The authors did not try with the efficacy of the catalyst using actual feed / in the presence of other hydrocarbons
9	Process for oligomerisation of alpha-olefin	Sarin et al. *(NCL Pune, India)*	• Heterogeneous catalyst is developed for alpha olefin oligomerization	The authors did not try with the efficacy of the catalyst using actual feed / in the presence of other hydrocarbons
10	Utilization of linear alpha olefins in the production metallocene catalyzed polyalpha olefins	Hagemeister et al. *(Exxonmobil Chemical Patents Inc., US)*	• A Process has been developed for the synthesis of lubricant base stock from alphaolefin by metallocene based catalyst.	The authors did not report the effect of mixed olefins from refinery streams.

S. No.	Title & Publication	Author	Major Key Findings	Gaps
11	Manufacture of low viscosity polyalpha-olefins	Goze et al. *(Exxonmobil Chemical Patents Inc., US)*	• Discussed on Synthesis of PAOs from mixture of olefins like octene, decene and dodecene.	Authors did not try to synthesize PAOs from other alpha olefin feeds.
12	Synthesis of poly-alpha olefin and Use thereof	Song et al. *(Shell Oil Company, US)*	• Catalyst formulations based on Metallocene were developed. • Pure C14 alpha olefins are used. • Optimized reaction temperature was reported as 60 ^{o}C	The authors did not try with the efficacy in the presence of mixed olefins / other hydrocarbons.
13	Lubricants from Mixed alpha olefin feeds	Wu et al. *(Exxonmobil Chemical Patents Inc., US)*	• Metallocene based catalyst is used for PAO production • PAO synthesis was carried out mixture of alpha olefins (C3 – C30) at different ratios at reaction temperature of 60 ^{o}C • Conversions ranging 84 - 94 wt% were reported with selectivity to lube ranging from 76 – 92 wt%.	Authors did not study the efficacy of the process in the presence of other hydrocarbons

S. No.	Title & Publication	Author	Major Key Findings	Gaps
14	Polyalphaolefins prepared using modified Salan catalyst compounds	Bruce et al. *(Exxonmobil Chemical Patents Inc.)*	• Zr based catalyst is reported • Different novel boron based activators are reported • Viscosity index up to 180 are reported • Experiments were conducted for pure alpha olefins	The effect of other hydrocarbons and impurities of refinery streams are not discussed
15	Method for making polyalphaolefins using aluminum halide catalyzed oligomerization of olefins	Gee et al. (*Chevron Phillips Chemical Company, US)*	• Lewis acid (AlCl3) catalyst based PAO synthesis is reported • Reactions were performed at 100 ^{o}C with the pure decene • Reaction kinetics were studied with various time intervals	Tested with pure alpha olefins. Effects of actual feed not discussed.

S. No.	Title & Publication	Author	Major Key Findings	Gaps
16	Method for manufacturing high viscosity polyalphaolefins using ionic liquid catalysts	Hope et al. *(Chevron Phillips Chemical Company, US)*	• Continuous process for manufacturing high viscosity poly alphaolefins sing ionic liquid catalysts was proposed. • Synthesized polyalphaolefins from pure dodecane	Authors did not test the oligomerization process with other alphaolefins and with refinery streams containing olefins.
17	The use of ionic liquids in the oligomerization of alkenes	Csaba et al. *(University of Pannonia, Hungary)*	• Ionic liquids are used as catalysts for alkene oligomerization • A good overview about various ionic liquids are reported • Ionic liquids based on AlCl3 are also reported	Model compound study
18	Synthesis of high viscosity index base stock and study on the lubricating properties	Wang et al. *(Dalian Maritime University, China)*	• Discussed on polymerization of 1-decene to PAO using ionic liquids ([Emim]Cl/$AlCl_3$) as a catalyst	Model compound study

S. No.	Title & Publication	Author	Major Key Findings	Gaps
			• Influence of following process parameters were studied Catalyst dosage, W: 1.5 – 17 wt% Rxn temperature, T: 40 – 120 ^oC Rxn time, t: 1 – 8 hr • Optimum conditions suggested are W: 3-6 wt%, t: 4h and T: based on target viscosity • Achieved maximum VI of 160 and yields >85% •	
19	Process for separating linear alpha olefins from saturated hydrocarbons	Black et al. *(Shell Internationale Research Maatschappij B.V.)*	• A process has been developed to separate linear alaphaolefins from a Fischer Tropsch stream containing alphaolefin, internal olefin and other hydrocarbons	The study is on FT Wax as feed stock

S. No.	Title & Publication	Author	Major Key Findings	Gaps
20	Process for separating linear internal olefins from branched internal olefins	Slaugh et al. *(Shell Oil Company, Texas)*	• Described the process scheme for the separation of linear internal olefins from branched internal olefins using linear poly aromatic compound	The study is on internal olefins, which are not good feed stock for PAOs.
21	Poly-a-olefin-based synthetic lubricants: a short review on various synthetic routes	Ray et al. *(BPCL, India)*	• Different types of catalysts are covered for the production of alphaolefins up to 2012 • Typical conditions and process parameters are included for important publications	Review article
22	Process Variables in the Manufacture of Polyalpha olefins	James et al. *(Edwin Copper Division, England)*	• Compared the performance of Ziegler type and cationic polymerization (BF_3) complexed catalysts for the polymerization of 1-decene to PAO over the rxn conditions of 30 – 85 °C and water / proponal as promoters	Model compound study

S. No.	Title & Publication	Author	Major Key Findings	Gaps
			• BF_3 based catalysts are more controllable and selective in product distribution compared to Ziegler type catalysts	
23	Kinetics of wax cracking for alpha olefin production	Worrell et al. *(Atlantic Richfield Go., Philadelphia)*	• Thermal cracking of paraffin wax was studied in isothermal bench scale and pilot unit reactors • Kinetics studies for the operating conditions of T: 538 -627 ^{o}C, Wax Partial pressure: 0.25 – 4 atm, t: 1.5 – 12 sec • Data well correlated with reaction order of 1.3 and E_a of 49.6 kcal/mole	High temperature process

S. No.	Title & Publication	Author	Major Key Findings	Gaps
24	Thermal cracking wax to normal alphaolefns	Perciful et al. *(Texaco Inc., Newyork)*	• Thermal cracking of wax was studied • Cracking temperature of 350 ^oC to 426 ^oC • Olefins were reported to be 12 %	Observed less olefins percentage on feed (wax) basis.
25	Treatment of Slack Wax by Thermal Cracking Process	Halim et al. *(University of Bhagdad)*	• Thermal cracking of slack wax was studied in continuous cracking unit • Recommended cracking temp is 500 ^oC and LHSV is 1.0 hr^{-1} • Maximum of 83 wt% conversion observed	Author didn’t discuss about the potential of LAO production

2.13 Summary & Research Objectives

i. Not much research work was found in identifying the alternate feed stocks. Few literatures were found on using wax as alternate feed stock. Thus in the proposed work, identification of low value feed stocks to bring down the cost of synthetic lubes is taken as one of the objectives.

ii. Most of the research is carried using model compounds like 1-hexene, 1-octene and 1-decene or mixture of model compounds and little information is available using actual feeds. Hence, the consequences of actual feed on the catalysts reported are less known.

    In the current study, development of synthetic lubes of required commercial properties using actual feed stocks, which are more representative, instead of model compounds, is taken up.

iii. Different catalysts systems studied in the literature are either metellocene, Ziegler Natta, Zirconium, Lewis acid or ionic liquid based catalysts, on whom the study of resistance to sulphur impurities in the feed stocks is not reported.

    In the current research work, catalyst systems, which are resistant to sulphur impurities are studied; as actual feed stocks contain many heteroatoms such as sulfur.

iv. Kinetics of the oligomerization reactions was also not much discussed in the literature.

    This work also is taken up as one of the objectives in the current research.

CHAPTER 3

IDENTIFICATION OF SUITABLE LOW VALUE FEEDSTOCKS

3.1 Overview

Literature indicates that the olefin rich streams with high linear alpha olefins (LAOs) [44, 45] or the streams with potential to transform into high LAOs are good building blocks for PAO production [46].

In this thesis chapter, to identify linear alpha olefins (LAOs) rich feed stocks various refinery and non-refinery based streams (total 7) were screened such as 1. FCC-light cut naphtha (FCC LCN), 2. FCC-heavy cut naphtha (FCC HCN), 3. Delayed coker naphtha (DCN) 4. Visbreaker naphtha (VBN) 5. Wax 1 (C20 to C43), 6. Wax 2 (C30 to C70) and 7. Waste polyethylene (PE).

Currently the above streams including Wax 1 and Wax 2 are routed to fuel pools; thus they fetch low margins. Hence, by converting these streams into high value products such as PAOs, refineries/petrochemical complexes would be able to enhance their gross refinery margins (GRM). However, based on the secondary unit and cracking conditions, olefins percentage, nature and carbon number can vary in the obtained cracked naphtha products

The streams 1 and 2 are products out of a catalytic cracking process while streams 3 and 4 are produced out of thermal cracking units. These 4 streams were analysed for their LAO content using PONA. Streams 5 to 7 are heavy hydrocarbon materials and thus they are not directly suitable as feed stock for PAO production. Thus they needed to be thermally cracked before being analysed for LAO content.

Detailed flow chart of the methodology followed in the current chapter is depicted in Figure 3.1. As shown in the figure, streams such as Wax and PE were subjected to fast pyrolysis before they were characterized using PONA techniques.

.

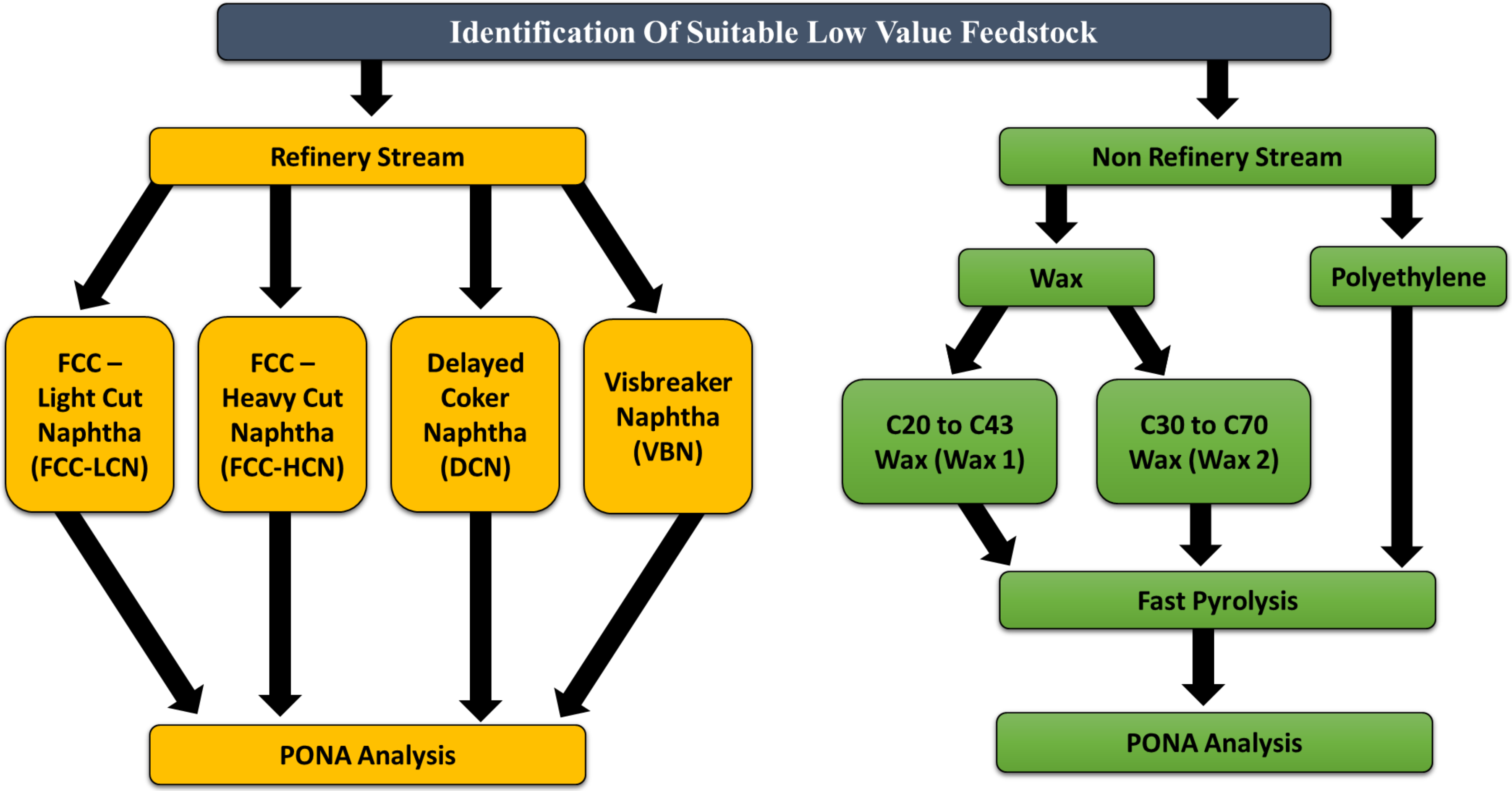

Figure 3.1: Flow chart of the study performed in the current chapter

3.2 Cracking Process Methods

In a refinery, cracking is performed by two methods detailed below:

Method 1: Thermal cracking

a) Cracking is facilitated by high temperature and without catalyst

b) Follows the radical pathway (Scheme illustrated in Figure 3.2

c) Isomerization is not possible

d) Leads to only alpha olefins production

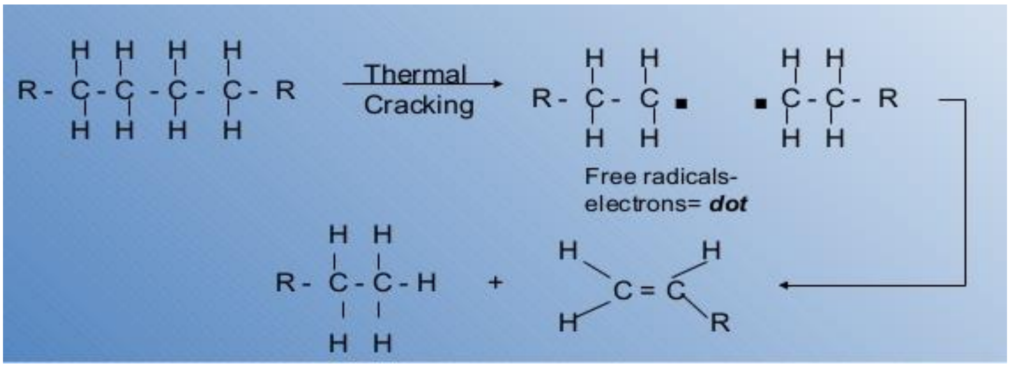

Figure 3.2: Thermal cracking – radical pathway

Method 2: Catalytic cracking

a) Cracking is facilitated by FCC catalyst at slightly low temperature

b) Follows the carbocation pathway

c) Isomerization possible

d) Leads to mainly internal olefins

3.3 Characterization of Refinery Streams (Streams 1 to 4)

Different refinery streams contain variable amounts of olefins with different carbon numbers. For synthesis of PAO, it is to be understood that carbon number of the feedstock has appreciable impact on the PAO properties [47, 48] and thus its value gradation. Thus, PONA analysis was performed on naphtha obtainable from different refinery streams mentioned below to quantify the olefin percentage and carbon number:

- FCC - low cut naphtha (FCC - LCN)
- FCC - high cut naphtha (FCC - HCN)

- Delayed coker naptha (DCN)
- Visbreaker naphtha (VBN)

Results of PONA for the streams mentioned are shown in Table 3.1. It can be observed that FCC-LCN contains maximum amount of olefins among the studied naphtha, up to 55%, mainly as C5 and C6. FCC-HCN contains up to 28.5% olefins with maximum contribution from C6-C8. DCN contains up to 30% olefins with maximum contribution from C8 and C9. VBN contains up to 37% olefins with carbon number spread over C4-C10. Thus, it can be confirmed from the PONA analysis that distribution of olefins, *i.e.*, carbon numbers and the corresponding olefin percentage, is very specific to the particular naphtha selected.

Table 3.1: Summary of PONA analysis – specifically the olefin content

Carbon number	**% Olefin from various refinery streams**			
	FCC-LCN	**FCC-HCN**	**DCN**	**VBN**
C4	1.7	0.13	0.02	2.25
C5	28.7	1.42	0.06	5.31
C6	19.7	10.63	0.52	7.61
C7	4.1	8.95	3.64	7.05
C8	0.5	6.97	11.92	7.7
C9	-	0.27	10.5	5.23
C10+	-	0.06	2.91	1.85
Total Olefin %	**54.7**	**28.43**	**29.57**	**37.0**

As per the literature reports, the PAO production requires LAOs with carbon number ranging between C8 and C14. The highest fraction of olefins in this carbon range is for naphtha from delayed coker. It is also reported that internal olefins do not yield PAOs. To identify the type of olefins in the feed streams 1H NMR analyses were carried out. NMR spectra obtained for LAO from FCC-HCN, FCC-LCN and DCN are illustrated in Figures 3.3 to 3.5, respectively.

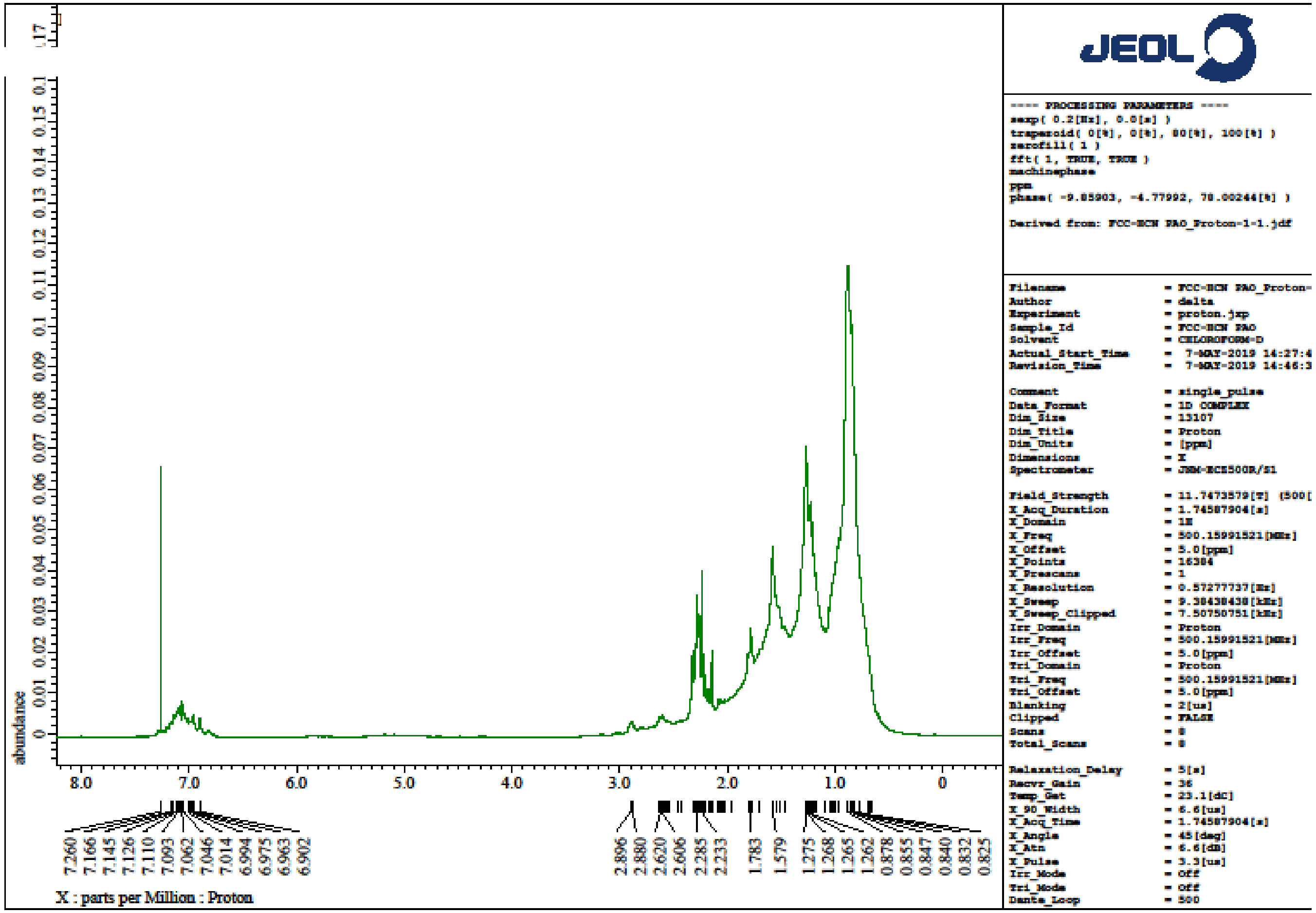

```
---- PROCESSING PARAMETERS ----
sexp( 0.2[Hz], 0.0[s] )
trapezoid( 0[%], 0[%], 80[%], 100[%] )
zerofill( 1 )
fft( 1, TRUE, TRUE )
machinephase
ppm
phase( -9.85903, -4.77992, 78.00244[%] )

Derived from: FCC-HCN PAO_Proton-1-1.jdf

Filename                = FCC-HCN PAO_Proton-
Author                  = delta
Experiment              = proton.jxp
Sample_Id               = FCC-HCN PAO
Solvent                 = CHLOROFORM-D
Actual_Start_Time       =  7-MAY-2019 14:27:4
Revision_Time           =  7-MAY-2019 14:46:3

Comment                 = single_pulse
Data_Format             = 1D COMPLEX
Dim_Size                = 13107
Dim_Title               = Proton
Dim_Units               = [ppm]
Dimensions              = X
Spectrometer            = JNM-ECZ500R/S1

Field_Strength          = 11.7473579[T] (500[
X_Acq_Duration          = 1.74587904[s]
X_Domain                = 1H
X_Freq                  = 500.15991521[MHz]
X_Offset                = 5.0[ppm]
X_Points                = 16384
X_Prescans              = 1
X_Resolution            = 0.57277737[Hz]
X_Sweep                 = 9.38438438[kHz]
X_Sweep_Clipped         = 7.50750751[kHz]
Irr_Domain              = Proton
Irr_Freq                = 500.15991521[MHz]
Irr_Offset              = 5.0[ppm]
Tri_Domain              = Proton
Tri_Freq                = 500.15991521[MHz]
Tri_Offset              = 5.0[ppm]
Blanking                = 2[us]
Clipped                 = FALSE
Scans                   = 8
Total_Scans             = 8

Relaxation_Delay        = 5[s]
Recvr_Gain              = 36
Temp_Get                = 23.1[dC]
X_90_Width              = 6.6[us]
X_Acq_Time              = 1.74587904[s]
X_Angle                 = 45[deg]
X_Atn                   = 6.6[dB]
X_Pulse                 = 3.3[us]
Irr_Mode                = Off
Tri_Mode                = Off
Dante_Loop              = 500
```

Figure 3.3: 1H-NMR spectra of FCC-HCN

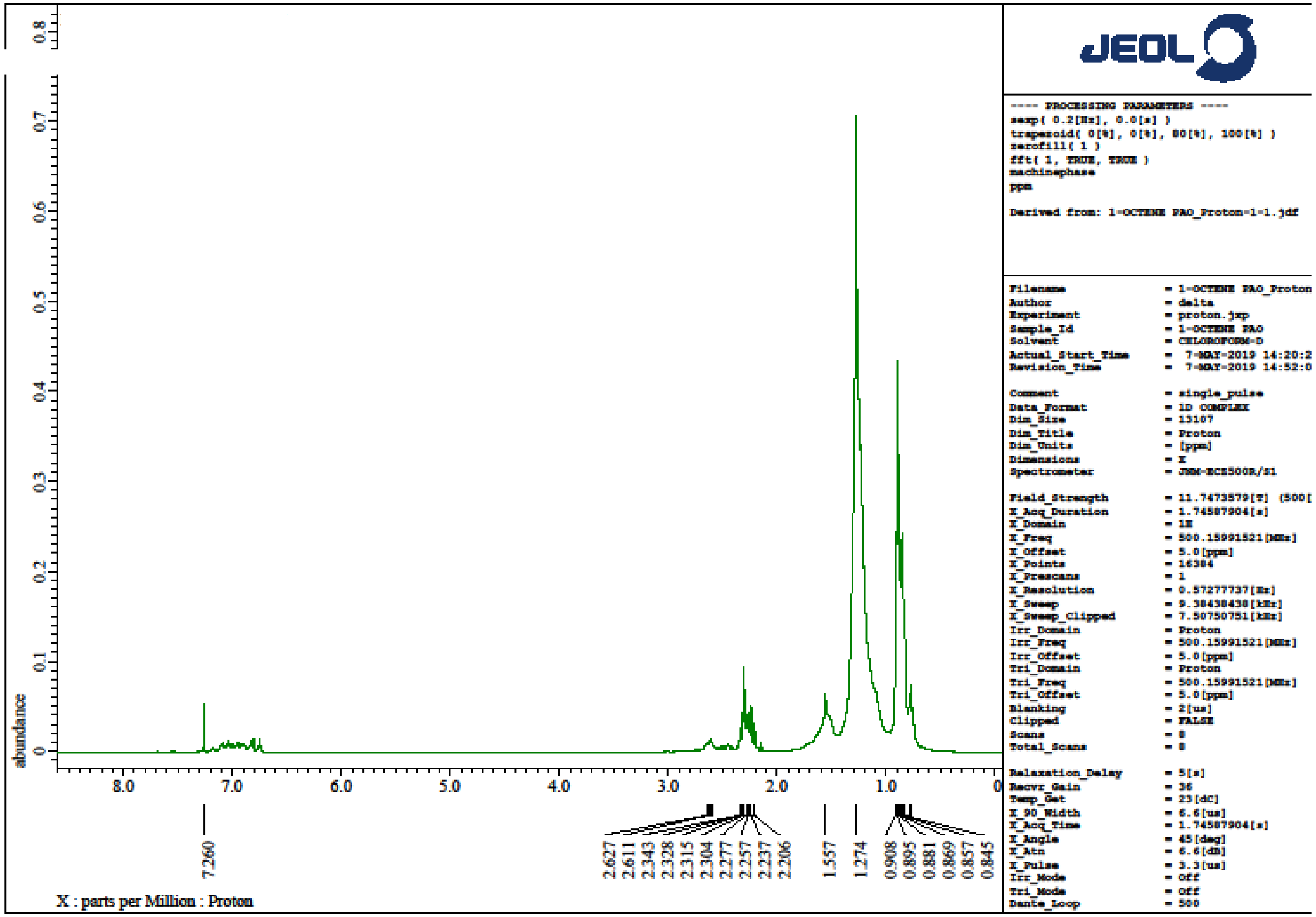

```
---- PROCESSING PARAMETERS ----
sexp( 0.2[Hz], 0.0[s] )
trapezoid( 0[%], 0[%], 80[%], 100[%] )
zerofill( 1 )
fft( 1, TRUE, TRUE )
machinephase
ppm

Derived from: 1-OCTENE PAO_Proton-1-1.jdf
```

```
Filename              = 1-OCTENE PAO_Proton
Author                = delta
Experiment            = proton.jxp
Sample_Id             = 1-OCTENE PAO
Solvent               = CHLOROFORM-D
Actual_Start_Time     =  7-MAY-2019 14:20:2
Revision_Time         =  7-MAY-2019 14:52:0

Comment               = single_pulse
Data_Format           = 1D COMPLEX
Dim_Size              = 13107
Dim_Title             = Proton
Dim_Units             = [ppm]
Dimensions            = X
Spectrometer          = JNM-ECS500R/S1

Field_Strength        = 11.7473579[T] (500[
X_Acq_Duration        = 1.74587904[s]
X_Domain              = 1H
X_Freq                = 500.15991521[MHz]
X_Offset              = 5.0[ppm]
X_Points              = 16384
X_Prescans            = 1
X_Resolution          = 0.57277737[Hz]
X_Sweep               = 9.38438438[kHz]
X_Sweep_Clipped       = 7.50750751[kHz]
Irr_Domain            = Proton
Irr_Freq              = 500.15991521[MHz]
Irr_Offset            = 5.0[ppm]
Tri_Domain            = Proton
Tri_Freq              = 500.15991521[MHz]
Tri_Offset            = 5.0[ppm]
Blanking              = 2[us]
Clipped               = FALSE
Scans                 = 8
Total_Scans           = 8

Relaxation_Delay      = 5[s]
Recvr_Gain            = 36
Temp_Get              = 23[dC]
X_90_Width            = 6.6[us]
X_Acq_Time            = 1.74587904[s]
X_Angle               = 45[deg]
X_Atn                 = 6.6[dB]
X_Pulse               = 3.3[us]
Irr_Mode              = Off
Tri_Mode              = Off
Dante_Loop            = 500
```

Figure 3.4: 1H-NMR spectra of FCC-LCN

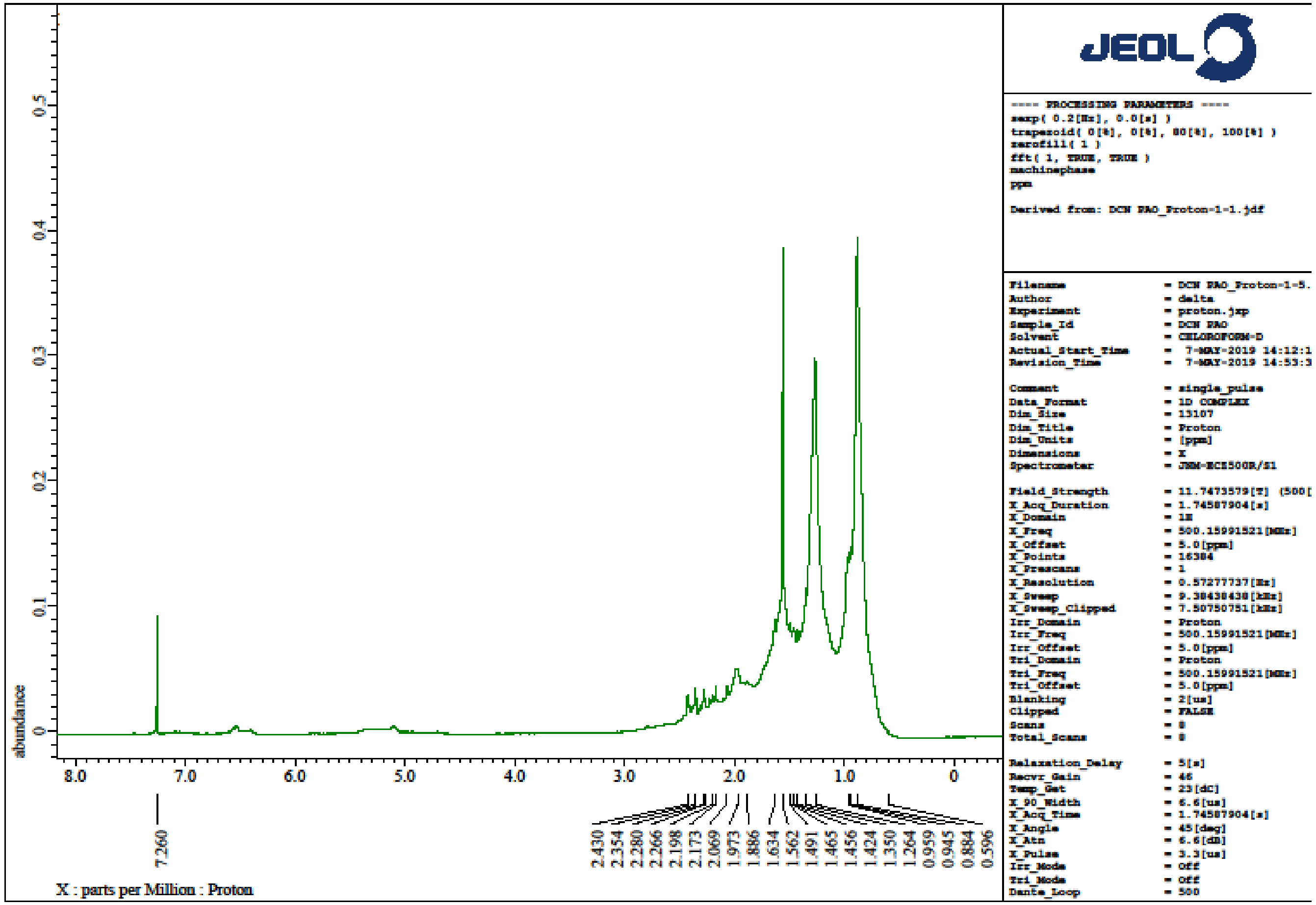

```
---- PROCESSING PARAMETERS ----
sexp( 0.2[Hz], 0.0[s] )
trapezoid( 0[%], 0[%], 80[%], 100[%] )
zerofill( 1 )
fft( 1, TRUE, TRUE )
machinephase
ppm

Derived from: DCN FAO_Proton-1-1.jdf
```

```
Filename                  = DCN FAO_Proton-1-5.
Author                    = delta
Experiment                = proton.jxp
Sample_Id                 = DCN FAO
Solvent                   = CHLOROFORM-D
Actual_Start_Time         =  7-MAY-2019 14:12:1
Revision_Time             =  7-MAY-2019 14:53:3

Comment                   = single_pulse
Data_Format               = 1D COMPLEX
Dim_Size                  = 13107
Dim_Title                 = Proton
Dim_Units                 = [ppm]
Dimensions                = X
Spectrometer              = JNM-ECZ500R/S1

Field_Strength            = 11.7473579[T] (500[
X_Acq_Duration            = 1.74587904[s]
X_Domain                  = 1H
X_Freq                    = 500.15991521[MHz]
X_Offset                  = 5.0[ppm]
X_Points                  = 16384
X_Prescans                = 1
X_Resolution              = 0.57277737[Hz]
X_Sweep                   = 9.38438438[kHz]
X_Sweep_Clipped           = 7.50750751[kHz]
Irr_Domain                = Proton
Irr_Freq                  = 500.15991521[MHz]
Irr_Offset                = 5.0[ppm]
Tri_Domain                = Proton
Tri_Freq                  = 500.15991521[MHz]
Tri_Offset                = 5.0[ppm]
Blanking                  = 2[us]
Clipped                   = FALSE
Scans                     = 8
Total_Scans               = 8

Relaxation_Delay          = 5[s]
Recvr_Gain                = 46
Temp_Get                  = 23[dC]
X_90_Width                = 6.6[us]
X_Acq_Time                = 1.74587904[s]
X_Angle                   = 45[deg]
X_Atn                     = 6.6[dB]
X_Pulse                   = 3.3[us]
Irr_Mode                  = Off
Tri_Mode                  = Off
Dante_Loop                = 500
```

Figure 3.5: 1H-NMR spectra of delayed coker naphtha

In the 1 H NMR spectra, two types of signals can be observed in the ratio of 1:2. A doublet of doublet (dd) peak at ~5 ppm corresponds to the C1 protons (CH2=CH), whereas the multiplet at ~6 ppm corresponds to C2 H of the alpha olefins (CH2=CH). The ratio is 2:1 as expected for alpha olefins. In the case of catalytic cracking streams, a multiplet at 5.5 ppm observed corresponds to the internal olefins.

3.4 Pyrolysis of Non-Refinery Streams (Streams 5 to 7)

Currently, due to the market demand of petrochemical and polymers, many new petrochemical units are being set-up. These units are majorly being integrated with existing refinery. During start-up of these units, there are lot of waste plastics generated, such as polypropylene, polyethylene and/or their copolymer. Thermal cracking of the obtained waste polyethylene [49] can be an attractive alternate route to obtain linear alpha olefins.

Similarly, wax streams (Wax 1 and Wax 2) produced in the making of conventional Group-I base oils are routed to a catalytic conversion unit such as FCC, producing internal olefinic product. Production of LAOs from waxes can be a definite step towards value addition [50, 51, 52].

Thermal cracking follows the homolytic bond fission to generate the radical intermediates, which cannot rearrange and lead to the formation of alpha olefins. However, the product distribution of thermal cracking is dependent on feed, temperature and residence time.

The traditional approach to obtain the “optimal parameters” for the required LAO synthesis, in batch or continuous process, involves the reactions at different temperatures with various feed stocks in the quantities of ∼100 g scale and the separation of the fractions for speciation analysis through GC-MS. In order to avoid the large sample and time-consuming process, development of alternate quick and reliable analytical method to obtain the feed/temperature product distribution relation in short time and with low sample quantities is desirable.

In current study, the pyrolysis system coupled with the gas chromatography/mass spectrometry (Py–GC/MS) has been shown to be an excellent analytical tool to obtain the detailed product distribution of fast pyrolysis of heavy petroleum feed stock such as Wax 1 and Wax 2, and waste plastics with low quantity of feed in very short time.

3.4.1 Characterization of Non-Refinery streams

The physical characteristics of waxes are given in Table 3.2, in which Wax 1 carbon chain length is in the rage of C20 to C43 (determined in the range 5% to 95% using simulated distillation (simdis) recovery analysis method as per ASTM D7169) and Wax 2 in the range of C30 to C70 (determined in the range 5% to 95% using simulated distillation (simdis) recovery analysis method as per ASTM D7169).

Table 3.2: Physical characteristics of waxes

Simdis recovery	Wax-1 Temperature (°C)	Boiling point of carbon number	Wax-2 Temperature (°C)	Boiling point of carbon number
IBP	291	C19	379	C24
5	352	C20	335	C30
25	392	C24	541	C43
50	421	C27	581	C51
75	455	C30	625	C65
95	541	C43	680	C70
FBP	678	C70	723	> C70

3.4.2 Fast Pyrolysis experiments with Py-GC-MS

The pyrolysis system coupled with the gas chromatography/mass spectrometry (Py–GC/MS) has been shown to be an excellent analytical tool to obtain the detailed product distribution of fast pyrolysis of heavy petroleum feed stock, waste plastics and biomass with low quantity of feed in very short time. The technology can also be extended for catalytic screening for various cracking experiments, with a variation in the pyrolysis design to accommodate catalyst, feed and required gases at micro level.

The Gas Chromatography/Mass Spectrometry (GC/MS) instrument separates chemical components based on boiling point and polarity. The mass spectrometry coupled with the GC identifies the components at a molecular level. It is one of the most accurate tools for hydrocarbon samples. The pyrolyzer acts as inlet for GC in the present studies. The samples were subjected to fast pyrolysis at very high temperatures for short time and the corresponding cracked products were sent to GC for separation. Py-GC-MS equipment provides the feed pyrolysis and product identification in a single run.

The fast pyrolysis is performed at 600–800°C and the product distribution of distillates up to C20 are analysed by GC-MS technique. The Gas Chromatography/Mass Spectrometry (GC/MS) instrument separates chemical components based on boiling point and polarity. The mass spectrometry coupled with the GC identifies the components at a molecular level. It is one of the most accurate tools for hydrocarbon samples. The pyrolyzer acts as inlet for GC in the present studies. The samples are subjected to fast pyrolysis at very high temperatures for short time and the corresponding cracked products are sent to GC for separation. Photo of Py-GC-MS equipment is shown in Figure 3.6; whereas, the typical configuration of the Py-GC-MS is demonstrated in Figure 3.7.

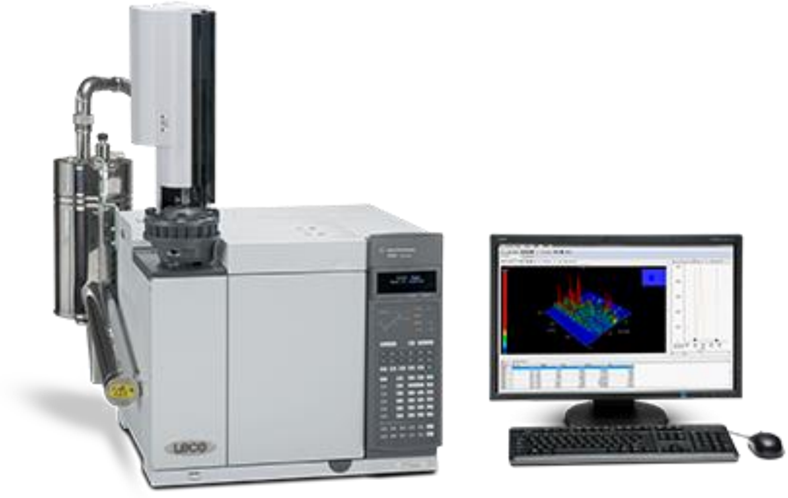

Figure 3.6: Py-GC-MS equipment

3.4.3 Pyrolyzer conditions

Pyrolysis studies were performed on Frontier lab Py3030 S model. In the pyrolyzer, the heating rate is very fast and is uncontrollable. Typically, it is less than one minute. The flowrate of He gas in the Pyrolyzer post heating time was maintained at 1.2 mL/minute.

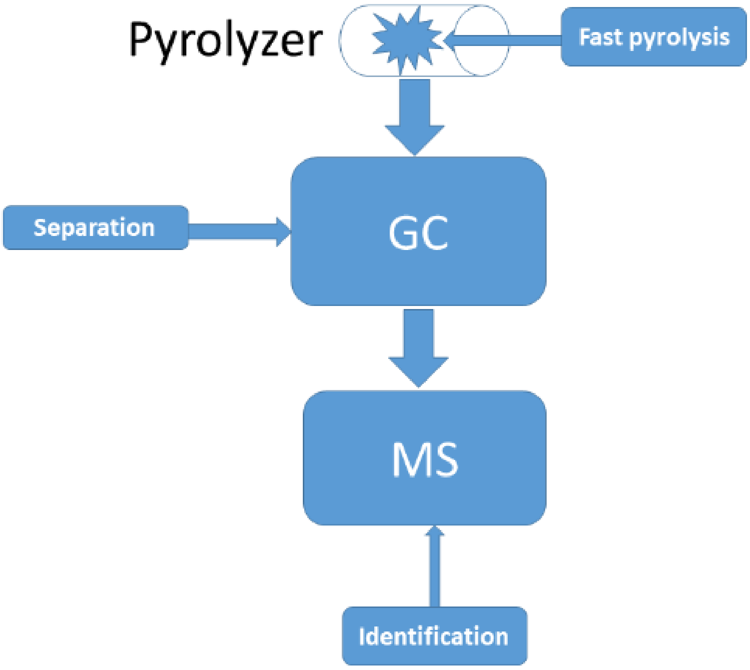

Figure 3.7: Configuration of a pyrolyzer

3.4.4 GC-MS analysis conditions

Feed: Wax 1/Wax 2/PE in pyrolyzer unit

Pyrolysis temperature: 600 ℃ to 800 ℃

Column details:

- Name: DB-624
- Length: 30m
- Diameter: 0.25
- Film Thickness: 1.4

Split/Split less Inlet conditions:

- Initial Temperature: 250°C
- Flow Rate: 1.2ml/min
- Split Ratio: 100

Oven Conditions:

- Initial Temperature: 40°C
- Initial Hold time: 2 min
- Ramp details are provided in Table 3.3

Heating ramp rate used in the study is detailed in Table 3.3.

Table 3.3: Heating ramp details

Parameter	Step 1	Step 2
Heating rate (°C / min)	5	5
Temperature (°C)	200	230
Hold time (min)	10	10

The feed and temperature dependent LAOs product distribution was obtained by conducting fast pyrolysis of structurally similar long-chain paraffin wax and PE. The polyethylene (PE) is waste LDPE, typically used bag materials.

3.4.5 Results and discussions

A typical GC/MS plot obtained after sample analysis is illustrated in Figure 3.8 (GC/MS graph obtained for PE sample at 600°C); wherein, it uses combination of gas-chromatography and mass spectrometry to determine various components within the specimen.

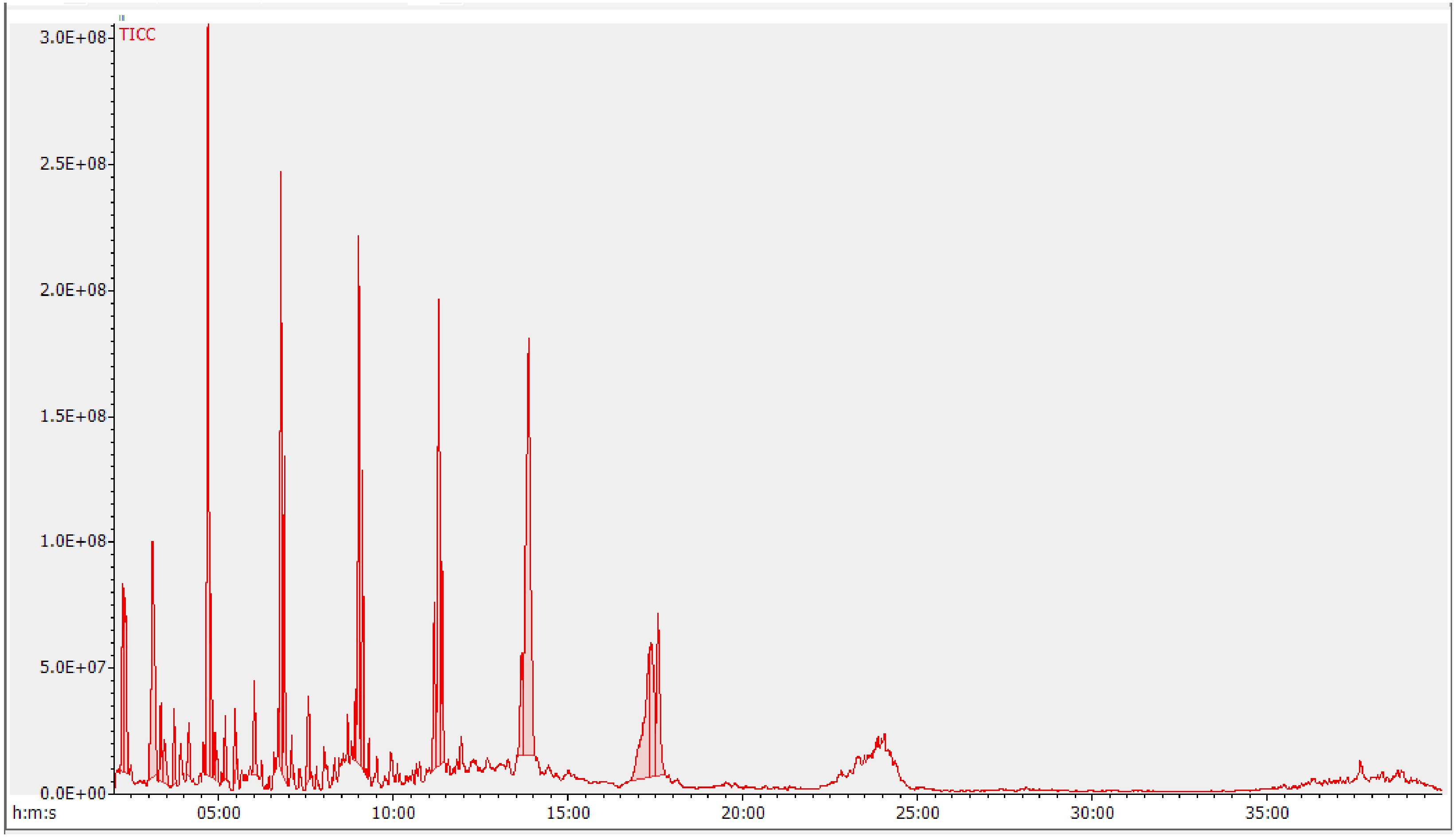

Figure 3.8: A representative GC/MS trace after fast pyrolysis of PE at 600 °C

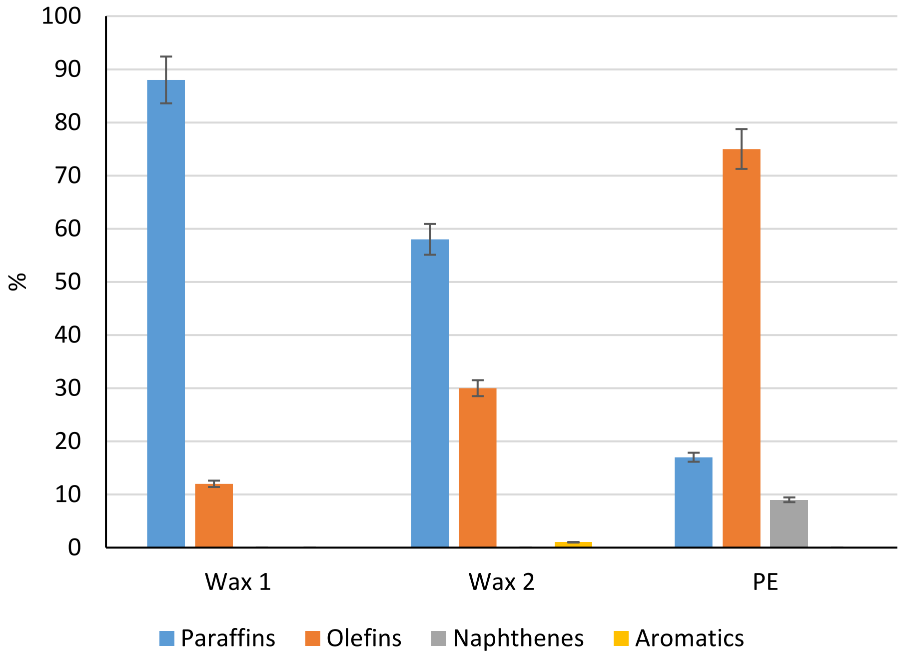

Figure 3.9: Effect of Feed type

The effect of feed type at constant temperature (600 °C) is given in Figure 3.9, which shows the percentage of olefin in the product increases with chain length or molecular weight of the feed, PE>Wax 2>Wax 1. This trend is attributed to the fact that longer chains lead to formation of more free radicals due to higher probability of bond scission kinetics. Whereas, for paraffin, naphthene and aromatics content showed following trend in values: Wax 1>Wax 2>PE, PE>Wax 1=Wax 2, and Wax 2>Wax 1 = PE. Furthermore, the naphthenic percentage is also increased in the order of PE> Wax 2>Wax 1, indicating the cyclic carbon chain formation tendency is higher with increase in carbon chain length.

The mechanism for the formation of naphthenic compounds follows either recombination of bi-radical intermediate or intramolecular cyclization involving an alkene radical containing intermediate. The cyclization can occur from 1–5, 1–6 and 1–7 position through transit state of five, six or seven membered ring containing naphthenes. As the PE can form the bi-radical due to simultaneous cracking at multiple position, the naphthenic percentage is high.

The mechanism for formation of aromatics is via cyclization and sequential dehydrogenation reactions.

Thus, it can be concluded that at GC temperature of 600^{o}C, PE provides highest olefin content, Wax 1 gives highest paraffin content; whereas, Wax 2 gives moderate amount of olefin and higher amount of paraffin. Aromatic content was observed only in Wax 2. Similarly, naphthene content was detected only in PE. To understand the effect of varied temperature of GC on the PONA content, same study was performed at temperatures of 600, 650, 700, 750 and 800 ^{o}C, and discussed in further sections.

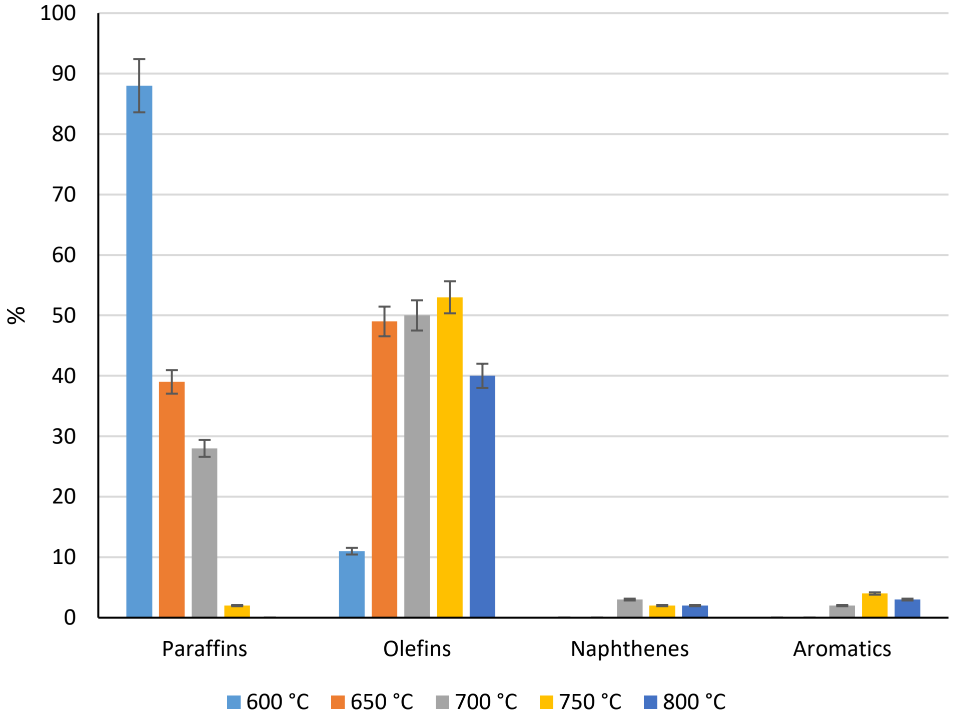

Figure 3.10.a: PONA (paraffin, olefin, naphthene and aromatics) percentage in fast pyrolysis of Wax 1 at different temperatures (600 to 800 ℃)

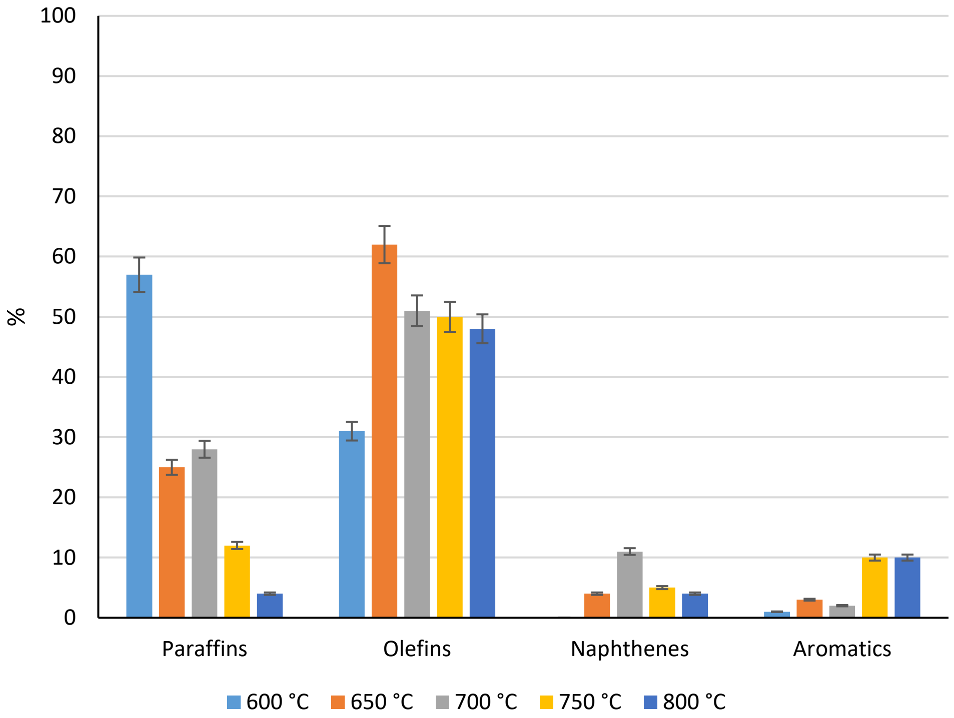

Fig 3.10.b: PONA (paraffin, olefin, naphthene and aromatics) percentage in fast pyrolysis of Wax 2 at different temperatures (600 to 800 °C)

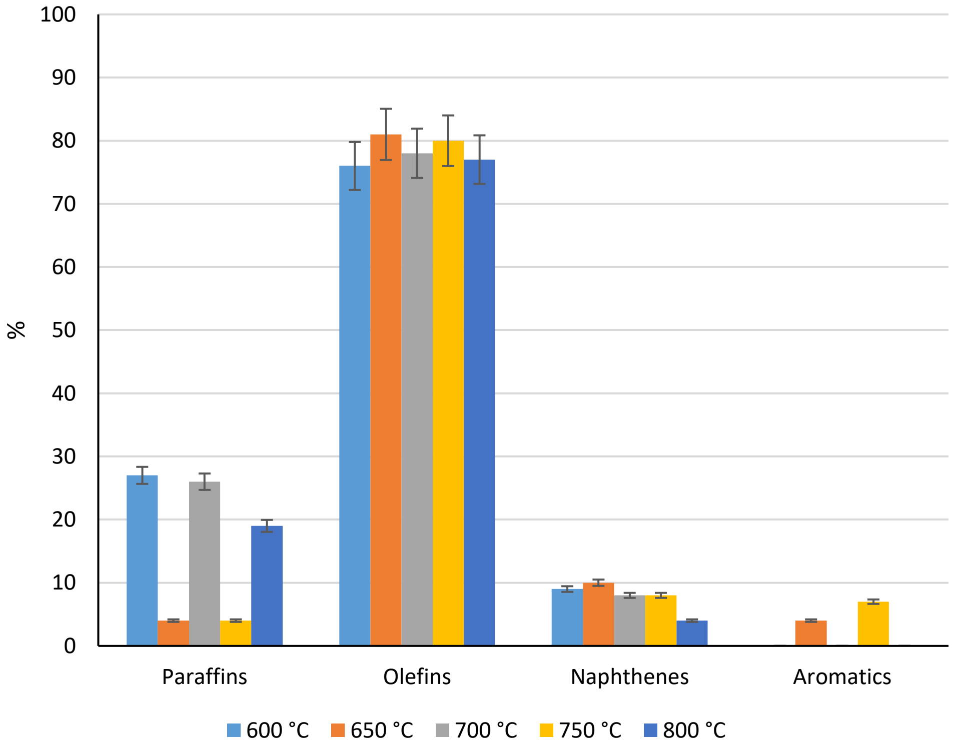

Figure 3.10.c: PONA (paraffin, olefin, naphthene and aromatics) percentage in fast pyrolysis of PE at different temperatures (600 to 800 °C)

The PONA (paraffin, olefin, naphthene and aromatics) distribution in Fast Pyrolysis of Wax 1, Wax 2 and polyethylene (PE) at different temperatures (600 to 800 °C) are given in Figures 3.10.a to 3.10.c. Observations are reported in Table 3.4:

Table 3.4: Trends in the values of PONA at different pyrolysis temperatures for Wax 1, Wax 2 and PE

Material in GC/MS	Trend with increase in pyrolysis temperature			
	Paraffins	Olefins	Naphthalenes	Aromatics
Wax 1	⬇	⬆	▼	▲
Wax 2	⬇	⬆	▼	▲
PE	↓	⬌	▼	▲

⬇ ⬆ = Appreciable increase or decrease

↓ ↑ = Moderate increase or decrease

▼ ▲ = Slight increase or decrease

In the case of lighter Wax 1, as it can be seen from the Figure 3.10.a, with increase in the temperature from 600 to 750 °C, there is an increase in the olefin percentage. However further increase in the temperature to 800 °C resulted a decrease in the olefin percentage, which may be due to side reactions. In the case of wax 2, the optimal temperature for olefins is 650 °C and with an increase in the pyrolysis temperature to 800 °C, the naphthenic and aromatic percentage is increased. It is interesting to note that the PONA distribution in the fast pyrolysis of PE remains same in the range 600 to 800 °C, even though the different components of olefins are varied.

Detailed analysis of olefins content in the pyrolyzed Wax 1, Wax 2 and PE, obtained after pyrolysis at different temperatures, is illustrated in Figure 3.11.

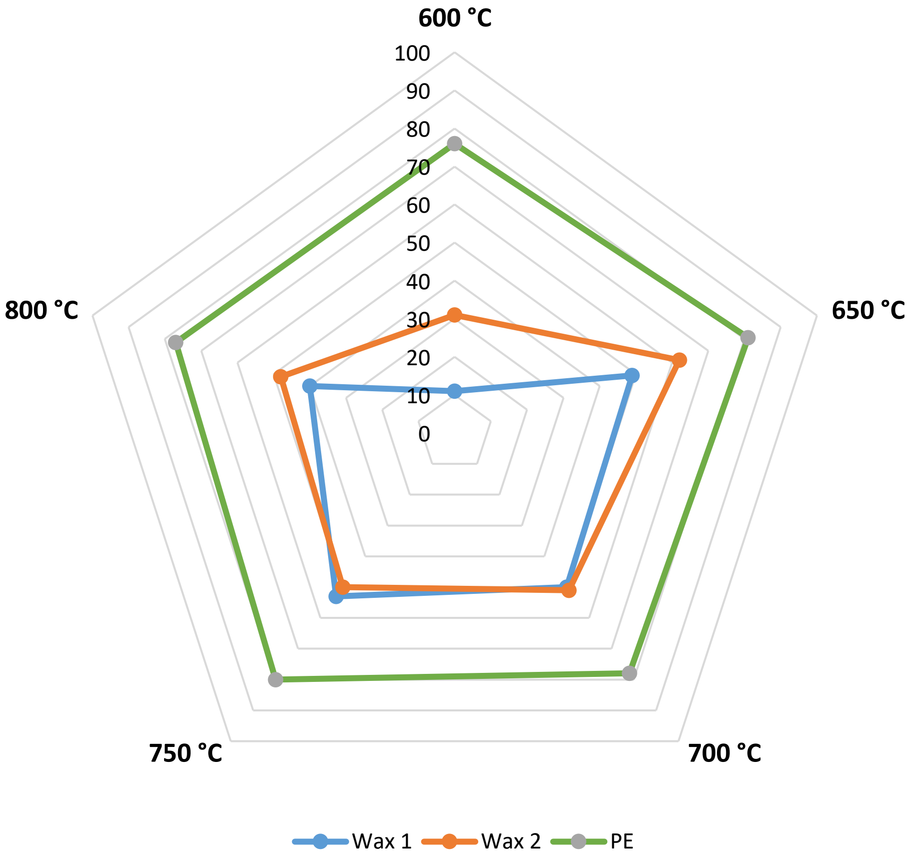

Figure 3.11: Comparison of percentage olefin obtained after fast pyrolysis of Wax 1, Wax 2 and PE at varied pyrolysis temperatures

From Figure 3.11 it can be observed that PE provides highest amounts of olefins at all range of pyrolysis temperatures followed by Wax 2; whereas, Wax 1 gives least amount olefins of the three. PE provides about 75 to 80% olefin content in all the temperature ranges; while, for Wax 2 and Wax 1 provides highest amounts, ~55% and 40% respectively, at 650 ^{o}C. This again corroborates our earlier discussion that longer the feed carbon chain length lower the optimal temperature and higher the olefin yield.

The olefins of the pyrolysis product are further classified into linear α-olefins (LAO), dienes and cyclic olefins (including cyclic dienes). The optimal temperature required for higher LAO percentage in fast pyrolysis is dependent on feed carbon length. The optimal temperature for Wax 1 is 700°C, Wax 2 is 650°C and polyethylene is 600°C. The longer the feed carbon chain length lower the optimal temperature. In chemical transformations of alpha olefins to various applications (for instance lubricants, surfactants etc.), the dienes and cyclic olefins potentially undergo side reactions and leads to complications. Hence, it is desirable to limit the dienes and cyclic olefins to the minimum possible level. Olefins distribution is presented in Figures 3.12.a, 3.12.b, 3.12.c

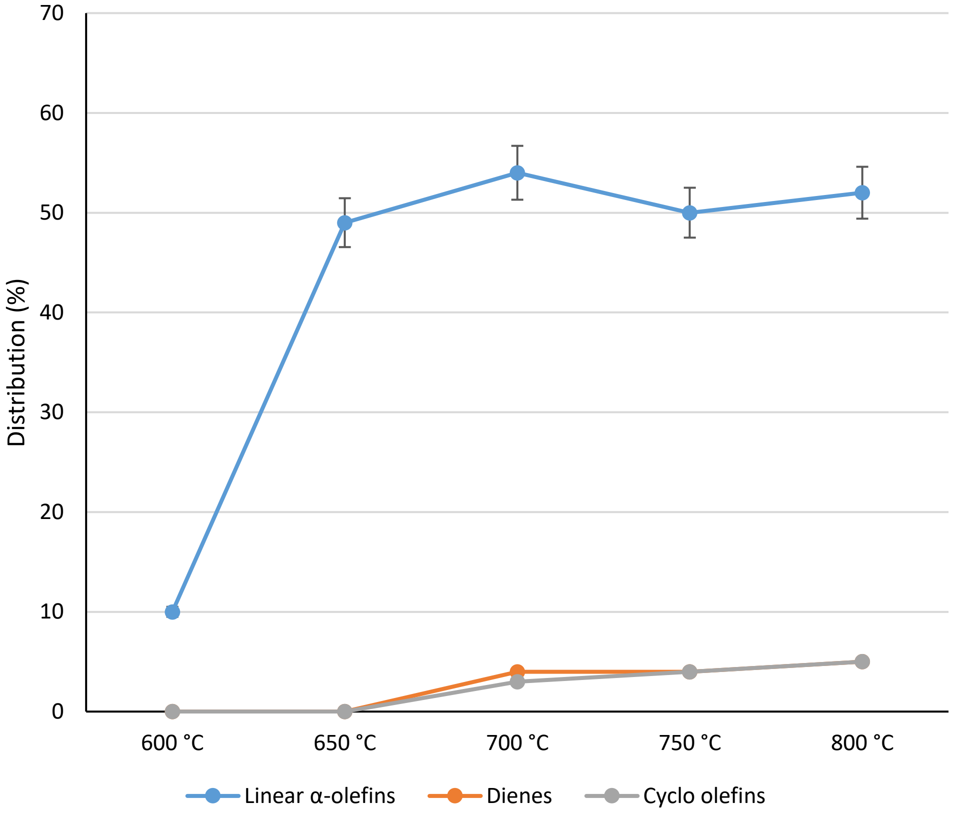

Figure 3.12.a: Olefin percentage in fast pyrolysis of Wax 1

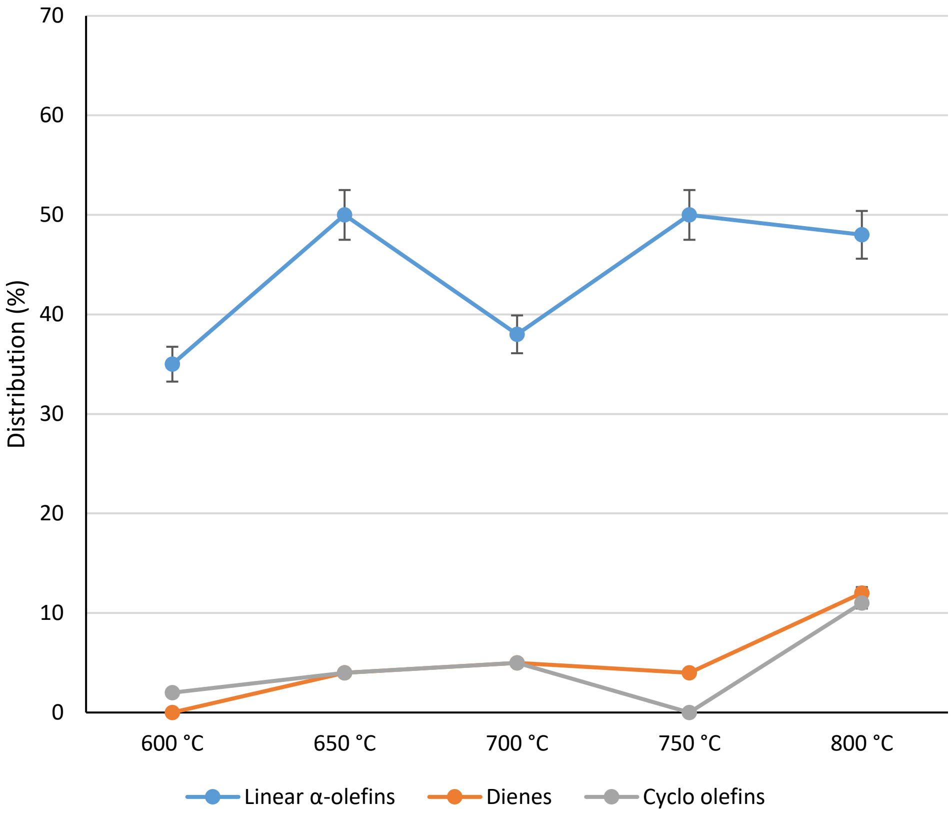

Figure 3.12.b: Olefin percentage in fast pyrolysis of Wax 2

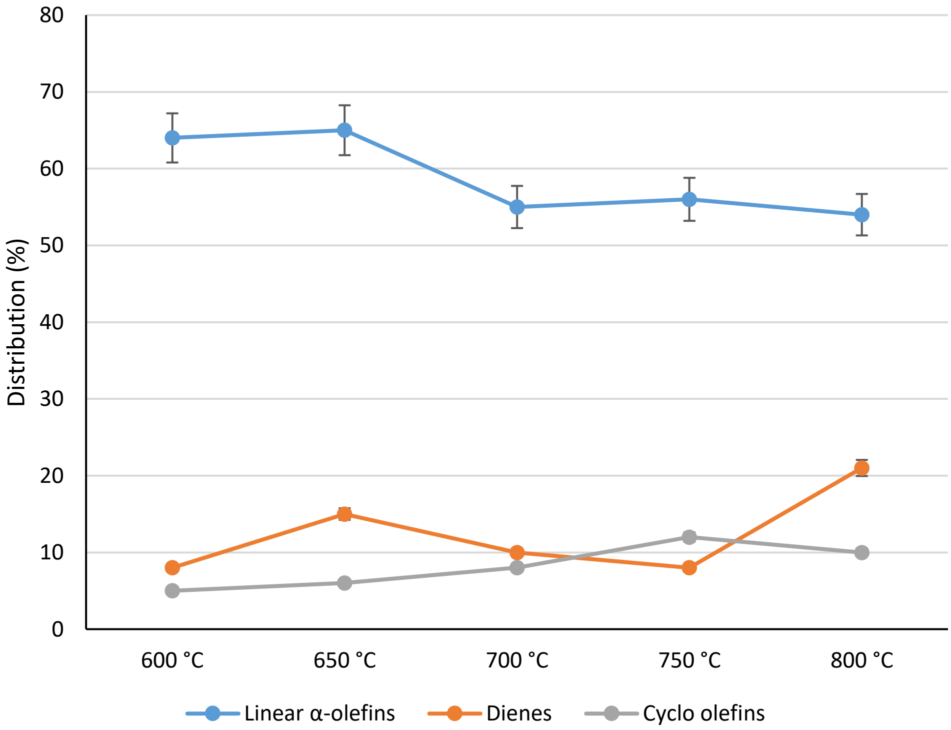

Figure 3.12.c: Olefin percentage in fast pyrolysis of PE

The carbon wise distributions of LAO from fast pyrolysis is given in Figure 3.13.a-3.13.c. As mentioned earlier, in the case of feed wax1, the cracking at 600 °C is minimum and at 700 to 800 °C, the relative percentage of LAOs from C5 to C14 is varied in the range of 4–6%. In the case of wax-2, the relative percentage of LAOs from C5 to C14 is varied in the range of 4–7%. In the case of poly ethylene, the ratio of 1-hexene (10 to 12%) and 1- decene (15 to 20%) was found to be higher at all the temperatures, whereas the reaming olefins varied in the range of 6 to 8%. One of the important feature of the LAO distribution pattern is the increase in lighter LAO percentage (< C6) with an increase in carbon chain of the feed. Furthermore, pyrolysis of PE fractions did not show LAOs of carbon numbers C12 and above. It can be explained by the fact the multiple cracking throughout the polymer chain, led to the smaller fragments. The longer the feed is, higher the smaller LAOs percentage (C5 and C6) and lower the higher LAOs (>C12) percentage.

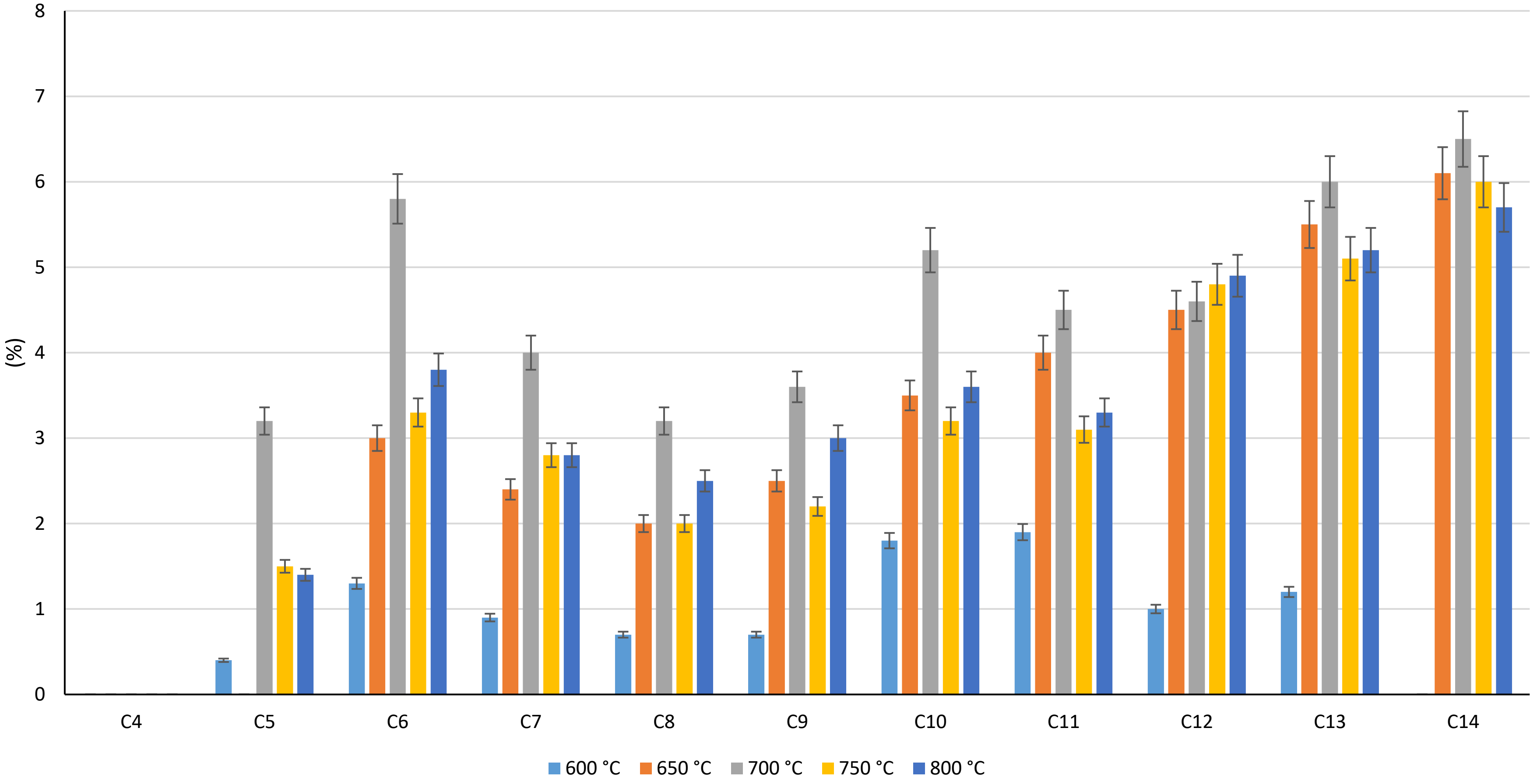

Figure 3.13.a: Carbon wise distribution of LAO obtained from Wax 1

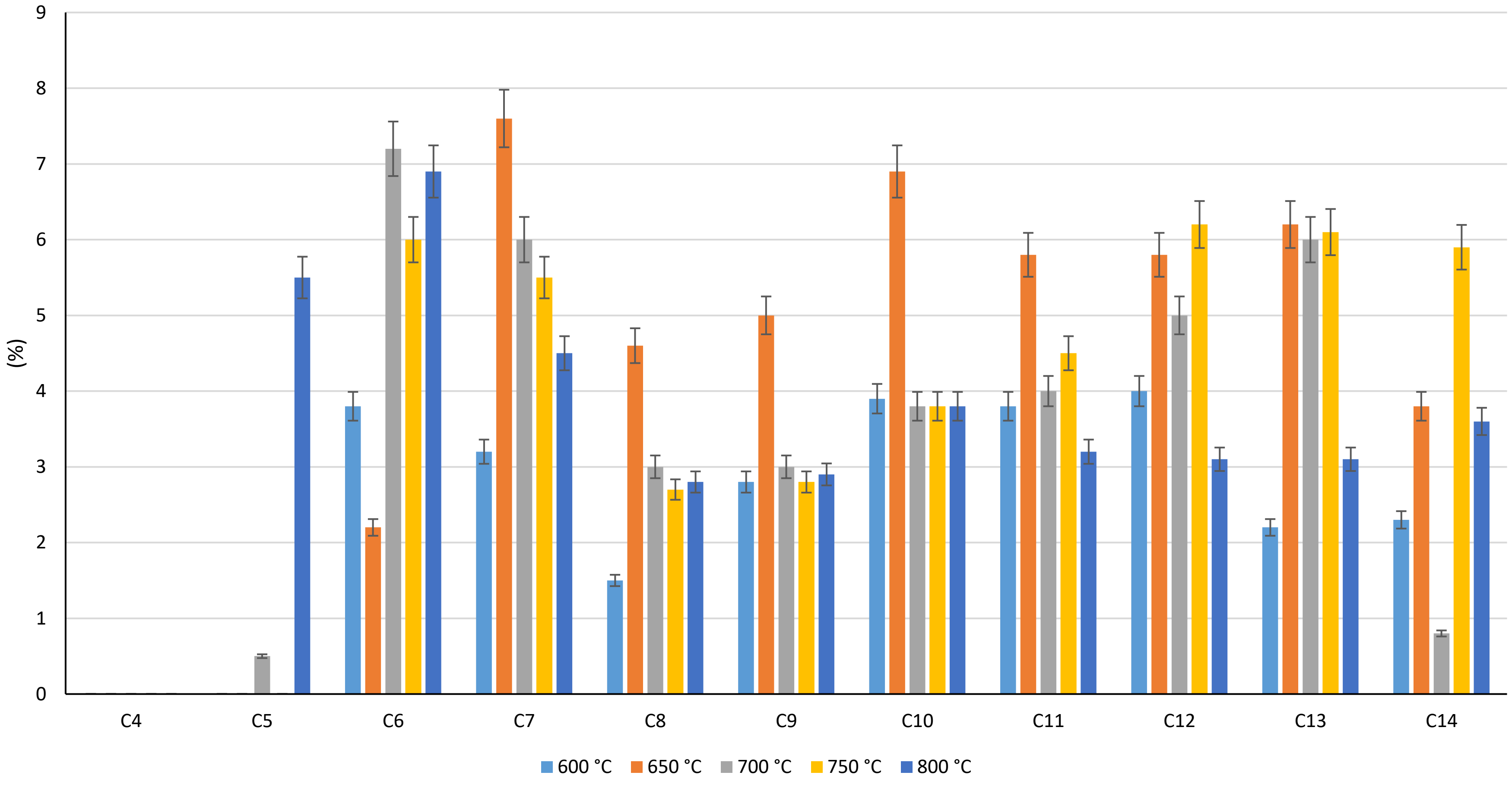

Figure 3.13.b: Carbon wise distribution of LAO obtained from Wax 2

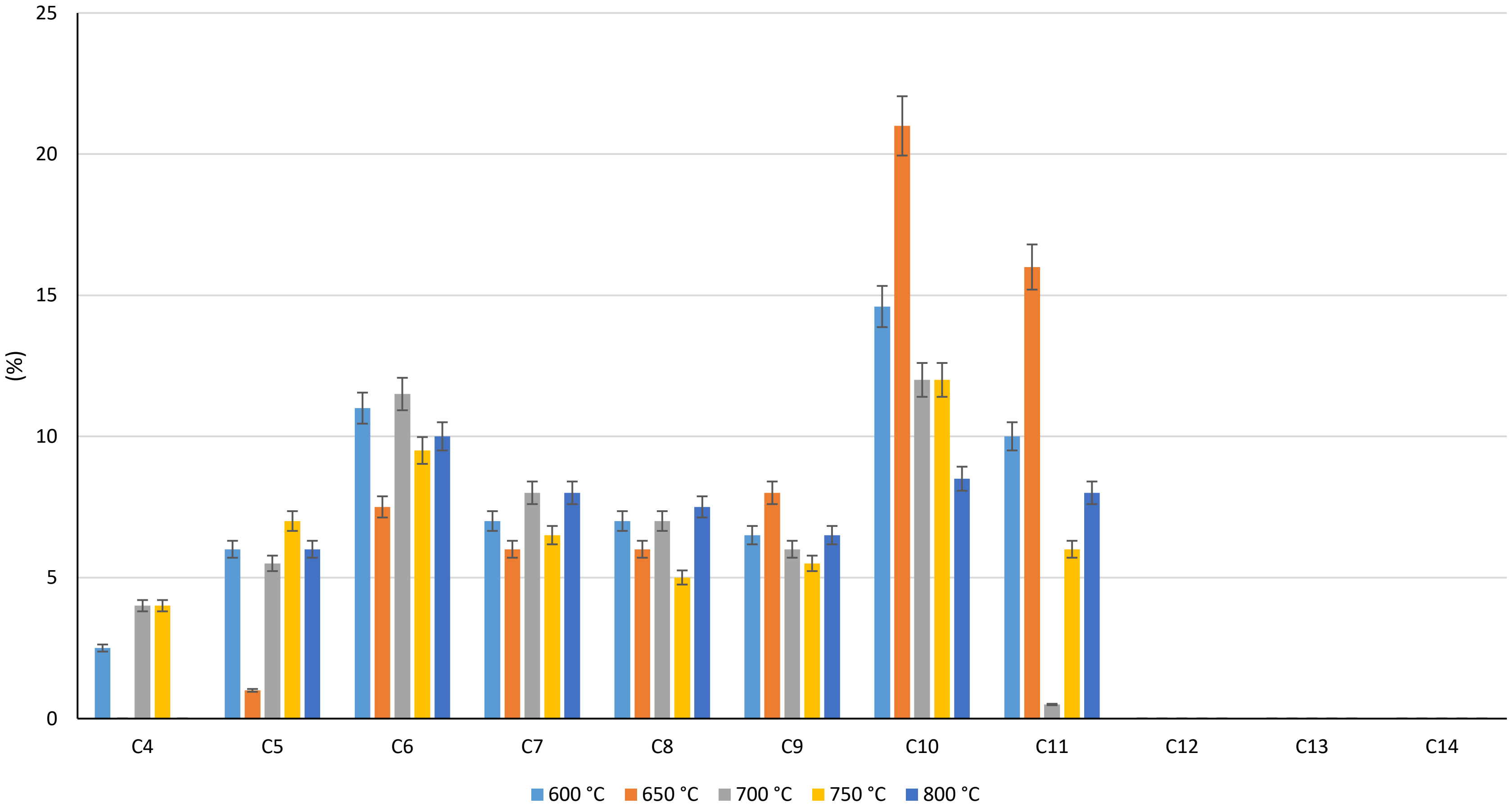

Figure 3.13.c: Carbon wise distribution of LAO obtained from PE

3.5 Scale up studies of Wax 2 Cracking

In order to verify the linear alpha olefin potential from the cracking of wax molecules at large scale, the Wax 2 was subjected to thermal cracking using Mini Pot still (MPS) Equipment (Figure 3.14). Experiments were carried out at 420 °C, atm pressure and three different reaction times (30 min, 60 min and 120 min). Distillate yield from the three experiments is provided in the Figure 3.15.

Figure 3.14: Mini Pot Still equipment

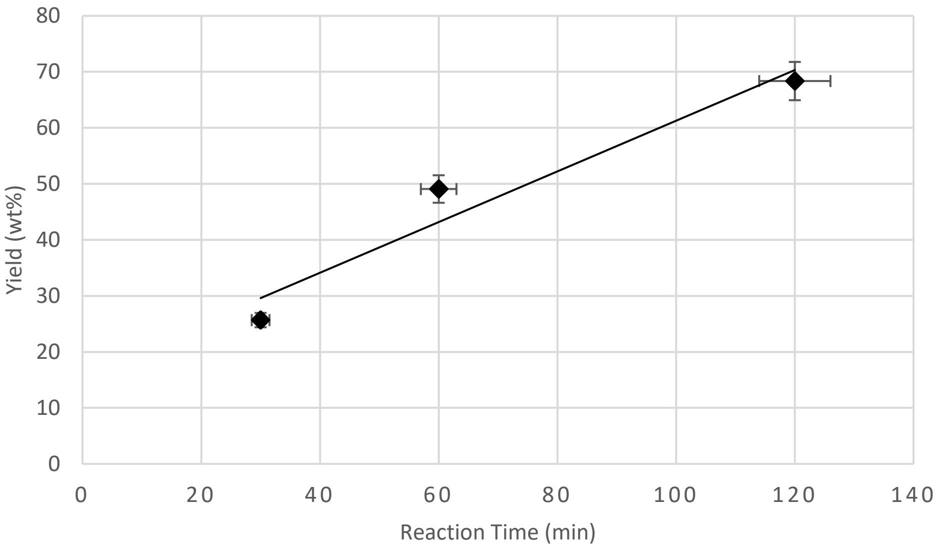

Figure 3.15: Time versus yield graph obtained during the wax cracking experiments in MPS

It was found that highest liquid yield of about 70% was obtained when the thermal cracking process was performed at 420 ^{o}C for 120 min. The result was quite expected as cracking would increase with more the residence time of the feedstock in the pot still, giving improved yield. Wax cracked naphtha (WCN) thus obtained was further analyzed for PONA. % LAO in WCN is listed in Table 3.5. The naphtha was characterized by GC/MS, and it was determined that these values were well correlated to those obtained by fast pyrolysis of Wax 2.

Table 3.5 GC/MS analysis of wax cracked naphtha (WCN)

Carbon number	**Linear alpha Olefin % in WCN**
C4	-
C5	0.71
C6	1.65
C7	1.33
C8	1.77
C9	2.01
C10+	19.6
Total Olefin %	**27.07**

3.6 Summary

Determination of feedstock source providing highest LAO was investigated from both refinery and non-refinery streams. From the refinery streams tried (FCC-LCN, FCC-HCN, DCN and VBN), DCN was determined to supply highest % of LAO in the desired carbon range of C8 to C14. Thus, if one has to choose refinery stream to make LAO for further synthesis of PAO, DCN would be the best available stream.

In non-refinery low value feedstock streams, Wax 1 (lower carbon number content), Wax 2 (higher carbon number content) and polyethylene (PE) were investigated, and it was found that alpha olefin (LAO) content was obtained in the following sequence PE>Wax 2> Wax 1, and the olefin yield was found to have direct correlation with the feed carbon chain length. Cracking of the feedstock was performed in pyrolyzer attached directly to GC/MS unit, and detailed analysis of PONA, olefin content and carbon numbers of the obtained olefin content was performed. Wax 2 was further utilized for thermal cracking in a pot still arrangement. Obtained product was characterized by PONA and further characterized for olefin and carbon number content, which was found to be similar to that obtained from fast pyrolysis.

Wax cracked naphtha (23.4% of linear alpha olefins of C8 to C14 range) and the delayed coker naphtha (25.3% of linear alpha olefins of C8 to C14 range) were shortlisted for further studies.

CHAPTER 4

DEVELOPMENT OF CATALYST SYSTEM USING MODEL COMPOUNDS

4.1 Overview

Lewis acids play an important role in chemical transformations as catalysts, reagents etc. Alpha olefin oligomerization, such as, 1-decene mediated by Lewis acids is an industrially important process for synthetic group IV Poly Alpha olefin (PAO) lubricants. The key lubricant properties such, as viscosity indices and pour points are governed by the molecular structure. PAOs typically are characterized by high viscosity indices >120, which indicates minimal changes in viscosity as a function of temperature, and low pour point <-40, which ensure the low temperature fluidity. The ideal balance between the linear (responsible for high viscosity index) versus branched structure (responsible high pour point) in the PAOs is critical for excellent lubricant properties. Furthermore, the viscosity grades of PAOs are much dependent on the oligomer length. Therefore, to achieve optimal lubricant performance, critical parameters such as catalyst design and reaction conditions (temperature and time) should be strenuously looked into.

Although a varied array of Lewis acid catalysts is reported, the industrial process is still dominated by $BF_3.OEt_2$ to obtain the low viscosity grade PAO lubricants. The commercial process involves the oligomerization, followed by distillation to separate the 1-decene oligomers and blending the components in required ratios to obtain the different grades of PAO lubricants. Same is also illustrated in the Figure 4.1. However, the process involves evolution of toxic gas, which is irritant to pulmonary system and reacts with water to form corrosive toxic HF fumes. Furthermore, to obtain the required oligomer ratio necessary for different viscosity grades is problematic, which depends on different strengths of Lewis acids.

One way is to achieve the fine tuning of Lewis acidity via ionic liquids [53, 54] or liquid coordination complexes [55- 59] *etc*, which are well studied for PAO synthesis. However, their synthesis typically involves anhydrous conditions and expensive quaternary ammonium reagents. An alternate way is to achieve the tuneable Lewis acidity [60 - 68] through judicious combinations of different Lewis acids with varied strength reagents. For instance, group 13 halides are strong Lewis acids (BF_3, $AlCl_3$) whereas transition metals halides ($FeCl_3$) salts are milder. Though the transition metal halide-based Lewis acids are reported for other key organic transformations, use in alpha olefin oligomerization is barely explored. [63, 64]

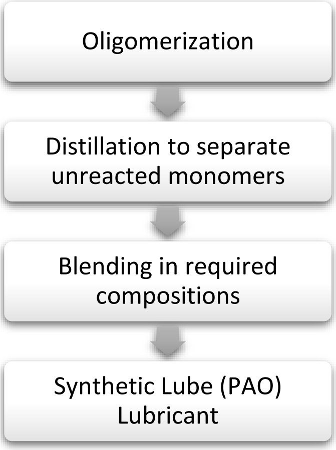

Figure 4.1 Flowchart depicting the conventional synthetic lube (PAO) steps

Experimental Studies with 1-decene: 1-decene was used as the model compound to represent alpha olefins and this compound was used as the feed for screening various catalyst systems to obtain the desired ratios of oligomers. A series of catalysts comprising of $AlCl_3/FeCl_3$ in different molar ratios [$AlCl_3$, $AlCl_3/FeCl_3$ (0.7:0.3), $AlCl_3/FeCl_3$ (0.5:0.5), $AlCl_3/FeCl_3$ (0.3:0.7), $FeCl_3$], which vary in terms of Lewis acid strength, were chosen. The oligomerization reactions were performed at 50 ℃, 75 ℃ and 100 ℃ and product distribution is monitored for 120 minutes with an interval of 20 min.

Experimental Studies on effect of Sulfur impurities: The effect of sulphur-based compound impurity on the PAO synthesis and properties was studied.

Experimental Studies on Effect of 1-octene / 1-dodecene monomer ratio: In addition, effect of 1-octene / 1-dodecene monomer ratio on the properties of synthesized synthetic lubricant (PAO), in presence of $AlCl_3$ or ionic liquid is also studied.

4.2 Characterization of commercial PAOs

Three PAOs were obtained from commercial suppliers, values of whose dimer, trimer, tetramer and higher oligomer content were determined from their technical data sheets and plotted in Figure 4.2. Also, PAO from one of the high volume suppliers was characterized for properties such as viscosity at 40 °C & 100 °C, viscosity index (as per ASTM D2270) and pour point (as per ASTM D7346), values of which are listed in Table 4.1.

Figure 4.2 shows PAO-1 predominantly consisting of dimer (~ 95 %) whereas PAO-2 base oil contains mainly trimer (~75 %) and tetramer (~20 %). On the other hand, tetramer (~46 %) was found to be the major constituent in PAO-3; while the rest is either trimer or other oligomers.

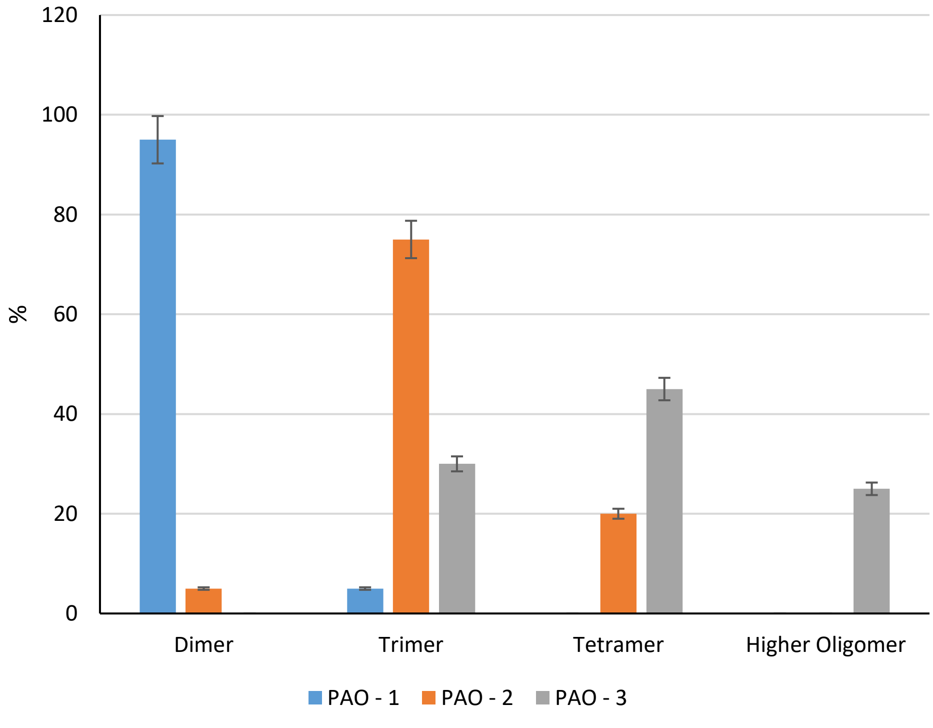

Figure 4.2: Dimer, trimer, tetramer and higher oligomer profile reported for commercial PAO lubricants

Table 4.1: Performance properties determined for one of the high volume supplied commercial PAO

Properties	Commercial PAO
Viscosity at 40 ^{o}C (cSt)	19
Viscosity at 100 ^{o}C (cSt)	4.1
Viscosity Index (ASTM D2270)	126
Pour point (ASTM D7346) (^{o}C)	-66

4.3 Experimental Materials and Methods

Table 4.2 lists the names, specifications and source of chemicals used in the current research work. The HT-SIMDIS (high temperature simulated distillation profile)-Carbon, is performed on AC Analytical Controls system. Mass spectrum was recorded on Shimadzu technologies LC-MS system.

Table 4.2: Chemicals, their specifications & source of supply, used in the study

Sr. No.	Chemical Name	Specification	Source
1	1-Hexene	>97.0%(GC)	TCI Chemicals
2	1-Octene	>99.0%(GC)	
3	1-Decene	>95.0%(GC)	
4	1-Dodecene	>95.0%(GC)	
5	*N*-butyl, *N*-methyl imidazolium chloride	≥98.5%	Sigma Aldrich
6	4- Methyl benzothiol	97%	
7	$AlCl_3$	98%	
8	$FeCl_3$	97%	
9	Wax cracked naphtha (WCN)	HPCL, Mumbai Refinery, India	
10	DIW	Type I	Milli-Q® Type 1 Ultrapure Water System
11	PAO-1	From commercial supplier	
12	PAO-2	From commercial supplier	
13	PAO-3	From commercial supplier	

4.4 Experimental Studies with 1-decene

4.4.1 Reaction procedure

To a stirred solution of 1-decene (20 mL), catalysts formulations of various ratios of $AlCl_3/FeCl_3$ (2 wt %) were added at room temperature. Water was added (0.4 eq with respect to catalyst) and the reaction mixture was heated at predesignated temperatures (50 °C, 75 °Cand 100 °C). The reaction aliquots were collected at a particular time (20 min, 40 min, 60 min, 80 min, 100 min and 120 min) intervals and analyzed with GC. The HT-SIMDIS (high temperature simulated distillation profile) was used to identify the oligomer ratio with FID detector. The SIMDIS recovery software was used to obtain the oligomer ratio. The HT-SIMDIS boiling point standard ASTM D7169 was used to identify the oligomer retention time**.** The experiment procedure is pictorially depicted in Figure 4.3.

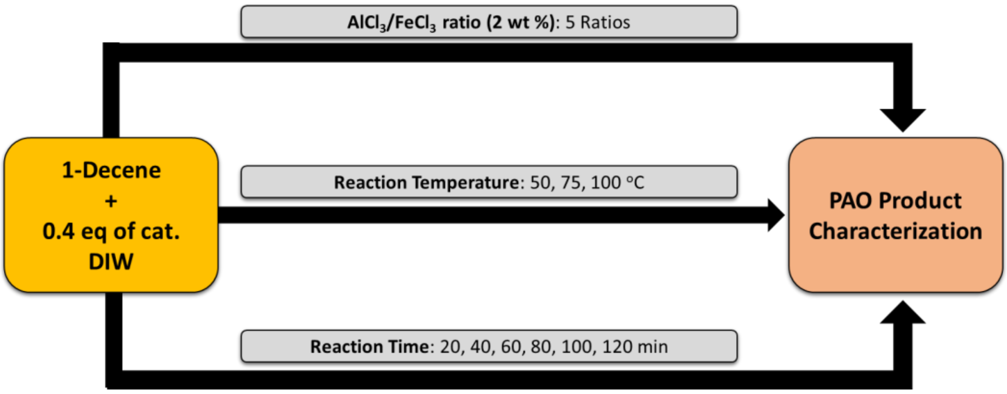

Figure 4.3: Flowchart of Experimental studies with 1 decene

4.4.2 Reaction mechanism

$$AlCl_3 \xrightarrow{H_2O} AlCl_3(OH)^{\ominus} + H^+$$

$$FeCl_3 \xrightarrow{H_2O} FeCl_3(OH)^{\ominus} + H^+ \qquad FeCl_3 \xrightarrow{H_2O} FeCl_2(OH) + HCl$$

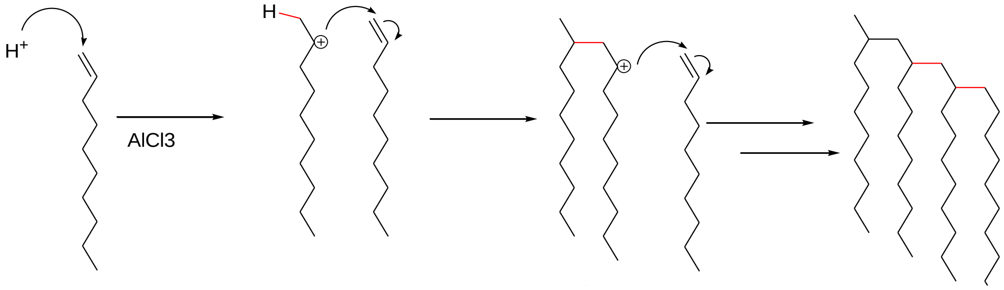

Figure 4.4: PAO oligomerization mechanism in the presence of Lewis acids

In the conventional pathway, depicted in Figure 4.4, the Lewis acid undergo hydrolysis to form proton, which initiates the oligomerization reaction. The rate of hydrolysis, which in turn depends on the strength of Lewis acid determines the rate of the reaction. Once initiated, the active carbonium ion can react with another olefin in the propagation step to form the higher oligomers. On the other hand, the active carbonium ion can undergo proton transfer termination reaction to form the oligomer product. In the case of the iron-based catalysts, the mechanism is not clear and possibly due to formation of mono or multi-metallic iron-carbon species. It is interesting to note that the conversion for catalyst with equal proportion of $AlCl_3/FeCl_3$ is similar for all temperatures. The commercial process involves the distillation of various oligomers from 1-decene and blending in suitable ratio to obtain the different grades of PAO lubricants.

In the present work, to obtain the desired ratios of oligomers, a series of catalysts comprising of $AlCl_3/FeCl_3$ in different molar ratios [$FeCl_3$ (designated as FA1), $FeCl_3:AlCl_3$ = 0.7:0.3 (designated as FA2), $FeCl_3:AlCl_3$ = 0.5:0.5 (designated as FA3), $FeCl_3:AlCl_3$ = 0.3:0.7 (designated as FA4), and $AlCl_3$ (designated as FA5)], which vary in terms of Lewis acid strength, were chosen for the 1-decene oligomerization. The oligomerization reactions were performed at 50 °C, 75 °C and 100 °C and product distribution is monitored for 120 minutes with the interval of 20 min.

4.4.3 Conversion studies

The conversions for Lewis acid blend catalysts at various temperatures is given in Figure 4.5. The conversion for catalyst $AlCl_3$ was found to be increasing with temperature and same is well documented. On the other hand, for the catalysts containing $FeCl_3$, the conversions decreased with increase in temperature from 50 to 100 °C. The abnormal behavior of the $FeCl_3$ may be due to different mechanistic pathway different from conventional pathway shown in Fig 4.4.

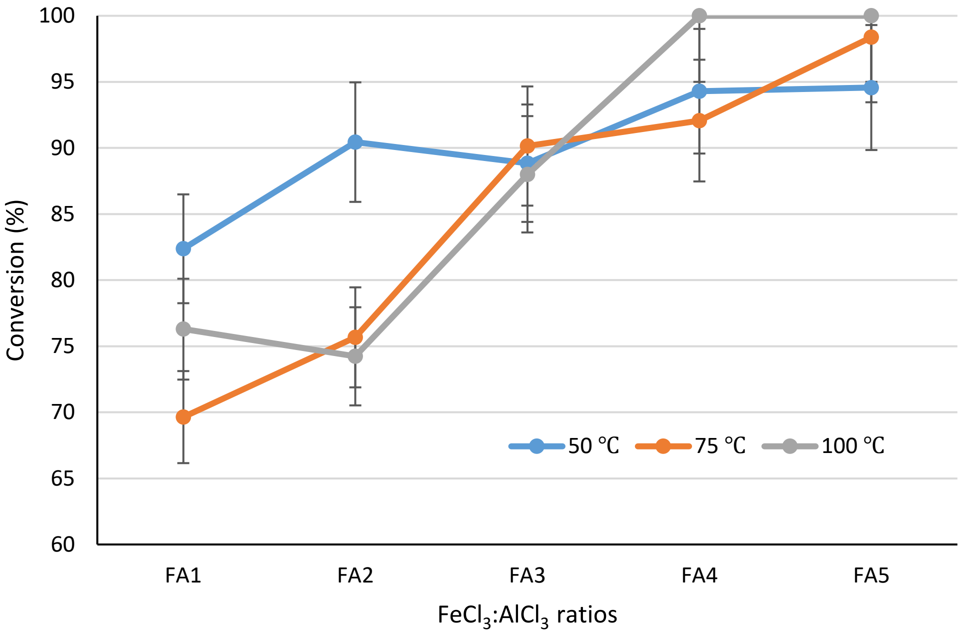

Figure 4.5: The temperature dependent conversions in the 1-decene oligomerization with Lewis acid blend oligomerization catalysts after 120 minutes of reaction time

4.4.4 Effect of reaction temperature

As can be seen from Figure 4.6.a, among the catalysts studied, the $FeCl_3$ and its blends with lower percentage of $AlCl_3$, led to the higher amount of dimers at all temperatures.

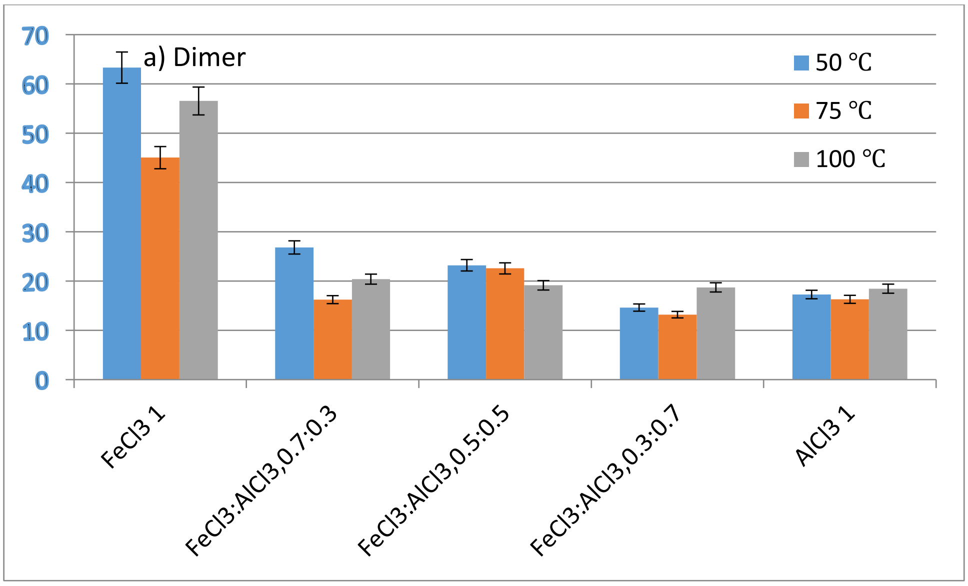

Figure 4.6.a: The temperature dependent dimer conversions in the 1-decene oligomerization with Lewis acid blend catalysts after 120 min reaction time

In the case of trimer and higher oligomers (refer Figures 4.6.b, 4.6.c and 4.6.d), at any temperature, their ratio (trimer and higher oligomers) is increased with an increase in $AlCl_3$ composition in the catalyst formulations. The trend can be explained on the basis of Lewis acid strength of $FeCl_3$ and $AlCl_3$. For a given catalyst, the ratio of smaller oligomer (dimer and trimer) increased with an increase in the temperature, whereas the ratio of higher oligomers (tetramer and higher) decreased with an increase in the temperature. It can be explained by the kinetics of propagation and termination. With increase in the temperature, the termination rate increases rapidly than the propagation leading to formations of lower oligomers. Whereas at lower temperature, the propagation rate is faster than the termination step, leading to higher oligomers.

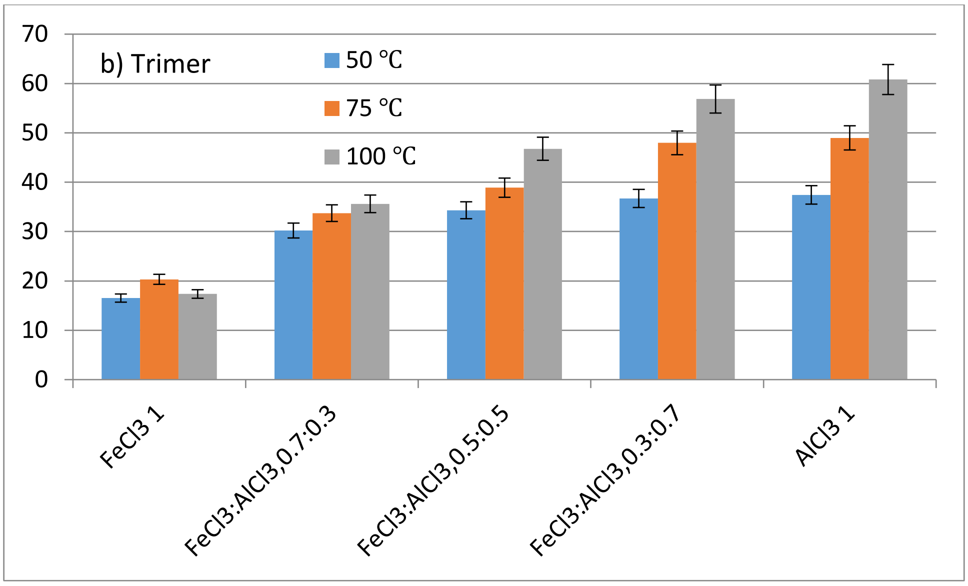

Figure 4.6.b: The temperature dependent trimer conversions in the 1-decene oligomerization with Lewis acid blend catalysts after 120 min reaction time

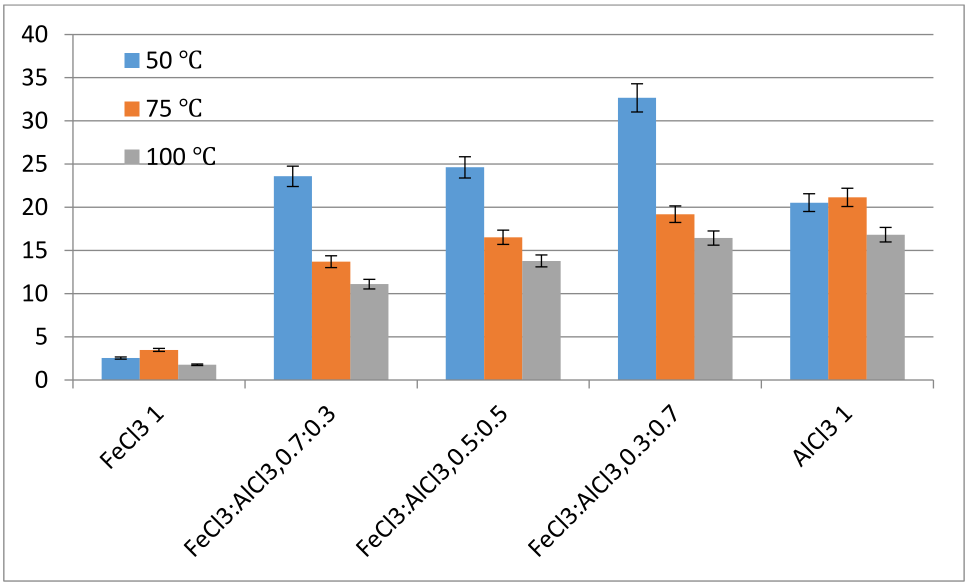

Figure 4.6.c: The temperature dependent tetramer conversions in the 1-decene oligomerization with Lewis acid blend catalysts after 120 min reaction time

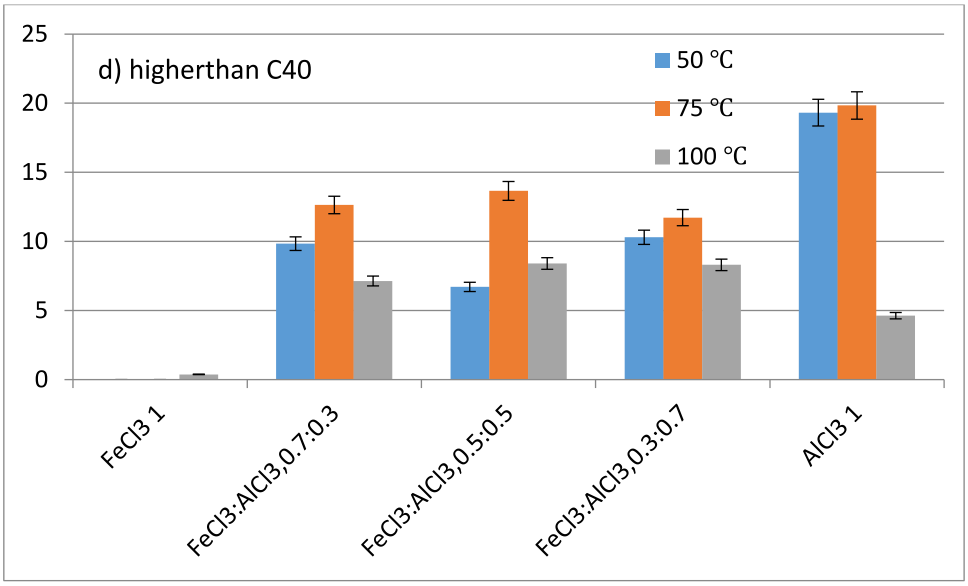

Figure 4.6.d: The temperature dependent higher oligomer conversions in the Lewis acid blend catalysts after 120 min reaction time

4.4.5 Effect of reaction time at 50˚C reaction temperature

The plots of oligomer ratio at different time intervals of Lewis acid blend catalysts at 50 °C reaction temperature are given in Figures 4.7.a to 4.7.e. In the case of $FeCl_3$ (Figure 4.7.a), the products are predominantly dimer and trimer, and the variation is also minimal with time interval. In the case of the blends of $FeCl_3$:$AlCl_3$ (0.7:0.3, Figure 4.7.b), $FeCl_3$:$AlCl_3$ (0.5:0.5, Figure 4.7.c), the dimer is the predominant species in the initial phases of the reaction but is consumed to produce higher olefins as the reaction progresses. This trend continued up to 80 min, post which the effects are minimal, indicating the optimal time for oligomerization reaction is 80 min at 50 °C for the catalysts $FeCl_3$:$AlCl_3$ (0.7:0.3, Figure 4.7.b), $FeCl_3$:$AlCl_3$ (0.5:0.5, Figure 4.7.c). With increase in $AlCl_3$ composition in the catalyst (Figures 4.7.d & 4.7.e), the oligomer ratio is moved towards higher oligomer ratio and composition remains same after 60-80 minutes.

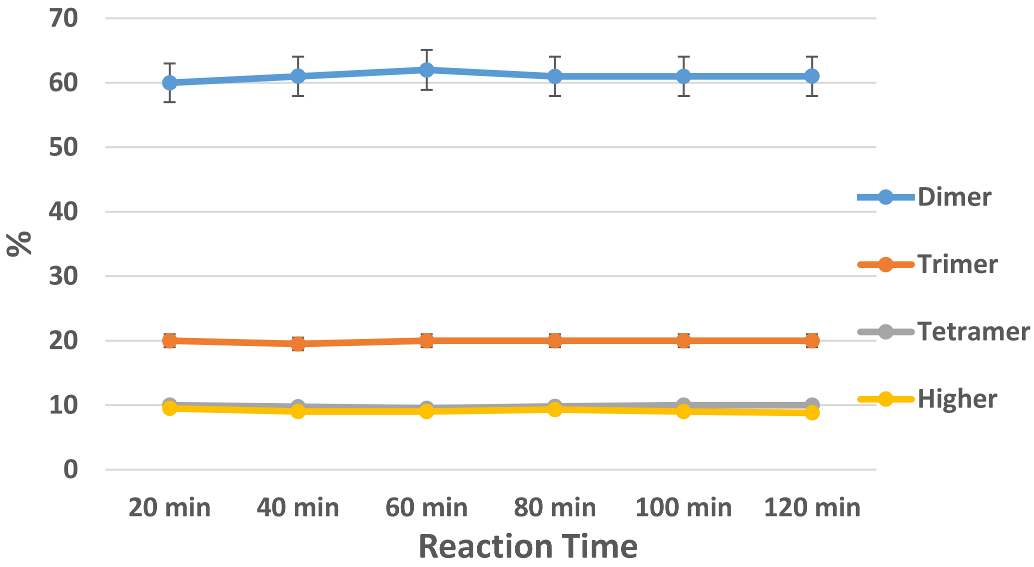

Figure 4.7.a: % dimer, trimer, tetramer and higher oligomers at different time intervals of FA1 catalysts at 50 °C

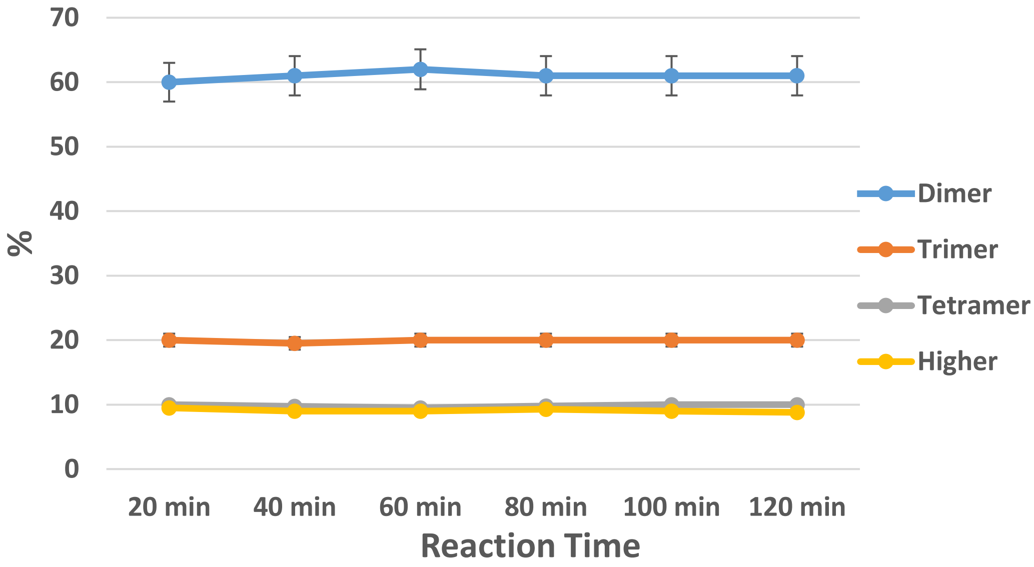

Figure 4.7.b: % dimer, trimer, tetramer and higher oligomers at different time intervals of FA2 catalysts at 50 °C

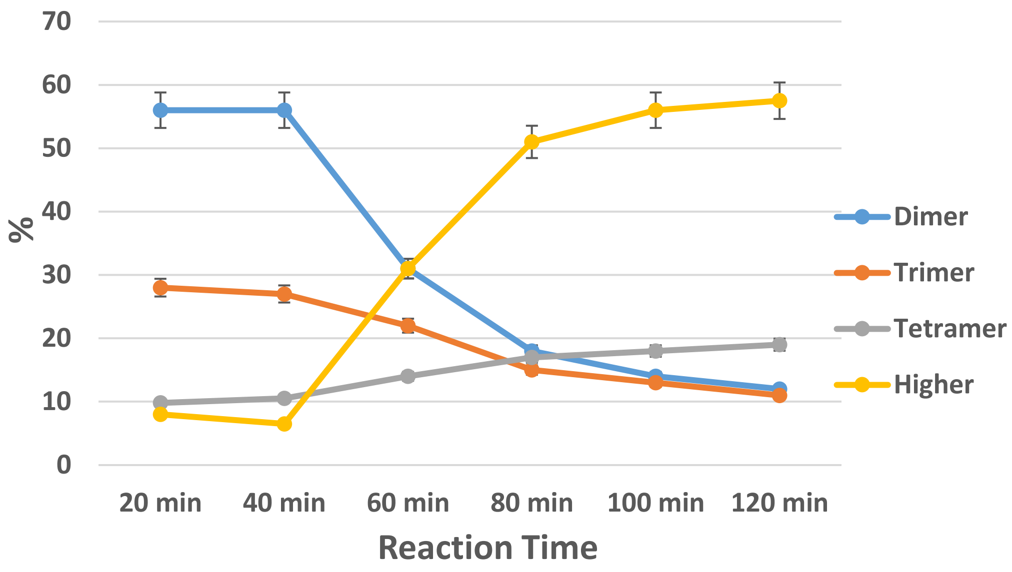

Figure 4.7.c: % dimer, trimer, tetramer and higher oligomers at different time intervals of FA3 catalysts at 50 °C

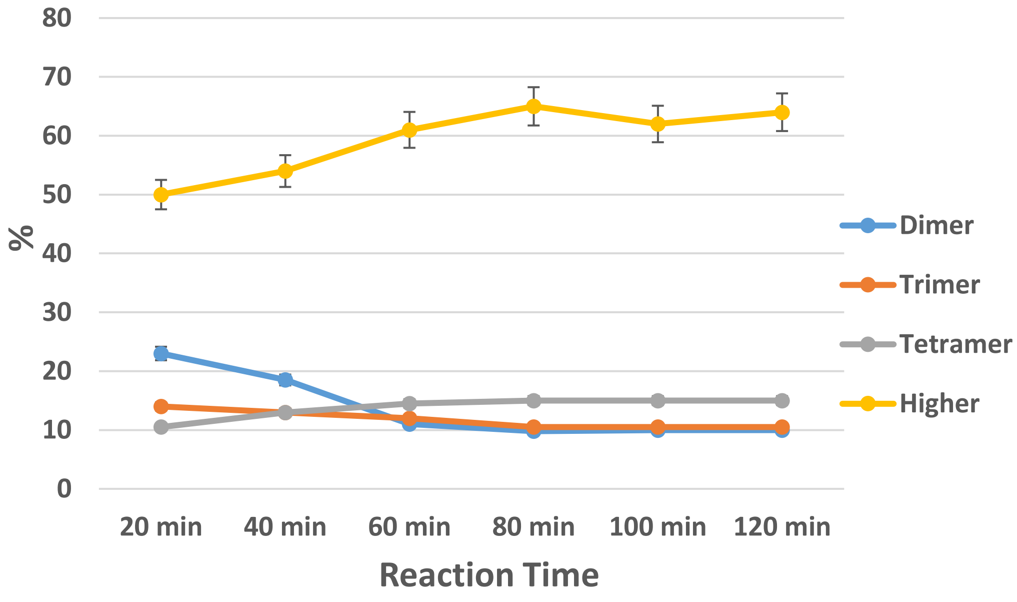

Figure 4.7.d: % dimer, trimer, tetramer and higher oligomers at different time intervals of FA4 catalysts at 50 °C

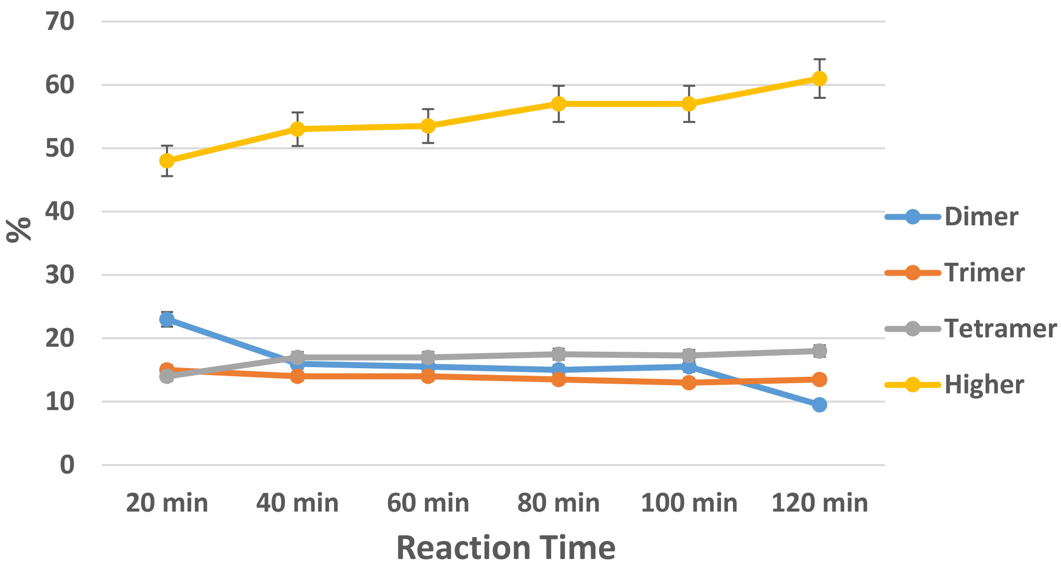

Figure 4.7.e: % dimer, trimer, tetramer and higher oligomers at different time intervals of FA5 catalysts at 50 °C

4.4.6 Effect of reaction time at 75˚C reaction temperature

Similar to the trend of 50 °C, the $FeCl_3$ catalyst at 75 °C (Figure 4.8.a), led to formation of mainly dimer and trimer. In the case of the blend catalysts $FeCl_3$:$AlCl_3$ (0.7:0.3, Figure 4.8.b), $FeCl_3$:$AlCl_3$ (0.5:0.5, Figure 4.8.c), with reaction progress, the dimer ratio decreased with the corresponding increase in higher oligomers. The product distribution remains constant after 60 minutes. Whereas the higher $AlCl_3$ in the catalyst blend (Figure 4.8.d and Figure 4.8.e), led to increase in the higher oligomer ratios (tetramer and higher) in comparison with the other catalysts.

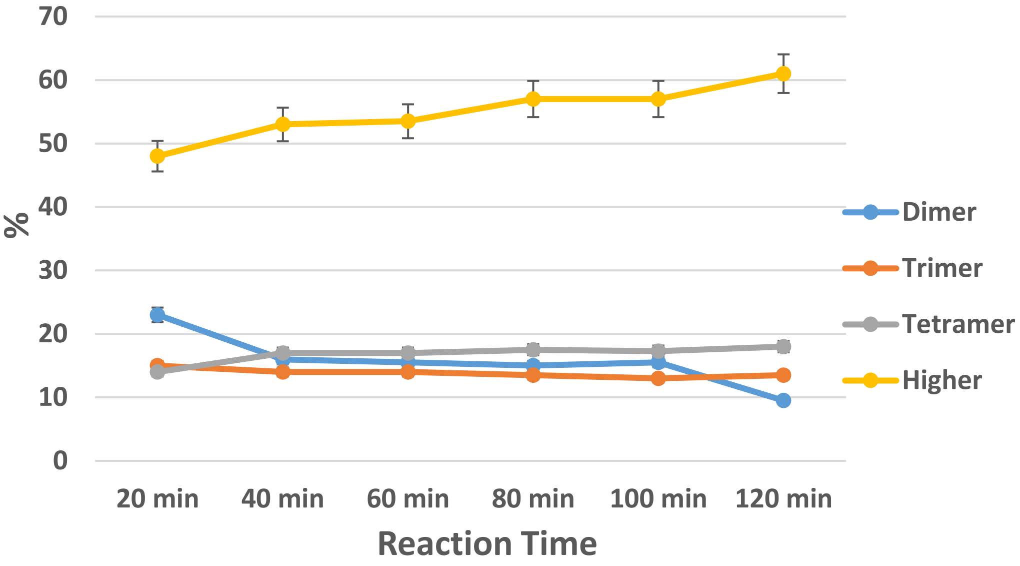

Figure 4.8.a: % dimer, trimer, tetramer and higher oligomers at different time intervals of FA1 catalysts at 75 °C

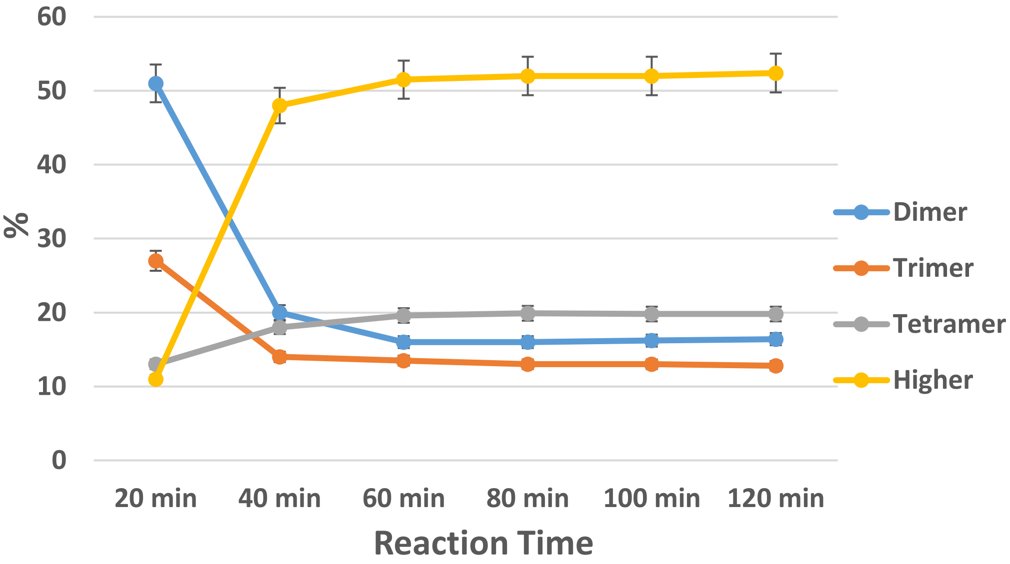

Figure 4.8.b: % dimer, trimer, tetramer and higher oligomers at different time intervals of FA2 catalysts at 75 °C

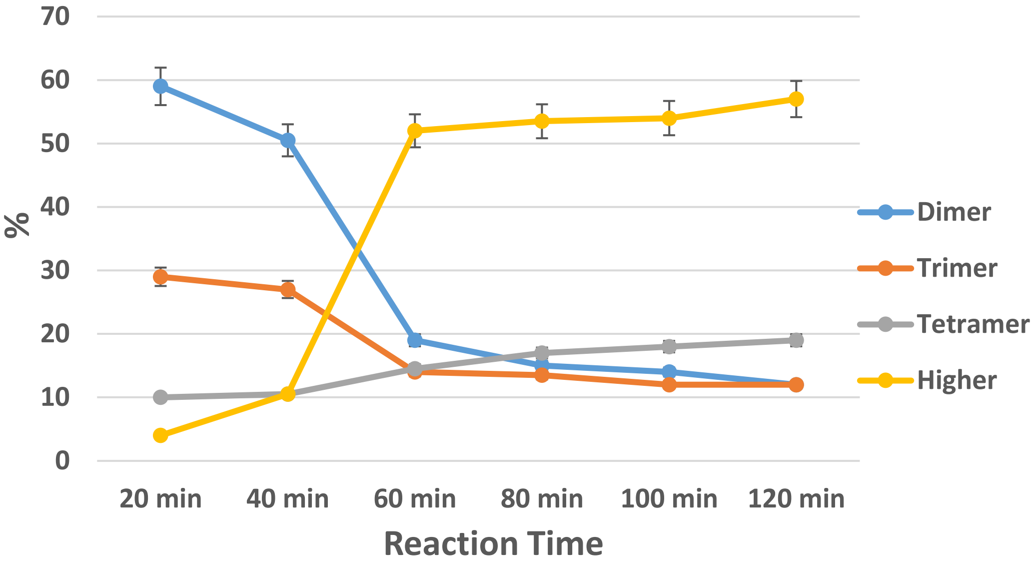

Figure 4.8.c: % dimer, trimer, tetramer and higher oligomers at different time intervals of FA3 catalysts at 75 °C

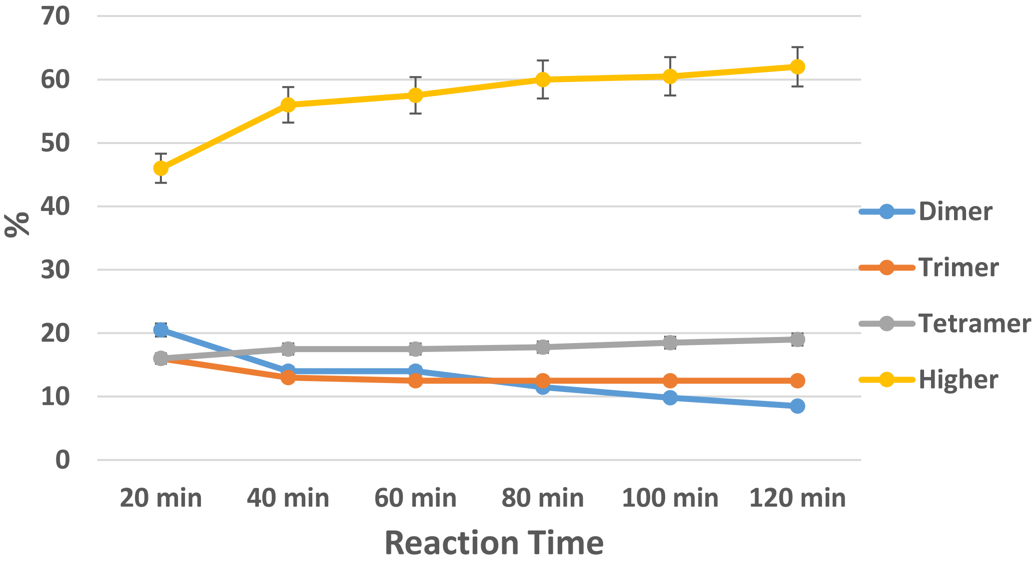

Figure 4.8.d: % dimer, trimer, tetramer and higher oligomers at different time intervals of FA4 catalysts at 75 °C

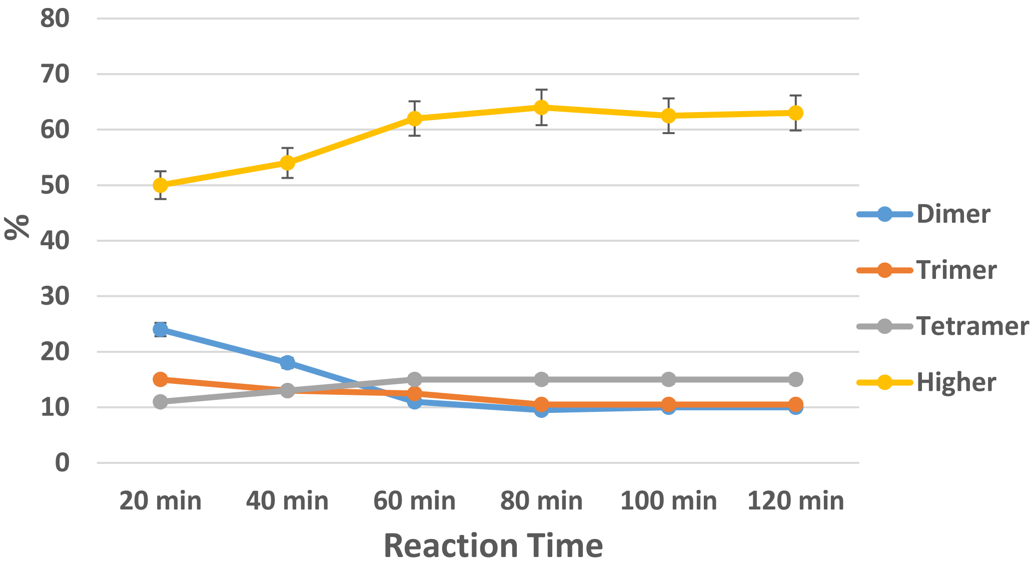

Figure 4.8.e: % dimer, trimer, tetramer and higher oligomers at different time intervals of FA5 catalysts at 75 °C

4.4.7 Effect of reaction time at 100˚C reaction temperature

In the case of 100 °C, similar to the earlier case, the $FeCl_3$ based catalyst oligomerization reaction of 1-decene, led to formation of dimer and trimer oligomers (Figure 4.9.a). In the case of the blend catalysts $FeCl_3$:$AlCl_3$ (0.7:0.3, Figure 4.9.b), $FeCl_3$:$AlCl_3$ (0.5:0.5, Figure 4.9.c), the equilibrium composition reached at 40 minutes and did not change further. Whereas the $AlCl_3$ dominated catalysts (Figure 4.9.d and Figure 4.9.e) ratios showed higher oligomer ratios in comparison with other catalyst ratios.

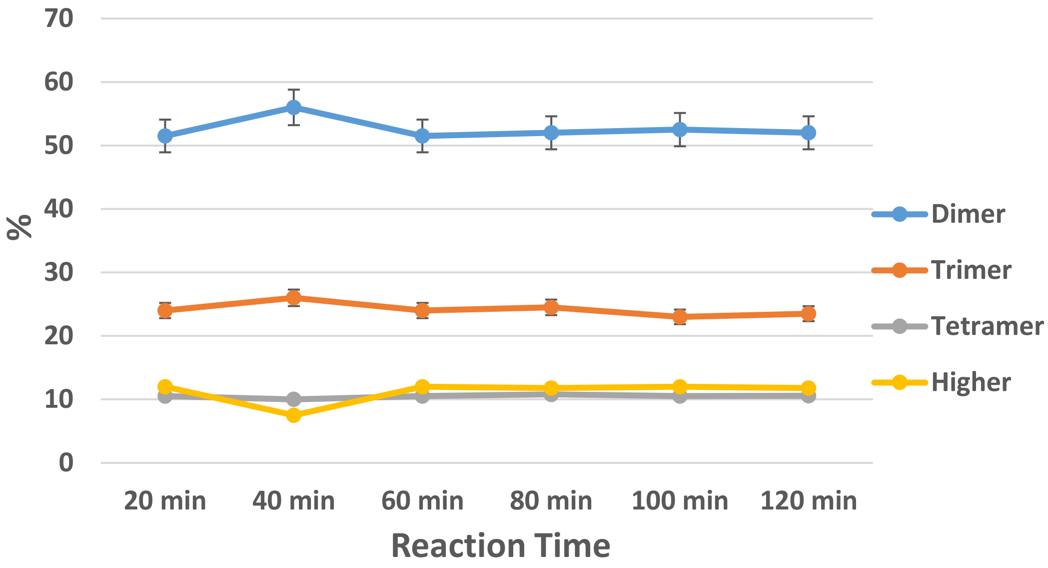

Figure 4.9.a: % dimer, trimer, tetramer and higher oligomers at different time intervals of FA1 catalysts at 100 °C

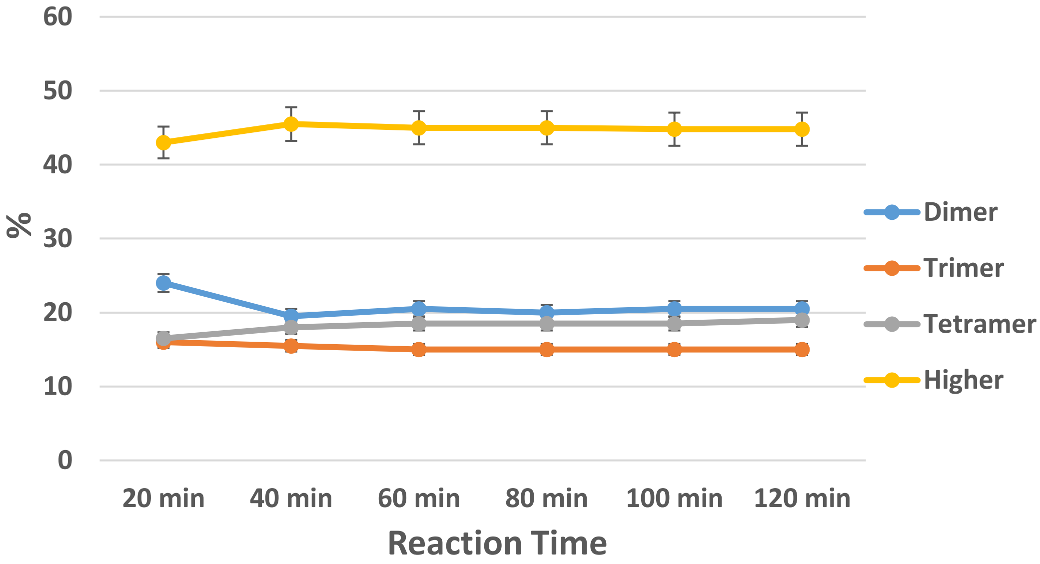

Figure 4.9.b: % dimer, trimer, tetramer and higher oligomers at different time intervals of FA2 catalysts at 100 °C

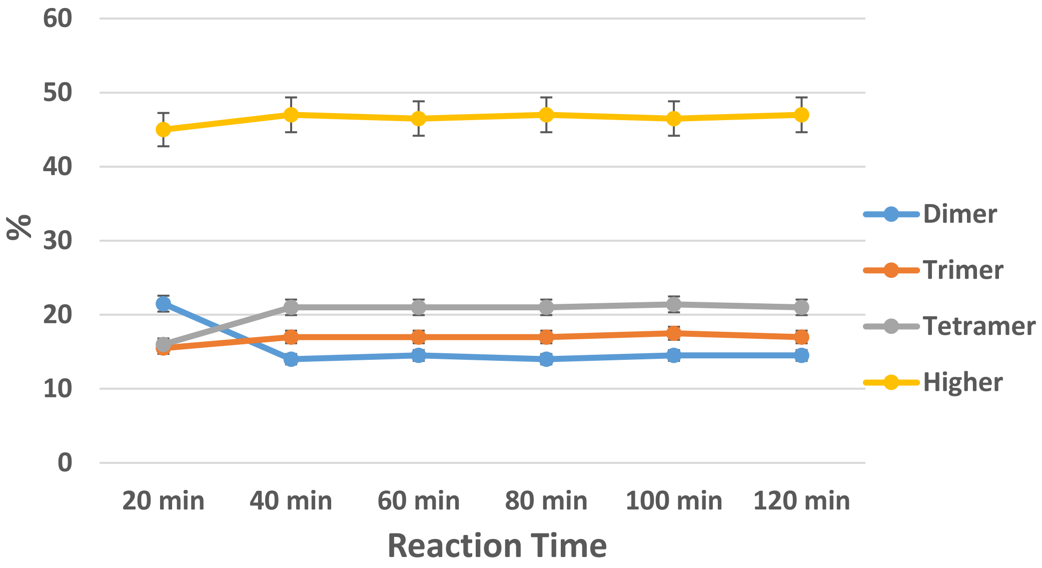

Figure 4.9.c: % dimer, trimer, tetramer and higher oligomers at different time intervals of FA3 catalysts at 100 °C

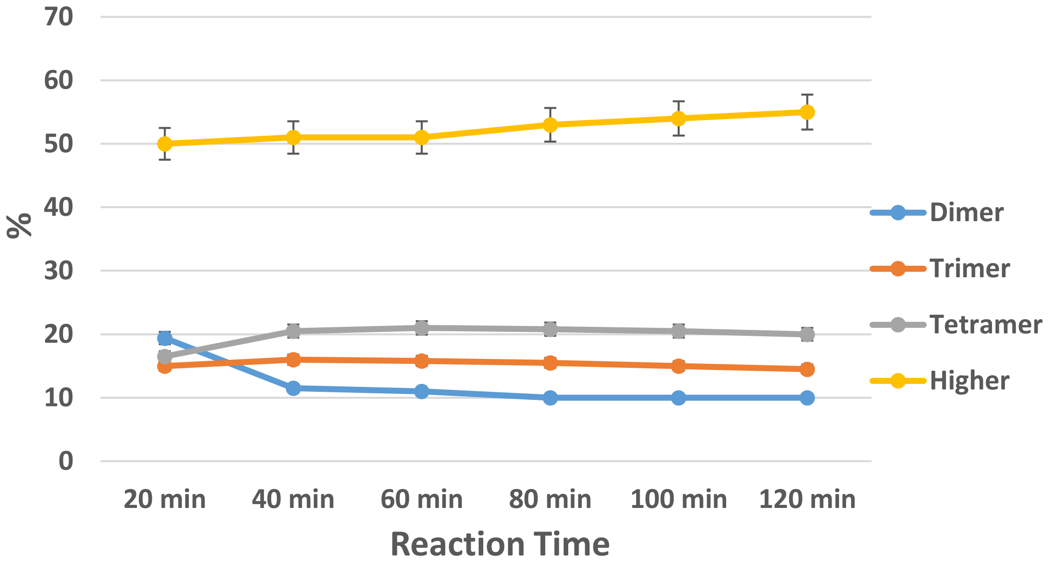

Figure 4.9.d: % dimer, trimer, tetramer and higher oligomers at different time intervals of FA4 catalysts at 100 °C

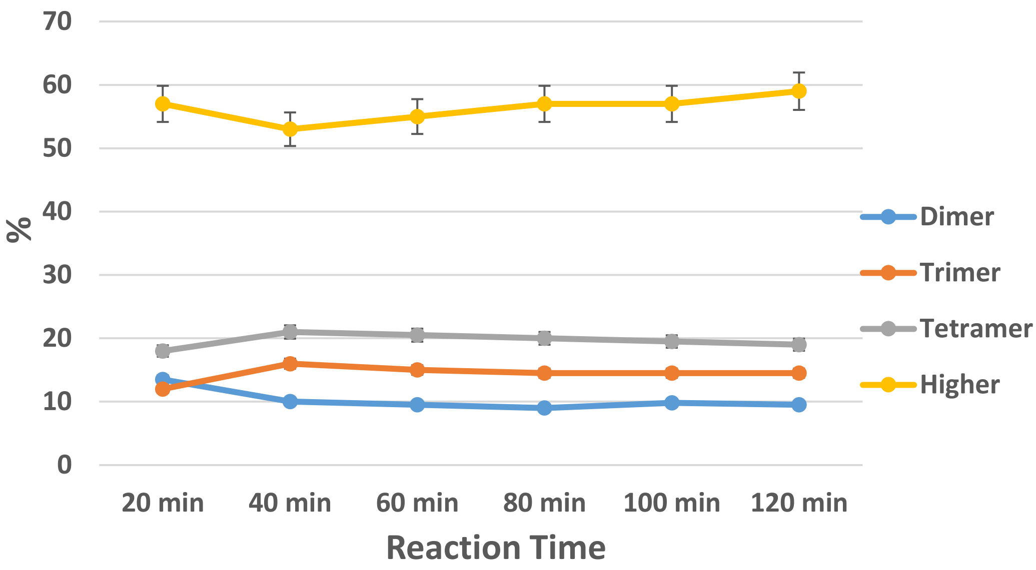

Figure 4.9.e: % dimer, trimer, tetramer and higher oligomers at different time intervals of FA5 catalysts at 100 °C

The product composition for 1-decene oligomerization was found to be critically dependent on temperature and residence time. The conversion with $AlCl_3$ was found to increase with increase in temperature, whereas the iron-based catalysts showed the reverse trend. The iron-based catalysts selectively yielded dimer or 2 cst grade PAO whereas with increasing $AlCl_3$ in the catalyst blend the oligomer ratio shifted towards to tetramer and higher oligomers. For a particular catalyst, with increase in temperature, the oligomer ratio is shifted towards lighters (dimer and trimer) due to faster termination kinetics in comparison with the propagation.

To understand the effect of temperature on oligomer ratio, the oligomer profile obtained for the $FeCl_3$:$AlCl_3$ (0.5:0.5) (FA3) catalyst is illustrated in Figure 4.10. For the catalyst with the same ratio of $FeCl_3$:$AlCl_3$, the higher oligomer ratio decreased at 100 ºC due to faster termination kinetics in comparison with the propagation phenomenon. The oligomer ratio of variation with respect to the catalyst formulations is shown in Figure 4.11.

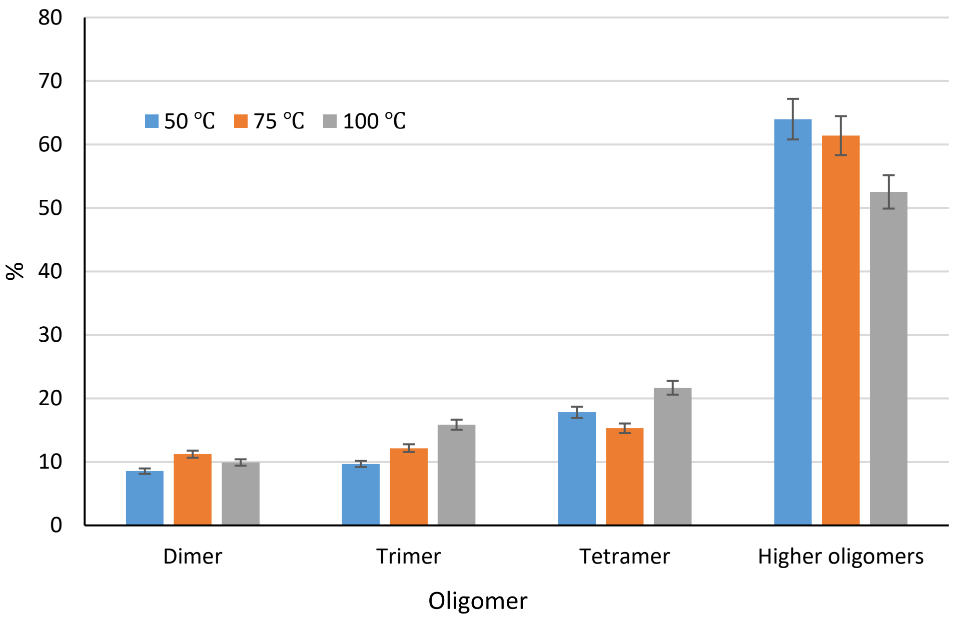

Figure 4.10: Temperature dependent oligomer % obtained at different temperatures for FA3 [$FeCl_3$:$AlCl_3$ (0.5:0.5)] catalyst

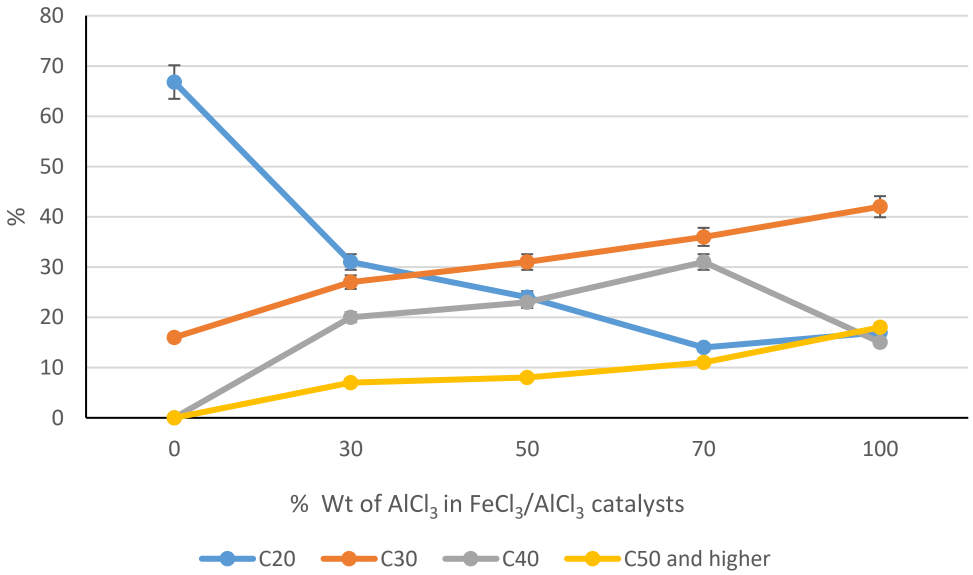

Figure 4.11: The oligomer % (C20 to C40) variation with respect to the catalyst formulations

Thus, $AlCl_3$ was determined to be the best catalyst system for PAO synthesis as per the research work. Ability of the catalyst in the presence of sulphur compound is studied in the next part

4.5 Experimental Studies on effect of Sulfur impurities

In order to verify the thio-affinity of $FeCl_3$ and $AlCl_3$ blend catalysts, a model synthetic mixture containing propane thiol in 1-decene was chosen for oligomerization reaction. The possible mechanistic pathways for oligomerization reaction in the presence of model thiopropane is given in Figure 4.12 below. In the case of Lewis acid catalyst, the oligomerization reaction follows the carbonium ion (2) pathway initiated by proton, which is formed from the hydrolysis of Lewis acids. The carbonium ion further reacts with alkene to form dimer carbonium ion 3 which is further continued to form alpha olefin oligomers 4. However, in the presence of nucleophylic thiol or H_2S compounds, the carbonium ion can be trapped by sulfur compounds to form the alpha olefin oligomers containing sulfur in their backbone (6-7). On the other hand, the thiol compound can undergo thiol-ene reaction with the alkene to form compound 5.

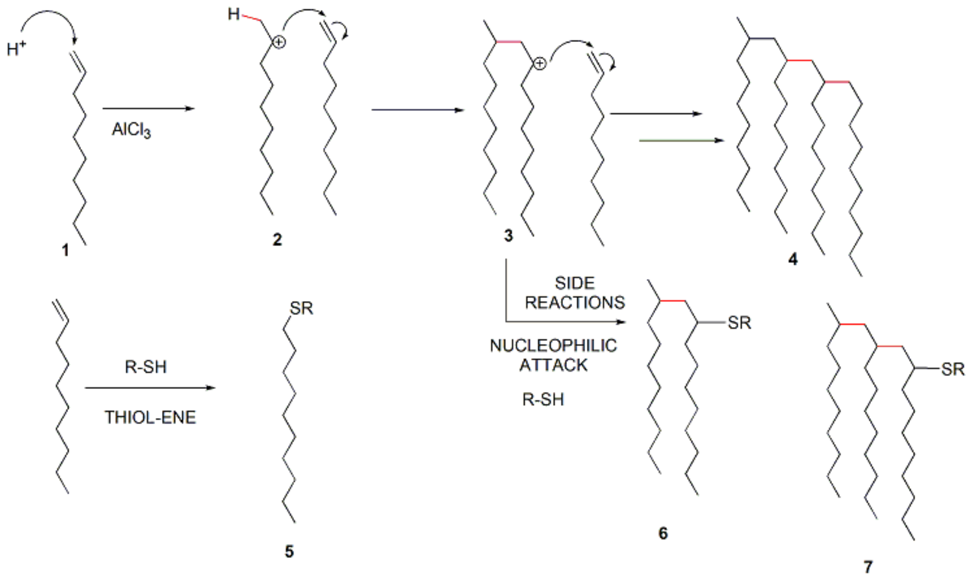

Figure 4.12: 1-decene oligomerization reaction and possible side reactions with thiol compound

4.5.1 Reaction procedure

To a stirred solution of propane thiol (0. 2 wt %) in 1-decene, catalysts formulations of $AlCl_3$, $AlCl_3/FeCl_3$ (1:1) (2 wt %) were added at room temperature. Water was added (0.4 eq with respect to catalyst) and the reaction mixture was heated at predesignated temperatures 50 °C. After work up with water, the organic layer was analysed by HT-sulfur SimDis (high temperature simulated distillation profile) with sulfur Chemiluminescence (SCD) detector. The experiment procedure is illustrated in the Figure 4.13.

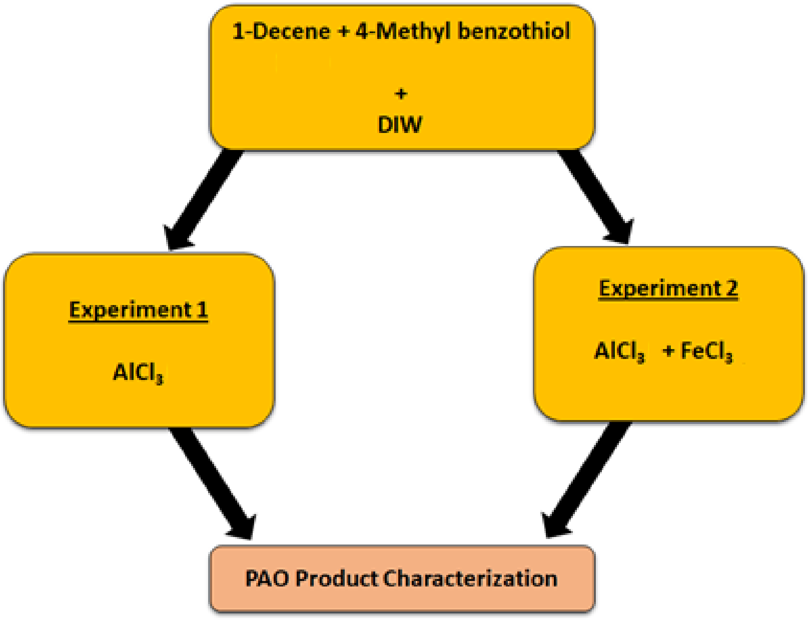

Figure 4.13: Flowchart for Experimental Studies on effect of Sulphur impurities

4.5.2 Experiment 1 1-Decene and 4-methylbenzothiol mixture with only $AlCl_3$

To a stirred solution of 1-Decene (99 g) + 4-methylbenzothiol (1 g) in flask, $AlCl_3$ (2 wt%) followed by catalytic amount of de-ionized water (0.4 eq with respect to catalyst) is added. The flask was quickly set-up with condenser and the reaction was continued at 100 °C for 6 h. This temperature and time values were kept constant for all the further experiments. For stopping the reaction, firstly the temperature is decreased to room temperature and then the reactor contents were transferred to another separating funnel and then quenched with water (20 mL). The separated water-layer (bottom layer) from the separating funnel was collected and discarded. The top layer in the separating funnel was washed again with water (2 x 20 mL) and the separated water layer was discarded. Top layer was then collected and dried over anhydrous sodium sulfate and filtered. Collected filtrate was concentrated using rotary evaporator to obtain the polyalphaolefin product. Collected filtrate is submitted for Sulphur quantification using WD XRF.

Sulfur percentage in the feed: 1%
Sulfur percentage in the PAO product: 0.7%

4.5.3 Experiment 2: 1-Decene and 4-methylbenzothiol mixture with $AlCl_3$ + $FeCl_3$ (1:1)

To a stirred solution of 1-Decene (99 g) + 4-methylbenzothiol (1 g) in flask, $AlCl_3$ (2 wt%) + $FeCl_3$ (3 g) followed by catalytic amount of de-ionized water (0.4 eq with respect to catalyst) is added. The flask was quickly set-up with condenser and the reaction was continued at 100 ^oC for 6 h. For stopping the reaction, firstly the temperature is decreased to room temperature and then the reactor contents were transferred to another separating funnel and then quenched with water (20 mL). The separated water-layer (bottom layer) from the separating funnel was collected and discarded. The top layer in the separating funnel was washed again with water (2 x 20 mL) and the separated water layer was discarded. Top layer was then collected and dried over anhydrous sodium sulfate and filtered. Collected filtrate was concentrated using rotary evaporator to obtain the polyalphaolefin product. Collected filtrate is submitted for Sulphur quantification using WD XRF. Collected filtrate is submitted for Sulphur quantification using WD XRF.

Sulfur percentage in the feed: 1%
Sulfur percentage in the PAO product: < 30 ppm

Comparison of sulphur content in feed and PAO for 1-decene oligomerized with only $AlCl_3$ and $AlCl_3$ + $FeCl_3$ (1:1) mixture is listed in Table 4.3.

Table 4.3: Comparison of sulphur content in feed and PAO for 1-decene oligomerized with only $AlCl_3$ and $AlCl_3$ + $FeCl_3$ (1:1) mixture

Sr. No.	Experiment no. & Catalyst system	Feed sulphur content (%)	Sulphur content in PAO
1	Exp. 1 $AlCl_3$ only	1	0.7 %
2	Exp. 2 $AlCl_3$ + $FeCl_3$ (1:1)	1	< 30 ppm

From Table 4.3, it can be observed that sulphur content was lower in PAO synthesized using experiment 2 as compared to experiment 1, indicating less incorporation of sulphur in the product, assuring product of controllable quality.

4.5.4 Results & Discussions

The oligomerization was conducted with conventional $AlCl_3$ catalyst and blend containing $FeCl_3$ and $AlCl_3$ in 1:1 ratio. Subsequent to the reaction, the oligomer product mixture was characterized with High Temperature-sulfur simdis and LC-MS analysis. In the sulfur simdis analysis, the sulfur compound distribution mediated by $AlCl_3$ catalyst (Figure 4.14.b) showed over a wide range of PAO boiling point (250 to 700 °C). Whereas the $AlCl_3$/$FeCl_3$ (1:1) blend sulfur simdis (Figure 4.14.a) exhibited a major peak appears at 200 °C, indicating the ability of blend catalyst preventing the incorporation of thiol group onto the PAO backbone. Furthermore, in the crude reaction mixture LC-MS spectrum mediated by $AlCl_3$ (Figure 4.15), the several peaks were observed in the range of 1-decene oligomers, indicating the side reactions of thiol during the 1-decene oligomerization reaction. In the case of blend catalyst, the crude reaction mixture LC-MS spectrum (Figure 4.16) exhibited the peaks corresponded to the adducts of dimer and trimer with formic acid without any significant side products, indicating the ability of $AlCl_3/FeCl_3$ blend catalysts trapping the thiol compound.

HT-SIMDIS carbon profiles of 1-decene oligomerization with $AlCl_3/FeCl_3$ blend catalysts after 120 minutes of reaction time.

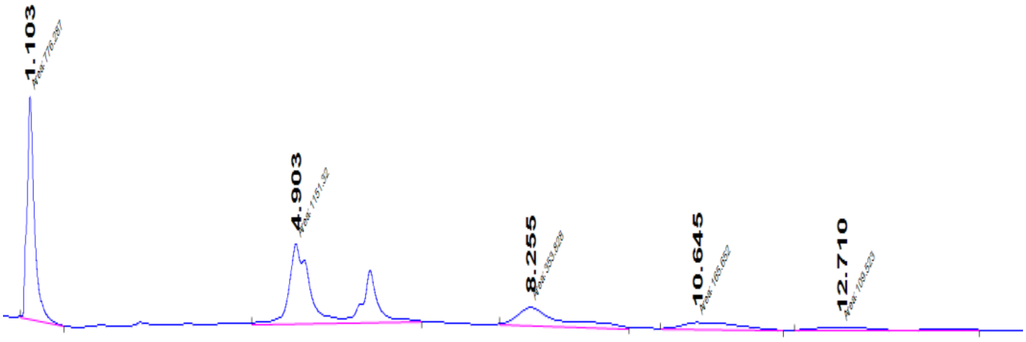

Figure 4.14.a 1-decene oligomerization carbon simdis profile with $FeCl_3$ at 75^0C

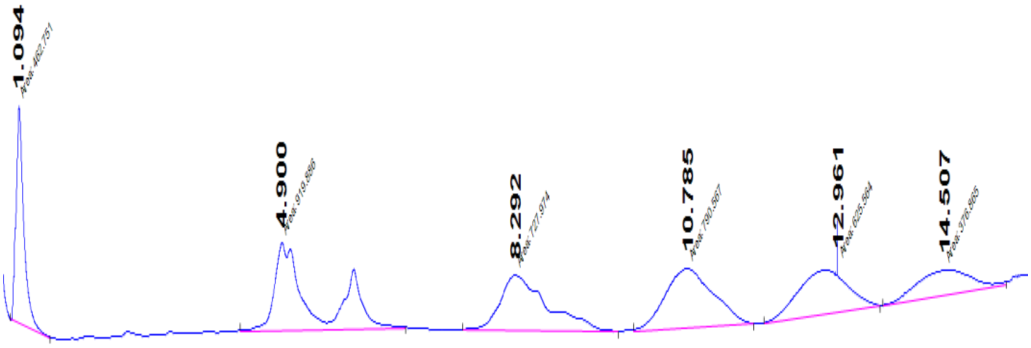

Figure 4.14.b 1-decene oligomerization carbon simdis profile with $FeCl_3:AlCl_3$ (0.5:0.5) at 75^0C

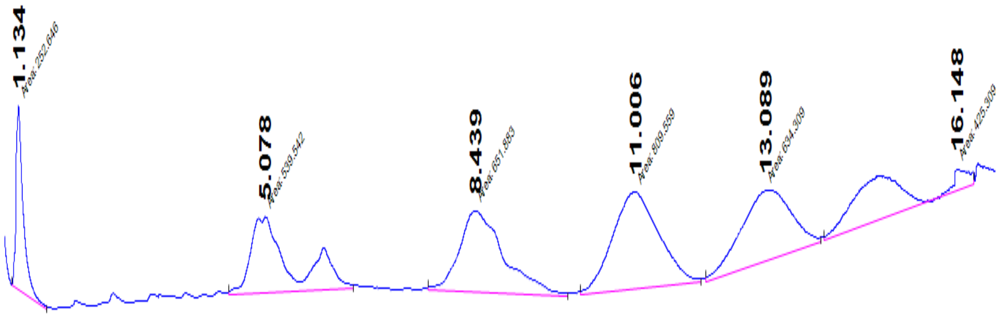

Figure 4.14.c 1-decene oligomerization carbon simdis profile with $AlCl_3$ at 75^0C

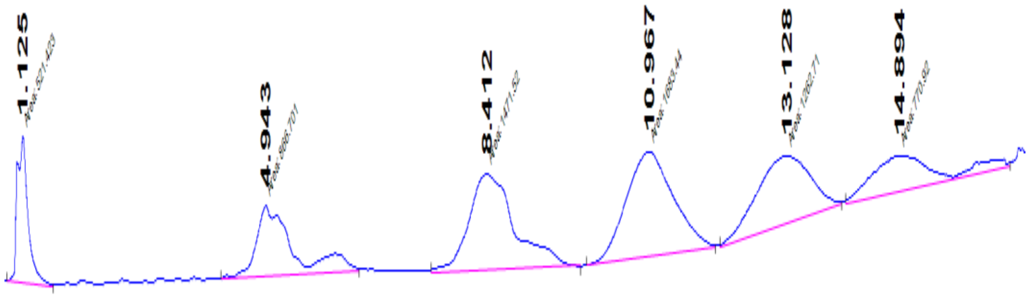

Figure 4.14.d 1-decene oligomerization carbon simdis profile with $FeCl_3$:$AlCl_3$ (0.3:0.7) at 75^0C

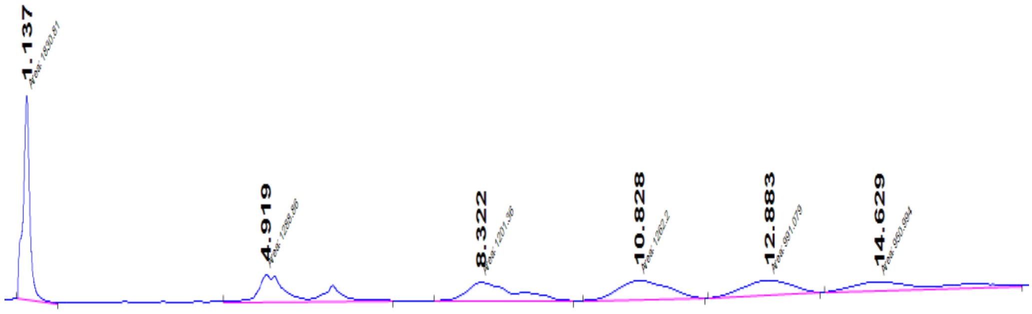

Figure 4.14.e 1-decene oligomerization carbon simdis profile with $FeCl_3$:$AlCl_3$ (0.7:0.3) at 75^0C

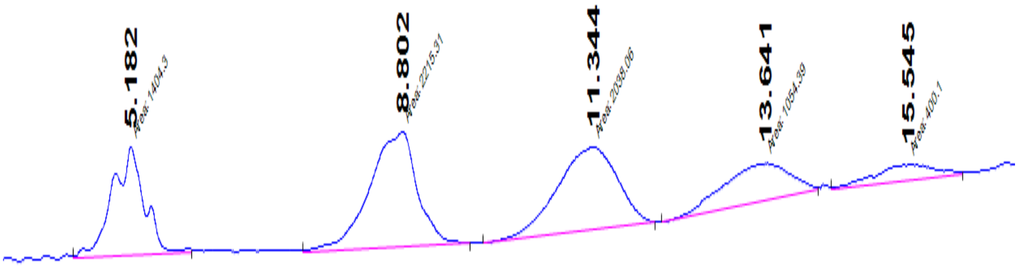

Figure 4.14.f 1-decene oligomerization carbon simdis profile with $AlCl_3$ at 100^0C

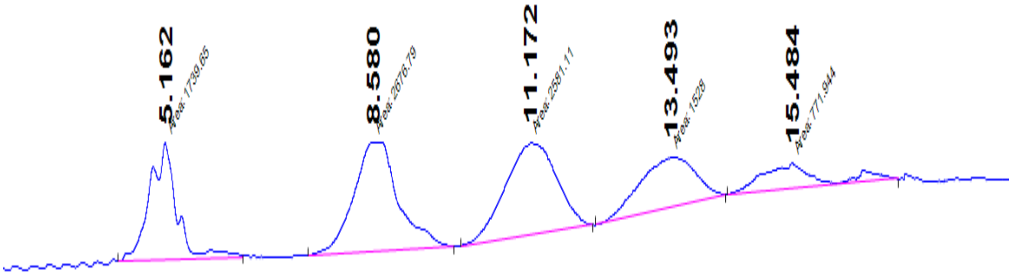

Figure 4.14.g 1-decene oligomerization carbon simdis profile with $FeCl_3$:$AlCl_3$ (0.3:0.7) at 100^0C

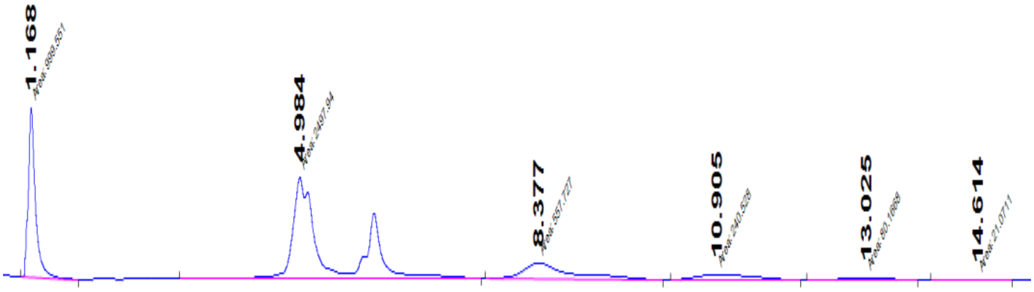

Figure 4.14.h 1-decene oligomerization carbon simdis profile with $FeCl_3$ at 100^0C

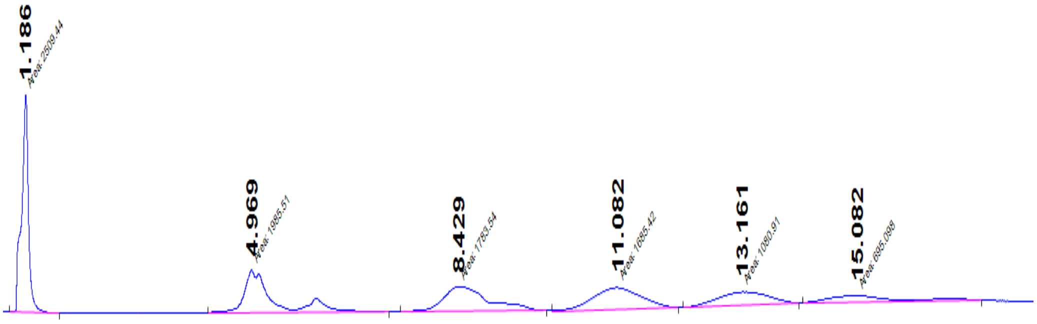

Figure 4.14.i 1-decene oligomerization carbon simdis profile with $FeCl_3$:$AlCl_3$ (0.7:0.3) at 100^0C

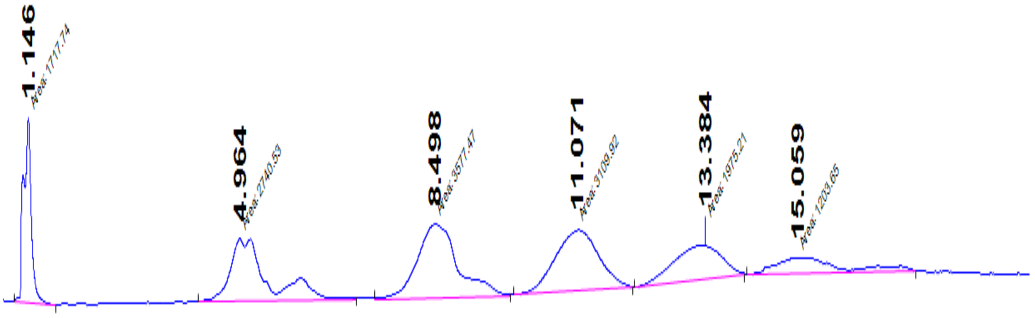

Figure 4.14.j 1-decene oligomerization carbon simdis profile with $FeCl_3$:$AlCl_3$ (0.5:0.5) at 100 ^{0}C

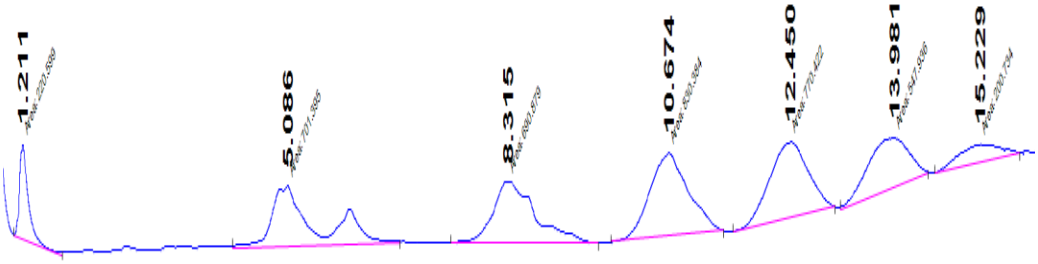

Figure 4.14.k 1-decene oligomerization carbon simdis profile with $AlCl_3$ at 50 ^{0}C

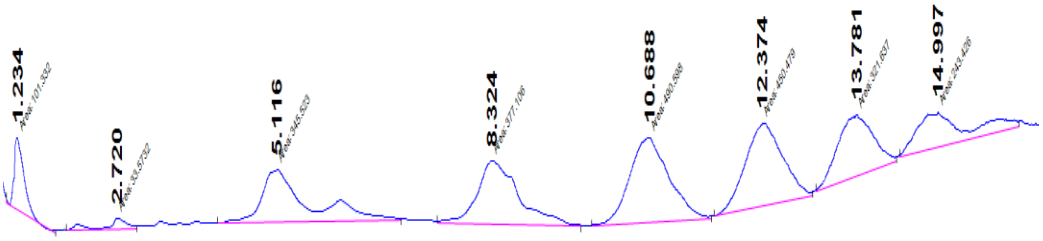

Figure 4.14.l 1-decene oligomerization carbon simdis profile with $FeCl_3$:$AlCl_3$ (0.3:0.7) at 50 ^{0}C

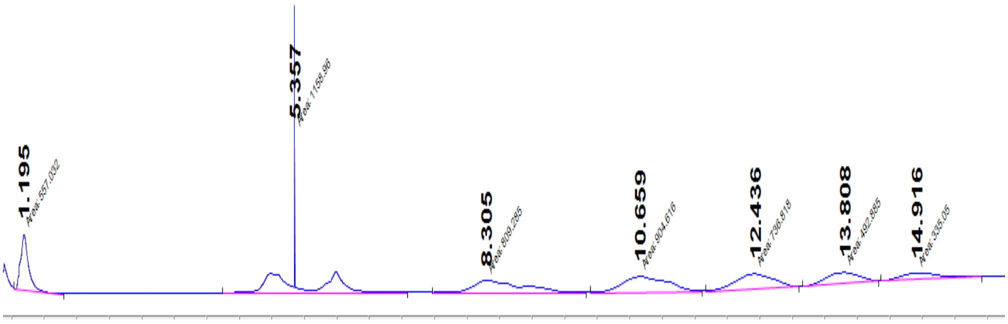

Figure 4.14.m 1-decene oligomerization carbon simdis profile with $FeCl_3$:$AlCl_3$ (0.5:0.5) at 50^{0}C

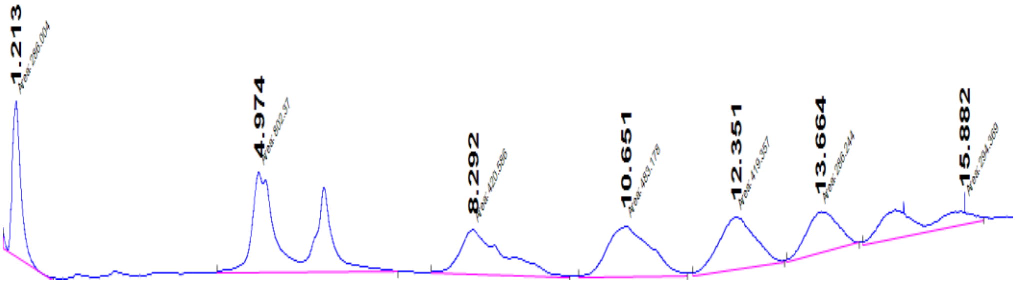

Figure 4.14.n 1-decene oligomerization carbon simdis profile with $FeCl_3$:$AlCl_3$ (0.7:0.3) at 50^{0}C

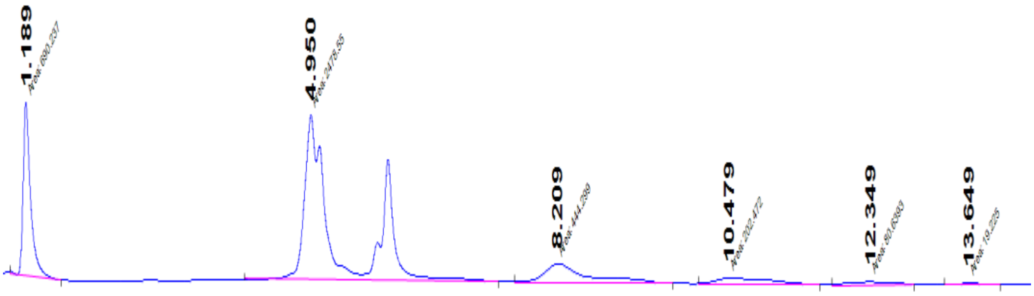

Figure 4.14.o 1-decene oligomerization carbon simdis profile with $FeCl_3$ at 50^0C

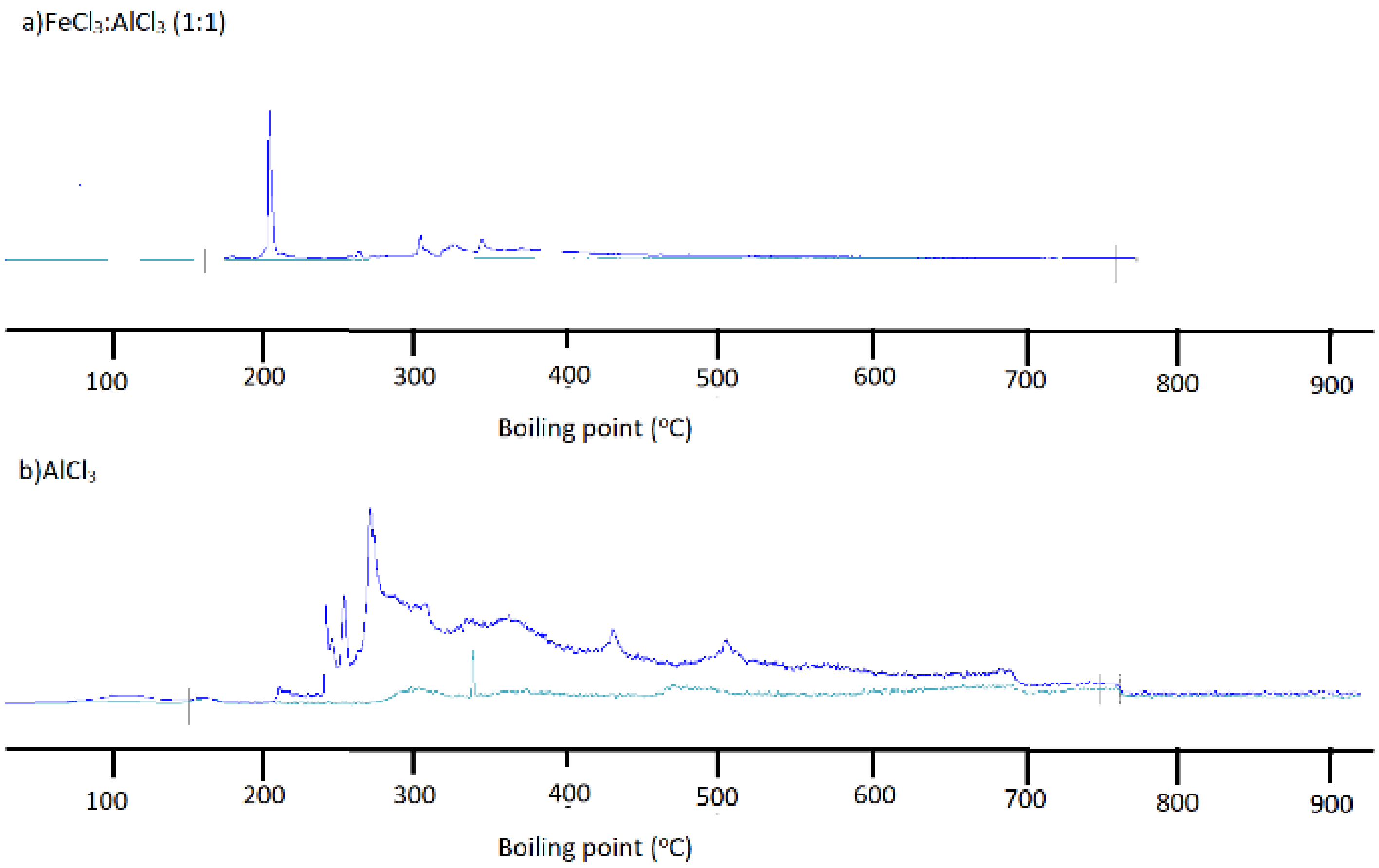

Figure 4.15: The sulfur Simdis profile of 1-decene oligomerization reaction with thiol compound in the presence of $AlCl_3$ and $FeCl_3$:$AlCl_3$ catalyst. Blank spectrum is also shown for both the samples

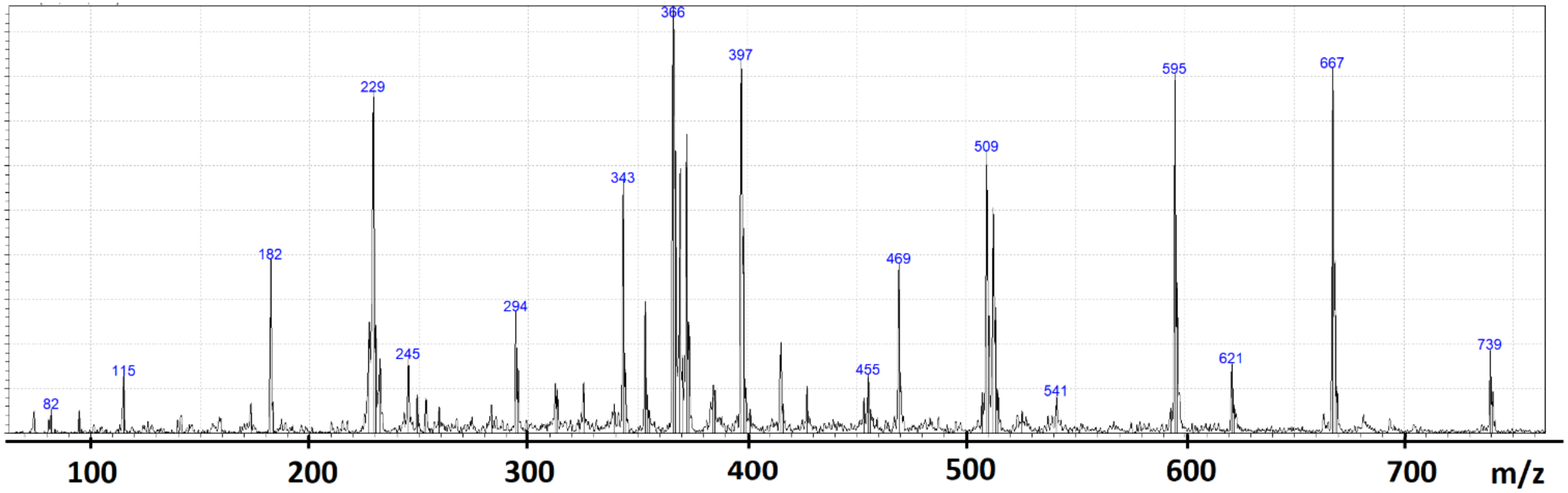

Figure 4.16: The LC-MS spectrum of 1-decene oligomerization reaction with thiol compound in the presence of $AlCl_3$ catalyst

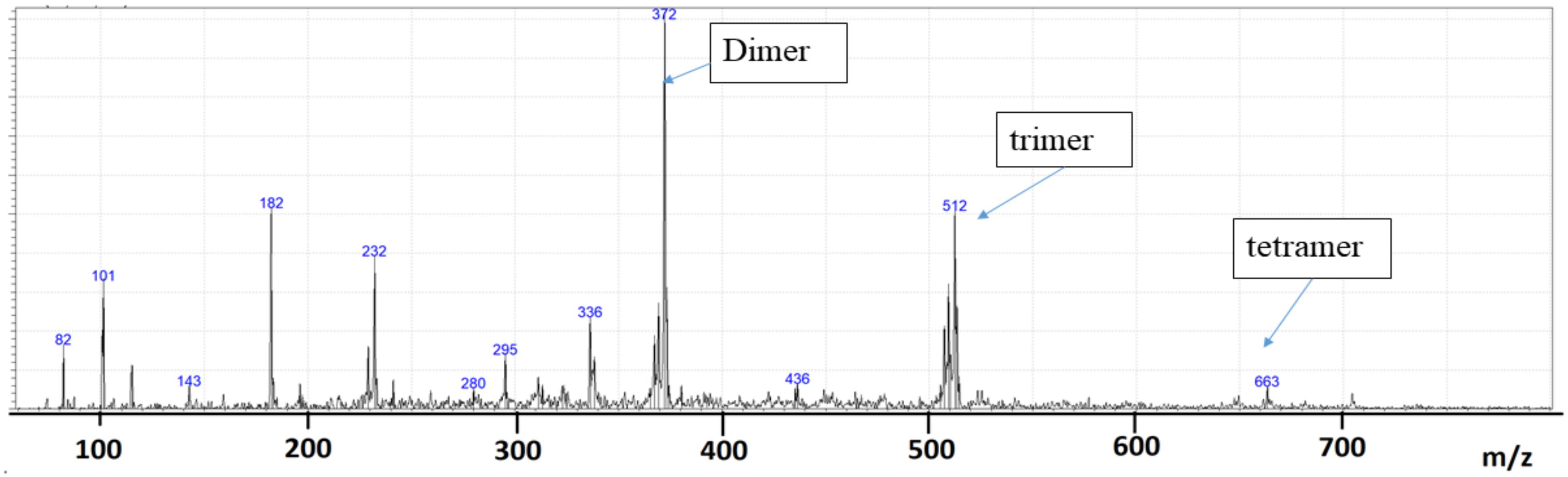

Figure 4.17: The LC-MS spectrum of 1-decene oligomerization reaction with thiol compound in the presence of $FeCl_3$:$AlCl_3$ catalyst

4.6 Experimental Studies on Effect of 1-octene / 1-dodecene monomer ratio

4.6.1 Reaction procedure

To a stirred solution of 1-octene (30 mL) and $AlCl_3$ (2 wt%) were stirred together, followed by addition of catalytic amount of de-ionized water (0.4 eq with respect to catalyst). The flask was quickly set-up with condenser and the reaction was continued at 50 °C for a duration of about 16 h. With this as the base, multiple variants of experiments have been deigned. The various experimental procedures carried out are illustrated in the Figure 4.18

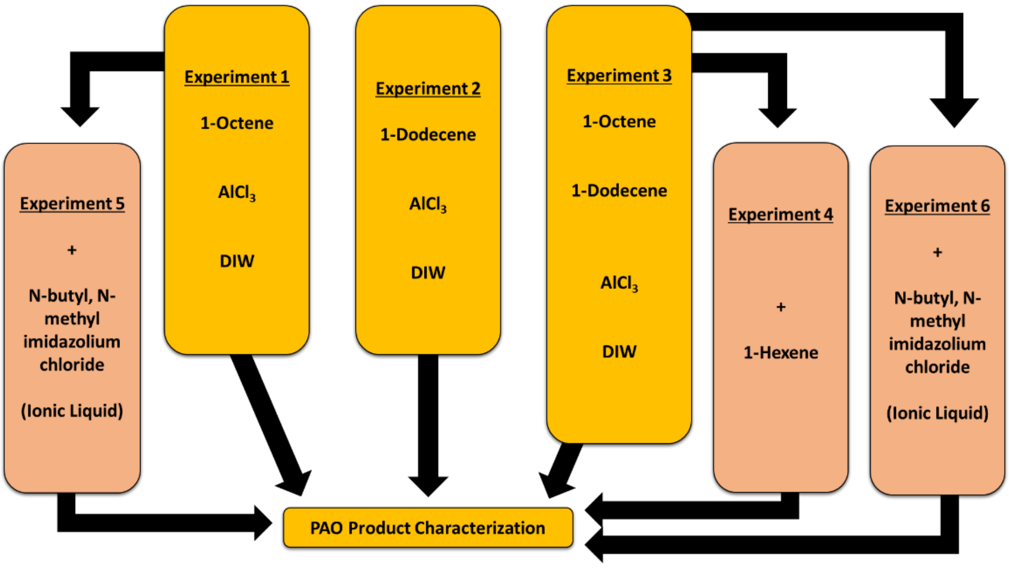

Figure 4.18: Flowchart for Experimental Studies on effect of 1-octene / 1-dodecene monomer ratio

4.6.2 Experiment 1: Only 1-octene

To a stirred solution of 1-octene (30 mL) and $AlCl_3$ (2 wt%) were stirred together, followed by addition of catalytic amount of de-ionized water (0.4 eq with respect to catalyst). The flask was quickly set-up with condenser and the reaction was continued at 50 °C for a duration of about 16 h. This temperature and time values were kept constant for all the further experiments. For stopping the reaction, firstly the temperature is decreased to room temperature and then the reactor contents were transferred to another separating funnel and then quenched with water (20 mL). The separated water-layer (bottom layer) from the separating funnel was collected and discarded. The top layer in the separating funnel was washed again with water (2 x 20 mL) and the separated water layer was discarded. Top layer was then collected and dried over anhydrous sodium sulfate and filtered. Collected filtrate was concentrated using rotary evaporator to obtain the polyalphaolefin product.

Properties of the obtained PAO product is detailed below:

- Viscosity at 40 ^{o}C (cSt): 35.2
- Viscosity at 100 ^{o}C (cSt): 6.4
- Viscosity Index (ASTM D2270): 136
- Pour point (ASTM D7346, ^{o}C): -66

4.6.3 Experiment 2: Only 1-dodecene

To a stirred solution of 1-dodecne (30 mL) and $AlCl_3$ (2 wt%) were stirred together, followed by addition of catalytic amount of de-ionized water (0.4 eq with respect to catalyst). The flask was quickly set-up with condenser and the reaction was continued at 50 ^{o}C for a duration of about 16 h. This temperature and time values were kept constant for all the further experiments. For stopping the reaction, firstly the temperature is decreased to room temperature and then the reactor contents were transferred to another separating funnel and then quenched with water (20 mL). The separated water-layer (bottom layer) from the separating funnel was collected and discarded. The top layer in the separating funnel was washed again with water (2 x 20 mL) and the separated water layer was discarded. Top layer was then collected and dried over anhydrous sodium sulfate and filtered. Collected filtrate was concentrated using rotary evaporator to obtain the polyalphaolefin product.

Properties of the obtained PAO product is detailed below:

- Viscosity at 40 ^{o}C (cSt): 94.4
- Viscosity at 100 ^{o}C (cSt): 14.3
- Viscosity Index (ASTM D2270): 158

- Pour point (ASTM D7346, ^{o}C): -53

4.6.4 Experiment 3: Mixture of 1-octene and 1-dodecene (1:1)

To a stirred solution of 1-octene (15mL), 1-dodecne (15 mL) and $AlCl_3$ (2 wt%) were stirred together, followed by addition of catalytic amount of de-ionized water (0.4 eq with respect to catalyst). The flask was quickly set-up with condenser and the reaction was continued at 50 ^{o}C for a duration of about 16 h. This temperature and time values were kept constant for all the further experiments. For stopping the reaction, firstly the temperature is decreased to room temperature and then the reactor contents were transferred to another separating funnel and then quenched with water (20 mL). The separated water-layer (bottom layer) from the separating funnel was collected and discarded. The top layer in the separating funnel was washed again with water (2 x 20 mL) and the separated water layer was discarded. Top layer was then collected and dried over anhydrous sodium sulfate and filtered. Collected filtrate was concentrated using rotary evaporator to obtain the polyalphaolefin product.

Properties of the obtained PAO product is detailed below:

- Viscosity at 40 ^{o}C (cSt): 214.4
- Viscosity at 100 ^{o}C (cSt): 23.5
- Viscosity Index (ASTM D2270): 136
- Pour point (ASTM D7346, ^{o}C): -48

Table 4.4 compares the properties of PAOs obtained from experiments 1 to 3.

Table 4.4: Comparison of properties of PAO obtained from experiments 1 to 3

Properties	Experiment 1	Experiment 2	Experiment 3	Commercial PAO
Viscosity @ 40 oC (cSt)	35.2	94.4	214.4	19
Viscosity @ 100 ^{o}C(cSt)	6.4	14.3	23.5	4.1

Viscosity Index (ASTM D2270)	136	158	136	126
Pour point (ASTM D7346), ^{o}C	-66	-53	-48	-66

It can be observed that PAO prepared using 1-dodecene demonstrated higher values of performance properties than that prepared using 1-octene. Moreover, on mixing them in1:1 ratio and subsequent PAO synthesis, the synthesized PAO copolymer PAO showed values even higher than that of PAOs prepared with individual monomers. Also, it can be seen that PAO prepared in experiment 1 (only 1-octene) showed performance properties closer to commercial PAO.

However, for the study purpose, extreme cases obtained in the study were re-synthesized with the presence of ionic liquid, and were prepared in experiments 5 and 6.

As illustrated in Figure 18, experiment 4 was performed as an extension of experiment 3 to investigate if addition of low molecular weight monomer (1-hexen) can bring down the properties of the synthesized PAO as per experiment 3 to nearer to commercial PAO, and the obtained properties were compared to those of experiment 3 and commercial PAO subsequently.

4.6.5 Experiment 4: Mixture of 1-octene, 1-dodecene and 1-hexene (1:1:1)

To a stirred solution of 1-octene (15mL), 1-dodecne (15 mL), 1-hexene (15 mL) and $AlCl_3$ (2 wt%) were stirred together, followed by addition of catalytic amount of de-ionized water (0.4 eq with respect to catalyst). The flask was quickly set-up with condenser and the reaction was continued at 50 ^{o}C for a duration of about 16 h. This temperature and time values were kept constant for all the further experiments. For stopping the reaction, firstly the temperature is decreased to room temperature and then the reactor contents were transferred to another separating funnel and then quenched with water (20 mL). The separated water-layer (bottom layer) from the separating funnel was collected and discarded. The top layer in the separating funnel was washed again with water (2 x 20 mL) and the separated water layer was discarded. Top layer was then collected and dried over anhydrous sodium sulfate and filtered. Collected filtrate was concentrated using rotary evaporator to obtain the polyalphaolefin product.

Properties of the obtained PAO product is detailed below:
Viscosity @ 40 ^{o}C (cSt): 201.8
Viscosity @ 100 ^{o}C (cSt): 22.1
Viscosity Index (ASTM D2270): 133
Pour point (ASTM D7346, ^{o}C): -48

Comparison of PAO synthesized in experiment 3 (1-octene:1-dodecene = 1:1), experiment 4 (1-octene:1-dodecene:1-hexene = 1:1:1) and commercial PAO is performed in Table 4.4.

Table 4.5: Comparison of properties of PAO obtained from experiments 3 and 4 with commercial PAO

Properties	**Experiment 3**	**Experiment 4**	**Commercial PAO**
Viscosity @ 40 oC (cSt)	214.4	201.8	19
Viscosity @ 100 ^{o}C(cSt)	23.5	22.1	4.1
Viscosity Index (ASTM D2270)	136	133	126
Pour point (ASTM D7346), ^{o}C	-48	-48	-66

It can be seen that addition of 1-hexene has no appreciable effect on the performance properties of PAO synthesized using experiment 3.

As discussed earlier, extreme cases obtained in the study were re-synthesized with the presence of ionic liquid, and were prepared in experiments 5 and 6.

4.6.6 Experiment 5: Mixture of 1-octene with ionic liquid

To a flask ionic liquid (*N*-butyl, *N*-methyl imidazolium chloride) (3 g) is added in glove box and sealed properly. The flask is taken out from glove box and 1-octene (30 mL), $AlCl_3$ (2 wt%) are added into the flask in fume hood under nitrogen supply. The flask was quickly set-up with condenser and the reaction was continued at 50 ^oC for a duration of about 16 h. This temperature and time values were kept constant for all the further experiments. For stopping the reaction, firstly the temperature is decreased to room temperature and then the reactor contents were transferred to another separating funnel and then quenched with water (20 mL). The separated water-layer (bottom layer) from the separating funnel was collected and discarded. The top layer in the separating funnel was washed again with water (2 x 20 mL) and the separated water layer was discarded. Top layer was then collected and dried over anhydrous sodium sulfate and filtered. Collected filtrate was concentrated using rotary evaporator to obtain the polyalphaolefin product.

The PAO product is then characterized and results are given below.
Viscosity @ 40 ^oC (cSt): 47.3
Viscosity @ 100 ^oC (cSt): 8.3
Viscosity Index (ASTM D2270): 152
Pour point (ASTM D7346, ^oC): -66

4.6.7 Experiment 6: Mixture of 1-octene and 1-dodecene with ionic liquid

To a flask ionic liquid (*N*-butyl, *N*-methyl imidazolium chloride) (3 g) is added in glove box and sealed properly. The flask is taken out from glove box and 1-octene + 1-dodecene (1:1 volume ratio) (30 mL), $AlCl_3$ (6 g) are added into the flask in fume hood under nitrogen supply. The flask was quickly set-up with condenser and the reaction was continued at 50 ^{o}C for a duration of about 16 h. This temperature and time values were kept constant for all the further experiments. For stopping the reaction, firstly the temperature is decreased to room temperature and then the reactor contents were transferred to another separating funnel and then quenched with water (20 mL). The separated water-layer (bottom layer) from the separating funnel was collected and discarded. The top layer in the separating funnel was washed again with water (2 x 20 mL) and the separated water layer was discarded. Top layer was then collected and dried over anhydrous sodium sulfate and filtered. Collected filtrate was concentrated using rotary evaporator to obtain the polyalphaolefin product.

The PAO product is then characterized and results are given below.
Viscosity @ 40 ^{o}C (cSt): 71.7
Viscosity @ 100 ^{o}C (cSt): 11.5
Viscosity Index (ASTM D2270): 155
Pour point (ASTM D7346, ^{o}C): -56

Comparison of PAO synthesized in experiments 1 (1-octene), experiment 2 (1-octene:1-dodecene = 1:1), experiment 5 (mixture of 1-octene with ionic liquid) and experiment 6 (mixture of 1-octene and 1-dodecene with ionic liquid) with commercial PAO is performed in Table 4.6.

Table 4.6: Comparison of properties of PAO obtained from experiments 1, 3, 5 and 6 with commercial PAO

Properties	**Experiment 1**	**Experiment 3**	**Experiment 5**	**Experiment 6**	**Commercial PAO**
Viscosity @ 40 oC (cSt)	35.2	214.4	47.3	71.7	19
Viscosity @ 100 ^{o}C(cSt)	6.4	23.5	8.3	11.5	4.1

Viscosity Index (ASTM D2270)	136	136	152	155	126
Pour point (ASTM D7346), °C	-66	-48	-66	-56	-66

Thus, it can be seen that PAO prepared with addition of ionic liquid had no directional effect in upgrading the properties of the PAOs and were no where match to that of commercial PAO sample.

Study with 1-decene (one of the very important monomer for PAO synthesis) was performed separately, and is explained next in the chapter.

4.7 Summary

Various experiments were conducted using model compounds. Tuneable Lewis acidity was tried through judicious combinations of different Lewis acids with varied strength reagents. For instance, group 13 halides are strong Lewis acids (BF_3, $AlCl_3$) whereas transition metals halides ($FeCl_3$) salts are milder. Though the transition metal halide-based Lewis acids are reported for other key organic transformations, use in alpha olefin oligomerization is barely explored.

The conversions for Lewis acid blend catalysts at various temperatures were studied. The conversion for catalyst $AlCl_3$ was found to be increasing with temperature and same is well documented. On the other hand, for the catalysts containing $FeCl_3$, the conversions decreased with increase in temperature from 50 to 100 °C. The abnormal behavior of the $FeCl_3$ may be due to different mechanistic pathway different from conventional pathway.

The product composition for 1-decene oligomerization was found to be critically dependent on temperature and residence time. The conversion with $AlCl_3$ was found to increase with increase in temperature, whereas the iron-based catalysts showed the reverse trend. The iron-based catalysts selectively yielded dimer or 2 cst grade PAO whereas with increasing $AlCl_3$ in the catalyst blend the oligomer ratio shifted towards to tetramer and higher oligomers. For a particular catalyst, with increase in temperature, the oligomer ratio is shifted towards lighters (dimer and trimer) due to faster termination kinetics in comparison with the propagation.

In order to verify the thio-affinity of $FeCl_3$ and $AlCl_3$ blend catalysts, a model synthetic mixture containing propane thiol in 1-decene was chosen for oligomerization reaction. It was observed that sulphur content was lower in PAO synthesized using $FeCl_3$ and $AlCl_3$ as compared to experiment using only $AlCl_3$, indicating less incorporation of sulphur in the product, assuring product of controllable quality.

CHAPTER 5

SYNTHESIS OF PAO FROM LOW VALUE FEED STOCKS

5.1 Overview

5.1.1 Conventional process for PAO synthesis

The conventional PAO synthesis [69,70, 71] is achieved in two major steps involving (i) Oligomerization of ethylene to make linear alpha olefins (ii) Oligomerization / polymerisation of linear alpha olefins to PAOs as depicted in Figure 5.1. In the first step, ethylene is subjected to controlled polymerization to obtain the mixture of higher alkenes. The mixture of alkenes on further upon separation yields the desired linear alpha olefins, which are starting materials for PAO synthesis. In the second step, the linear alpha olefins are subjected to oligomerization / polymerisation to obtain the polymers of low molecular weight. The catalysts used for these two oligomerization processes are slightly different and mostly product driven. [65-68]

Figure 5.1: Conventional process for PAO synthesis

Synthesis of PAO is executed using the cationic polymerization technique. Some of the catalysts used in the cationic polymerization technique are generally Lewis acids namely aluminium chloride ($AlCl_3$) or boron trifluoride (BF_3); whereas some of the promoters used are water (H_2O), carboxylic acid (R-COOH), alkyl halides (RX), alcohols (R-OH) and ethers (R-O-R). Some research papers had reported synthesis of synthetic lubricants by oligomerization of α-olefins using a group IV metal oxide bed. Hamilton *et al*. reported synthesis of PAO oligomers from α-olefins using organic peroxide, Friedel-Crafts catalysts and also by thermal initiation polymerization method; stability of which is increased by further hydrogenation step.

5.1.2 Limitations of Conventional PAO Synthesis

In spite of the advantages and the market demand of the PAOs, their use as synthetic base oils is still limited because of the cost and availability of feed stocks, which face competition from other applications. The conventional PAO synthesis route suffers from high cost, as this route is from high value ethylene. Hence there is a need for development of alternative cost effective routes for the production of PAO lubricants. Furthermore, there is a need to produce the polyalphaolefin lubricants with the improvement in the performance to meet the market demand.

It is imperative to reduce the production costs of PAO base oils stocks. The production cost can be reduced by either developing a low value feedstock which has the potential to produce PAO or selecting a process which can be cost effective. However, as the major factor in cost of PAO is the availability and cost of feed stocks.

5.2 Proposed Alternate process for PAO Synthesis

The focus in this particular research has been to select a low value feedstock and development of a novel process [72 - 79] for production of PAOs as depicted in Figure 5.2.

Refineries being complex and integrated with various unit operations / processes like distillation, catalytic cracking, thermal cracking, coking, solvent extraction, solvent dewaxing, reforming, hydrogenation, etc., for handling of different feed stocks and meeting the desired fuel specifications, numerous options will be available for selecting the right feed stock. However, selecting the appropriate feeds stock from the options available is the most critical task. Literature indicates that the olefin rich streams with high linear alpha olefins (LAOs) or the streams with potential to transform into high LAOs are good building blocks for PAO production.

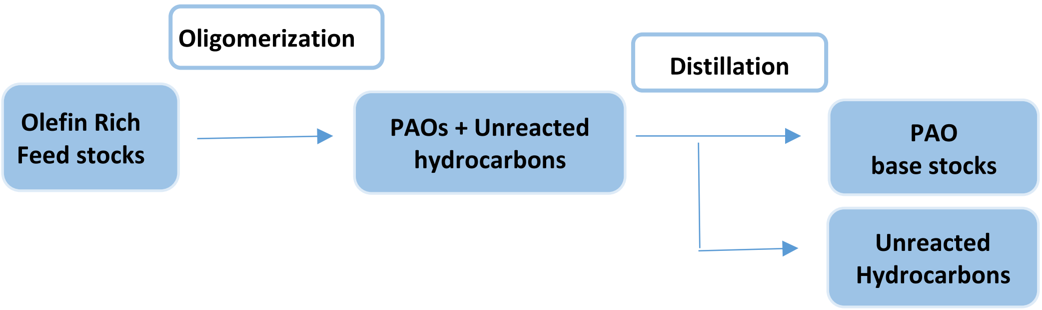

Figure 5.2: Proposed process for PAO synthesis

As discussed in Chapter 3, various refinery and non-refinery based streams (total 7) were studied such as 1. FCC-light cut naphtha (FCC LCN), 2. FCC-heavy cut naphtha (FCC HCN), 3. Delayed coker naphtha (DCN) 4. Visbreaker naphtha (VBN) 5. Wax 1 (C20 to C43), 6. Wax 2 (C30 to C70) and 7. Waste polyethylene (PE). The streams 1 and 2 are products out of a catalytic cracking process while streams 3 and 4 are produced out of thermal cracking units. These 4 streams were analysed for their LAO content using PONA. Streams 5 to 7 are heavy hydrocarbon materials and thus they are not directly suitable as feed stock for PAO production. Thus they needed to be thermally cracked before being analysed for LAO content.

As discussed in Chapter 4 of this thesis, by conducting a number of experiments with model compounds various judicious combinations of catalysts comprising of $AlCl_3/FeCl_3$ in different molar ratios [$AlCl_3$, $AlCl_3/FeCl_3$ (0.7:0.3), $AlCl_3/FeCl_3$ (0.5:0.5), $AlCl_3/FeCl_3$ (0.3:0.7), $FeCl_3$] varying in terms of Lewis acid strength, were identified. The identified catalyst system was also studied for scavenging of sulphur compounds present in the feed stocks.

5.3 Experimental Methodology for Oligomerization

Oligomerization of alpha olefin is performed using Lewis acids to produce synthetic group IV lubricants (PAO) in the current study [80 - 86] as depicted in the Figure 5.3. Some of the important lubricant properties are: viscosity index and pour point; which has strong correlation to its molecular structure. Generally, PAOs possess viscosity index of greater than 120, and pour point lower than -40 ^{o}C. Some of the factors of molecular structures affecting PAOs performance properties are:

- Higher the linear structure, higher the viscosity index
- Higher the branching structure, higher the pour point
- Length of the oligomer used in PAO synthesis also has significant effect on PAOs performance properties

Appropriate balance between linear and branched structure is required for production of lubricants with excellent lubricant properties. Other factors of

PAO synthesis [87 - 93] which can affect performance properties are: catalyst type and concentration, reaction conditions such as, temperature, time etc.

Of the numerous Lewis acids used as catalysts in PAO synthesis $BF_3.OEt_2$ dominate commercially. The commercial process involves oligomerization followed by distillation and blending the components in required ratios to obtain the different grades of PAO lubricants.

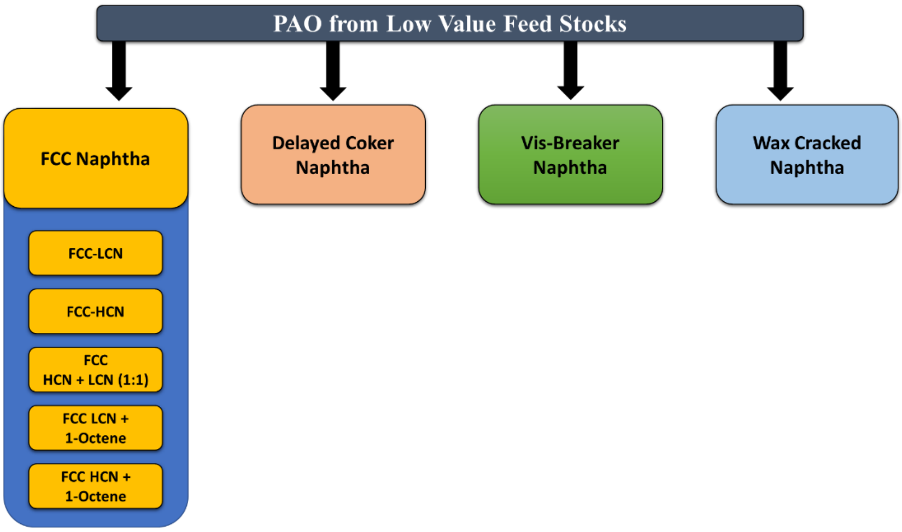

Figure 5.3: Flow chart of the study performed in the current chapter

5.3.1 Experimental Studies with FCC naphtha

The naphtha from FCC, namely, LCN and HCN were subjected to oligomerization in the presence of $AlCl_3$. The data obtained is summarized in Table 5.1. In the case of FCC-LCN and FCC-HCN, due to the presence of internal olefins, the VI values of the products of the oligomerization reaction are low (Exp. 1 and 2). The VI values did not improve even in the case of blend as a feed (Exp. 3). However, the pour point values are low due to high branching caused by oligomerizaiton of internal olefins. To improve the VI properties of the oligomers, 1-Octene was used as a co-monomer in the oligomerization reaction. With the addition of the 1-octene at the 1:1 volume ratio to that of FCC-LCN, the VI of the combined product was found to be 131 with the pourpoint of -70 ^{o}C. Whereas the VI of the oligomer product formed from the 1:1 volume ratio to that of FCC-LCN is 105 with the pour point of -67 ^{o}C. The addition of 1-Octene as co-monomer to the FCC naphtha helped in improving the key lubricant properties, namely, VI and pour point.

Table 5.1: Properties comparison of PAOs synthesized from FCC naphtha

Exp. No.	Alpha-olefin	Viscosity @ 40 °C (mm^2/s)	Viscosity @ 100 °C (mm^2/s)	Viscosity index	Pour point
1	FCC-LCN	4.99	1.59	---	-73 °C
2	FCC-HCN	5.25	1.61	---	-73 °C
3	FCC-LCN + FCC-HCN (1:1)	7.19	1.95	33	-69 °C
4	FCC-LCN + 1-Octene (1:1)	5.94	1.98	131	-70 °C
5	FCC-HCN + 1-Octene (1:1)	18.22	3.87	105	-67 °C

Details of the above experiments carried out using FCC Naphtha are described in the following sections.

5.3.1.1 Experiment 1: PAO from FCC-LCN

To a stirred solution in a round bottom flask consisting of FCC-LCN (400 mL), $AlCl_3$ (2 wt%) followed by catalytic amount of de-ionized water (0.4 eq with respect to catalyst) was added. The flask was quickly set-up with condenser and the reaction was continued at 50 °C for 16 h. Later, the reaction mixture was cooled down to room temperature and reaction contents were transferred into separating funnel. To this, 200 ml water for extracting the catalyst from the reaction mixture was added. The separated water-layer (bottom layer) from the separating funnel was collected and discarded. The top layer in the separating funnel was washed again with water (2 x 100 mL) and the separated water layer was discarded. Top layer was then collected and dried over anhydrous sodium sulfate. The collected filtrate was concentrated using rotary evaporator to obtain polyalphaolefin (PAO)

5.3.1.2 Experiment 2: PAO from FCC-HCN

To a stirred solution in a round bottom flask consisting of FCC-HCN (400 mL), $AlCl_3$ (2 wt%) followed by catalytic amount of de-ionized water (0.4 eq with respect to catalyst) was added. The flask was quickly set-up with condenser and the reaction was continued at 50 ^oC for 16 h. Later, the reaction mixture was cooled down to room temperature and reaction contents were transferred into separating funnel. To this, 200 ml water for extracting the catalyst from the reaction mixture was added. The separated water-layer (bottom layer) from the separating funnel was collected and discarded. The top layer in the separating funnel was washed again with water (2 x 100 mL) and the separated water layer was discarded. Top layer was then collected and dried over anhydrous sodium sulfate. The collected filtrate was concentrated using rotary evaporator to obtain polyalphaolefin (PAO).

5.3.1.3 Experiment 3: PAO from FCC-LCN + FCC-HCN (1:1)

To a stirred solution in a round bottom flask consisting of FCC-LCN + FCC-HCN (1:1: volume ratio) (400 mL), $AlCl_3$ (2 wt%) followed by catalytic amount of de-ionized water (0.4 eq with respect to catalyst) was added. The flask was quickly set-up with condenser and the reaction was continued at 50 ^oC for 16 h. Later, the reaction mixture was cooled down to room temperature and reaction contents were transferred into separating funnel. To this, 200 ml water for extracting the catalyst from the reaction mixture was added. The separated water-layer (bottom layer) from the separating funnel was collected and discarded. The top layer in the separating funnel was washed again with water (2 x 100 mL) and the separated water layer was discarded. Top layer was then collected and dried over anhydrous sodium sulfate. The collected filtrate was concentrated using rotary evaporator to obtain polyalphaolefin (PAO).

5.3.1.4 Experiment 4: PAO from FCC-LCN + 1-octene

To a stirred solution in a round bottom flask consisting of FCC-LCN + 1-octene (1:1 volume ratio) (60 mL), $AlCl_3$ (2 wt%) followed by catalytic amount of de-ionized water (0.4 eq with respect to catalyst) was added. The flask was quickly set-up with condenser and the reaction was continued at 50 ^oC for 16 h. Later, the reaction mixture was cooled down to room temperature and reaction contents were transferred into separating funnel. To this, 50 ml water for extracting the catalyst from the reaction mixture. The separated water-layer (bottom layer) from the separating funnel was collected and discarded. The top layer in the separating funnel was washed again with water (2 x 20 mL) and the separated water layer was discarded. Top layer was then collected and dried over anhydrous sodium sulfate. The collected filtrate was concentrated using rotary evaporator to obtain polyalphaolefin (PAO).

5.3.1.5 Experiment 5: PAO from FCC-HCN + 1-octene

To a stirred solution in a round bottom flask consisting of FCC-HCN + 1-Octene (1:1 volume ratio) (60 mL), $AlCl_3$ (2 wt%) followed by catalytic amount of de-ionized water (0.4 eq with respect to catalyst) was added. The flask was quickly set-up with condenser and the reaction was continued at 50 ^oC for 16 h. Later, the reaction mixture was cooled down to room temperature and reaction contents were transferred into separating funnel. To this, 50 ml water for extracting the catalyst from the reaction mixture. The separated water-layer (bottom layer) from the separating funnel was collected and discarded. The top layer in the separating funnel was washed again with water (2 x 20 mL) and the separated water layer was discarded. Top layer was then collected and dried over anhydrous sodium sulfate. The collected filtrate was concentrated using rotary evaporator to obtain polyalphaolefin (PAO).

5.3.2 Experimental Studies using delayed coker naphtha (DCN)

The $AlCl_3$ mediated oligomerization of DCN led to the PAOs with good viscosity index of 92 and the pour point of -71 ^oC at a temperate of 50^O C. By decreasing the acidity of the $AlCl_3$ with the combination of $FeCl_3$ yielded the PAOs with the Viscosity index of 134 and the pour point of -67 ^oC at a temperate of 100^O C. Due to the presence of linear alpha olefins, DCN naphtha could be a potential feedstock for PAO production. Table 5.2 provides comparison of properties of PAOs synthesized from DCN under two temperature conditions.

Table 5.2: Properties comparison of PAOs synthesized from DCN

Exp. No.	Alpha-olefin	Viscosity @ 40 °C (mm^2/s)	Viscosity @ 100 °C (mm^2/s)	Viscosity index	Pour point
1	DCN at 50°C	9.81	2.59	92	-71 °C
2	DCN at 100°C	9.1	2.64	130	-67 °C

Details of the above experiments carried out using DCN are described in the following sections:

5.3.2.1 Experiment 1: PAO from DCN at 50 °C

To a stirred solution in a round bottom flask consisting of Delayed Coker Naphtha (400 mL), $AlCl_3$ (2 wt%): $FeCl_3$(2 wt%) followed by catalytic amount of de-ionized water (0.4 eq with respect to catalyst) was added. The flask was quickly set-up with condenser and the reaction was continued at 50 °C for 16 h. Later, the reaction mixture was cooled down to room temperature and reaction contents were transferred into separating funnel. To this, 200 ml water for extracting the catalyst from the reaction mixture was added. The separated water-layer (bottom layer) from the separating funnel was collected and discarded. The top layer in the separating funnel was washed again with water (2 x 100 mL) and the separated water layer was discarded. Top layer was then collected and dried over anhydrous sodium sulfate. The collected filtrate was concentrated using rotary evaporator to obtain polyalphaolefin (PAO).

5.3.2.2 Experiment 2: PAO from DCN at 100 °C

To a stirred solution in a round bottom flask consisting of Delayed Coker Naphtha (400 mL), $AlCl_3$ (2 wt%): $FeCl_3$(2 wt%) followed by catalytic amount of de-ionized water (0.4 eq with respect to catalyst) was added. The flask was quickly set-up with condenser and the reaction was continued at 100 °C for 16 h. Later, the reaction mixture was cooled down to room temperature and reaction contents were transferred into separating funnel. To this, 200 ml water for extracting the catalyst from the reaction mixture was added. The separated water-layer (bottom layer) from the separating funnel was collected and discarded. The top layer in the separating funnel was washed again with water (2 x 100 mL) and the separated water layer was discarded. Top layer was then collected and dried over anhydrous sodium sulfate. The collected filtrate was concentrated using rotary evaporator to obtain polyalphaolefin (PAO).

5.3.3 Experimental Studies using Vis Breaker Naphtha (VBN)

Due to the presence lower olefins in the VBU naphtha, the viscosity of the oligomer product is too low for the synthetic lubes production. Table 5.3 provides comparison of properties of PAOs synthesized from VBN under two temperature conditions.

Table 5.3: Synthesis of PAOs from visbreaker naphtha

Exp. No.	Alpha-olefin	Viscosity at 40 °C(mm²/s)	Viscosity at 100 °C(mm²/s)	Viscosity index	Pour point
1	VBN at 50°C	3.61	1.34	---	-73 °C
2	VBN at 100°C	4.36	1.50	---	-73 °C

Details of the above experiments carried out using VBN are described in the following sections:

5.3.3.1 Experiment 1: PAO from VBN @ 50 °C

To a stirred solution in a round bottom flask consisting of Vis-breaker naphtha (400 mL), $AlCl_3$ (2 wt%) followed by catalytic amount of de-ionized water (0.4 eq with respect to catalyst) was added. The flask was quickly set-up with condenser and the reaction was continued at 50 °C for 16 h. Later, the reaction mixture was cooled down to room temperature and reaction contents were transferred into separating funnel. To this, 200 ml water for extracting the catalyst from the reaction mixture was added. The separated water-layer (bottom layer) from the separating funnel was collected and discarded. The top layer in the separating funnel was washed again with water (2 x 100 mL) and the separated water layer was discarded. Top layer was then collected and dried over anhydrous sodium sulfate. The collected filtrate was concentrated using rotary evaporator to obtain polyalphaolefin (PAO).

5.3.3.2 Experiment 2: PAO from VBN @ 100 °C

To a stirred solution in a round bottom flask consisting of Vis-breaker naphtha (400 mL), $AlCl_3$ (2 wt%) followed by catalytic amount of de-ionized water (0.4 eq with respect to catalyst) was added. The flask was quickly set-up with condenser and the reaction was continued at 100 °C for 16 h. Later, the reaction mixture was cooled down to room temperature and reaction contents were transferred into separating funnel. To this, 200 ml water for extracting the catalyst from the reaction mixture was added. The separated water-layer (bottom layer) from the separating funnel was collected and discarded. The top layer in the separating funnel was washed again with water (2 x 100 mL) and the separated water layer was discarded. Top layer was then collected and dried over anhydrous sodium sulfate. The collected filtrate was concentrated using rotary evaporator to obtain polyalphaolefin (PAO).

5.3.4 Synthetic lubricant (PAO) from Wax Cracked Naphtha (WCN)

The thermally cracked naphtha was oligomerized in the presence of $AlCl_3$. The VI of the product was found to be 166 with the pour point of -73 °C. The product meeting the specifications of synthetic lubricants, indicating the potential of wax cracked naphtha. Table 5.4 provides details of PAO synthesized from WCN in this experiment.

Table 5.4: Synthesis of PAOs from wax cracked naphtha

Exp. No.	Alpha-olefin	Viscosity at 40 °C (mm^2/s)	Viscosity at 100 °C(mm^2/s)	Viscosity index	Pour point
1	Wax cracked naphtha	6.08	2.08	166	-73 °C

Details of the above experiment carried out using WCN are described in the following sections:

5.3.4.1 Experiment 1: PAO from WCN

To a stirred solution in a round bottom flask consisting of Wax cracked naphtha, $AlCl_3/FeCl_3$ (9:1) (2 wt%), followed by catalytic amount of de-ionized water (0.4 eq with respect to catalyst) was added. The flask was quickly set-up with condenser and the reaction was continued at 100 ^{o}C for 16 h. Later, the reaction mixture was cooled down to room temperature and reaction contents were transferred into separating funnel. To this, 200 ml water for extracting the catalyst from the reaction mixture was added. The separated water-layer (bottom layer) from the separating funnel was collected and discarded. The top layer in the separating funnel was washed again with water (2 x 100 mL) and the separated water layer was discarded. Top layer was then collected and dried over anhydrous sodium sulfate. The collected filtrate was concentrated using rotary evaporator to obtain polyalphaolefin (PAO).

5.4 Benchmarking with Commercial PAO

Viscosity Index (VI) of various PAOs produced the experiments in this chapter using various feed stocks were benchmarked with the commercial PAO performance parameters (VI & Pour Point).

5.4.1 Commercial PAO Performance Properties

Performance properties determined for various grades of commercial PAOs, such as viscosity index and viscosities @40 ^{o}C and 100 ^{o}C are listed in Table 5.5. These values are helpful in comparing the in-house developed PAOs with the commercially available grades.

Table 5.5: Commercial grade PAOs

S.No	Commercial PAO grades	Visc at 40^{o}C	Visc at 100^{o}C	VI	Pour point ^{o}C
1	2 cSt	5.1	1.7	120	-73
2	4 cSt	16.8	3.8	124	-69
3	6 cSt	30.8	5.9	139	-62
4	8 cSt	46.2	7.8	138	-56

5.4.2 Experimental PAO Performance Properties Benchmarking

Viscosity Index (VI) of various PAOs produced the experiments in this chapter using various feed stocks were benchmarked with the commercial PAO performance parameters (VI & Pour Point). The results from the analysis are presented in Table 5.6

Table 5.6: Table benchmarking experimental results with commercial PAO

S. No.	Alpha-olefin	Visc at 40 °C	Visc at 100 °C	VI	Pour point	Benchmarking with Commercial PAO grades
1	FCC-LCN	4.99	1.59	VLV	-73 °C	Not meeting any commercial grade
2	FCC-HCN	5.25	1.61	VLV	-73 °C	Not meeting any commercial grade
3	FCC-LCN + FCC-HCN	7.19	1.95	33	-69 °C	Not meeting any commercial grade
4	FCC-LCN + 1-Octene	5.94	1.98	131	-70 °C	Meeting 2 & 4 cSt grades
5	FCC-HCN + 1-Octene	18.22	3.87	105	-67 °C	Not meeting any commercial grade
6	DCN at 50°C	9.81	2.59	92	-71 °C	Not meeting any commercial grade.
7	DCN at 100°C	9.1	2.64	130	-67 °C	Meeting 2 & 4 cSt grades
8	VBN at 50°C	3.61	1.34	VLV	-73 °C	Not meeting any commercial grade.
9	VBN at 100°C	4.36	1.50	VLV	-73 °C	Not meeting any commercial grade
10	Wax cracked naphtha	6.08	2.08	166	-73 °C	Meets VI requirement for ALL grades

The above analysis indicates that only Wax Cracked Naphtha (WCN) & Delayed Cocker Naphtha (DCN) meet the feed stock requirements for PAO production. It is interesting to note that these results are in line with the analysis made in Chapter 3 based on LAO content in feed stock.

FCC-LCN can also be used as Feed stock provided only if it is mixed with 1-Octene in 1:1 ratio. However, 1-Octene is fine material which is a costly input material not very suitable for large scale production.

5.5 Proposed Flow scheme for PAO production using feed stocks

Using WCN/DCN as feedstock, a process scheme was developed for production of PAO. The details of the proposed process scheme is outlined in Figure 5.4:

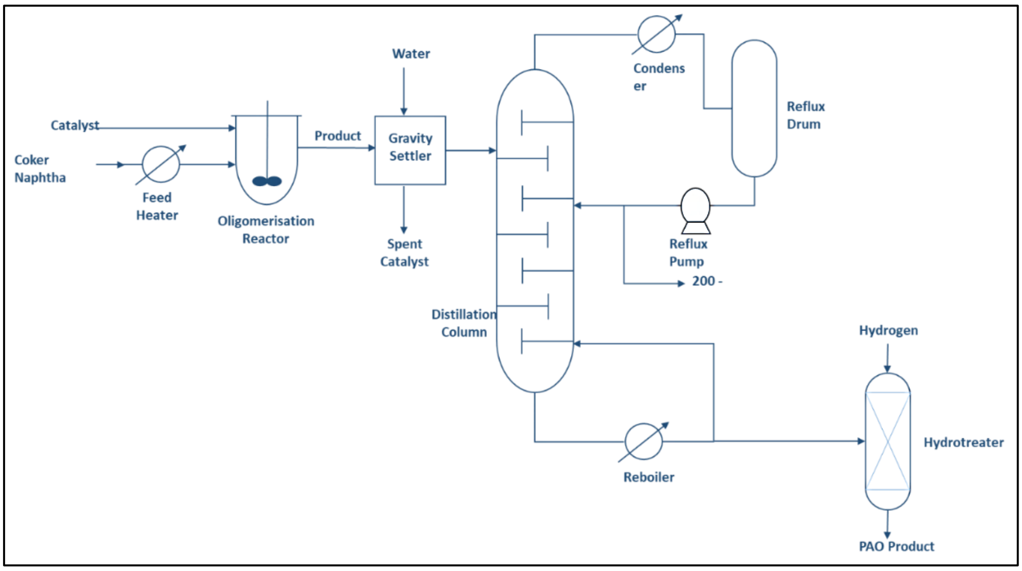

Figure 5.4: Process flow scheme for PAO production

Feed stream from a refinery unit is routed to a feed preheater where the feed stream is heated to the desired temperature for oligomerisation reaction. The feed along with the catalyst is routed through the Oligomerisation Reactor. The reactor is designed for a volume considering the required residence time for oligomerisation reaction to occur. During the oligomerisation reaction, the alpha-olefins in the feed are converted to poly alpha olefins. The product stream from the oligomerisation reactor will have a mixture of poly alpha olefins, spent catalyst and unreacted feedstock.

In the next step the product is mixed with water in a specific ratio and routed to a Gravity Settler. The water wash step will enhance the removal of spent catalyst from the product stream. The catalyst rich water stream is separated out from the remaining stream in the Gravity Settler due to the difference in densities. The balance stream is routed to a binary Distillation Column to separate out unreacted feed from the PAO product. The top draw from the column will have product which consists of the unreacted feed stocks. The bottom product consists of PAO rich streams.

Also, the effluent comprising of catalyst formulations ($AlCl_3$/$FeCl_3$) are treated with caustic. Upon reaction with caustic, the catalyst formulations are converted into Alumina, sodium chloride and iron oxide. These compounds are not toxic and can be treated along with process effluents in a refinery as per environmental norms.

5.6 Summary

In this study, various feed stocks such as FCC Naphtha (LCN, HCN & with 1-Octene), Delayed Coker Naphtha (DCN), Vis-Breaker Naphtha (VBN) and Wax Cracked Naphtha (WCN) were considered ad potential feedstock for PAO production using various combinations of Lewis acid catalysts.

The PAOs produced from the above feeds were benchmarked with performance parameters of commercial PAO grades. The resulting analysis indicated that only FCC LCN with 1-Octene, DCN & WCN were suitable as feed stocks for PAO production. However FCC-LCN can only be used if it is mixed with 1-Octene in 1:1 ratio. 1-Octene is a fine material which is a costly input material not very suitable for large scale production. Therefore, FCC LCN with 1-Octene is not recommended as a suitable feed stock.

A prospective process flow sheet for industrial production of PAO with feed stock was developed using WCN/DCN as feedstock.

CHAPTER 6

PROCESS MODELLING AND DESIGN

6.1 Overview

Process simulation models are used for scale up and design of Process plants. Several authors [94 - 106] have developed models for PAO production through the conventional ethylene oligomerization route.

Kinetic model was developed for ethylene oligomerization using zirconium/aluminium, and nickel/zinc-based catalyst system. The model predicted C4-C8 composition, within 10% confidence limits. The model prediction was good for low carbon components. However, as the carbon number increased, the model failed to predict the correct concentration of higher carbon components. Single event kinetic modelling of ethylene oligomerization, with elementary steps of protonation/de-protonation, isomerization, alkylation, beta-scission, cyclization and hydride transfer was also attempted. In this, 10,456 elementary steps involving 2,567 species up to C8 range were considered.

Also, structure-oriented lumping in their kinetic modelling was studied. In this approach a large number of key molecules were generated by assembling 6 structural groups in various ways. However, the use of lumps, i.e., pseudo- or key-components, leads to the rate coefficients depending on the feedstock composition.

Although the above research gives us directional inputs for designing a process model, none of them can be directly used to simulate PAO production using WCN/DCN as feed stocks. Here we have developed a model to find the kinetic parameter estimation for the proposed oligomerization reaction pathways using MATLAB. Further, these kinetic parameters were then used in Aspen HYSYS for developing a process model for scale up studies.

6.2 Kinetic Model Development

6.2.1 Model Carbon Range

During oligomerization of naphtha materials such as DCN and WCN, alpha olefins (LAO) are oligomerized over the catalyst system to produce poly alpha olefins (PAO). Cracked naphtha usually contains C6-C14 hydrocarbons comprising of paraffins, iso-paraffins, olefins, naphthenes and aromatics. Olefins are two types: alpha olefins and internal olefins. Only alpha olefins present in the feed participate in oligomerization, whereas the remaining components remain unreacted. Usually, the product, poly alpha olefins, PAO, consist of carbon range of C15-C40. Thus the reaction mixture was modelled to represent the hydrocarbon material with carbon range of C6 to C40.

6.2.2 Model Lumping

As presented in Table 6.1, limited number of lumps were assumed to decrease the complexity of model without compromising the accuracy of the model:

Table 6.1: Boiling range of lumps considered for model development

S. No	Lump	Boiling range, ºC
1	C6	63-64
2	C7	93-94
3	C8	121-122
4	C9	147-148
5	C10	170-172
6	C12	196-235
7	C14	235-270
8	C16	270-303
9	C18	303-330
10	C20	330-343
11	C21	343-369
12	C24	369-401
13	C27	401-422
14	C28	422-441

S. No	Lump	Boiling range, ºC
15	C30	441-458
16	C32	458-474
17	C35	474-490
18	C36	490-511
19	C40	511-524

6.2.3 Model Reactions

Assuming only oligomerization and cracking reactions take place, all the possible reactions are depicted in the Table 6.2 below:

Table 6.2: Reactions involved in the process

Oligomerization reactions	
1. $C_6 + C_6 \rightarrow C_{12}$, $k_{6,6}$	2. $C_6 + C_{12} \rightarrow C_{18}$, $k_{12,6}$
3. $C_6 + C_{18} \rightarrow C_{24}$, $k_{18.6}$	4. $C_6 + C_{24} \rightarrow C_{30}$, $k_{24,6}$
5. $C_6 + C_{30} \rightarrow C_{36}$, $k_{30,6}$	6. $C_7 + C_7 \rightarrow C_{14}$, $k_{7,7}$
7. $C_7 + C_{14} \rightarrow C_{21}$, $k_{14,7}$	8. $C_7 + C_{21} \rightarrow C_{28}$, $k_{21,7}$
9. $C_7 + C_{28} \rightarrow C_{35}$, $k_{28,7}$	10. $C_8 + C_8 \rightarrow C_{16}$, $k_{8,8}$
11. $C_8 + C_{16} \rightarrow C_{24}$, $k_{16,8}$	12. $C_8 + C_{24} \rightarrow C_{32}$, $k_{24,8}$
13. $C_8 + C_{32} \rightarrow C_{40}$, $k_{32,8}$	14. $C_9 + C_9 \rightarrow C_{18}$, $k_{9,9}$
15. $C_9 + C_{18} \rightarrow C_{27}$, $k_{18,9}$	16. $C_9 + C_{27} \rightarrow C_{35}$, $k_{27,9}$
17. $C_{10} + C_{10} \rightarrow C_{20}$, $k_{10,10}$	18. $C_{10} + C_{20} \rightarrow C_{30}$, $k_{20,10}$
19. $C_{10} + C_{30} \rightarrow C_{40}$, $k_{30,10}$	
Cracking Reactions	
20. $C_{40} \rightarrow C_{20} + C_{20}$, k_{40}	21. $C_{36} \rightarrow C_{18} + C_{18}$, k_{36}

6.2.4 Mole Balance Equations

General mole balance equation for steady state batch reaction:

$$F_{i0} - F_i + \int_0^V r_i \, dV = \frac{dN_i}{dt}$$

Considering no inflow and out flow, the equation changes to

$$\int_0^V r_i dV = \frac{dN_i}{dt}$$

$$\int_0^V r_i dV = r_i \int_0^V dV = \frac{dN_i}{dt}$$

If volume of the reactor is constant, $V = V_0$

$$\frac{dN_i}{dt} = r_i V_0$$

$$\frac{d(N_i/V_0)}{dt} = (r_i V_0)/(V_0)$$

$$\frac{dC_i}{dt} = r_i$$

Following Table 6.3 lists the appearance/disappearance of the components during the reaction:

Table 6.3: Rate of appearance/disappearance of component i

Rate of appearance/disappearance of component *i*	
$\frac{dC_6}{dt}$	$-K_{(6,6)}C_6C_6 - K_{(12,6)}C_{12}C_6 - K_{(18,6)}C_{18}C_6 - K_{(24,6)}C_{24}C_6 - K_{(30,6)}C_{30}C_6$
$\frac{dC_7}{dt}$	$-K_{(7,7)}C_7C_7 - K_{(14,7)}C_{14}C_7 - K_{(21,7)}C_{21}C_7 - K_{(28,7)}C_{28}C_7$
$\frac{dC_8}{dt}$	$-K_{(8,8)}C_8C_8 - K_{(16,8)}C_{16}C_8 - K_{(24,8)}C_{21}C_7 - K_{(32,8)}C_{32}C_8$
$\frac{dC_9}{dt}$	$-K_{(9,9)}C_9C_9 - K_{(18,9)}C_{18}C_9 - K_{(27,9)}C_{27}C_9$
$\frac{dC_{10}}{dt}$	$-K_{(10,10)}C_{10}C_{10} - K_{(20,10)}C_{20}C_{10} - K_{(30,10)}C_{30}C_{10}$
$\frac{dC_{12}}{dt}$	$K_{(6,6)}C_6C_6 - K_{(12,6)}C_{12}C_6$

Rate of appearance/disappearance of component *i*	
$\frac{dC_{14}}{dt}$	$K_{(7,7)}C_7C_7 - K_{(14,7)}C_{14}C_7$
$\frac{dC_{16}}{dt}$	$K_{(8,8)}C_8C_8 - K_{(16,8)}C_{16}C_8$
$\frac{dC_{18}}{dt}$	$K_{(9,9)}C_9C_9 - K_{(18,9)}C_{18}C_9 + K_{(12,6)}C_{12}C_6 - K_{(18,6)}C_{18}C_6$ $+ K_{36}\,C_{36}$
$\frac{dC_{20}}{dt}$	$K_{(10,10)}C_{10}C_{10} - K_{(20,10)}C_{20}C_{10}+K_{40}\,C_{40}$
$\frac{dC_{21}}{dt}$	$K_{(14,7)}C_{14}C_7 - K_{(21,7)}C_{21}C_7$
$\frac{dC_{24}}{dt}$	$K_{(18,6)}C_{18}C_6 - K_{(24,6)}C_{24}C_6 + K_{(16,8)}C_{16}C_8 - K_{(24,8)}C_{24}C_8$
$\frac{dC_{27}}{dt}$	$K_{(18,9)}C_{18}C_9 - K_{(27,9)}C_{27}C_9$
$\frac{dC_{28}}{dt}$	$K_{(21,7)}C_{21}C_7 - K_{(28,7)}C_{28}C_7$
$\frac{dC_{30}}{dt}$	$K_{(20,10)}C_{20}C_{10} - K_{(30,10)}C_{30}C_{10} + K_{(24,6)}C_{24}C_6 - K_{(30,6)}C_{30}C_6$
$\frac{dC_{32}}{dt}$	$K_{(24,8)}C_{24}C_8 - K_{(32,8)}C_{32}C_8$
$\frac{dC_{35}}{dt}$	$K_{(28,7)}C_{28}C_7$
$\frac{dC_{36}}{dt}$	$K_{(30,6)}C_{30}C_6 + K_{(27,9)}C_{27}C_9 - K_{36}\,C_{36}$
$\frac{dC_{40}}{dt}$	$K_{(30,10)}C_{30}C_{10} + K_{(32,8)}C_{32}C_8 - K_{40}\,C_{40}$

6.3 Experimental Studies with WCN

It is known from the current study that poly alpha olefins are produced from the wax cracked naphtha (WCN) feed. For the purpose of modelling, oligomerization experiments were carried out to generate the kinetic data.

6.3.1 WCN Feed Characteristics

Feed composition of WCN is shown in the Table 6.4.

Table 6.4: Feed composition

Carbon number	Naphthenes	i-Paraffins	n-Paraffins	Olefins	Aromatics	Total
6	0.21	1.17	0.76	0.3	0.09	2.53
7	7.07	7.05	8.83	6.79	2.68	32.42
8	6.19	6.37	6.69	13.23	5.33	37.81
9	7.67	-	4.85	11.67	0.92	25.11
10+	0.2	0.64	0.02	1.27	0	2.13
Total	21.34	15.23	21.15	33.26	9.02	100

6.3.2 WCN Kinetic data

Experiments were performed in a batch reactor at temperatures of 50^{o}C, 62.5^{o}C, 75^{o}C, 87.5^{o}C & 100^{o}C at residence times of 30 min, 60 min, 90 min & 120 min with known amount of catalyst volume under atmospheric conditions.

After the experiments, catalyst was separated/filtered out from the organic phase. Complete conversion of olefins in the feed to poly alpha olefins was observed. Hydrocarbon samples were analyzed in Simdist to understand the concentration of poly alpha olefins. Simdist generates data in a tabulated form as the mass% with boiling point values. As per the mentioned lumps boiling point, experimental concentrations of the products were calculated and reported in Tables 6.5 & Tables 6.6, respectively.

Table 6.5: Experimental concentrations at different temperatures and resident time

Wt. %	50 C, 30min	50 C, 60 min	50 C, 90 min	50 C, 120 min	62.5 C, 30 min	62.5 C, 60 min	62.5 C, 90 min	62.5 C, 120min	75 C, 30 min	75 C, 60 min
C6	0	0	0	0	0	0	0	0	0	0
C7	0	0	0	0	0	0	0	0	0	0
C8	0	0	0	0	0	0	0	0	0	0
C9	0	0	0	0	0	0	0	0	0	0
C10	0	0	0	0	0	0	0	0	0	0
C12	0.218	0.160	0.131	0.102	0.133	0.116	0.087	0.073	0.160	0.087
C14	0.275	0.287	0.287	0.250	0.316	0.275	0.262	0.212	0.300	0.250
C16	0.153	0.164	0.175	0.153	0.227	0.197	0.197	0.230	0.186	0.219
C18	0.058	0.049	0.049	0.058	0.056	0.049	0.049	0.058	0.049	0.049
C20	0.035	0.044	0.044	0.044	0.051	0.044	0.053	0.044	0.044	0.044
C21	0.100	0.117	0.125	0.142	0.154	0.134	0.134	0.134	0.117	0.134
C24	0.044	0.051	0.059	0.073	0.076	0.066	0.073	0.081	0.051	0.073
C27	0.033	0.033	0.033	0.039	0.038	0.033	0.033	0.039	0.033	0.033
C28	0.019	0.019	0.025	0.025	0.022	0.019	0.025	0.025	0.019	0.025
C30	0.006	0.012	0.006	0.012	0.014	0.012	0.012	0.012	0.006	0.012
C32	0.011	0.011	0.011	0.011	0.006	0.005	0.005	0.005	0.011	0.005
C35	0.005	0.005	0.005	0.005	0.006	0.005	0.010	0.010	0.005	0.010
C36	0.010	0.005	0.010	0.005	0.006	0.005	0.005	0.005	0.005	0.005
C40	0.031	0.026	0.018	0.022	0.021	0.018	0.013	0.013	0.018	0.013
Inert.	4.461	4.461	4.461	4.461	4.461	4.461	4.461	4.461	4.461	4.461

Table 6.6: Experimental concentrations at different temperatures and resident time

Wt. %	75 C, 90 min	75 C, 120 min	87.5C, 30 min	87.5C, 60 min	87.5C, 90 min	87.5 C, 120 min	100C, 30 min	100C, 60 min	100C, 90 min	100 C, 120 min
C6	0	0	0	0	0	0	0	0	0	0
C7	0	0	0	0	0	0	0	0	0	0
C8	0	0	0	0	0	0	0	0	0	0
C9	0	0	0	0	0	0	0	0	0	0
C10	0	0	0	0	0	0	0	0	0	0
C12	0.073	0.058	0.160	0.073	0.058	0.044	0.044	0.044	0.044	0.044
C14	0.250	0.212	0.312	0.225	0.187	0.162	0.175	0.162	0.162	0.137
C16	0.241	0.241	0.197	0.230	0.230	0.230	0.241	0.219	0.219	0.208
C18	0.049	0.058	0.058	0.049	0.058	0.058	0.068	0.068	0.058	0.058
C20	0.044	0.035	0.044	0.035	0.035	0.035	0.035	0.035	0.035	0.035
C21	0.134	0.134	0.100	0.134	0.125	0.125	0.109	0.117	0.117	0.109
C24	0.073	0.088	0.059	0.081	0.102	0.102	0.110	0.110	0.117	0.117
C27	0.033	0.039	0.026	0.039	0.033	0.046	0.033	0.039	0.039	0.046
C28	0.025	0.025	0.019	0.025	0.031	0.031	0.038	0.031	0.031	0.038
C30	0.012	0.012	0.006	0.012	0.018	0.018	0.012	0.023	0.023	0.023
C32	0.005	0.011	0.005	0.011	0.011	0.011	0.011	0.011	0.011	0.016
C35	0.005	0.005	0.005	0.005	0.005	0.010	0.010	0.005	0.010	0.010
C36	0.005	0.005	0.005	0.010	0.005	0.005	0.005	0.010	0.005	0.005
C40	0.013	0.013	0.018	0.013	0.018	0.018	0.018	0.018	0.018	0.022
Inert.	4.461	4.461	4.461	4.461	4.461	4.461	4.461	4.461	4.461	4.461

6.4 Model Objective Function

All differential equations were solved using MATLAB and kinetic parameters were obtained by minimizing the following objective function.

$$\text{Objective Function:} \quad \text{Min} \sum_{i=6}^{40} \left(C_{e,i} - C_{m,i}\right)^2$$

$$\text{Subjected to: } k>0$$

The objective function is formulated as sum of the squares of the difference between the experimental concentrations and the model concentrations. The minimization routine, GA (genetic algorithm) from global optimization tool box of MATLAB is used here for obtaining the rate constants. Genetic Algorithm is a stochastic global optimization routine based on classical evolutionary algorithm. It works on the population, consisting of solutions, where each solution is called as individual or gene. The best solutions / individuals / genes will be used for mutation or cross over to produce the children or new individuals. The bad solutions or individuals or genes will be replaced by the children or new individuals in next iteration.

MATLAB code is given in Annexure-I at the end of this chapter.

6.5 Kinetic Parameter Estimation

Model was developed with 15 set of experimental data available. 5 set of experimental data points are used for model validation. Following (Table 6.7) set of experimental data was used for rate constants estimation.

Table 6.7: Experiential data sets for model parameter estimation

50 C, 30 min	50 C, 90 min	50 C, 120 min	62.5C, 30 min	62.5C, 90 min	62.5 C, 120 min	75 C, 30 min	75 C, 90 min
75 C, 120 min	87.5 C, 30 min	87.5 C, 90 min	87.5 C, 120 min		100 C, 30 min	100 C, 90 min	100 C, 120 min

Experimental concentrations versus the model concentrations are plotted in Figures 6.1 – 6.5, obtained at different temperatures

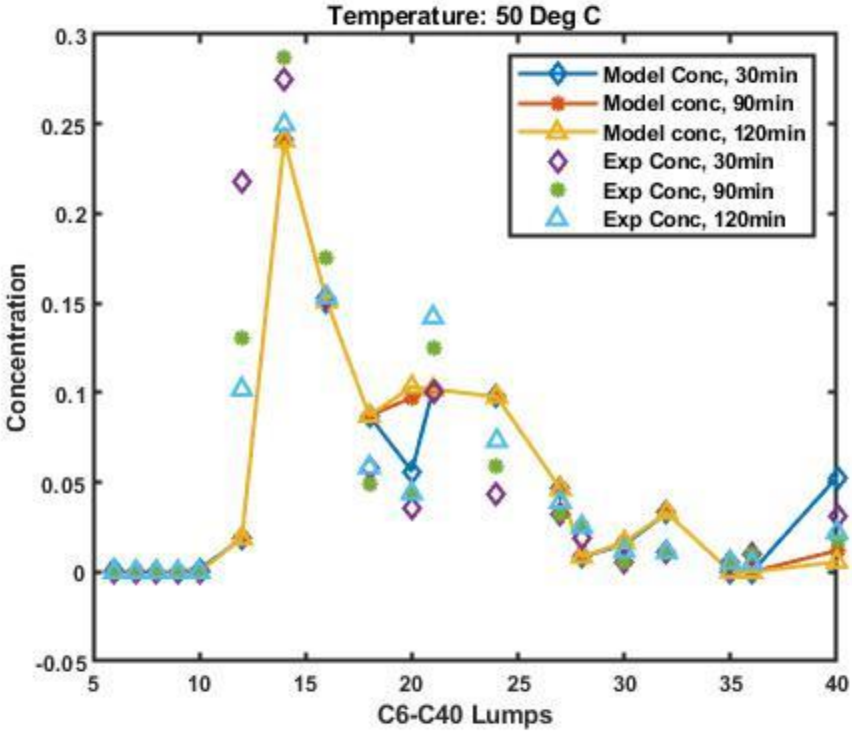

Figure 6.1: Experimental concentration vs model concentrations at 50^{o}C

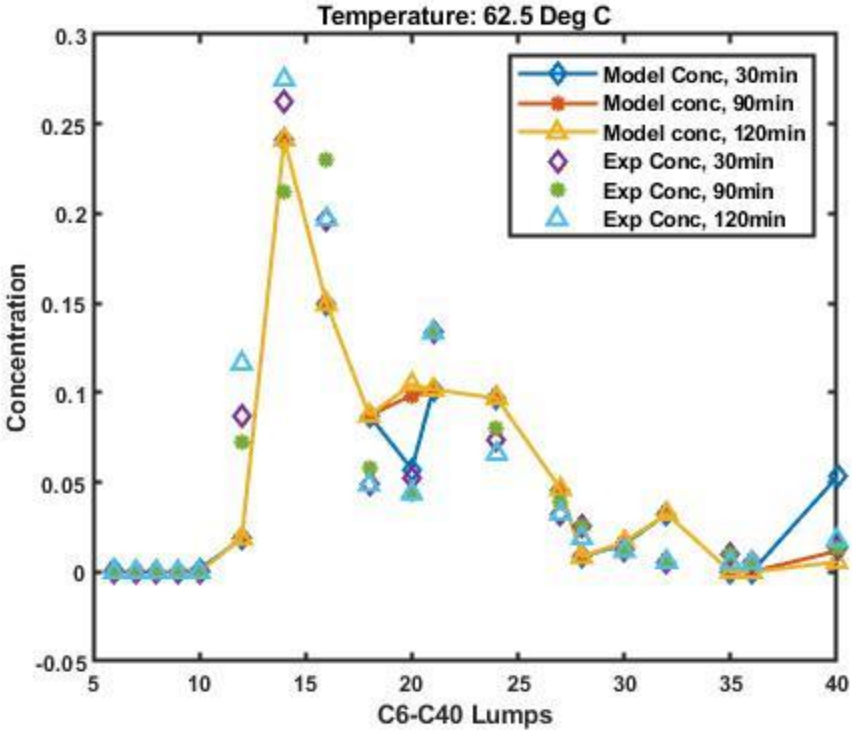

Figure 6.2: Experimental concentration vs model concentrations at 62.5^{o}C

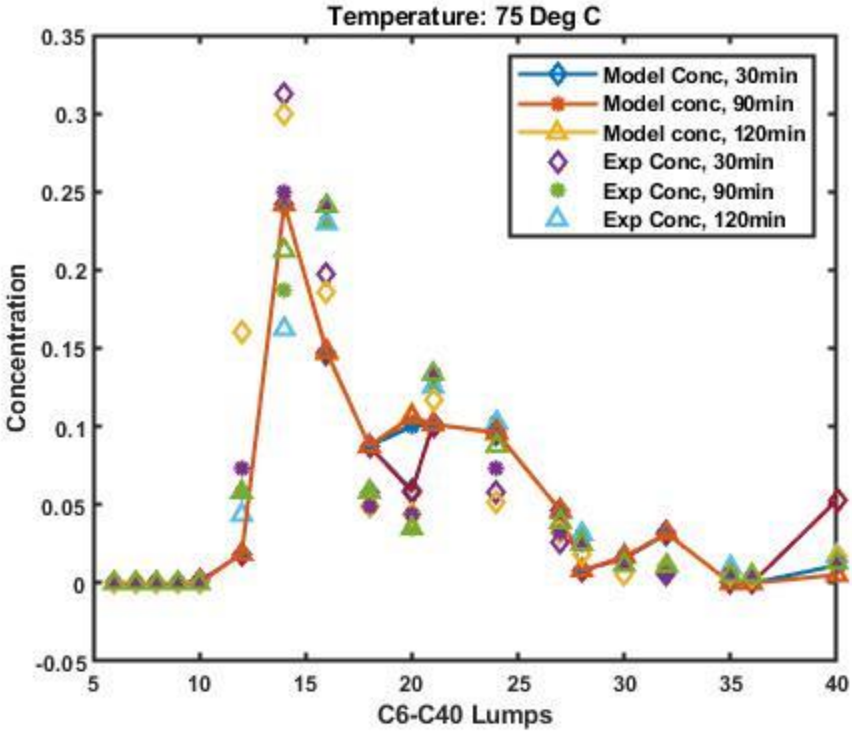

Figure 6.3: Experimental concentration vs model concentrations at 75°C

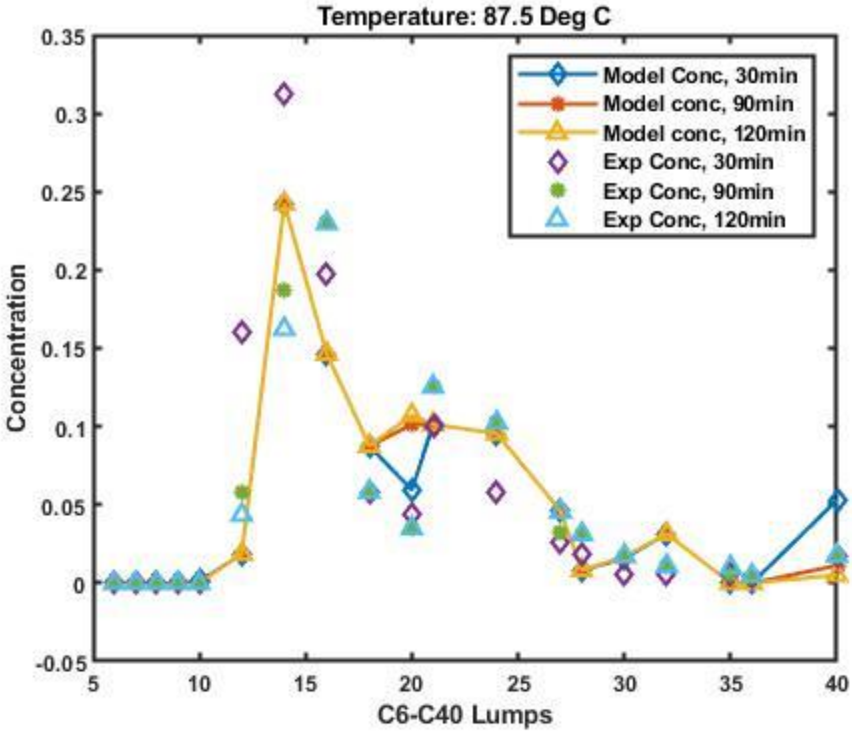

Figure 6.4: Experimental concentration vs model concentrations at 87.5°C

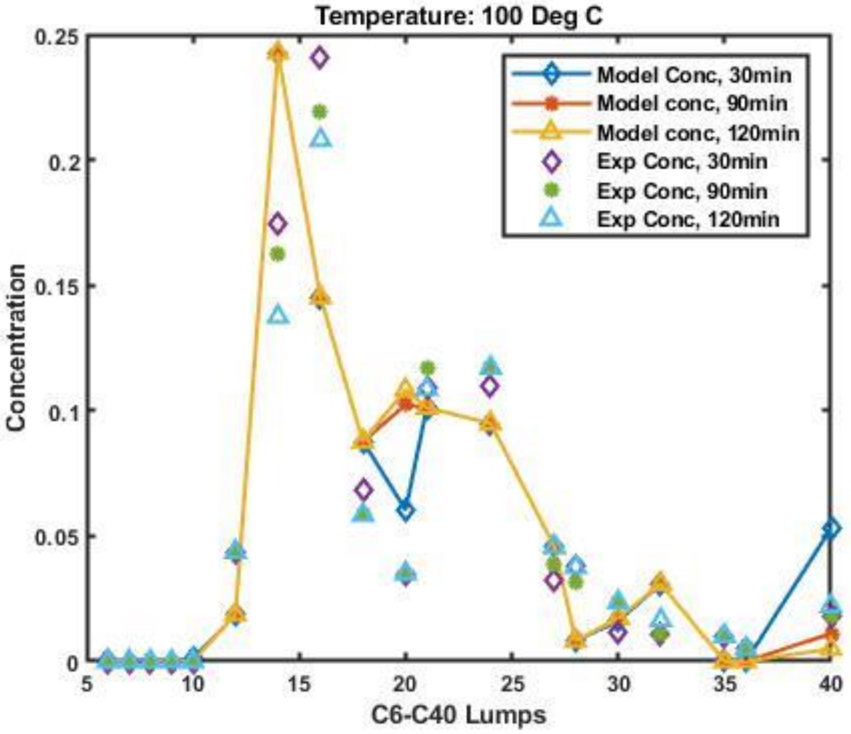

Figure 6.5: Experimental concentration vs model concentrations at 100^{o}C

Rate constants are estimated from minimizing the above mentioned objective function. And it is reported in the Table 6.8.

Activation energy & frequency factors of reactions are reported in Table 6.9.

Table 6.8: Rate constants of lumps at 100°C, 87.5 °C, 75 °C, 62 °C & 50°C

Rate equation no	Rate constant 100°C	Rate constant 87.5°C	Rate constant 75°C	Rate constant s62°C	Rate constant 50°C
1	51.203	58.666	62.227	55.551	65.155
2	0.374	0.033	0.063	0.112	0.096
3	0.162	0.041	0.004	0.024	0.045
4	0.649	0.088	0.048	0.104	0.034
5	1.900	0.043	0.091	0.300	0.174
6	15.487	23.858	18.316	24.634	19.717
7	9.378	7.777	4.310	6.143	3.945
8	6.457	3.500	0.045	0.050	0.111
9	2.403	0.075	0.087	0.247	0.201
10	8.265	8.427	3.006	5.855	5.257
11	7.778	8.146	2.852	6.112	7.431
12	10.910	15.781	7.229	13.593	16.125
13	32.808	36.641	14.724	30.934	23.542
14	0.244	0.231	0.261	0.059	0.227
15	14.528	14.942	19.758	11.936	19.103
16	20.282	22.934	27.471	11.272	26.222
17	24.851	36.545	23.548	24.107	19.993
18	2.902	2.758	11.368	1.139	0.628
19	0.112	0.152	0.014	0.030	0.007
20	5.915	7.997	12.737	0.928	6.136
21	10.640	17.940	0.057	5.096	1.253

Table 6.9: Activation energy & frequency factors of reactions

Rate equation no	Activation Energy, J/mole		Frequency factor, *k0*		Units
1	$E_{6,6}$	66.415	$k0_{6,6}$	63.310	L/(min. mole)
2	$E_{12,6}$	243.164	$k0_{12,6}$	0.015	L/(min. mole)
3	$E_{18,6}$	787.839	$k0_{18,6}$	0.022	L/(min. mole)
4	$E_{24,6}$	838.395	$k0_{24,6}$	0.003	L/(min. mole)
5	$E_{30,6}$	851.072	$k0_{30,6}$	0.125	L/(min. mole)
6	$E_{7,7}$	852.197	$k0_{7,7}$	9.618	L/(min. mole)
7	$E_{14,7}$	428.679	$k0_{14,7}$	2.065	L/(min. mole)
8	$E_{21,7}$	505.453	$k0_{21,7}$	0.771	L/(min. mole)
9	$E_{28,7}$	295.610	$k0_{28,7}$	0.028	L/(min. mole)
10	$E_{8,8}$	466.324	$k0_{8,8}$	2.168	L/(min. mole)
11	$E_{16,8}$	1399.091	$k0_{16,8}$	5.150	L/(min. mole)
12	$E_{24,8}$	1526.590	$k0_{24,8}$	8.889	L/(min. mole)
13	$E_{32,8}$	2478.074	$k0_{32,8}$	35.896	L/(min. mole)
14	$E_{9,9}$	684.654	$k0_{9,9}$	0.292	L/(min. mole)
15	$E_{18,9}$	784.875	$k0_{18,9}$	12.879	L/(min. mole)
16	$E_{27,9}$	958.992	$k0_{27,9}$	17.246	L/(min. mole)
17	$E_{10,10}$	128.192	$k0_{10,10}$	4.586	L/(min. mole)
18	$E_{20,10}$	571.348	$k0_{20,10}$	2.882	L/(min. mole)
19	$E_{30,10}$	461.827	$k0_{30,10}$	0.004	L/(min. mole)
20	E_{40}	330.218	$k0_{40}$	1.512	L/(min. mole)
21	E_{36}	979.654	$k0_{36}$	0.036	L/(min. mole)

6.6 Kinetic Model Validation

Model was validated with the following set of experimental data as given in Table 6.10. Model concentration were calculated based on the obtained kinetic parameters and the eexperimental concentrations were plotted versus the model concentrations in the Figure 6.6 - 6.10

Table 6.10: Experiential data sets for model validation

50 C, 60 min	62.5 C, 60 min	75 C, 60 min	87.5 C, 60 min	100 C, 60 min

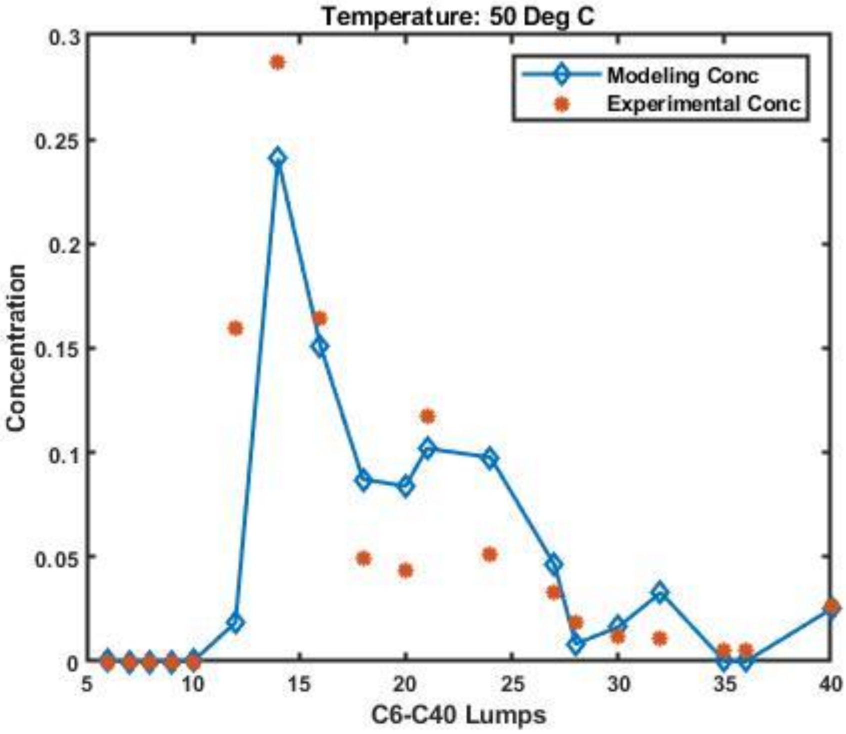

Figure 6.6: Experimental concentration vs model concentrations at 50°C

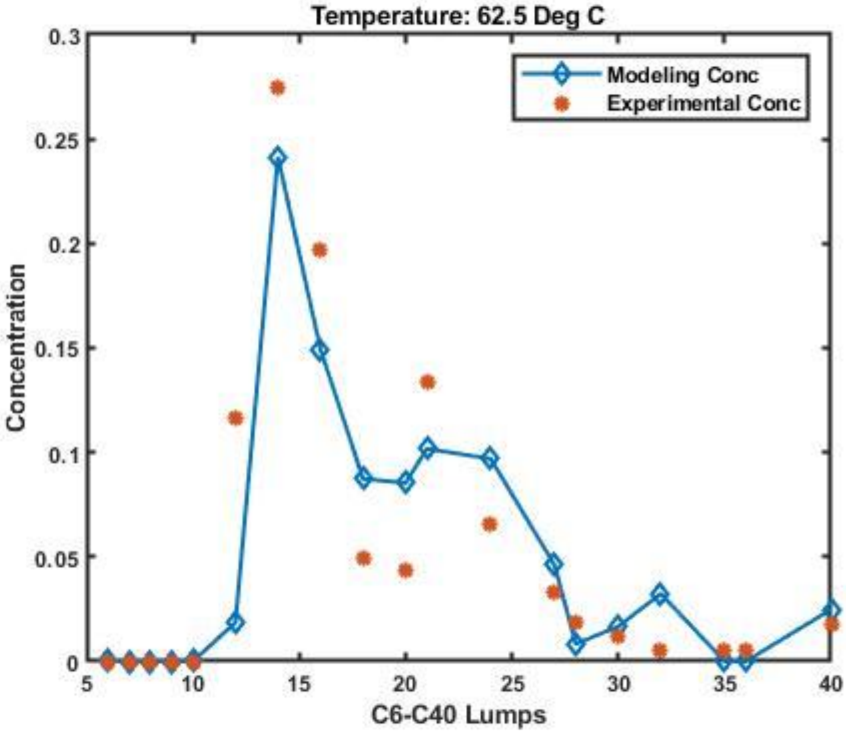

Figure 6.7: Experimental concentration vs model concentrations at 62.5^{0}C

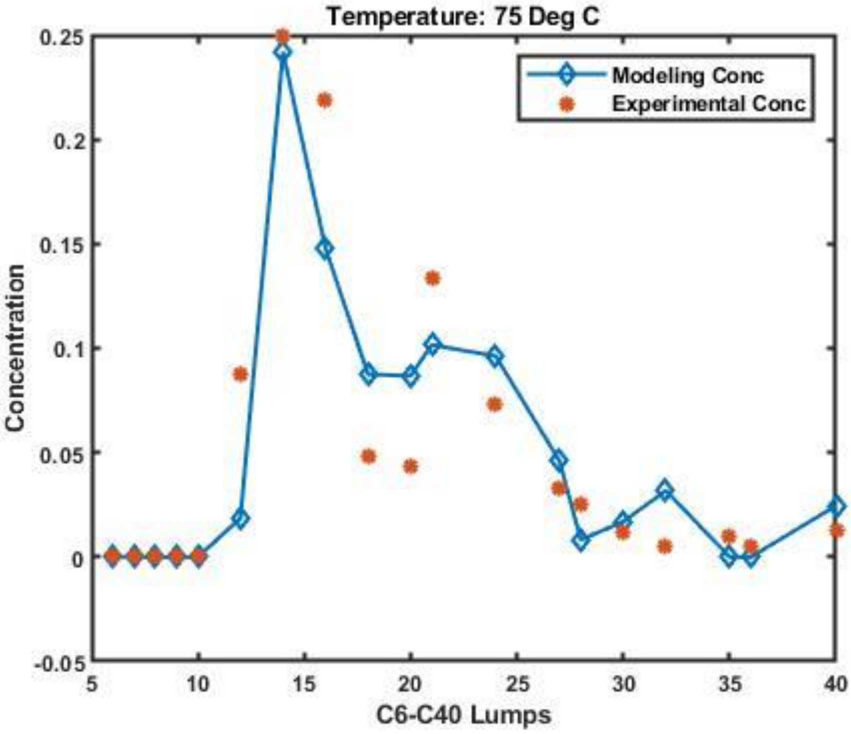

Figure 6.8: Experimental concentration vs model concentrations at 75°C

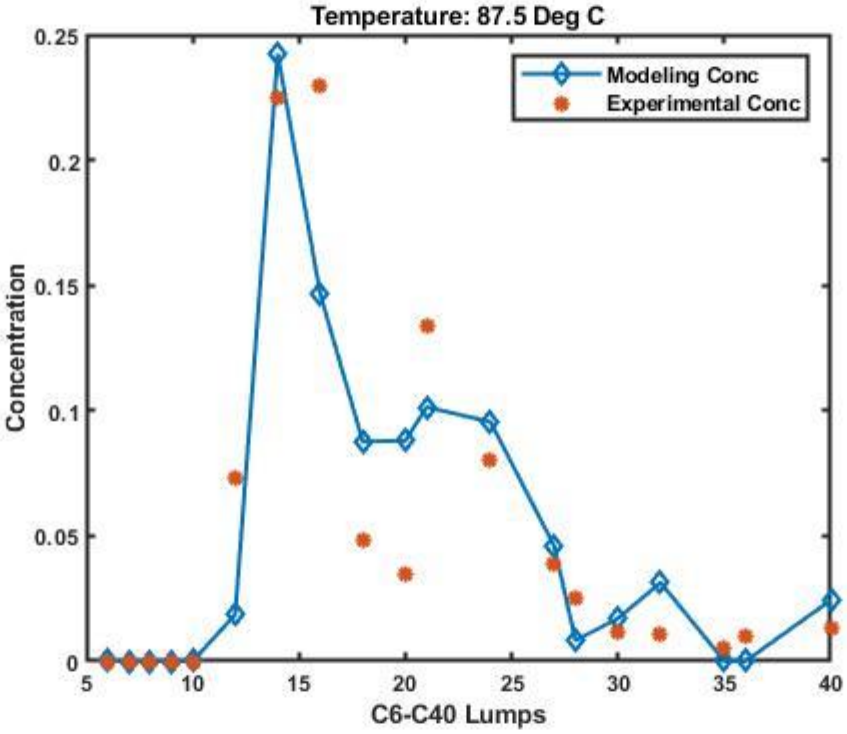

Figure 6.9: Experimental concentration vs model concentrations at 87.5 ^{0}C

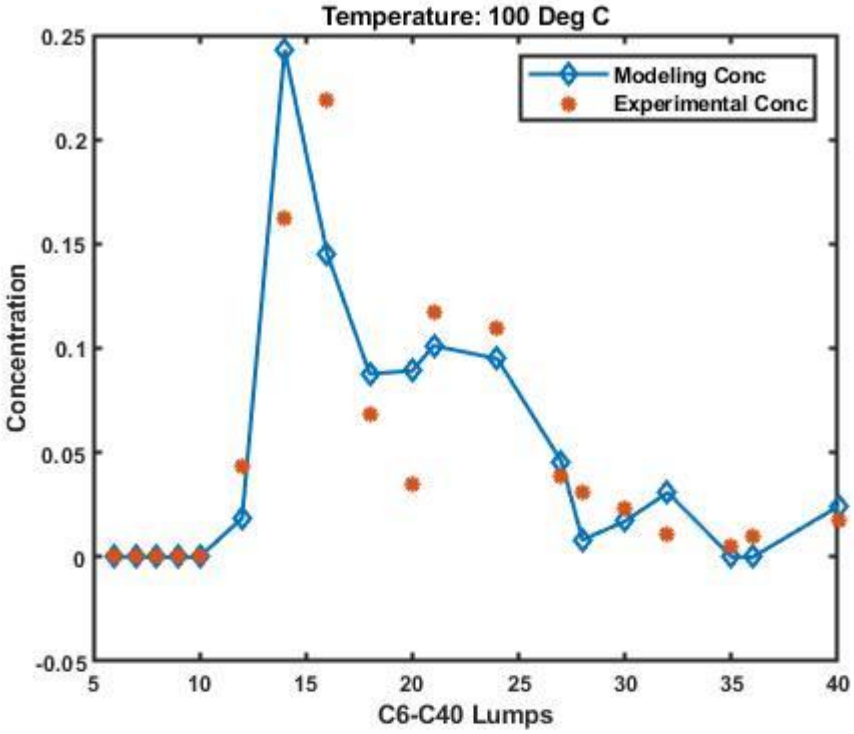

Figure 6.10: Experimental concentration vs model concentrations at 100 ^{0}C

Based on the above validation, it is inferred that, the proposed model predicts the concentrations of the components with ±10 % confidence intervals. It is observed that at higher temperature, lower carbon number hydrocarbons are formed due to the fast termination reactions. The same is obtained by the model kinetics.

Kinetic parameters of all considered rate equations are shown in the Table 6.9. The results show that the proposed model predicts the products concentrations, with the estimated kinetic parameters. These kinetic parameters are used in the ASPEN HYSYS for the process development for commercial scale plant. Activation energy of the C_{40} cracking reactions are observed high. It can be inferred that at higher temperatures cracking reactions are favorable.

6.7 Process Simulation Model Development

Process model was developed in ASPEN HYSYS V.11 for production of PAOs from cracked naphtha streams. The parameters estimated from kinetic modelling using MATLAB were incorporated in the model.

6.7.1 Property Package Selection

The Peng-Robinson (PR) model is ideal for VLE calculations for hydrocarbon systems. The PR property package rigorously solves any single-, two-, or three-phase system with a high degree of efficiency and reliability and is applicable over a wide range of conditions:

- ✓ Temperature Range > -271 °C or -456 °F
- ✓ Pressure Range < 100,000 kPa or 15,000 psia

The PR property package also contains enhanced binary interaction parameters for all library hydrocarbon-hydrocarbon pairs (a combination of fitted and generated interaction parameters), as well as for most hydrocarbon-non-hydrocarbon binaries, such as N2, CO2, H2S, H2, and H2O. For non-library or hydrocarbon hypo components, HC-HC interaction parameters are generated automatically by HYSYS for improved VLE property predictions. Accordingly, Peng Robinson model was selected to develop the process model.

6.7.2 Equation of State

The Peng Robinson equation of state applies functionality to some specific component-component interaction parameters. Formulations used in HYSYS for the PR equations of state:

$$P = \frac{RT}{V-b} - \frac{a}{V(V+b)+b(V-b)}$$

$$Z^3 - \left(1-B\right)Z^2 + \left(A-2B-3B^2\right)Z - \left(AB-B^2-B^3\right) = 0$$

Where:

$$A = \frac{aP}{(RT)^2}$$

$$B = \frac{bP}{RT}$$

$$b = \sum_{i=1}^{N} x_i \left(0.077796 \frac{RT_{ci}}{P_{ci}} \right)$$

$$a = \sum_{i=1}^{N} \sum_{j=1}^{N} x_i x_j \left[\left(0.457235 \frac{(RT_{ci})^2}{P_{ci}} \right) \alpha_i \left(0.457235 \frac{(RT_{cj})^2}{P_{cj}} \right) \alpha_j \right]^{0.5} \left(1 - k_{ij} \right)$$

$$\alpha_i^{0.5} = 1 + m_i \left(1 - T_{ri}^{0.5} \right)$$

$$m_i = 0.37464 + 1.54226\omega_i - 0.26992\omega_i^2$$

6.7.3 Enthalpy & Entropy

For the Peng-Robinson Equation of State, the enthalpy and entropy departure calculations use the following relations:

$$\frac{H - H^{ID}}{RT} = Z - 1 - \frac{1}{2^{1.5} bRT} \left[a - T\frac{\mathrm{d}a}{\mathrm{d}t} \right] \ln \left(\frac{V + (2^{0.5} + 1)b}{V - (2^{0.5} - 1)b} \right)$$

$$\frac{S - S_{\circ}^{ID}}{R} = \ln(Z - B) - \ln \frac{P}{P^{\circ}} - \frac{A}{2^{1.5} bRT} \left[\frac{T}{a} \frac{\mathrm{d}a}{\mathrm{d}t} \right] \ln \left(\frac{V + (2^{0.5} + 1)b}{V - (2^{0.5} - 1)b} \right)$$

Where:

H^{ID} = Ideal Gas Enthalpy basis used by HYSYS changes with temperature according to the coefficients for each individual component.

$$a = \sum_{i=1}^{n}\sum_{j=1}^{n} x_i x_j (a_i a_j)^{0.5}\left(1 - k_{ij}\right)$$

$$b_i = 0.077796\frac{RT_{ci}}{P_{ci}}$$

$$a_i = 0.457235\frac{(RT_{ci})^2}{P_{ci}}\alpha_i$$

$$\sqrt{\alpha_i} = 1 + m_i\left(1 - T_{ri}^{0.5}\right)$$

$$m_i = 0.37464 + 1.54226\omega_i - 0.26992\omega_i^2$$

R = Ideal Gas constant

H = Enthalpy

S = Entropy

^{ID} = indicates Ideal Gas

$^{\circ}$ = indicates reference state

The list of property models used under Peng Robinson property package is listed in the Table 6.11 below.

Table 6.11: Property Models

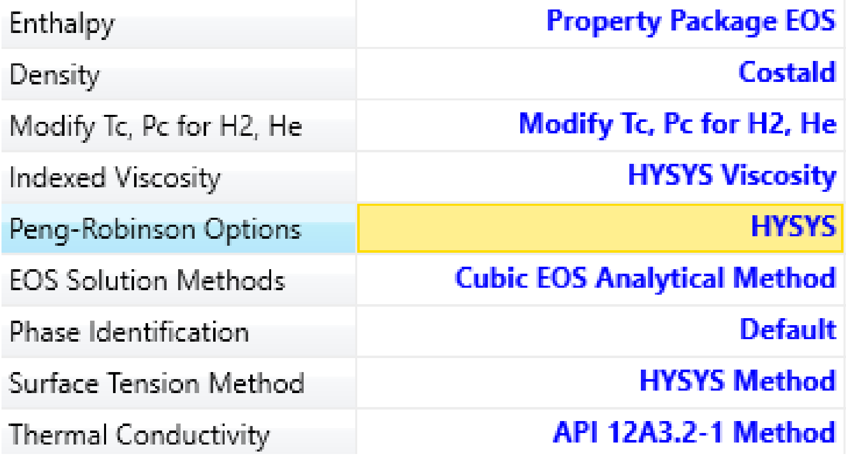

Enthalpy	Property Package EOS
Density	Costald
Modify Tc, Pc for H2, He	Modify Tc, Pc for H2, He
Indexed Viscosity	HYSYS Viscosity
Peng-Robinson Options	HYSYS
EOS Solution Methods	Cubic EOS Analytical Method
Phase Identification	Default
Surface Tension Method	HYSYS Method
Thermal Conductivity	API 12A3.2-1 Method

6.8 Process flow sheet

ASPEN HYSYS flow sheet is presented in Figure 6.11 below.

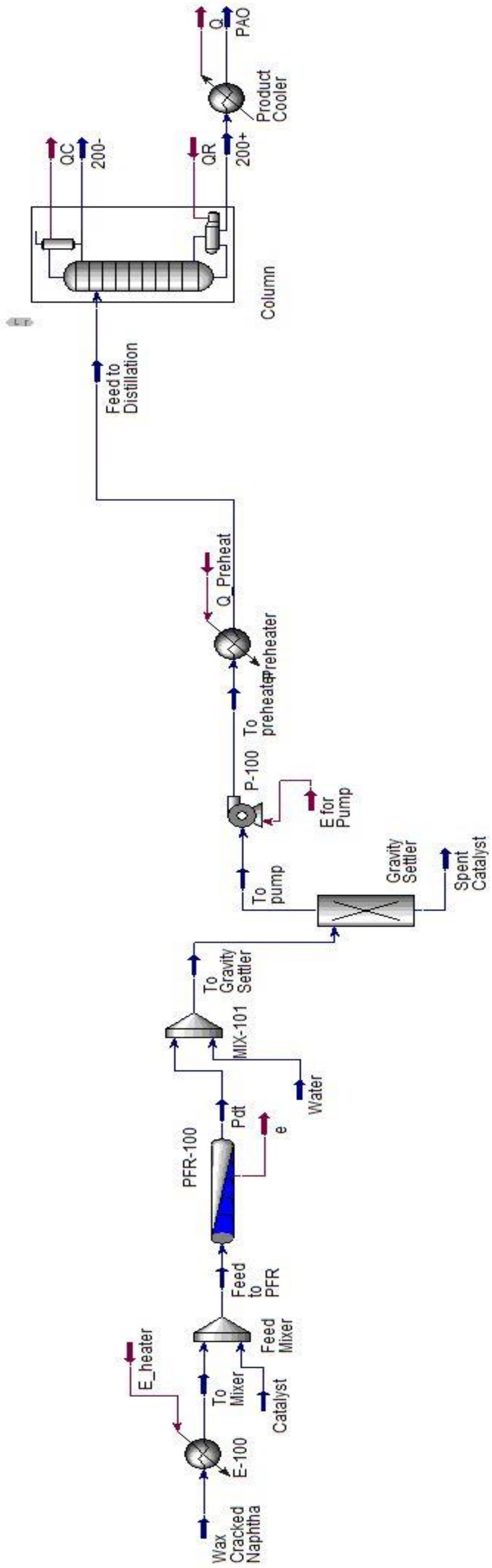

Figure 6.11: Process flow sheet

(a) Component list

The components for process modelling were selected from the ASPEN HYSYS databank. The components were linked to the PR property package for carrying out simulation. The selected list of components are as listed below in Figure 6.12:

Table 6.12: List of components selected

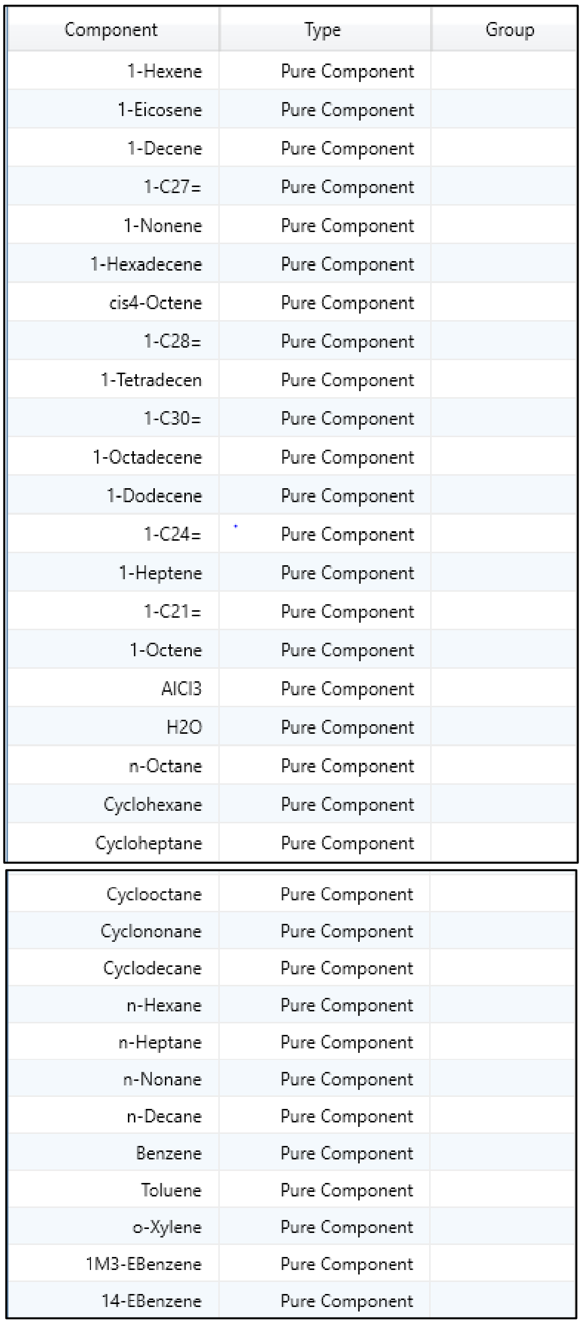

Component	Type	Group
1-Hexene	Pure Component	
1-Eicosene	Pure Component	
1-Decene	Pure Component	
1-C27=	Pure Component	
1-Nonene	Pure Component	
1-Hexadecene	Pure Component	
cis4-Octene	Pure Component	
1-C28=	Pure Component	
1-Tetradecen	Pure Component	
1-C30=	Pure Component	
1-Octadecene	Pure Component	
1-Dodecene	Pure Component	
1-C24=	Pure Component	
1-Heptene	Pure Component	
1-C21=	Pure Component	
1-Octene	Pure Component	
AlCl3	Pure Component	
H2O	Pure Component	
n-Octane	Pure Component	
Cyclohexane	Pure Component	
Cycloheptane	Pure Component	
Cyclooctane	Pure Component	
Cyclononane	Pure Component	
Cyclodecane	Pure Component	
n-Hexane	Pure Component	
n-Heptane	Pure Component	
n-Nonane	Pure Component	
n-Decane	Pure Component	
Benzene	Pure Component	
Toluene	Pure Component	
o-Xylene	Pure Component	
1M3-EBenzene	Pure Component	
14-EBenzene	Pure Component	

Components with Carbon number > 30 are not considered, as the experimental results indicates very low concentration of these molecules post oligomerisation reaction.

(b) Feed specifications

Naphtha from thermal cracker was shortlisted as one of the promising feed stock for PAO production based on experimental studies discussed in previous chapters. This is used as the starting material to develop the current model. The properties and compositions of the feed is listed in the Table 6.13 below:

Table 6.13: Feed properties

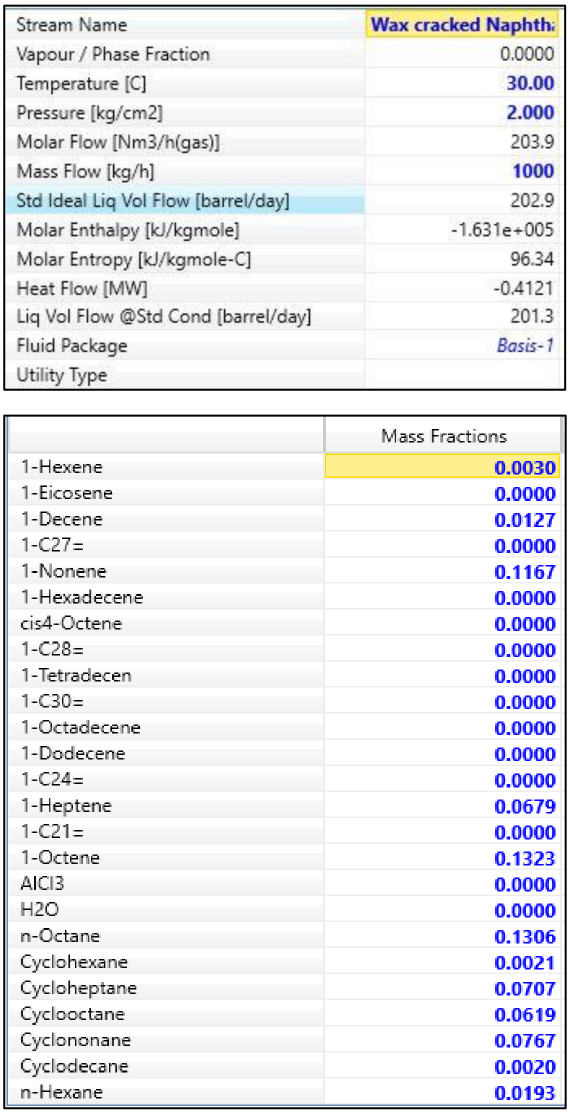

Stream Name	Wax cracked Naphth
Vapour / Phase Fraction	0.0000
Temperature [C]	30.00
Pressure [kg/cm2]	2.000
Molar Flow [Nm3/h(gas)]	203.9
Mass Flow [kg/h]	1000
Std Ideal Liq Vol Flow [barrel/day]	202.9
Molar Enthalpy [kJ/kgmole]	-1.631e+005
Molar Entropy [kJ/kgmole-C]	96.34
Heat Flow [MW]	-0.4121
Liq Vol Flow @Std Cond [barrel/day]	201.3
Fluid Package	Basis-1
Utility Type	

	Mass Fractions
1-Hexene	0.0030
1-Eicosene	0.0000
1-Decene	0.0127
1-C27=	0.0000
1-Nonene	0.1167
1-Hexadecene	0.0000
cis4-Octene	0.0000
1-C28=	0.0000
1-Tetradecen	0.0000
1-C30=	0.0000
1-Octadecene	0.0000
1-Dodecene	0.0000
1-C24=	0.0000
1-Heptene	0.0679
1-C21=	0.0000
1-Octene	0.1323
AlCl3	0.0000
H2O	0.0000
n-Octane	0.1306
Cyclohexane	0.0021
Cycloheptane	0.0707
Cyclooctane	0.0619
Cyclononane	0.0767
Cyclodecane	0.0020
n-Hexane	0.0193

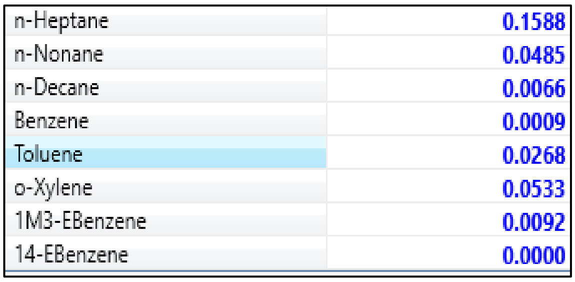

n-Heptane	0.1588
n-Nonane	0.0485
n-Decane	0.0066
Benzene	0.0009
Toluene	0.0268
o-Xylene	0.0533
1M3-EBenzene	0.0092
14-EBenzene	0.0000

6.9 Oligomerisation Reactions

The oligomerisation reactions were modelled in a continuous plug flow reactor. The reactions considered for the modelling are listed in Table 6.14 below and Details of reactions kinetics are given in Table 6.15.

Table 6.14: List of oligomerisation reactions for process modelling

1. $C_6 + C_6 \rightarrow C_{12}, k_{6,6}$	**2.** $C_6 + C_{12} \rightarrow C_{18}, k_{12,6}$
3. $C_6 + C_{18} \rightarrow C_{24}, k_{18.6}$	**4.** $C_6 + C_{24} \rightarrow C_{30}, k_{24,6}$
5. $C_7 + C_7 \rightarrow C_{14}, k_{7,7}$	**6.** $C_7 + C_{14} \rightarrow C_{21}, k_{14,7}$
7. $C_7 + C_{21} \rightarrow C_{28}, k_{21,7}$	**8.** $C_8 + C_8 \rightarrow C_{16}, k_{8,8}$
9. $C_8 + C_{16} \rightarrow C_{24}, k_{16,8}$	**10.** $C_9 + C_9 \rightarrow C_{18}, k_{9,9}$
11. $C_9 + C_{18} \rightarrow C_{27}, k_{18,9}$	$C_{10} + C_{10} \rightarrow C_{20}, k_{10,10}$
13. $C_{10} + C_{20} \rightarrow C_{30}, k_{20,10}$	

Carbon range upto C30 is assumed to avoid the complexity.

Table 6.15: Details of kinetic reactions

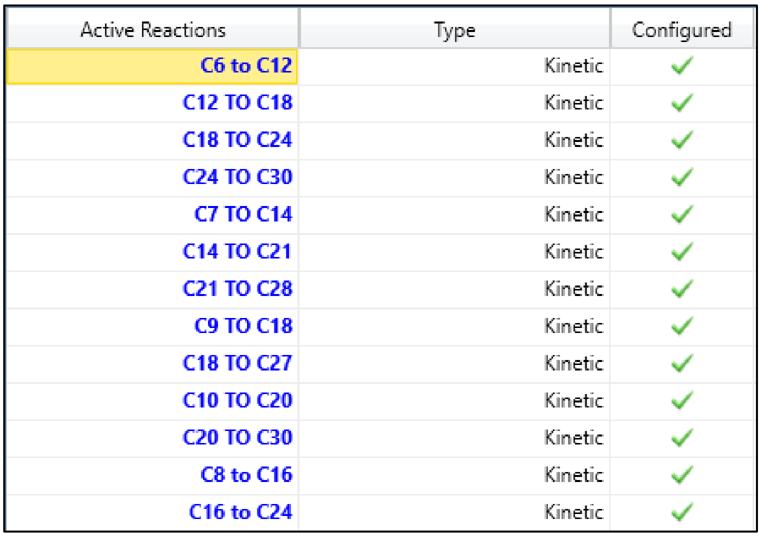

Active Reactions	Type	Configured
C6 to C12	Kinetic	✓
C12 TO C18	Kinetic	✓
C18 TO C24	Kinetic	✓
C24 TO C30	Kinetic	✓
C7 TO C14	Kinetic	✓
C14 TO C21	Kinetic	✓
C21 TO C28	Kinetic	✓
C9 TO C18	Kinetic	✓
C18 TO C27	Kinetic	✓
C10 TO C20	Kinetic	✓
C20 TO C30	Kinetic	✓
C8 to C16	Kinetic	✓
C16 to C24	Kinetic	✓

Details of individual reactions, stoichiometry and parameters incorporated from the kinetic model are described in Figures 6.12 to 6.37 in the subsequent sub sections.

(a) Reaction 1:

Hexene to Dodecene

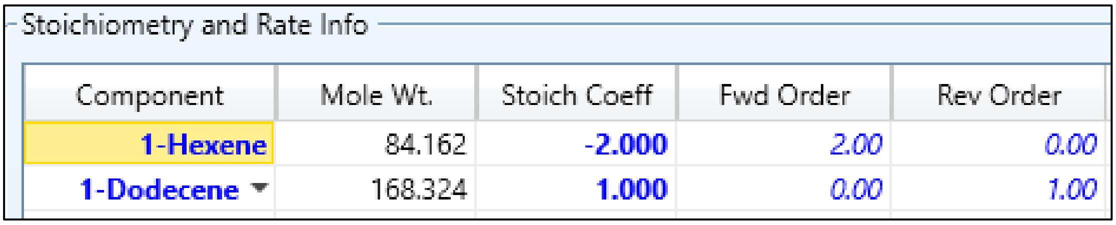

Component	Mole Wt.	Stoich Coeff	Fwd Order	Rev Order
1-Hexene	84.162	-2.000	2.00	0.00
1-Dodecene	168.324	1.000	0.00	1.00

Figure 6.12: Stoichiometry for Reaction 1

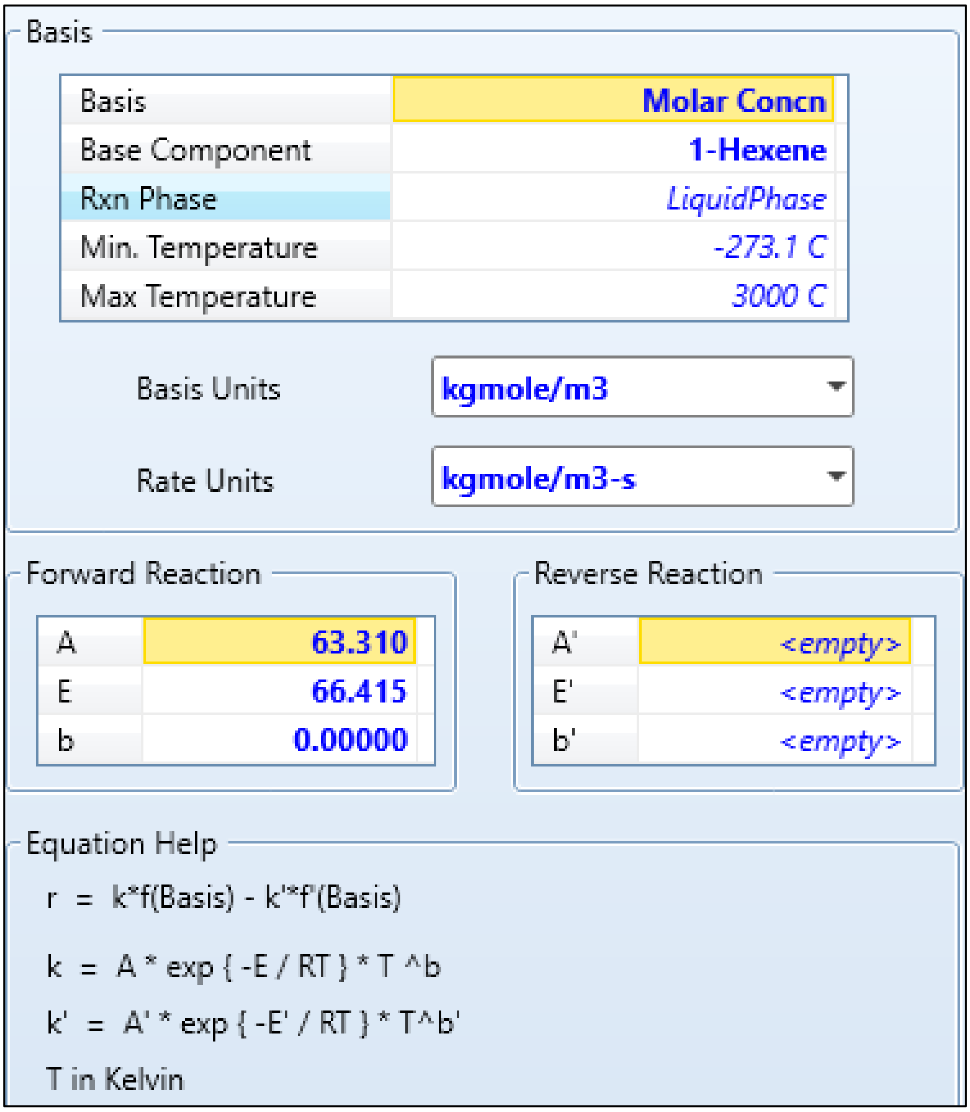

Basis

Basis	Molar Concn
Base Component	1-Hexene
Rxn Phase	*LiquidPhase*
Min. Temperature	*-273.1 C*
Max Temperature	*3000 C*

Basis Units: kgmole/m3

Rate Units: kgmole/m3-s

Forward Reaction

A	63.310
E	66.415
b	0.00000

Reverse Reaction

A'	*<empty>*
E'	*<empty>*
b'	*<empty>*

Equation Help

r = k*f(Basis) - k'*f'(Basis)

k = A * exp { -E / RT } * T ^b

k' = A' * exp { -E' / RT } * T^b'

T in Kelvin

Figure 6.13: Kinetic Parameters for Reaction 1

(b) Reaction 2:

Hexene & Dodecene to Octadecene

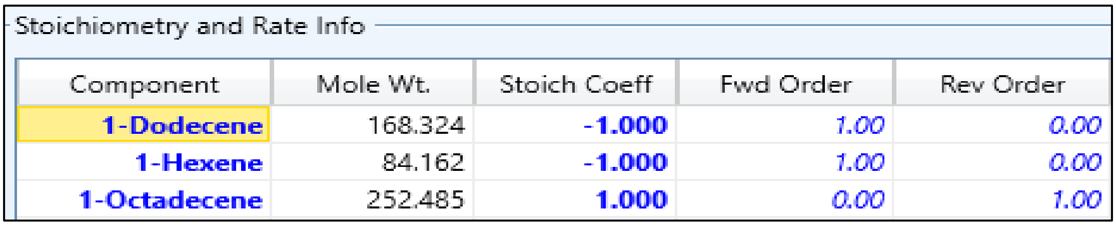

Stoichiometry and Rate Info

Component	Mole Wt.	Stoich Coeff	Fwd Order	Rev Order
1-Dodecene	168.324	-1.000	*1.00*	*0.00*
1-Hexene	84.162	-1.000	*1.00*	*0.00*
1-Octadecene	252.485	1.000	*0.00*	*1.00*

Figure 6.14: Stoichiometry for Reaction 2

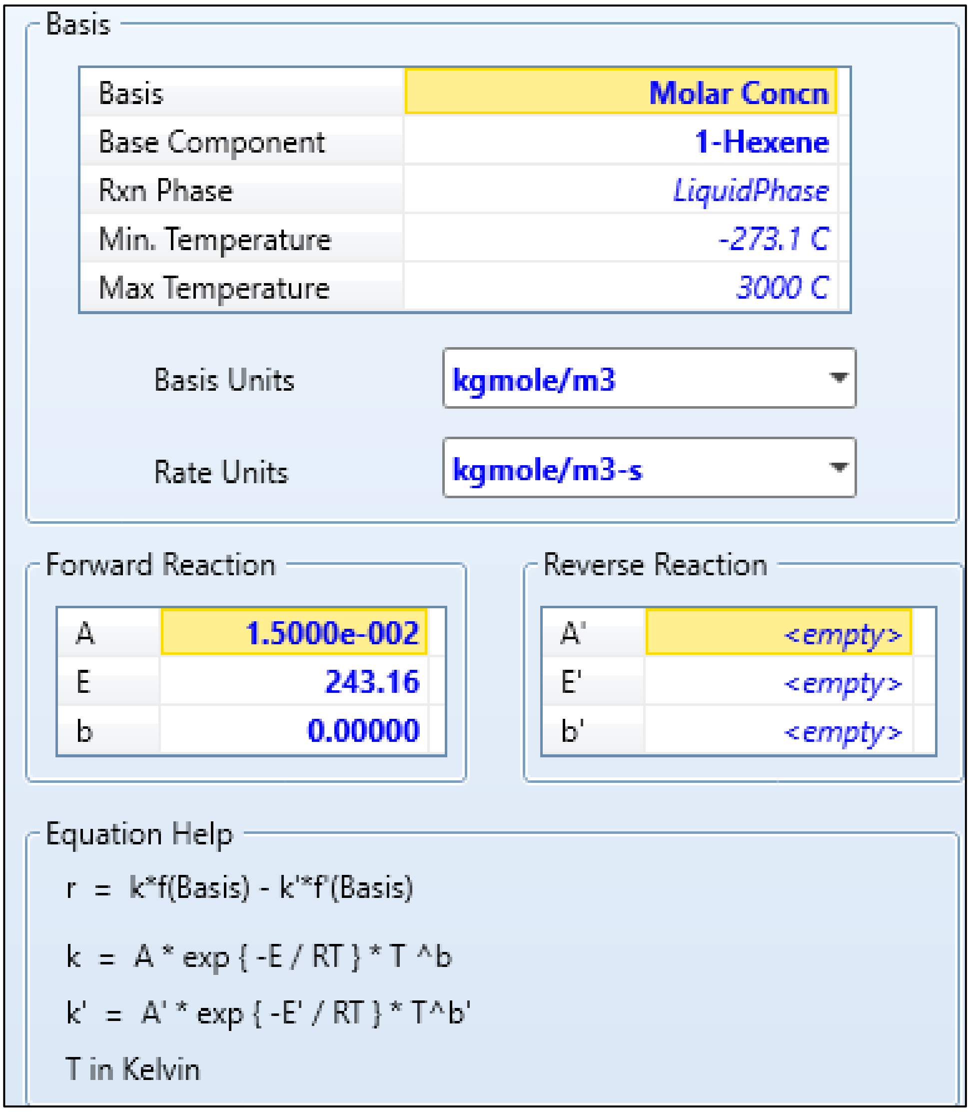

Basis

Basis	Molar Concn
Base Component	1-Hexene
Rxn Phase	LiquidPhase
Min. Temperature	-273.1 C
Max Temperature	3000 C

Basis Units: kgmole/m3

Rate Units: kgmole/m3-s

Forward Reaction

A	1.5000e-002
E	243.16
b	0.00000

Reverse Reaction

A'	<empty>
E'	<empty>
b'	<empty>

Equation Help

r = k*f(Basis) - k'*f'(Basis)

k = A * exp { -E / RT } * T ^b

k' = A' * exp { -E' / RT } * T^b'

T in Kelvin

Figure 6.15: Kinetic Parameters for Reaction 2

(c) Reaction 3:

Hexene and Octadecene to Tetracosene

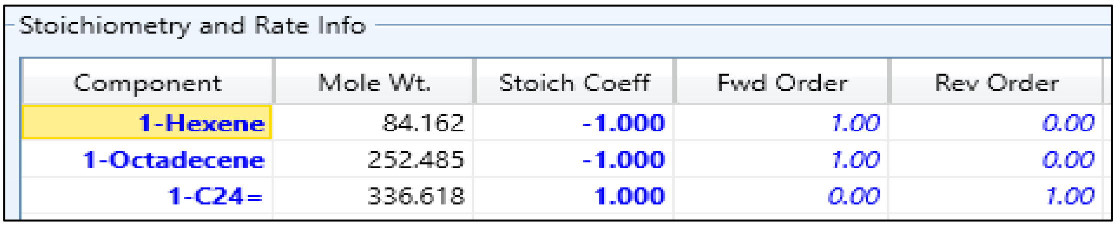

Stoichiometry and Rate Info

Component	Mole Wt.	Stoich Coeff	Fwd Order	Rev Order
1-Hexene	84.162	-1.000	1.00	0.00
1-Octadecene	252.485	-1.000	1.00	0.00
1-C24=	336.618	1.000	0.00	1.00

Figure 6.16: Stoichiometry for Reaction 3

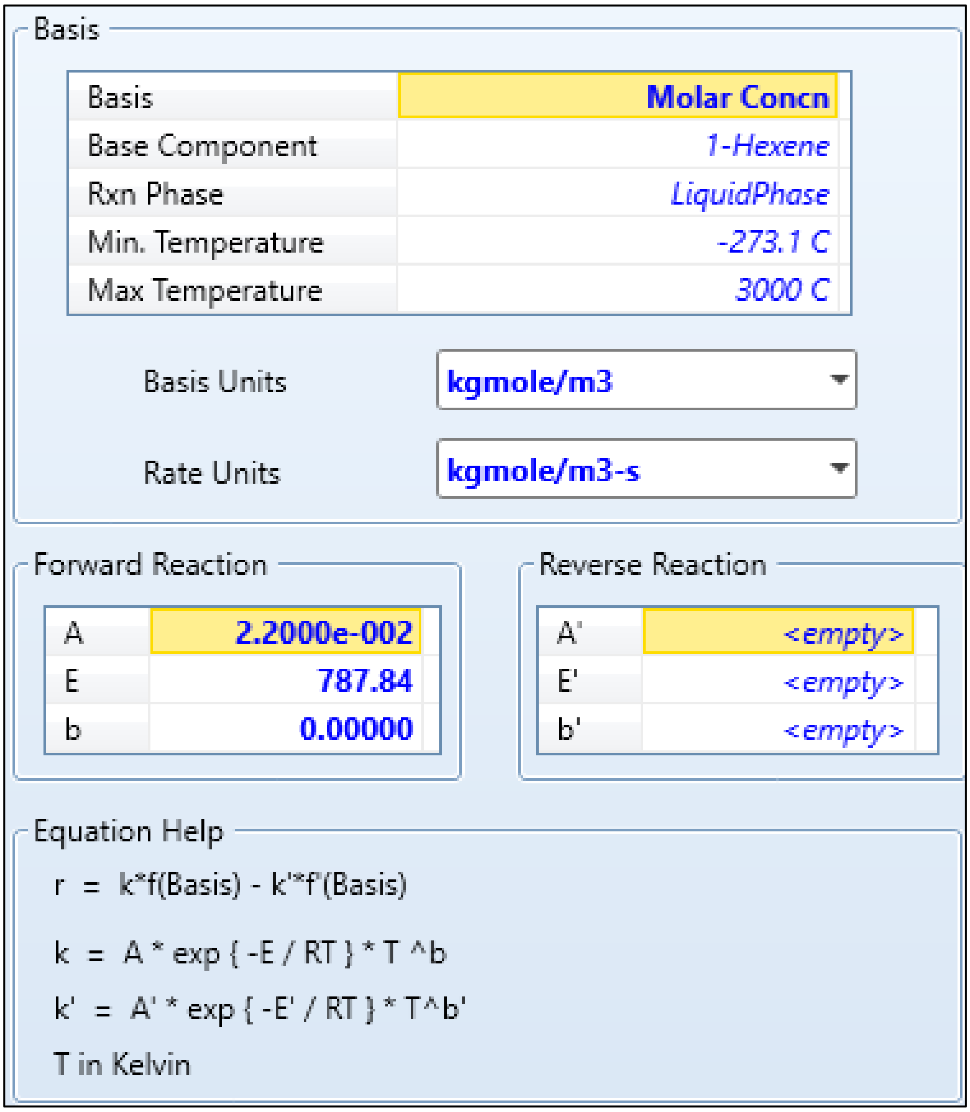

Basis

Basis	Molar Concn
Base Component	1-Hexene
Rxn Phase	LiquidPhase
Min. Temperature	-273.1 C
Max Temperature	3000 C

Basis Units: kgmole/m3

Rate Units: kgmole/m3-s

Forward Reaction

A	2.2000e-002
E	787.84
b	0.00000

Reverse Reaction

A'	<empty>
E'	<empty>
b'	<empty>

Equation Help

r = k*f(Basis) - k'*f'(Basis)

k = A * exp { -E / RT } * T ^b

k' = A' * exp { -E' / RT } * T^b'

T in Kelvin

Figure 6.17: Kinetic Parameters for Reaction 3

(d) <u>Reaction 4:</u>

<u>Hexene and Tetracosene to Triacontene</u>

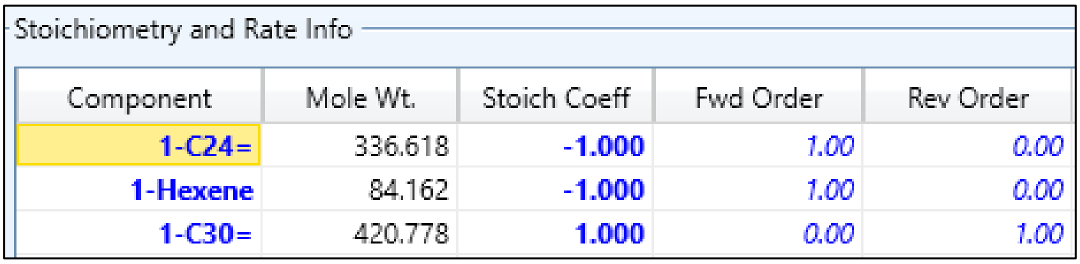

Stoichiometry and Rate Info

Component	Mole Wt.	Stoich Coeff	Fwd Order	Rev Order
1-C24=	336.618	-1.000	1.00	0.00
1-Hexene	84.162	-1.000	1.00	0.00
1-C30=	420.778	1.000	0.00	1.00

Figure 6.18: Stoichiometry for Reaction 4

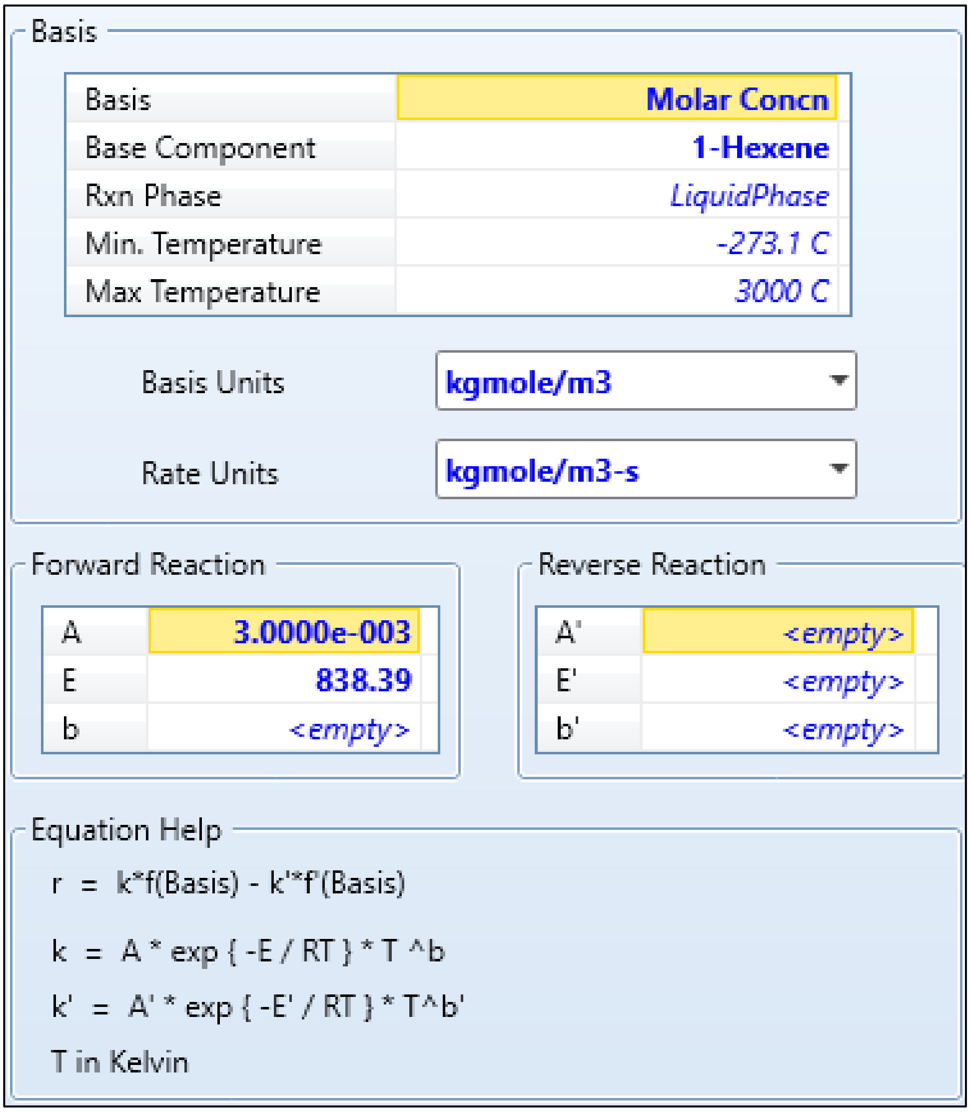

Basis

Basis	Molar Concn
Base Component	1-Hexene
Rxn Phase	LiquidPhase
Min. Temperature	-273.1 C
Max Temperature	3000 C

Basis Units: kgmole/m3

Rate Units: kgmole/m3-s

Forward Reaction

A	3.0000e-003
E	838.39
b	<empty>

Reverse Reaction

A'	<empty>
E'	<empty>
b'	<empty>

Equation Help

r = k*f(Basis) - k'*f'(Basis)

k = A * exp { -E / RT } * T ^b

k' = A' * exp { -E' / RT } * T^b'

T in Kelvin

Figure 6.19: Kinetic Parameters for Reaction 4

(e) Reaction 5:

Heptene to Tetradecene

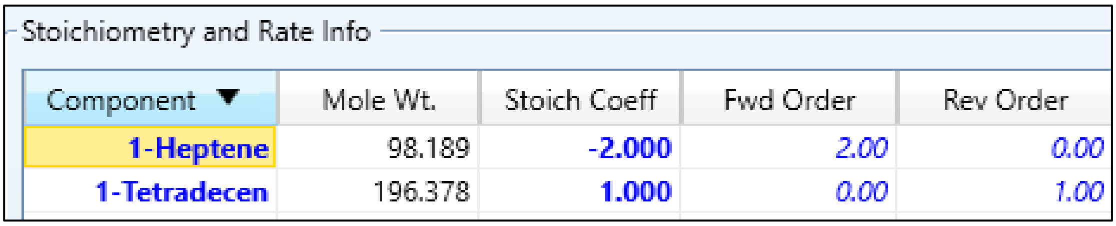

Stoichiometry and Rate Info

Component	Mole Wt.	Stoich Coeff	Fwd Order	Rev Order
1-Heptene	98.189	-2.000	2.00	0.00
1-Tetradecen	196.378	1.000	0.00	1.00

Figure 6.20: Stoichiometry for Reaction 5

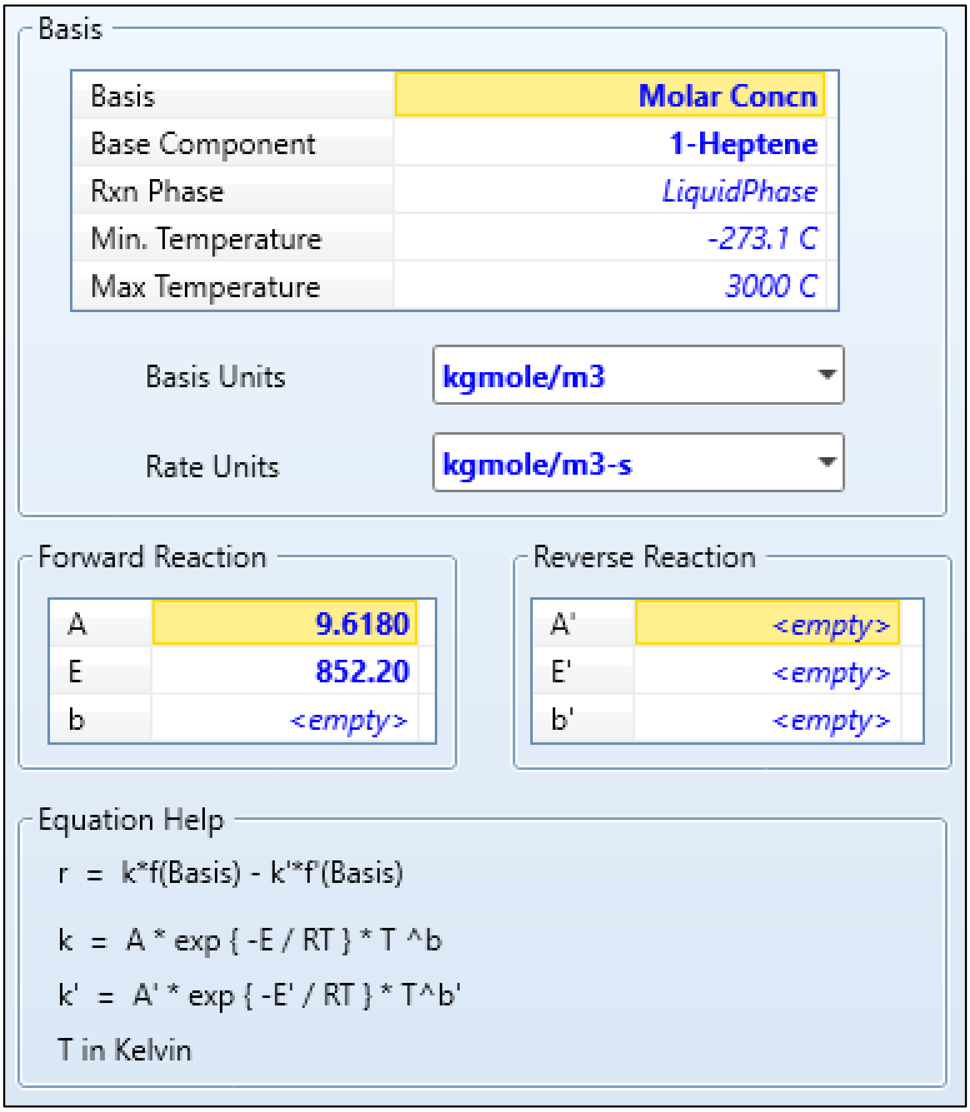

Basis

Basis	Molar Concn
Base Component	1-Heptene
Rxn Phase	LiquidPhase
Min. Temperature	-273.1 C
Max Temperature	3000 C

Basis Units: kgmole/m3

Rate Units: kgmole/m3-s

Forward Reaction

A	9.6180
E	852.20
b	<empty>

Reverse Reaction

A'	<empty>
E'	<empty>
b'	<empty>

Equation Help

r = k*f(Basis) - k'*f'(Basis)

k = A * exp { -E / RT } * T ^b

k' = A' * exp { -E' / RT } * T^b'

T in Kelvin

Figure 6.21: Kinetic Parameters for Reaction 5

(f) Reaction 6:

Heptene and Tetradecene to Heneicosene

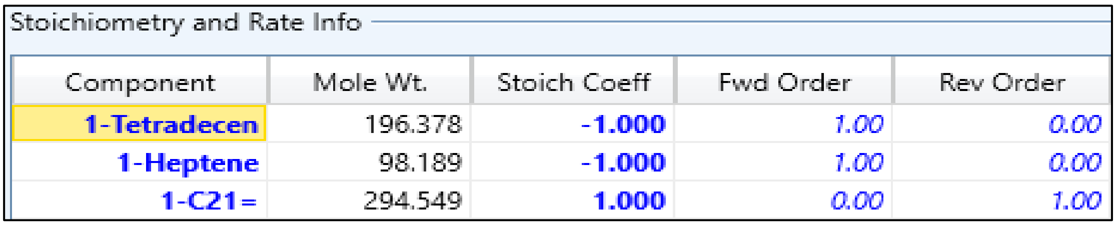

Stoichiometry and Rate Info

Component	Mole Wt.	Stoich Coeff	Fwd Order	Rev Order
1-Tetradecen	196.378	-1.000	1.00	0.00
1-Heptene	98.189	-1.000	1.00	0.00
1-C21=	294.549	1.000	0.00	1.00

Figure 6.22: Stoichiometry for Reaction 6

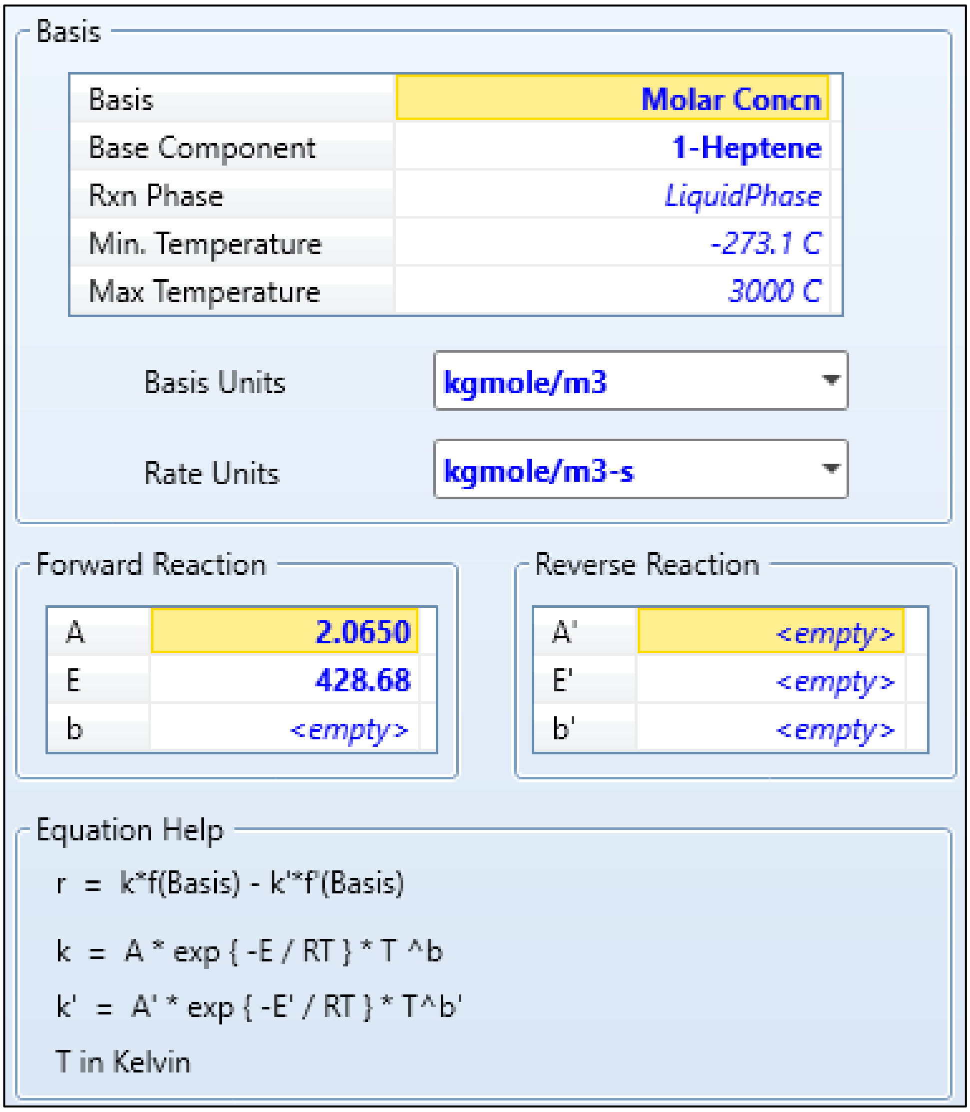

Basis

Basis	Molar Concn
Base Component	1-Heptene
Rxn Phase	LiquidPhase
Min. Temperature	-273.1 C
Max Temperature	3000 C

Basis Units: kgmole/m3

Rate Units: kgmole/m3-s

Forward Reaction

A	2.0650
E	428.68
b	<empty>

Reverse Reaction

A'	<empty>
E'	<empty>
b'	<empty>

Equation Help

r = k*f(Basis) - k'*f'(Basis)

k = A * exp { -E / RT } * T ^b

k' = A' * exp { -E' / RT } * T^b'

T in Kelvin

Figure 6.23: Kinetic Parameters for Reaction 6

(g) Reaction 7:

Heptene and Heneicosene to Octacosene

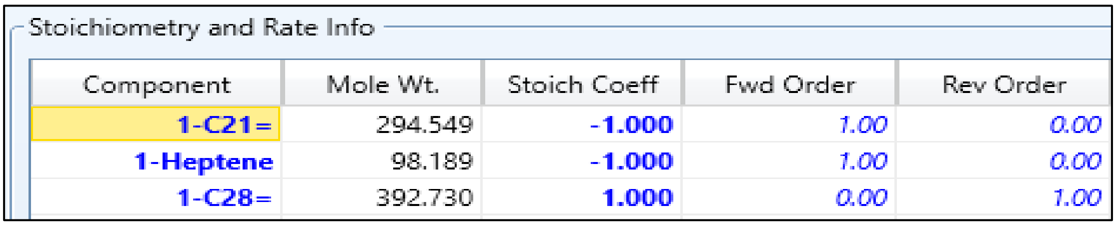

Stoichiometry and Rate Info

Component	Mole Wt.	Stoich Coeff	Fwd Order	Rev Order
1-C21=	294.549	-1.000	1.00	0.00
1-Heptene	98.189	-1.000	1.00	0.00
1-C28=	392.730	1.000	0.00	1.00

Figure 6.24: Stoichiometry for Reaction 7

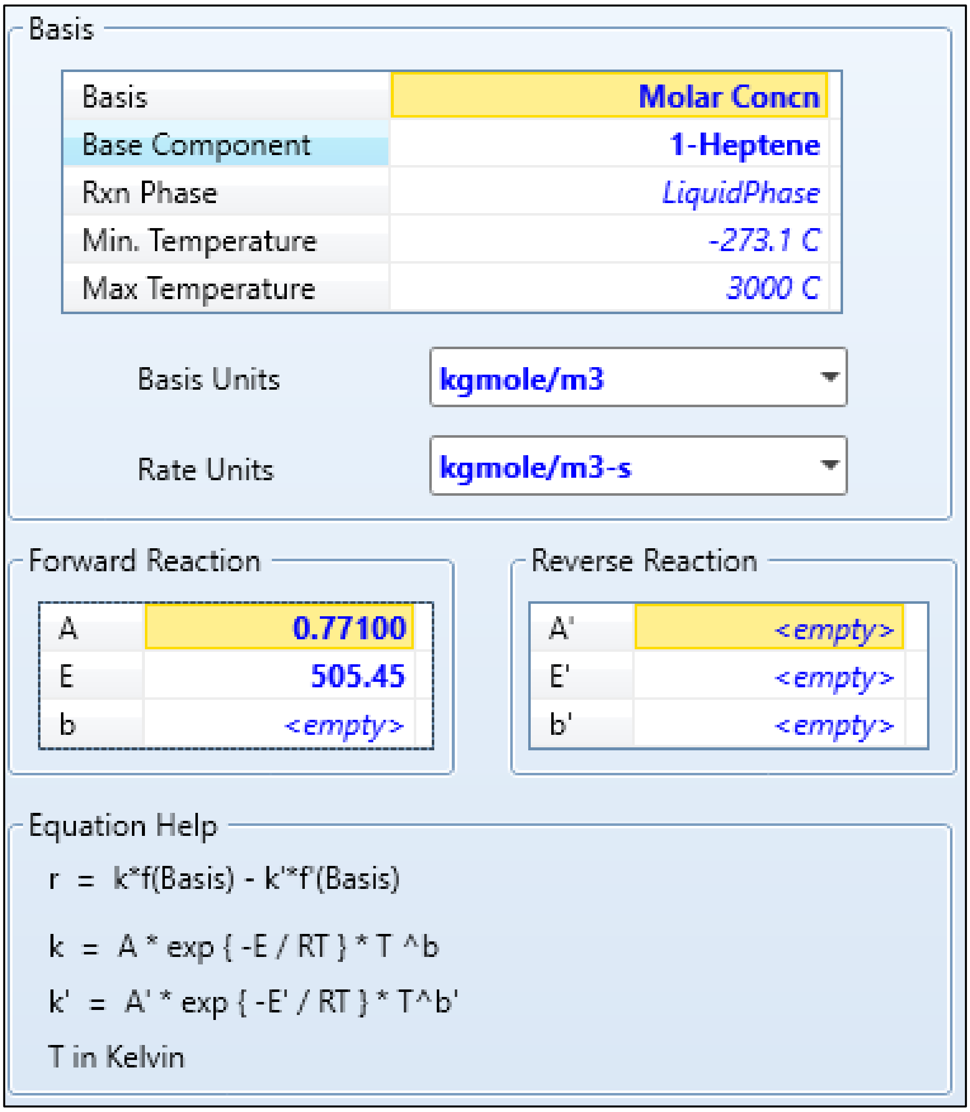

Basis

Basis	Molar Concn
Base Component	1-Heptene
Rxn Phase	LiquidPhase
Min. Temperature	-273.1 C
Max Temperature	3000 C

Basis Units: kgmole/m3

Rate Units: kgmole/m3-s

Forward Reaction

A	0.77100
E	505.45
b	<empty>

Reverse Reaction

A'	<empty>
E'	<empty>
b'	<empty>

Equation Help

r = k*f(Basis) - k'*f'(Basis)

k = A * exp { -E / RT } * T ^b

k' = A' * exp { -E' / RT } * T^b'

T in Kelvin

Figure 6.25: Kinetic Parameters for Reaction 7

(h) Reaction 8:

Octene to Hexadecene

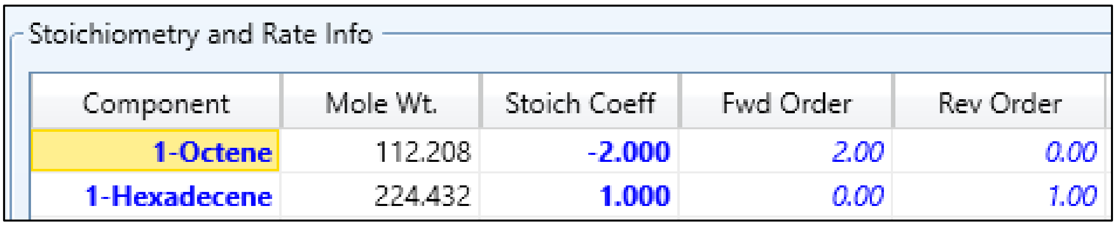

Stoichiometry and Rate Info

Component	Mole Wt.	Stoich Coeff	Fwd Order	Rev Order
1-Octene	112.208	-2.000	2.00	0.00
1-Hexadecene	224.432	1.000	0.00	1.00

Figure 6.26: Stoichiometry for Reaction 8

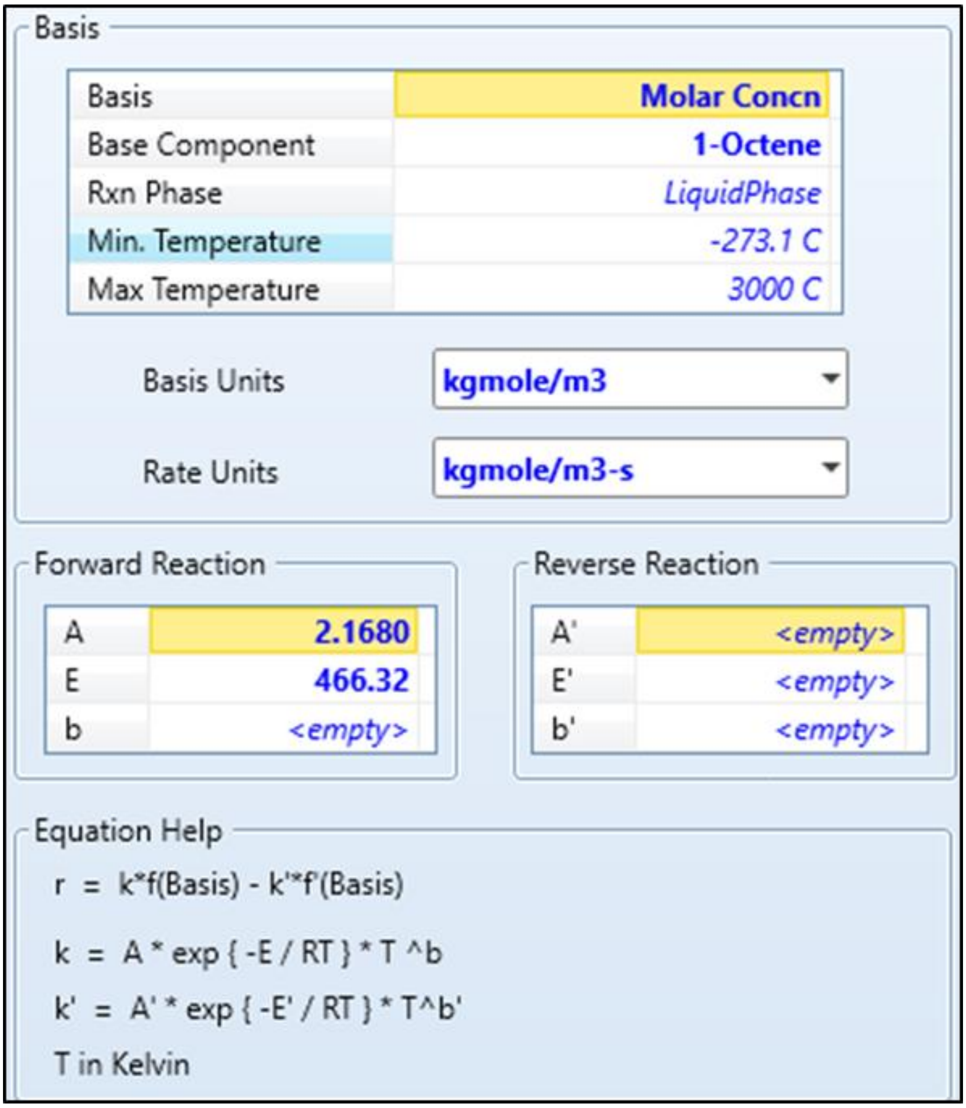

Basis

Basis	Molar Concn
Base Component	1-Octene
Rxn Phase	LiquidPhase
Min. Temperature	-273.1 C
Max Temperature	3000 C

Basis Units: kgmole/m3

Rate Units: kgmole/m3-s

Forward Reaction

A	2.1680
E	466.32
b	<empty>

Reverse Reaction

A'	<empty>
E'	<empty>
b'	<empty>

Equation Help

r = k*f(Basis) - k'*f'(Basis)

k = A * exp { -E / RT } * T ^b

k' = A' * exp { -E' / RT } * T^b'

T in Kelvin

Figure 6.27: Kinetic Parameters for Reaction 8

(i) <u>Reaction 9:</u>

Octene and Hexadecene to Tetracosene

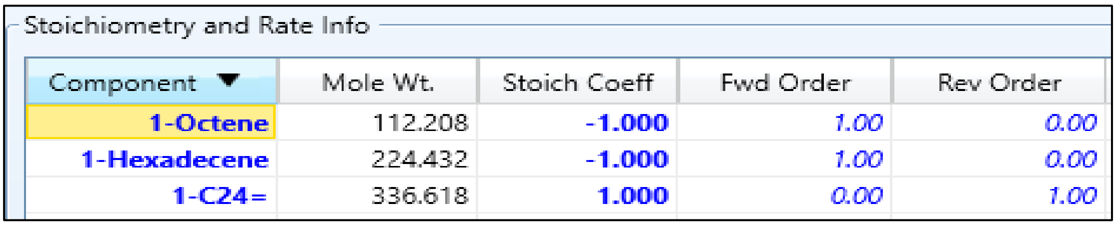

Stoichiometry and Rate Info

Component	Mole Wt.	Stoich Coeff	Fwd Order	Rev Order
1-Octene	112.208	-1.000	1.00	0.00
1-Hexadecene	224.432	-1.000	1.00	0.00
1-C24=	336.618	1.000	0.00	1.00

Figure 6.28: Stoichiometry for Reaction 9

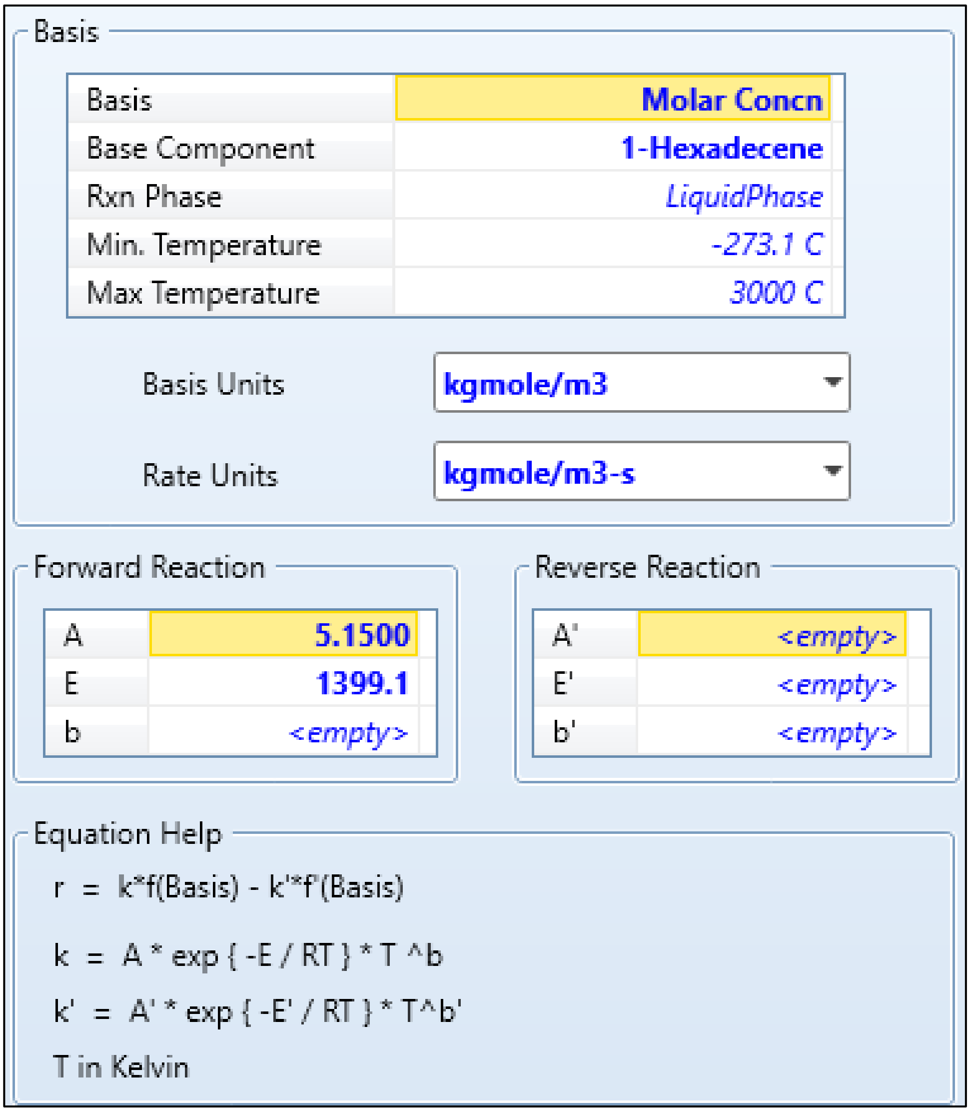

Basis	Molar Concn
Base Component	1-Hexadecene
Rxn Phase	LiquidPhase
Min. Temperature	-273.1 C
Max Temperature	3000 C

Basis Units: kgmole/m3

Rate Units: kgmole/m3-s

Forward Reaction

A	5.1500
E	1399.1
b	<empty>

Reverse Reaction

A'	<empty>
E'	<empty>
b'	<empty>

Equation Help

r = k*f(Basis) - k'*f'(Basis)

k = A * exp { -E / RT } * T ^b

k' = A' * exp { -E' / RT } * T^b'

T in Kelvin

Figure 6.29: Kinetic Parameters for Reaction 9

(j) Reaction 10:

Nonene to Octadecene

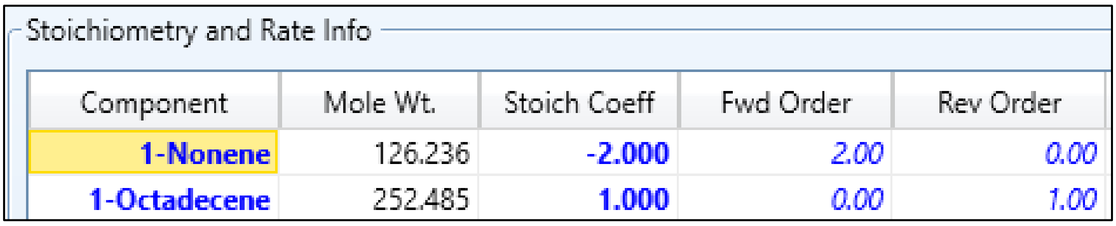

Stoichiometry and Rate Info

Component	Mole Wt.	Stoich Coeff	Fwd Order	Rev Order
1-Nonene	126.236	-2.000	2.00	0.00
1-Octadecene	252.485	1.000	0.00	1.00

Figure 6.30: Stoichiometry for Reaction 10

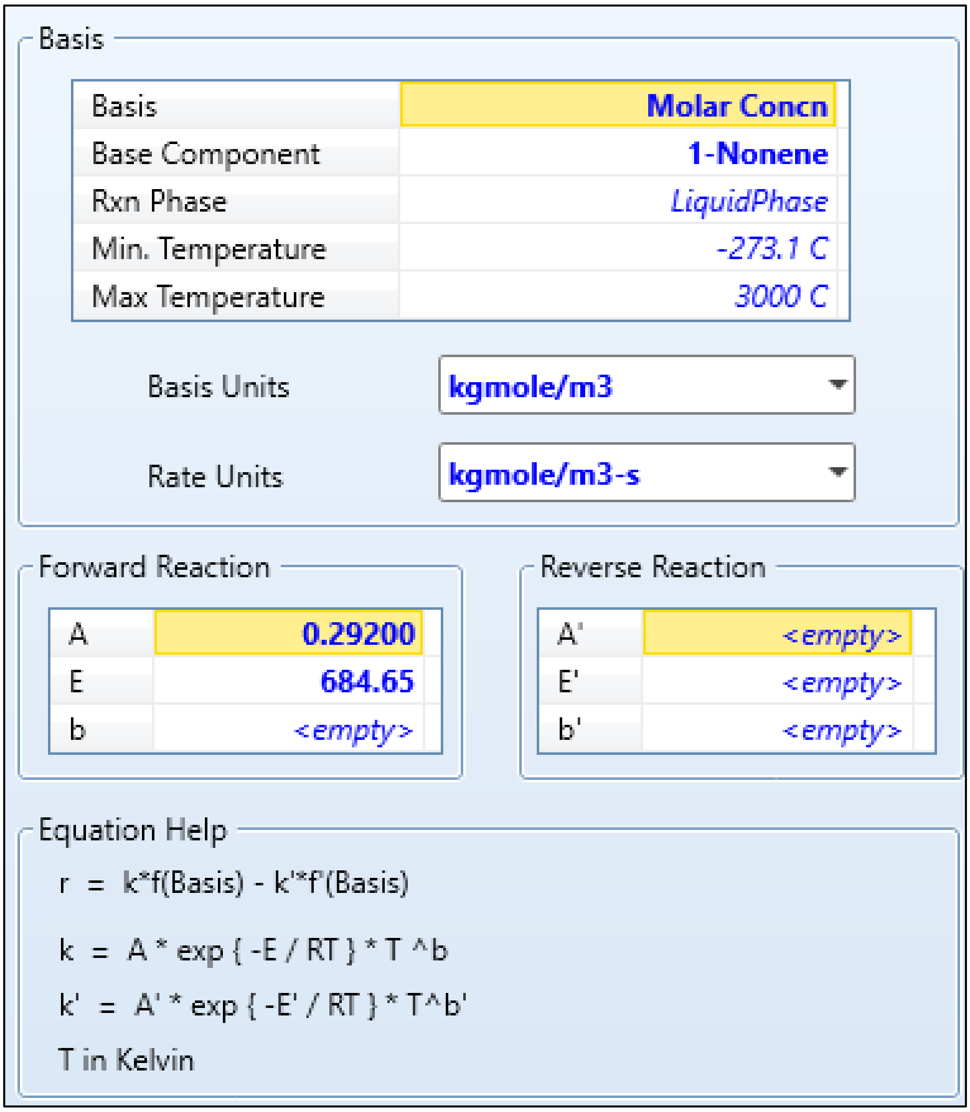

Basis	Molar Concn
Base Component	1-Nonene
Rxn Phase	LiquidPhase
Min. Temperature	-273.1 C
Max Temperature	3000 C

Basis Units: kgmole/m3

Rate Units: kgmole/m3-s

A	0.29200
E	684.65
b	<empty>

A'	<empty>
E'	<empty>
b'	<empty>

r = k*f(Basis) - k'*f'(Basis)

k = A * exp { -E / RT } * T ^b

k' = A' * exp { -E' / RT } * T^b'

T in Kelvin

Figure 6.31: Kinetic Parameters for Reaction 10

(k) <u>Reaction 11:</u>

<u>Nonene and Octadecene to Heptacosene</u>

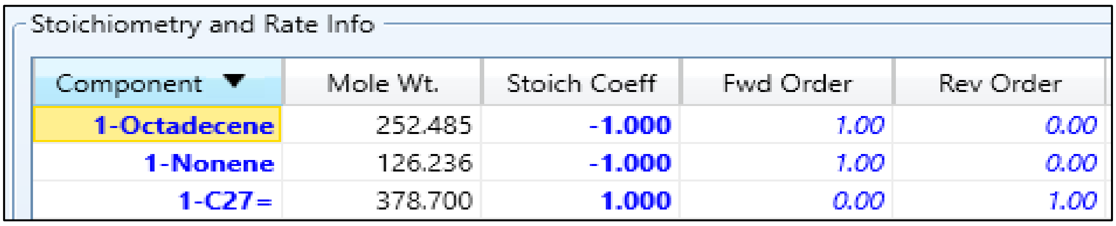

Component	Mole Wt.	Stoich Coeff	Fwd Order	Rev Order
1-Octadecene	252.485	-1.000	1.00	0.00
1-Nonene	126.236	-1.000	1.00	0.00
1-C27=	378.700	1.000	0.00	1.00

Figure 6.32: Stoichiometry for Reaction 11

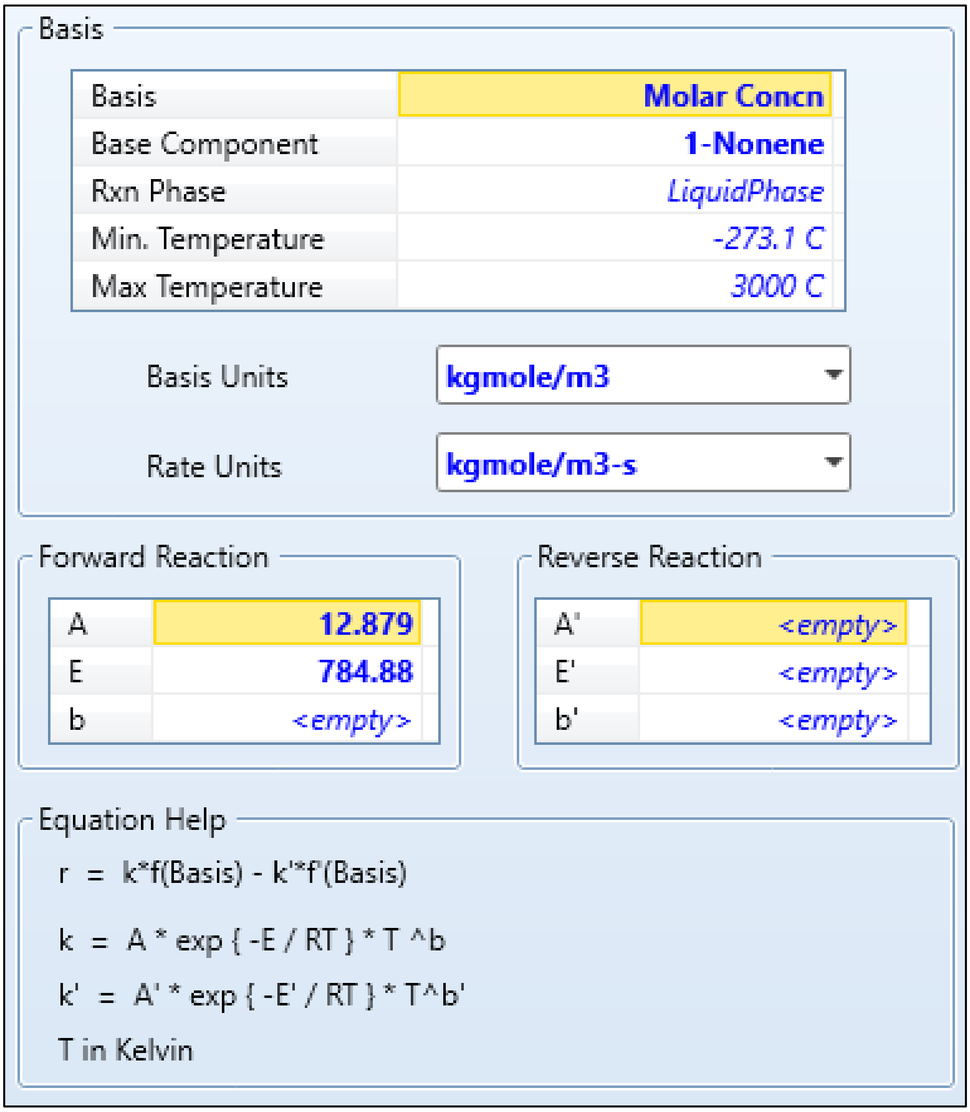

Basis

Basis	Molar Concn
Base Component	1-Nonene
Rxn Phase	*LiquidPhase*
Min. Temperature	*-273.1 C*
Max Temperature	*3000 C*

Basis Units: kgmole/m3

Rate Units: kgmole/m3-s

Forward Reaction

A	12.879
E	784.88
b	*<empty>*

Reverse Reaction

A'	*<empty>*
E'	*<empty>*
b'	*<empty>*

Equation Help

r = k*f(Basis) - k'*f'(Basis)

k = A * exp { -E / RT } * T ^b

k' = A' * exp { -E' / RT } * T^b'

T in Kelvin

Figure 6.33: Kinetic Parameters for Reaction 11

(l) <u>Reaction 12:</u>

<u>Decene to Eicosene</u>

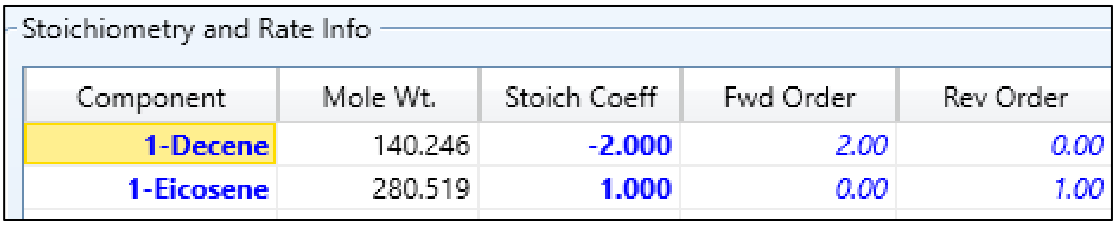

Stoichiometry and Rate Info

Component	Mole Wt.	Stoich Coeff	Fwd Order	Rev Order
1-Decene	140.246	-2.000	*2.00*	*0.00*
1-Eicosene	280.519	1.000	*0.00*	*1.00*

Figure 6.34: Stoichiometry for Reaction 12

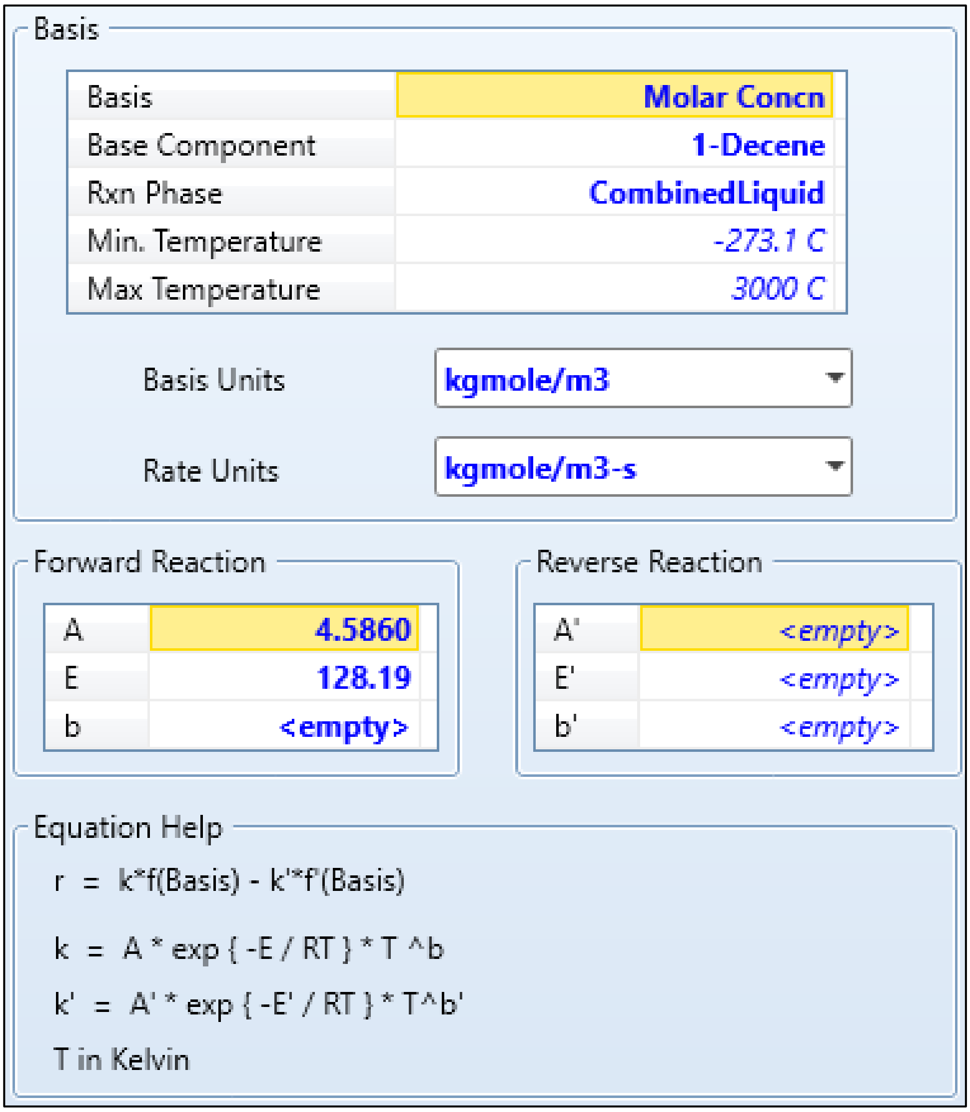

Basis

Basis	Molar Concn
Base Component	1-Decene
Rxn Phase	CombinedLiquid
Min. Temperature	-273.1 C
Max Temperature	3000 C

Basis Units: kgmole/m3

Rate Units: kgmole/m3-s

Forward Reaction

A	4.5860
E	128.19
b	<empty>

Reverse Reaction

A'	<empty>
E'	<empty>
b'	<empty>

Equation Help

r = k*f(Basis) - k'*f'(Basis)

k = A * exp { -E / RT } * T ^b

k' = A' * exp { -E' / RT } * T^b'

T in Kelvin

Figure 6.35: Kinetic Parameters for Reaction 12

(m) <u>Reaction 13:</u>

<u>Decene and Eicosene to Triacontene</u>

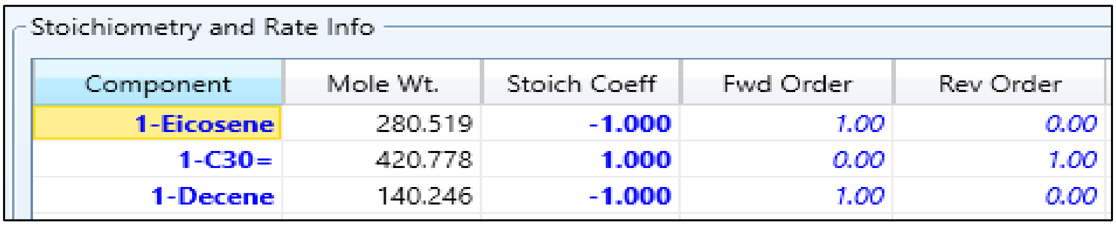

Stoichiometry and Rate Info

Component	Mole Wt.	Stoich Coeff	Fwd Order	Rev Order
1-Eicosene	280.519	-1.000	1.00	0.00
1-C30=	420.778	1.000	0.00	1.00
1-Decene	140.246	-1.000	1.00	0.00

Figure 6.36: Stoichiometry for Reaction 13

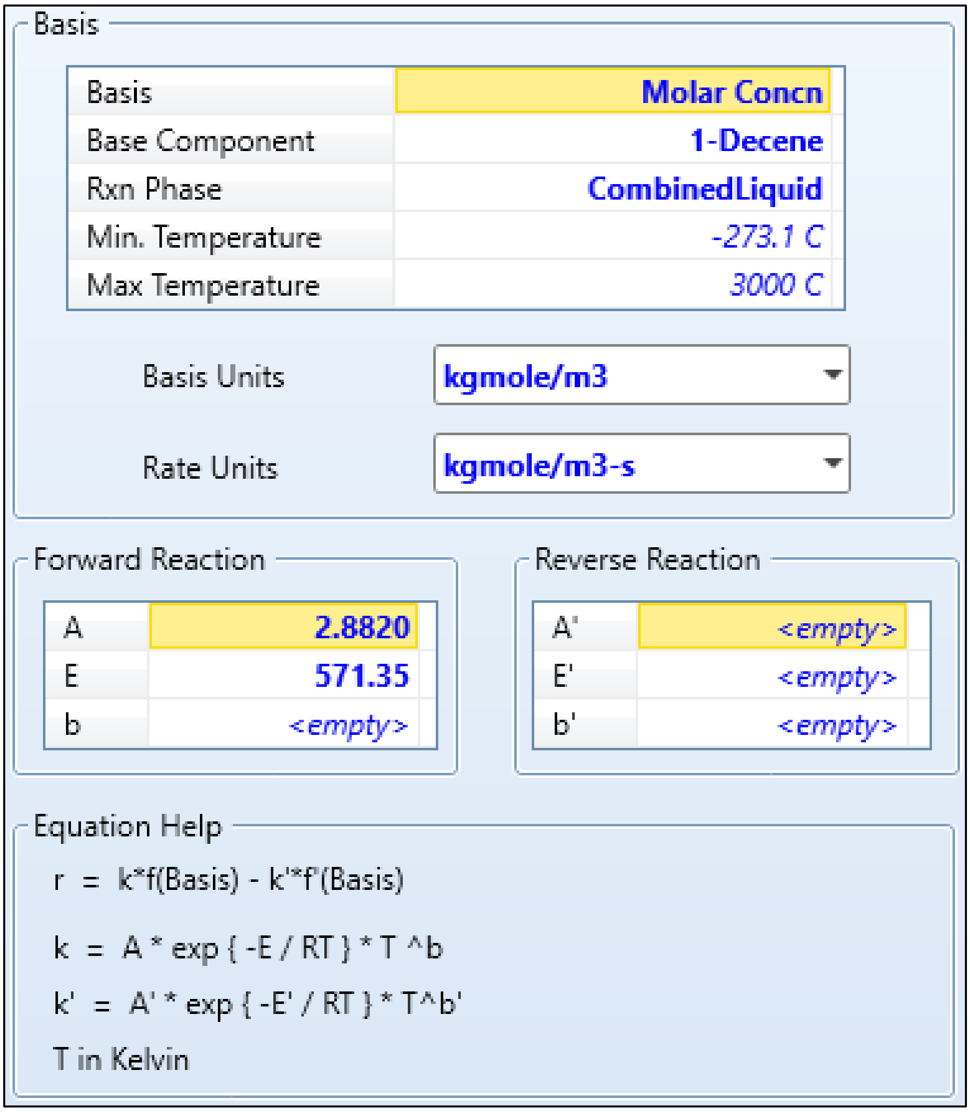

Basis

Basis	Molar Concn
Base Component	1-Decene
Rxn Phase	CombinedLiquid
Min. Temperature	-273.1 C
Max Temperature	3000 C

Basis Units: kgmole/m3

Rate Units: kgmole/m3-s

Forward Reaction

A	2.8820
E	571.35
b	<empty>

Reverse Reaction

A'	<empty>
E'	<empty>
b'	<empty>

Equation Help

r = k*f(Basis) - k'*f'(Basis)

k = A * exp { -E / RT } * T ^b

k' = A' * exp { -E' / RT } * T^b'

T in Kelvin

Figure 6.37: Kinetic Parameters for Reaction 13

6.10 Reactor Details

The oligomerisation reactions for 1 ton/hr of feed (WCN) was carried out in a plug flow oligomerisation reactor. The reactor details are given in the Table 6.16 below:

Table 6.16: Plug flow reactor details

Parameter	Volume
Total Volume (m^3)	5
Length (m)	50
Diameter (m)	0.36
Number of Tubes	1
Wall Thickness (m)	0.005

6.11 Reaction summary

Based on the simulation the below Table 6.17 represents the conversions of individual reactions:

Table 6.17: Reaction conversions

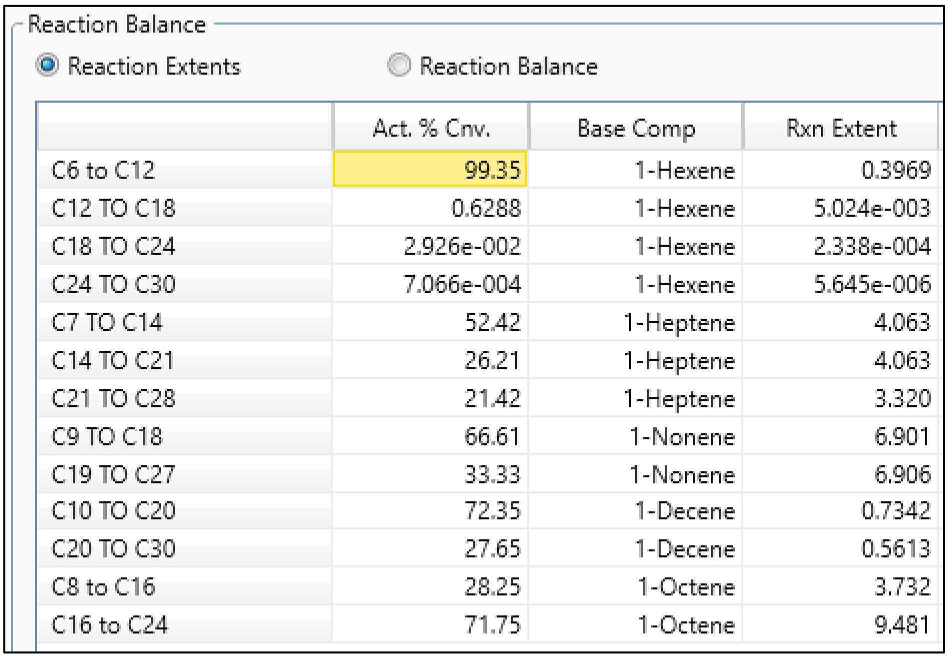

Reaction Balance

● Reaction Extents ○ Reaction Balance

	Act. % Cnv.	Base Comp	Rxn Extent
C6 to C12	99.35	1-Hexene	0.3969
C12 TO C18	0.6288	1-Hexene	5.024e-003
C18 TO C24	2.926e-002	1-Hexene	2.338e-004
C24 TO C30	7.066e-004	1-Hexene	5.645e-006
C7 TO C14	52.42	1-Heptene	4.063
C14 TO C21	26.21	1-Heptene	4.063
C21 TO C28	21.42	1-Heptene	3.320
C9 TO C18	66.61	1-Nonene	6.901
C19 TO C27	33.33	1-Nonene	6.906
C10 TO C20	72.35	1-Decene	0.7342
C20 TO C30	27.65	1-Decene	0.5613
C8 to C16	28.25	1-Octene	3.732
C16 to C24	71.75	1-Octene	9.481

The conversion indicates that the kinetic model predicts the formation of oligomers with higher carbon numbers (> C 20). The net conversion of PAO from cracked wax feedstock vide oligomerisation is 45% (wt. basis), i.e. upon 1 ton/hr of cracked wax naphtha feed stream, 450 kg/hr of Poly alpha olefins are produced after distillation.

The feed and product composition in the reactor is given in the Table 6.18 below:

Table 6.18: Reactor feed and product composition

Component	Feed Composition (mole %)	Product Composition (mole %)
1-Hexene	0.004	0.000
1-Eicosene	0.000	0.001
1-Decene	0.010	0.000
1-C27=	0.000	0.042
1-Nonene	0.101	0.000
1-Hexadecene	0.000	0.080
cis4-Octene	0.000	0.000
1-C28=	0.000	0.020
1-C30=	0.000	0.003
1-Octadecene	0.000	0.000
1-Dodecene	0.000	0.002
1-C24=	0.000	0.000
1-Heptene	0.076	0.000
1-C21=	0.000	0.004
1-Octene	0.129	0.000
n-Octane	0.125	0.156
Cyclohexane	0.003	0.003
Cycloheptane	0.079	0.098
Cyclooctane	0.060	0.075
Cyclononane	0.067	0.083
Cyclodecane	0.002	0.002
n-Hexane	0.025	0.031
n-Heptane	0.174	0.216
n-Nonane	0.041	0.052
n-Decane	0.005	0.006
Benzene	0.001	0.002
Toluene	0.032	0.040
o-Xylene	0.055	0.068
1M3-EBenzene	0.008	0.010

6.12 Product Separation

The product from oligomerisation reactions consists of Poly alpha olefins and unreacted olefins. The separation of these fractions is key for attaining the desired product specifications. Distillation is on the widely used separation unit operation for this purpose. In this model distillation unit is considered to separate the feed stream into two streams, a top stream which has a boiling point of less than 200 ^{0}C and the bottom stream which will be having boiling point greater than 200 ^{0}C. Unconverted olefins will typically have boiling point less than 200 ^{0}C and these will constitute the top product, whereas, the bottom product having the higher oligomers can be retrieved as the Poly alpha olefin product.

In the current process model, binary component distillation module has been used with partial reflux for separating out PAO stream from feed. The column was designed and sized using ASPEN HYSYS equipment sizing and rating tool The details of the column are given in Table 6.19 below.

Table 6.19: Distillation column design details

Distillation Column Details	
Tray Type	Sieve
Number of Trays	11
Diameter [m]	0.318693207
Tray Spacing [m]	0.6096
Number Of Passes	1
Hole Diameter [mm]	12.7
Hole Area to Active Area	0.1
Deck Gauge Thickness	10 Gauge
Deck Gauge Thickness Value [mm]	3.4036
Cross-Sectional Area [m2]	7.98E-02
Active Area [m2]	6.38E-02
Net Area [m2]	7.18E-02
Downcomer Geometry	
Downcomer Clearance (mm)	38.1
Downcomer Width Top (mm)	49.86770636
Downcomer Width Bottom (mm)	49.86770636

Downcomer Area Top (m2)	7.98E-03
Downcomer Area Bottom (m2)	7.98E-03
Weir Geometry	
Weir Height (mm)	50.8
Weir Length (m)	0.30
Panel Details	
Flow Path Length (m)	0.284090054
Bubbling Area (m2)	0.10742781

The design was validated using hydraulic plots, Figures 6.38 to Figures 6.41 where in flooding and weeping level in each tray was checked. Following are the hydrodynamic details of the column:

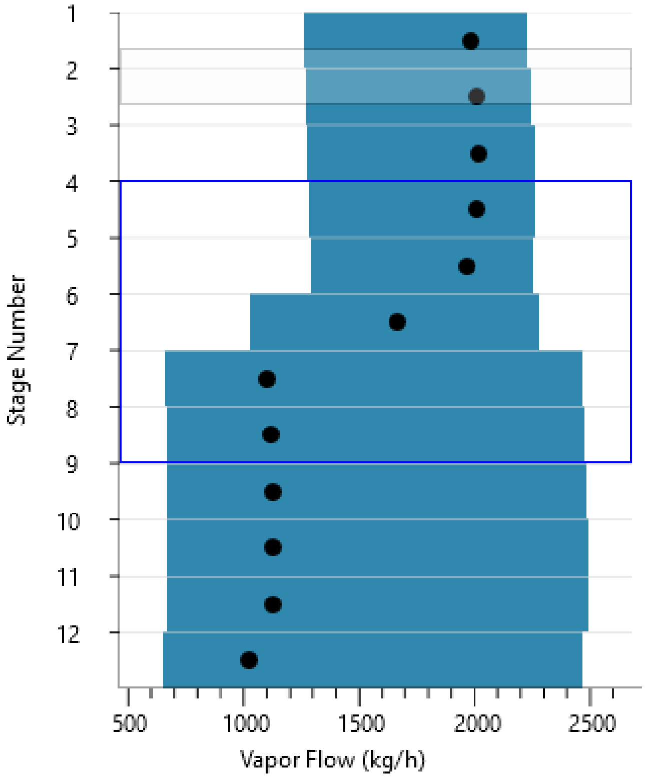

Figure 6.38: Vapor flow profile across the trays

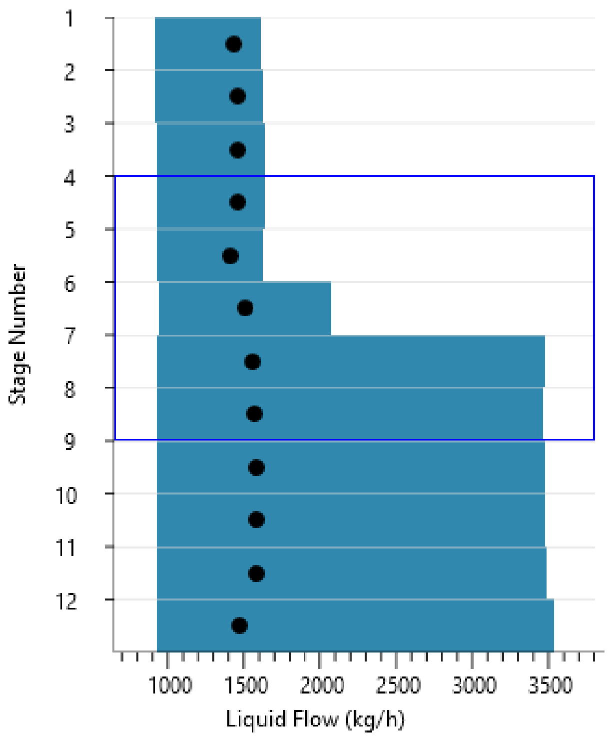

Figure 6.39: Liquid flow across the trays

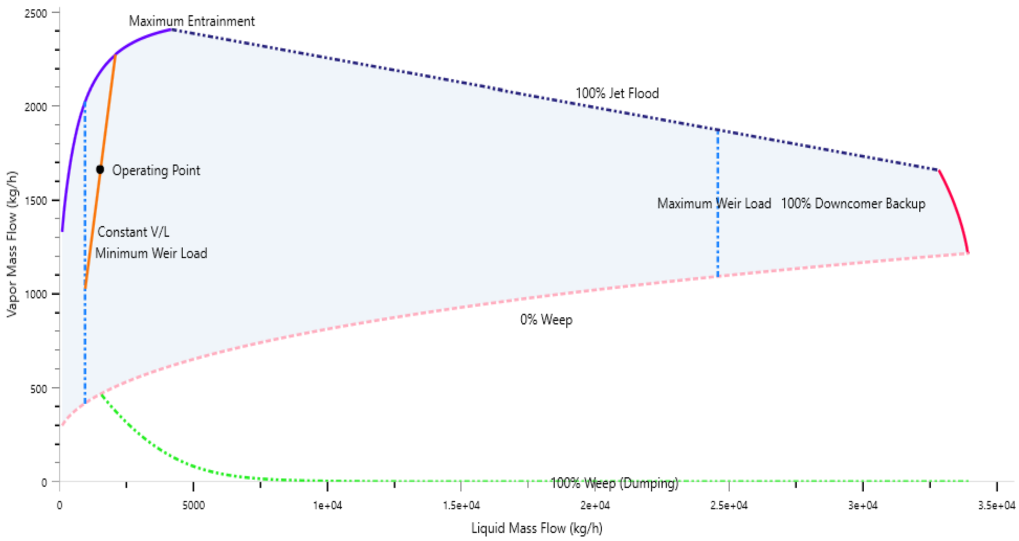

Figure 6.40: Hydraulic plot for trays

The hydraulic plot above for trays indicates that the operating point is well within the limits of maximum entrainment, weeping. The figure also indicates that further increase in liquid rate within the trays is possible without any hydrodynamic limitations. This provides an operating window for increasing reflux ratio to tune the operating parameters.

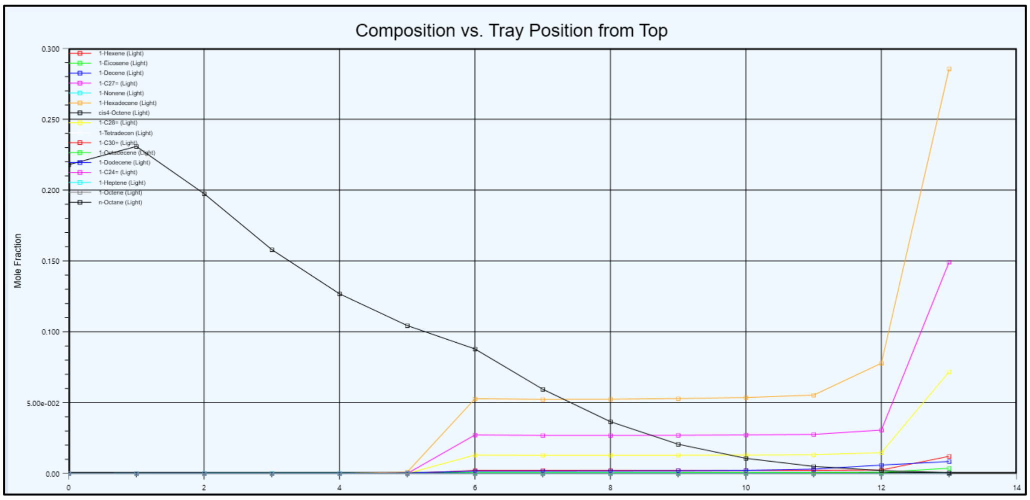

Figure 6.41: Composition profile across stages

The above profile indicates the variation of composition of various components across the trays. The concentration of olefins are higher to the top section where as the composition of poly olefins are concentrated at the bottom section of the column. This provides a clear insight of the proper separation that is taking place within the column.

The bottom product from the distillation column includes PAO. The property details are given in the Table 6.20 below:

Table 6.20: Physical properties of PAO product

PHYSICAL PROPERTIES OF PAO PRODUCT	
Molecular Weight	217.76
Molar Density [kgmole/m3]	3.72
Mass Density [kg/m3]	810.30
Mass Entropy [kJ/kg-C]	1.91
Heat Capacity [kJ/kgmole-C]	425.40
Mass Heat Capacity [kJ/kg-C]	1.95
Avg. Liq. Density [kgmole/m3]	3.69
Specific Heat [kJ/kgmole-C]	425.40

Cp/Cv	1.18
Kinematic Viscosity [cSt]	4.56
Molar Volume [m3/kgmole]	0.27
Mass Heat of Vap. [kJ/kg]	644.65
Surface Tension [dyne/cm]	26.70
Thermal Conductivity [W/m-K]	0.14
Viscosity [cP]	3.70
Reid VP at 37.8 C [kg/cm2]	0.01
Viscosity Index	18.51

6.13 Mass Balance Summary

Summary of Results from process model including process parameters, mass balance and material balance is given in the Table 6.21 below:

Table 6.21: Summary of process model results

	Feed Naphtha	**Product from reaction**	**Feed to Distillation Unit**	**200- cut from Distillation Unit**	**PAO Product**
Vapour Fraction	0.0	0.0	0.7	0.0	0.0
Temperature [C]	30.0	100.0	190.0	109.5	30.0
Pressure [kg/cm2]	2.0	1.9	1.9	1.0	1.0
Mass Flow [kg/h]	1000.0	1004.0	1000.0	550.0	450.0
Mole Fraction					
1-Hexene	0.003	0.000	0.000	0.000	0.000
1-Eicosene	0.000	0.002	0.001	0.000	0.004
1-Decene	0.013	0.000	0.000	0.000	0.000
1-C27=	0.000	0.116	0.042	0.000	0.149
1-Nonene	0.117	0.000	0.000	0.000	0.000
1-Hexadecene	0.000	0.132	0.081	0.000	0.285
cis4-Octene	0.000	0.000	0.000	0.000	0.000
1-C28=	0.000	0.058	0.020	0.000	0.072
1-Tetradecen	0.000	0.000	0.000	0.000	0.000
1-C30=	0.000	0.010	0.003	0.000	0.012

	Feed Naphtha	**Product from reaction**	**Feed to Distillation Unit**	**200- cut from Distillation Unit**	**PAO Product**
1-Octadecene	0.000	0.000	0.000	0.000	0.000
1-Dodecene	0.000	0.003	0.002	0.000	0.008
1-C24=	0.000	0.000	0.000	0.000	0.000
1-Heptene	0.068	0.000	0.000	0.000	0.000
1-C21=	0.000	0.010	0.005	0.000	0.016
1-Octene	0.132	0.000	0.000	0.000	0.000
AlCl3	0.000	0.004	0.000	0.000	0.000
n-Octane	0.131	0.130	0.156	0.218	0.001
Cyclohexane	0.002	0.002	0.003	0.005	0.000
Cycloheptane	0.071	0.070	0.099	0.137	0.000
Cyclooctane	0.062	0.062	0.076	0.089	0.041
Cyclononane	0.077	0.076	0.083	0.000	0.293
Cyclodecane	0.002	0.002	0.002	0.000	0.007
n-Hexane	0.019	0.019	0.031	0.043	0.000
n-Heptane	0.159	0.158	0.217	0.302	0.000
n-Nonane	0.049	0.048	0.052	0.054	0.046
n-Decane	0.007	0.007	0.006	0.000	0.022
Benzene	0.001	0.001	0.002	0.002	0.000
Toluene	0.027	0.027	0.040	0.056	0.000
o-Xylene	0.053	0.053	0.069	0.093	0.008
1M3-EBenzene	0.009	0.009	0.010	0.001	0.035

6.14 Summary

Based on the experimental data a model was developed in MATLAB for determining the kinetic parameters associated with various oligomerisation reactions. 19 lumps with 21 reactions were considered for the model development. The proposed model predicts the concentrations of the components with ±10 confidence intervals. These kinetic parameters were incorporated to develop a process simulation model in ASPEN HYSYS. A case study was carried out in ASPEN HYSYS for production of PAO from 1 ton/hour shortlisted low value feed stocks. The simulation results indicated that 45% of the wax cracked naphtha was converted to poly alpha olefins.

Annexure-I

Sample MATLAB codes for optimizing the objective function for estimating the rate constants are given below:

```
% Below we described the kinetic parameter estimation by optimizin
the sum of squared error function. This is the Main
optimizationfunction file,%%
clc
clear screen
bo=zeros(21,1);
Kk=ga(@optim50,21,[],[],[],[],bo,[],[],options) % K@ 50 0C are given
as Upper limits.
% below function consists the objective function. It claculates the
model cocentrations and pass the concntrations to objective function to
claculate the error

function Kopt=optim50(k)



C0=zeros(20,1);
C0(1:5,1)=[0.019;0.470;0.881;0.765;0.089]; C0(20,1)=4.463;
K1=k;

 [t1,C1]=ode45(@(t,C) Odesolkcra(t,C,K1),[0,30],C0);%30 min
residance time, 50 C
 [t2,C2]=ode45(@(t,C) Odesolkcra(t,C,K1),[0,90],C0);%90 min
residance time 50 C
 [t3,C3]=ode45(@(t,C) Odesolkcra(t,C,K1),[0,120],C0);%120 min
residance time 50 C
```

```
 C1experimental=[0.000 0.000 0.000 0.000 0.000 0.21830.2749 0.1533
       0.0584 0.0351 0.1003 0.0439 0.0326 0.0188 0.0059 0.0110 0.0050
       0.0098 0.0308 4.4607];
C2experimental=[0.000 0.000 0.000 0.000 0.000 0.1310 0.2874 0.1752
       0.0487 0.0439 0.1254 0.0586 0.0326 0.0251 0.0059 0.0110 0.0050
       0.0098 0.0176 4.4607];
C3experimental=[0.000 0.000 0.000 0.000 0.000 0.1019 0.2499 0.1533
       0.0584 0.0439 0.1421 0.0732 0.0391 0.0251 0.0117 0.0110 0.0050
       0.0049 0.0220 4.4607];

Kopt=(C1(end,:)-C1experimental)*(C1(end,:)-
C1experimental)'+(C2(end,:)-C2experimental)*(C2(end,:)-
C2experimental)'+(C3(end,:)-C3experimental)*(C3(end,:)-
C3experimental)'; %Objective function



end
% Rate of equations for claculating the fnal cocentrations are included
in the folowing function file
function dcdt=Odesolkcra(t,C,K)

% dc6dt(6)=-k(6,6)*C(6)*C(6)-k(12,6)*C(12)*C(6)-
k(18,6)*C(18)*C(6)-k(24,6)*C(24)*C(6)-
k(30,6)*C(30)*C(6)+k12*C(12);
% dcdt(7)=-k(7,7)*C(7)*C(7)-k(14,7)*C(14)*C(7)-
k(21,7)*C(21)*C(7)-k(28,7)*C(28)*C(7)+k14*C(14);
% dcdt(8)=-k(8,8)*C(8)*C(8)-k(16,8)*C(16)*C(8)-
k(24,8)*C(24)*C(8)-k(32,8)*C(32)*C(8)+k16*C(16);
% dcdt(9)=-k(9,9)*C(9)*C(9)-k(18,9)*C(18)*C(9)-
k(27,9)*C(27)*C(9)+k18*C(18);
% dcdt(10)=-k(10,10)*C(10)*C(10)-k(20,10)*C(20)*C(10)-
k(30,10)*C(30)*C(10)+k20*C(20)+k20*C(20)
```

```
% dcdt(12)=k(6,6)*C(6)*C(6)-k(12,6)*C(12)*C(6)+k24*C(24)-
k12*C(12);
% dcdt(14)=k(7,7)*C(7)*C(7)-k(14,7)*C(14)*C(7)-
k14*C(14)+k28*C(28);
% dcdt(16)=k(8,8)*C(8)*C(8)-k(16,8)*C(16)*C(8)-
k16*C(16)+k32*C(32);
% dcdt(18)=k(9,9)*C(9)*C(9)-
k(18,9)*C(18)*C(9)+k(12,6)*C(12)*C(6)-k(18,6)*C(18)*C(6)-
k18*C(18)+k36*C(36);
% dcdt(20)=k(10,20)*C(10)*C(20)-k(20,10)*C(20)*C(10)-
k20*C(20)+k40*C(40);
% dcdt(21)=k(14,7)*C(14)*C(7)-k(21,7)*C(21)*C(7);
% dcdt(24)=k(18,6)*C(18)*C(6)-
k(24,6)*C(24)*C(6)+k(16,8)*C(16)*C(8)-k(24,8)*C(24)*C(8)-
k24*C(24);
% dcdt(27)=k(18,9)*C(18)*C(9)-k(27,9)*C(27)*C(9);
% dcdt(28)=k(21,7)*C(21)*C(7)-k(28,7)*C(28)*C(7)-k28*C(28);
% dcdt(30)=k(20,10)*C(20)*C(10)-
k(30,10)*C(30)*C(10)+k(24,6)*C(24)*C(6)-k(30,6)*C(30)*C(6);
% dcdt(32)=k(24,8)*C(24)*C(8)-k(32,8)*C(32)*C(8)-k32*C(32);
% dcdt(35)=k(28,7)*C(28)*C(7);
% dcdt(36)=k(30,6)*C(30)*C(6)+k(27,9)*C(27)*C(9)-k36*C(36);
% dcdt(40)=k(30,10)*C(30)*C(10)+k(32,8)*C(32)*C(8)-k40*C(40);

k66=K(1);k126=K(2);k186=K(3);k246=K(4);k306=K(5);
k77=K(6);k147=K(7);k217=K(8);k287=K(9);
k88=K(10);k168=K(11);k248=K(12);k328=K(13);
k99=K(14);k189=K(15);k279=K(16);
k1010=K(17);k2010=K(18);k3010=K(19);

% k12=K(20);k14=K(21);k16=K(22);k18=K(23);%Cracking rate
constatnts
```

```
%
k20=K(24);k24=K(25);k28=K(26);k32=K(27);k36=K(28);k40=K(29)
k36=K(20);k40=K(21);
dcdt=zeros(19,1);
C6=C(1);C7=C(2);C8=C(3);C9=C(4);C10=C(5);
C12=C(6);C14=C(7);C16=C(8);C18=C(9);C20=C(10);
C21=C(11);C24=C(12);C27=C(13);C28=C(14);C30=C(15);
C32=C(16);C35=C(17);C36=C(18);C40=C(19);
%
dcdx=[dc6dx;dc7dx;dc8dx;dc9dx;dc10dx;dc12dx;dc13dx;dc16dx;dc18
dx;dc20dx;dc21dx;dc24dx;dc27dx;dc28dx;dc30dx;dc32dx;dc35dx;dc3
6dx;dc40dx];
dcdt(1)=-k66*C6*C6-k126*C12*C6-k186*C18*C6-k246*C24*C6-
k306*C30*C6;
dcdt(2)=-k77*C7*C7-k147*C14*C7-k217*C21*C7-k287*C28*C7;
dcdt(3)=-k88*C8*C8-k168*C16*C8-k248*C24*C8-k328*C32*C8;
dcdt(4)=-k99*C9*C9-k189*C18*C9-k279*C27*C9;
dcdt(5)=-k1010*C10*C10-k2010*C20*C10-k3010*C30*C10;
dcdt(6)=k66*C6*C6-k126*C12*C6;
dcdt(7)=k77*C7*C7-k147*C14*C7;
dcdt(8)=k88*C8*C8-k168*C16*C8;
dcdt(9)=k99*C9*C9-k189*C18*C9+k126*C12*C6-
k186*C18*C6+k36*C36;
dcdt(10)=k2010*C10*C20-k2010*C20*C10+k40*C40;
dcdt(11)=k147*C14*C7-k217*C21*C7;
dcdt(12)=k186*C18*C6-k246*C24*C6+k168*C16*C8-k248*C24*C8;
dcdt(13)=k189*C18*C9-k279*C27*C9;
dcdt(14)=k217*C21*C7-k287*C28*C7;
dcdt(15)=k2010*C20*C10-k3010*C30*C10+k246*C24*C6-
k306*C30*C6;
dcdt(16)=k248*C24*C8-k328*C32*C8;
dcdt(17)=k287*C28*C7;
```

```
dcdt(18)=k306*C30*C6+k279*C27*C9-k36*C36;
dcdt(19)=k3010*C30*C10+k328*C32*C8-k40*C40;
dcdt(20)=0;

end
```

```
% below codes will be used for the estimating the kietic parameters from
% the rate constants
clc
clear screen
bo=zeros(42,1);
options = gaoptimset('PlotFcns',{@gaplotbestf,@gaplotstopping});
 Kk=ga(@optimAF,42,[],[],[],[],bo,[],[],options);
A0=Kk(1:21)'
 E=Kk(22:42)'
function AF=optimAF(b)
k50=[65.15491123 0.095760702   0.045448327   0.034197484
     0.174290167   19.71665102   3.944517484   0.111095514
     0.200683884   5.256581442   7.431168751   16.12475417
     23.54241912   0.227395347   19.1031869    26.22186637
     19.99338993   0.628224625   0.006867009   6.136191162
     1.252725921];
k62=[55.5514       0.1118 0.0244 0.1044 0.3000 24.6344       6.1429
     0.0496 0.2470 5.8552 6.1122 13.5926       30.9344       0.0586
     11.9362       11.2721       24.1071       1.1386 0.0304 0.9285
     5.0958];
k75=[62.226825     0.062801804   0.00357177    0.047770073
     0.091196992   18.31649136   4.309968926   0.045005638
     0.086835057   3.005646531   2.852228826   7.22899518
     14.72413929   0.26113151    19.75764228   27.47148608
```

```
     23.54784805  11.36792515  0.013680941  12.73733122
     0.057019896];
k87=[58.66590335 0.03303309   0.041476375  0.088381163
     0.043220095  23.85807234  7.777223112  3.499971468
     0.074674917  8.426723947  8.146493767  15.78124502
     36.64120241  0.230914833  14.94184715  22.93355843
     36.54509061  2.758348232  0.152484609  7.996645519
     17.93955928];
k100=[51.20347462       0.373739053  0.162457555  0.64859677
     1.900015842  15.48654276  9.378135921  6.456973302
     2.403099889  8.264561242  7.777715693  10.91004022
     32.80801573  0.243537068  14.52751636  20.28246154
     24.85096274  2.902478986  0.111554343  5.914839872
     10.64021002];
A0=b(1:21)';E=b(22:42)';
AF =(k50-(A0.*exp(-E/(8.314*323)))')*((k50-(A0.*exp(-
E/(8.314*323)))'))'+...
   (k62-(A0.*exp(-E/(8.314*335)))')*((k62-(A0.*exp(-
E/(8.314*335)))'))'+...
   (k75-(A0.*exp(-E/(8.314*348)))')*((k75-(A0.*exp(-
E/(8.314*348)))'))'+...
   (k87-(A0.*exp(-E/(8.314*360)))')*((k87-(A0.*exp(-
E/(8.314*360)))'))'+...
   (k100-(A0.*exp(-E/(8.314*373)))')*((k100-(A0.*exp(-
E/(8.314*373)))'))';
end
```

CHAPTER 7

PROCESS ECONOMICS & SENSITIVITY ANALYSIS

7.1 Overview

At this point of time in the current research, it has been established that there are various refinery/non-refinery feed stocks such as WCN and DCN which can be oligomerized into poly alpha olefins. Also, a process has been developed using Aspen HYSYS with tuneable Lewis acid catalyst system. However, economic feasibility [107-108] of this process has not yet been established.

As a case study, this chapter intends to evaluate the economic benefits of large scale production of polyalpha olefins from WCN using the developed process compared to conventional process of routing wax as feed stock to FCC for production of fuels.

Economic viability of the process developed was carried out considering WCN availability at one of the Indian refineries. The refinery is equipped with Propane Deasphlating Unit (PDU) for production of Group-I base stocks for lubricants. Wax is a by-product from this unit, which is routed conventionally to a catalytic conversion unit for production of fuels.

The stream summaries from the process simulation model were considered for carrying out economic analysis for PAO production from the shortlisted feed stocks. Also, the effect of various key parameters on the process economics is studied using sensitivity analysis.

7.2 Process Design Basis

Currently, wax stream, which is a by-product from propane de-asphalting unit (PDU) of an Indian refinery is routed to the fluid catalytic cracking unit (FCCU), where it further undergoes catalytic cracking to yield wide range of fuel products such as fuel gas, propylene, petrol, diesel fraction and light cycle oil fractions.

In this refinery, about 25 T/hr of wax is generated as a by-product in PDU that operates 8000 hours in a year. Basis these numbers, Plant capacity of 0.2 MMTPA on feed basis is proposed as part of this study.

For arriving at the economics of the process, Refinery Transfer Price (RTP) of petroleum products corresponding to the period of September, 2019 to March, 2020 were considered for the purpose of this case study. The market price of PAO was considered based on the average market price of PAO by various commercial suppliers during the same period. Input feed cost (Wax) is considered as Rs. 25000 per MT.

7.3 Economics of Conventional Wax processing in FCC Plant

In this section, economic evaluation of the products from wax routing through fluid catalytic cracking was carried out. The schematic of the production path is given in the Figure 7.1 below:

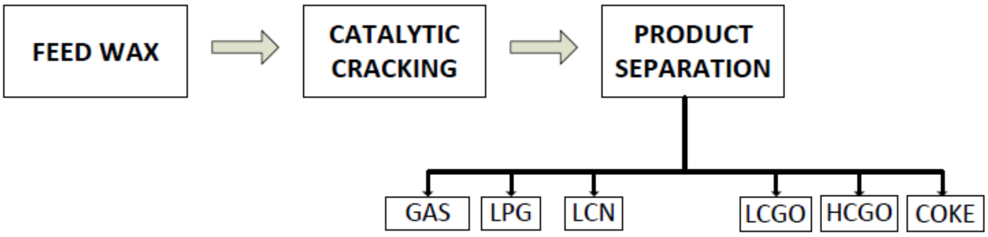

Figure 7.1: Value realization through catalytic cracking route

7.3.1 Product Valuation

As described above the fluid catalytic route processing of wax feedstock will yield wide variety of products. FCC units are flexible units and by fixing severity of operating parameters, the product yield pattern can be adjusted. These units typically run-in gasoline or diesel mode and when integrated in a Petrochemical unit, will mostly be run-in gas mode producing more of LPG boiling range olefin products.

Table 7.1 below indicates the typical yield patterns from FCC Unit and value of resulting products. The value realised from products per ton of feed is also indicated in the table.

Table 7.1: Product Yields and Value from wax cracking in FCCU

Stream	Typical Yield Composition (wt.%)	RTP (Rs./MT)	Value per Ton of feed (Rs./MT)
Gas	4	35000	1400
LPG	23	42000	9660
LCN	33	47000	15510
LCGO	21	53000	11130
HCGO	6	35000	2100
Resid	8	35000	2800
Coke	5	0	0
TOTAL Product Value (Rs./MT)			**42600**

Unit value of coke is considered as zero as it is being consumed within the unit operation. From the calculation in the Table 7.1, the total product value upon wax conversion into fuels is about Rs. 42,600 per MT.

7.3.2 Operating Expenses (OPEX)

The major operating costs in FCC units include:

a) Cost of utilities: include cost of steam, air used for regeneration

b) Cost of energy: includes cost for preheating the feed, electricity for unit operation

c) Catalyst Cost: Though FCC is a regenerative process, over several cycles the activity of catalyst gets deteriorated, hence make-up catalyst has to be added continuously.

d) LCO upgradation cost in downstream units: Light Cycle Oil is a heavy fraction and hydro-treating is required before it is used as a fuel blending stock.

Based on the above operational cost input factors, the typical total operational cost is about Rs.1500 per MT of feed processed.

7.3.3 Annual Gross Margin

Table 7.2: GM calculation for Conventional Wax Processing in FCC Unit

Parameters	Unit	Value
End Product Value (A)	Rs/ MT	42600
OPEX (B)	Rs/ MT	1500
Feed Cost (C)	Rs/ MT	25000
Gross Margin (D=A-B-C)	Rs/ MT	16100
Plant Capacity (E)	MMTPA	0.2
Annual Margin (D * E)	Rs Cr.	322

From the above calculations in Table 7.2, the estimated annual value generation of conventional process of converting Wax into Fuels is about **Rs. 322 Crores.**

7.4 Economics of Proposed Wax Cracking for PAO Production

The feed wax stream typically consists of long chain paraffins. When subjected to high temperature, these paraffins crack and form smaller chain alpha olefins, apart from other gas and liquid streams. These products are separated based on boiling ranges. Stream “C8 to C14” is routed for PAO production through oligomerization pathway. Unreacted stream is further routed to gasoline pool. The schematic of the production path is given in the Figure 7.2 below:

Figure 7.2: Value realisation through Wax-to-PAO route

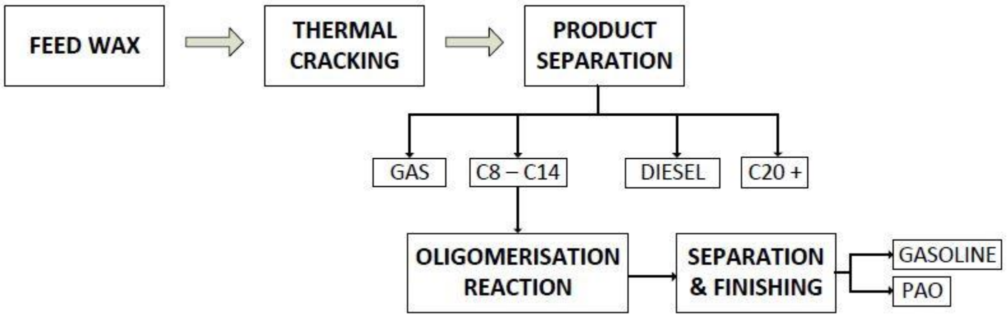

7.4.1 Product Valuation

As discussed earlier in this study, PAO from wax is obtained in a two-step process:

a. Thermal Cracking of Wax
b. Oligomerization of WCN/Wax cracked Naphtha (obtained from Step a)

The Table 7.3 below indicates the yield pattern established from previous studies conducted under this research work done for thermal cracking of wax stream.

Table 7.3: Yield pattern for thermal cracking of wax

Streams	Yield (wt.%)
Wax cracked Naphtha (C8-C14)	25
Diesel	25
C20+	48
Gases	2

From Table 7.3, it is to be noted that about 25% of Wax is converted into WCN (C8-C14).

WCN thus produced is further routed to Oligomerization reactor for PAO production. Aspen HYSYS simulation model developed earlier was used to predict the yield of PAO from WCN as depicted in the Table 7.4. Based on ASPEN Simulation, only 50% of input WCN is converted into PAO that meets commercial specifications. That is, of 100 parts of input Wax, only 12-13% parts of PAO is generated in the Proposed Process.

Table 7.4: Product Yields and Value Feed Basis (Wax)

Stream	Product Yields (wt. %)	Unit Value (Rs./MT)	Value per ton of feed (Rs./MT)
Gases	2	35000	700
PAO (Required product)	13	250000	32500

Gasoline	12	47000	5640
Diesel	25	53000	13250
C20+	48	35000	16800
TOTAL Product Value (Rs./MT)			**68890**

7.4.2 Operating Expenses (OPEX) (per ton of Wax Feed)

The major operational costs in this route include the costs incurred for thermal cracking of wax, oligomerization of alpha olefins, separation, etc. Viscosity Breaking Unit (VBU) is a unit similar to the thermal cracking process proposed under this study. Operational cost of VBU is about 1500 Rs/ MT of feed.

Experimental studies indicated that about 2 wt. % of Lewis acid catalyst is needed for oligomerization reactions. Therefore, catalyst requirement per ton of feed wax is 0.05 (25% x 2%). Cost of catalyst per ton is taken as Rs. 60000.

The operating cost for PAO separation is attributed majorly to the energy cost for pumps, preheaters, condenser and re-boiler. From Aspen HYSYS model LP steam requirement was about 700 kg/hr and total power load was 3.6 MW.

Table 7.5: **Total OPEX for PAO production**

Process Steps	**Cost (Rs).**	**Remarks**
OPEX for Thermal Cracking	1400	Same as VBU cost
OPEX for Oligomerization	300	Catalyst consumption (5 kg) multiplied by its cost (Rs 60 per kg)
OPEX for Separations & Utilities for PAO	1000	Estimated through Aspen HYSYS
Total OPEX	**2700**	

7.4.3 Annual Gross Margin

Table 7.6: **Annual Margin for PAO production**

Parameters	**Unit**	**Value**
Product Value (A)	Rs/ MT	68890
OPEX (B)	Rs/ MT	2700
Feed Cost (C)	Rs/MT	25000
Gross Margin (D=A-B-C)	Rs/ MT	38490
Plant Capacity (E)	MMTPA	0.2
Annual Margin (D* E)	Rs Cr.	770

7.5 Value Addition by PAO Production (0.2 MMTPA Capacity)

Table 7.6: **Value addition for PAO production**

Process Description	**Unit**	**Gross Margin**
Wax to PAO (Proposed Process in Section 7.4)	Rs. Cr	770
Wax to Fuels (Conventional Process in Section 7.3)	Rs. Cr.	322
Value Addition due to PAO production	Rs. Cr.	448

It is observed that the Value addition due to PAO production is 448 Crores as it is the difference of values obtained from the Proposed Wax to PAO process (770 Cr) and the conventional process of converting Wax to Fuels (322 Cr).

7.6 Capital Expenditure (CAPEX) for Proposed Process

The major equipment for production of PAO includes:

a) Feed storage tank
b) Wax cracking heater
c) Oligomerisation reactor

d) Preheater
e) Distillation column
f) Reboiler
g) Condenser

To calculate the CAPEX for equipment, sizing of the equipment was carried out. Heat exchangers, pumps and instrumentation ratings were evaluated based on Process simulation model developed in Aspen HYSYS. Other equipment were rated and sized based on first principles.

Based on the sizing of the equipment and further enquiries with equipment suppliers, the net cost for setting up of unit for PAO production inclusive of equipment cost, instrument cost, piping, civil and electrical cost is estimated as about Rs. 500 Crores.

7.7 Payback Period

Net Payback Period = CAPEX / Value Addition
= 500Cr / 448 Cr (Calculated in Section 7.5)
= 1.2 years

The net payback period is very short and Wax-to-PAO is highly attractive.

7.8 Sensitivity Analysis

The payback period and the economics of process for PAO production is dependent on various parameters. In this section the impact of these parameters on overall process economics is studied.

Sensitivity analysis was carried out to determine the effect of various cost parameters such as PAO price, catalyst cost and utility cost on the overall economics of PAO production process. The criteria for selection for these parameters are (a) Highest contributors to cost (b) Parameters with cost fluctuations according to market scenarios (c) Parameters which affect the production of PAOs.

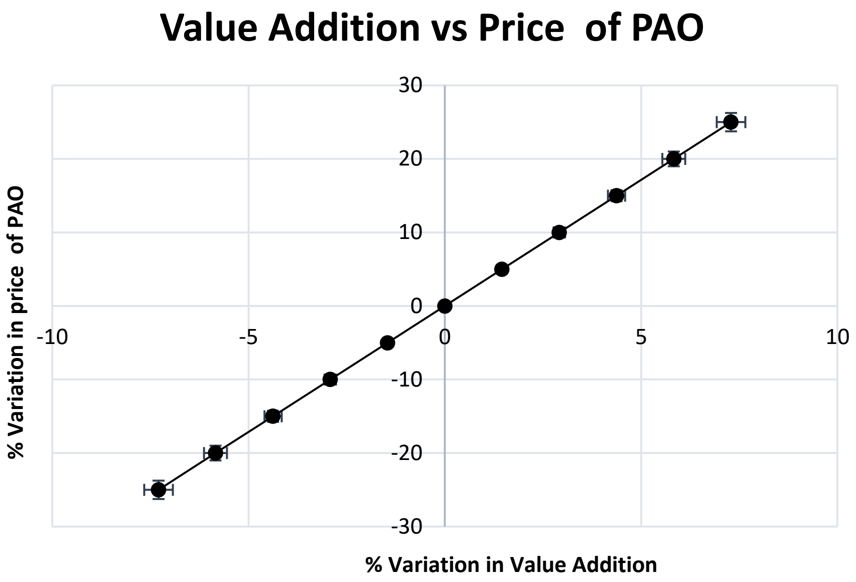

Figure 7.3: Sensitivity Analysis – Value Addition vs Variation in PAO Price

In the above plotted graph (Figure 7.3) coordinates (0, 0) represent the design case. However, it is observed that the value addition % varies marginally with variation in the PAO market price. Increase in PAO price increases the net value addition %.

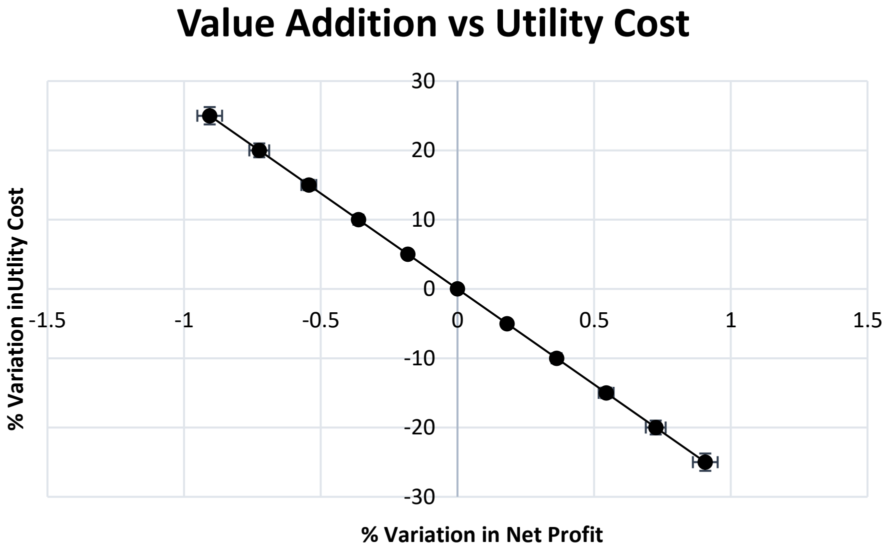

Figure 7.4: Sensitivity Analysis – Value Addition vs Utility Cost variation

The effect of utility cost was estimated to have marginal impact on the value addition % (refer Figure 7.4). About 20% reduction in the utility cost / utility consumption attributes to only 1% increase in value addition %. This highlights the low dependency of the process on utility consumption which is a favourable trait for any process.

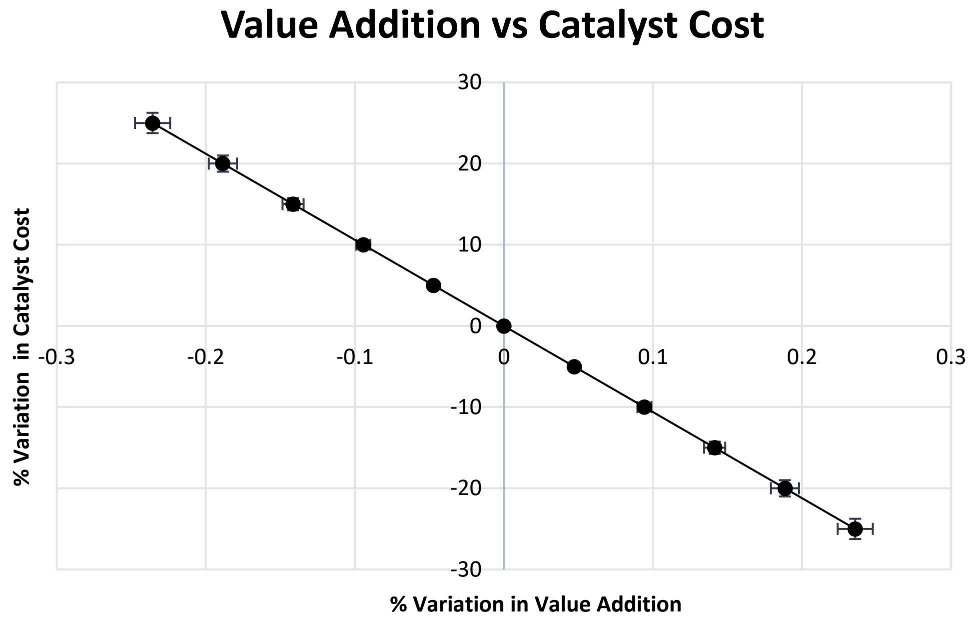

Figure 7.5: Value Addition % vs Catalyst Cost Variation

Catalyst cost variation is one of the least influential parameters for net process economics. The above graph (Figure 7.5) indicates that about 20% reduction in cost of the catalyst contributes to a 0.2% net increase in production. Hence, this gives an inference that the process is not dependent on the catalyst consumption and hence provides more window for enhancement of the process through additional catalyst usage or higher performance catalyst.

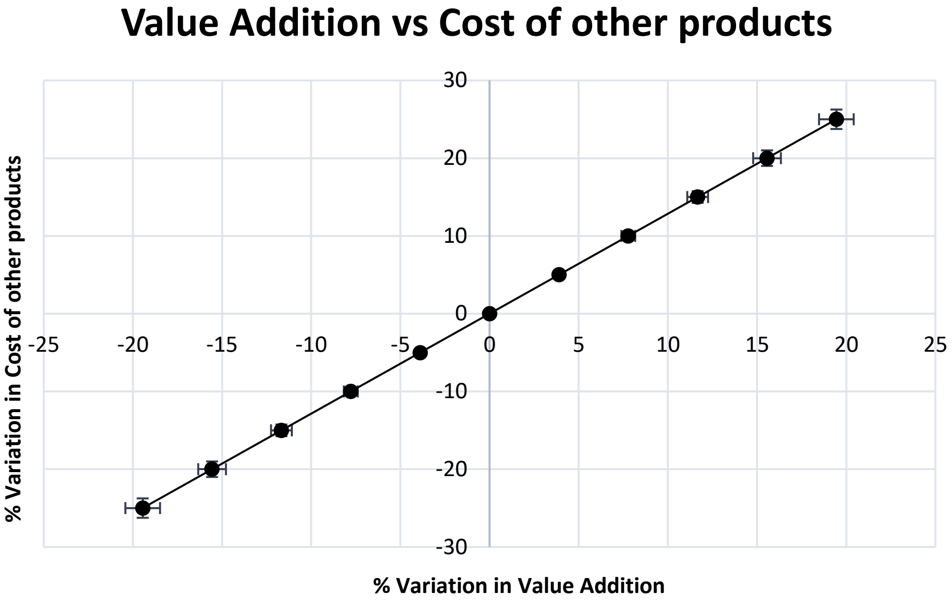

Figure 7.4: Value Addition vs Variation in cost of other products

The cost of other products from thermal wax cracking has significant impact on PAO production. If the cost of other products decreases, then process for conversion of these products to PAO or any other significant value products shall be considered. Otherwise thermal cracking will not be a feasible route due to lack of flexibility of operation unlike fluid catalytic cracking units.

7.9 Summary

Value addition due to Proposed PAO production process is Rs. 448 Cr PA corresponding to a Plant Capacity of 0.2 MMTPA. This was calculated as the difference of values obtained from Proposed Wax to PAO Process (Rs. 770 Cr PA) and the Conventional process of converting Wax into Fuels (Rs. 322 Cr PA)

Further, based on the sensitivity analysis carried out, it was assessed that the major cost parameters which contributes to the economics of PAO production process parameters are market price of PAO and other valuable products from wax cracking. It was observed that the impact of variation of catalyst cost and utility cost was insignificant compared to the feed parameters. Hence, it is inferred that the process is not economically dependent on utilities and catalyst.

With a CAPEX of Rs. 500 Cr to set up the proposed plant, and the Net value addition of 448 Cr PA, the Payback period is only 1.2 years. As this is a very small time frame for recovering the investment for a refinery, the proposed PAO production process is highly recommended.

CHAPTER 8

CONCLUSIONS & FUTURE RESEARCH

8.1 Conclusions

i. Despite the various advantages and super performance of PAOs compared to conventional lubricants, their use as synthetic base oils is still limited because of the cost and availability of feed stocks. The conventional PAO synthesis route involves high cost, as the feedstock is high value ethylene. Considering this, the current research is driven towards the search of low value feed stocks for production PAOs.

ii. Various refinery streams were identified and analyzed using PONA GC. Results indicated that FCC-LCN contains maximum amount of olefins among the studied naphthas, up to 55%, mainly as C5 and C6. FCC-HCN contains up to 28.5% olefins with maximum contribution from C6-C8. DCN contains up to 30% olefins with maximum contribution from C8 and C9. VBN contains up to 37% olefins with carbon number spread over C4-C10. Thus, it can be confirmed that distribution of olefins, *i.e.*, carbon numbers and the corresponding olefin percentage, is very specific to the particular naphtha selected.

iii. As per the literature reports, PAO production requires LAOs with carbon number ranging between C8 and C14. It is also reported that internal olefins do not yield PAOs. To identify the type of olefins in the feed streams, 1H NMR analyses were carried out. Feed stocks produced via thermal cracking process (VBN, DCN, WCN) were found to contain linear alpha olefins (LAOs) whereas feed stocks produced from catalytic processes such as FCC-LCN, FCC-LCN did not contain any linear alpha olefins.

iv. The fast pyrolysis (thermal cracking) was performed on heavy HC molecules such as Wax 1, Wax 2 and PE and the products were analysed. The results indicated that percentage of olefin in the product increases with chain length or molecular weight of the feed (PE>Wax 2>Wax 1). Also, the results showed that PE provides highest olefin content, Wax 1 gives highest paraffin content; whereas, Wax 2 gives moderate amount of olefin. However, all these product streams are suitable for PAO production as they contained only LAO.

v. The composition of PAOs (observed via model compound studies) was found to be critically dependent on temperature and residence time. The conversion with $AlCl_3$ was found to increase with increase in temperature, whereas the iron-based catalysts showed the reverse trend. The iron-based catalysts selectively yielded dimer or 2 cst grade PAO whereas with increasing $AlCl_3$ in the catalyst blend the oligomer ratio shifted towards to tetramer and higher oligomers. For a particular catalyst, with increase in temperature, the oligomer ratio is shifted towards lighters (dimer and trimer) due to faster termination kinetics in comparison with the propagation.

vi. In order to verify the thio-affinity of $FeCl_3$ and $AlCl_3$ blend catalysts, a model synthetic mixture containing propane thiol in 1-decene was chosen for oligomerization reaction. It was observed that sulphur content was lower in PAO synthesized using $FeCl_3$ and $AlCl_3$ as compared to experiment using only $AlCl_3$, indicating less incorporation of sulphur in the product, assuring product of controllable quality.

vii. The PAOs produced from various low value feed stocks were benchmarked with commercially available PAO grades. The resulting analysis indicated that only FCC LCN with 1-Octene, DCN & WCN were suitable as feed stocks for PAO production. However FCC-LCN can only be used if it is mixed with 1-Octene in 1:1 ratio. 1-Octene is a costly input material and hence not suggested for large scale production

viii. Based on experimental data, a kinetic model of various oligomerisation reactions was developed in MATLAB. Using this kinetic model, a Simulation Flow sheet was developed for design of large scale PAO production plants using Aspen HYSYS.

ix. Economic benefits of large scale production of PAOs (with WCN) using the process developed in this research work were estimated and the results were compared to the benefits currently accruing though conventional process of routing wax as feed stock to FCC for production of fuels. Value addition from production of PAO is about 448 Cr PA for a Plant Capacity of 0.2 MMTPA. With a CAPEX of Rs. 500 Cr to set up the proposed plant, the Payback period is only 1.2 years. As this is a very small time frame for recovering the investment for a refinery, the proposed PAO production process is highly recommended.

8.2 Future Research Work

The following future research work is suggested:

i. The conversion with $AlCl_3$ catalyst was found to be increasing with temperature and same is well documented. On the other hand, for the catalysts containing $FeCl_3$, the conversions decreased with increase in temperature. The abnormal behavior of the $FeCl_3$ may be due to a mechanistic pathway different from conventional pathway.

   Mechanistic studies may be taken up to better understand this observation.

ii. In order to verify and optimize the linear alpha olefin potential from cracking of wax molecules at large scale, wax material was subjected to thermal cracking using Mini Pot still (MPS) equipment. Experiments were carried out at various residence times. However, temperature was restricted to maximum temperature of 420°C due to the design limitations of the equipment.

   Scale-up studies can be taken up to further optimize LAO potential from thermal cracking of Wax.

REFERENCES

[1] B. Bhushan, & P. L. Ko, *Introduction to tribology:Appl. Mech.*, Rev., 56(1), B6-B7. 2003.

[2] A. Cameron, *Basic Lubrication Theory*, Ellis Horwood Ltd., 256, 1981.

[3] M. Torbacke, Å. K. Rudolphi, &, E. Kassfeldt, *Lubricants: introduction to properties and performance*. John Wiley & Sons, 2014.

[4] "Api base oil interchangeability guidelines for passenger car motor oils and diesel engine oils", *American Petroleum Institute*, March 2015.

[5] W. Keim, "Oligomerization of Ethylene to α-Olefins: Discovery and Development of the Shell Higher Olefin Process (SHOP)", *Angewandte Chemie International Edition*, 52(48), 12492-12496, 2013.

[6] Fan-Hua Kong & Ming-He Xie, "Catalysts for 1-hexene Synthesis from Ethylene Oligomerization", *J Nat Gas Chem* 8:256–263, 1999.

[7] R. F. de Souza, K. Bernardo-Gusma˜o, G. A. Cunha, C. Loup, F. Leca & R. Re´au R, "Ethylene dimerization into 1-butene using 2-pyridylphosphole nickel catalysts", J Catal 226:235–239, 2004.

[8] G. L. Tembe, M. Ravindranathan, "Oligomerization of ethylene to linear a-olefins by a titanium aryl oxide-alkylaluminum catalyst", Ind Eng Chem Res 30:2247–2252, 1991.

[9] Anon, *Poly Alpha Olefin (PAO) Market Analysis By Application (Gear Oil, Engine Oil, Compressor Oil, Grease) And Segment Forecast To 2025* [Online]. Available: https://www.grandviewresearch.com/industry-analysis/poly-alpha-olefin-pao-market visited 10.06.2021.

[10] Anon, Poly Alpha Olefin (PAO) Market Size, Industry Analysis Report, Regional Outlook, Application Development Potential, Price Trends, Competitive Market Share & Forecast, 2021 – 2027 [Online]. Available: https://www.gminsights.com/industry-analysis/poly-alpha-olefin-pao-market

[11] S. Ray, P. V Rao, & N. V Choudary, “Poly-α-olefin-based synthetic lubricants: a short review on various synthetic routes”, *Lubrication Science*, 24(1), 23-44M, 2012.

[12] P. Hetherington, “Inspiring the next generation of lubricant professionals”, *Tribology & Lubrication Technology*, 77(4), 6-7, 2021.

[13] Lappin (Ed.), Alpha olefins applications handbook, CRC press, 2014.

[14] G.R. Lappin, “Routes to Alpha Olefins”, *Alpha Olefins Applications Handbook*, 35, 1989.

[15] I. Zhen-hua, “Study on poly-alpha-olefin synthesis with 1-decene catalyzed by boron trifluoride”, *Applied Chemical Industry*, 2011.
I. Yamane & O. Okumura, *Alpha-olefins applications handbook*, 1989.

[16] E.I. Shaheen, Catalytic processing in petroleum refining, 1983.

[17] M. L. Occelli, Fluid Catalytic Cracking (No. CONF-870802-). Washington, DC (USA); American Chemical Society, 1988.

[18] L., T. R, *Process chemistry of lubricant base stocks*, CRC Press, 2007.

[19] Jr. K. J. Stippich, V. P. Thakkar, & J. A. Petri, No. 9,453,169, US, Washington, DC: U.S. Patent and Trademark Office, 2016.

[20] J. G. Speight, & D. I. Exall, *Refining used lubricating oils*, Vol., 99. Boca Raton: CRC Press, 2014.

[21] I. Madanhire, C. Mbohwa, *Mitigating environmental impact of petroleum lubricants*, pp. 17-34, Berlin, Germany:: Springer, 2016.

[22] T. Kaminski & M. M. Husein, “Thermal cracking of atmospheric residue versus vacuum residue”, *Fuel Processing Technology*, 181, 331-339, 2018.

[23] R. Sadeghbeigi, *R. Fluid catalytic cracking handbook* (p. 208). Houston, TX: Gulf publishing company, 1995.

[24] C. S. Hsu & P. R. Robinson, “Lubricant processes and synthetic lubricant”, *In Petroleum science and technology* (pp. 253-285). Springer, Cham, 2019.

[25] P. S. Coffin, C. M. Lindsay, A. J. Mills, H. Lindenkamp & J. Fuhrmann, “The application of synthetic fluids to automotive lubricant development:

trends today and tomorrow", *Journal of Synthetic Lubrication*, 7(2), 123-143, 1990.

[26] M. M. Wu, S. C. Ho, & T. R. Forbus, "Synthetic lubricant base stock processes and products", *In Practical advances in petroleum processing* (pp. 553-577). Springer, New York, NY, 2006,

[27] T. Mang, *Encyclopedia of lubricants and lubrication*, Berlin Heidelberg: Springer, (Ed.), 2014.

[28] T . Mang, & W. Dresel, *Lubricants and lubrication*, John Wiley & Sons, 2007.

[29] E. R. Booser, CRC Handbook of Lubrication and Tribology, Volume III: Monitoring, materials, synthetic lubricants, and applications, Vol. 3, CRC Press, 1993.

[30] C. Zerbe, *Lubrication and Lubricants,* Von ER Braithwaite, Elsevier Verlag, Amsterdam, Leinen, 568 S., 191 Abb, Preis ca. DM 95, 1967.

[31] D. M. Pirro, M. Webster, & E. Daschner, *Lubrication fundamentals, revised and expanded,* CRC Press, 2016.

[32] G., Childs, T. H. C. Dalmaz, D., & Taylor, C. M. Dowson, Lubricants and lubrication (Vol. 30), Elsevier, (Eds.), 1995.

[33] W. L. Robertson, Lubrication in practice (Vol. 27). CRC Press, 1984.

[34] Shahnazar, S. Bagheri & S. B. Abd, "Enhancing lubricant properties by nanoparticle additives", *International journal of hydrogen energy*, 41(4), 3153-3170, 2016.

[35] Z. Q. Fu, C. B. Wang, W. Zhang, W. Wang, W. Yue & X. Yu, "Influence of W content on tribological performance of W-doped diamond-like carbon coatings under dry friction and polyalpha olefin lubrication conditions", *Materials & Design*, 51, 775-779, 2013.

[36] B. M. O'Connor, L. F. Schiemann & R. L. Johnson, "Axle efficiency—response to synthetic lubricant components", *SAE Technical Paper*, No. 821181, 1982.

[37] R. W. Miller, *Lubricants and their applications*, McGraw-Hill Companies, 1993.

[38] S. P. Srivastava, “Developments in lubricant technology”, *John Wiley & Sons*, 2014.

[39] A. G. Fotopoulos & D. P. Margaris, “Computational Analysis of Air Lubrication System for Commercial Shipping and Impacts on Fuel Consumption”, *Computation*, 8(2), 38, 2020.

[40] Q. Lu, H. Wang, C. Ye, W. Liu & Q. Xue. “Room temperature ionic liquid 1-ethyl-3-hexylimidazolium-bis (trifluoromethylsulfonyl)-imide as lubricant for steel–steel contact”, *Tribology International*, 37(7), 547-552, 2004S.

[41] J. Randles, S. Pasquin, & P. T. Gibb, “A critical assessment of synthetic lubricant technologies for alternative refrigerants”, In *The 10th European Conference on Technological Innovations in Air-Conditioning and Refrigeration Industry*, Milan, 2003.

[42] O. O. Amund, “Utilization and degradation of an ester-based synthetic lubricant” by Acinetobacter lwoffi, *Biodegradation*, 7(2), 91-95, 1996.

[43] R. M. Mortier, S. T. Orszulik, & M. F Fox, *Chemistry and technology of lubricants*, Vol. 107115, pp. 56-75), Dordrecht: Springer, 2010.

[44] A.H. Turner, “Purity aspects of higher alpha olefins”, *Journal of the American oil chemists’ society*, 60(3), 623-627, A. H. 1983A. Sequeira, *Lubricant base oil and wax processing*, CRC press, 1994.

[45] G. P. Belov & P. E. Matkovsky, “Processes for the production of higher linear a-olefins”, Pet Chem 50:283–289, 2010

[46] M. M. Wu, S. C. Ho & T. R. Forbus, “Synthetic lubricant base stock processes and products”, *Practical advances in petroleum processing* (pp. 553-577). Springer, New York, NY, 2006.

[47] A. L. Mendes Siqueira, M. Beaumesnil, M. Hubert-Roux, C. Loutelier-Bourhis, C. Afonso, Y. Bai, & A. Racaud, “Atmospheric solid analysis probe coupled to ion mobility spectrometry-mass spectrometry, a fast and simple method for polyalphaolefin characterization”, *Journal of The American Society for Mass Spectrometry*, 29(8), 1678-1687, 2018.

[48] S. S. Scheuermann, S. Eibl & P. Bartl. “Detailed characterisation of isomers present in polyalphaolefin dimer and the effect of isomeric distribution on bulk properties”, *Lubrication Science*, 23(5), 221-232, 2011.

[49] S. Kumar & R. K. Singh, “Recovery of hydrocarbon liquid from waste high density polyethylene by thermal pyrolysis”, *Brazilian journal of chemical engineering*, 28(4), 659-667, 2011.

[50] G. R. Worrell, R. F. Chapman, & S. G. Woinsky, “Kinetics of wax cracking for alpha-olefin production”, *Industrial & Engineering Chemistry Process Design and Development*, 6(1), 89-95, 1967.

[51] A. H. A. Mohammed & S. M. Obeyed, “Treatment of Slack Wax by Thermal Cracking Process” *Iraqi Journal of Chemical and Petroleum Engineering*, 15(3), 1-7, 2014.

[52] G. P. Belov, & P. E Matkovsky, “Processes for the production of higher linear α-olefins”, *Petroleum Chemistry,* 50(4), 2010.

[53] C. Fehér, E. Kriván, Z. Eller, J. Hancsók & R. Skoda-Földes, “The Use of Ionic Liquids in the Oligomerization of Alkenes”, InTech, 2014.

[54] M. Tabrizi, N. Bahri-Laleh, S. Sadjadi, & M. Nekoomanesh-Haghighi, “The effect of ionic liquid containing AlCl3 catalytic systems on the microstructure and properties of polyalphaolefin based lubricants”, *Journal of Molecular Liquids*, 335, 116299. (2021)

[55] I.E. Nifant’ev, A.A. Vinogradov, I.V. Sedov, V.G. Dorokhov, A.S. Lyadov, & P.V. Ivchenko, “Structurally uniform 1-hexene, 1-octene, and 1-decene oligomers: Zirconocene/MAO-catalyzed preparation, characterization, and prospects of their use as low-viscosity low-temperature oil base stocks”, *Applied Catalysis A: General*, 549, 40-50, 2018

[56] H. Choo & L. Kevan, “Catalytic study of ethylene dimerization on Ni (II) -exchanged clinoptilolite”, *J Phys Chem B* 105:6353–6360, 2001.

[57] J. Skupinsk, “Oligomerization of a-olefins to higher oligomers”, Chem Rev 91:613–648, 1991.

[58] J. F. Knifton, J. R. Sanderson, & P. E. Dai, “Olefin oligomerization via zeolite catalysis.” *Catalysis Letters*, 28(2), 223-230, 1994.

[59] L. Ma, W. Li, H. Xi, X. Bai, E. Ma, X. Yan, & Z. Li, “Catalyzed Ring-Closing Carbonyl–Olefin Metathesis.”, *Angewandte Chemie International Edition*, 55(35), 10410-10413, 2016.

[60] Tobisch, “α-Olefin Dimerization by a Mono (imido) Tungsten Catalyst: Computational Evidence for the Role of Lewis Acid Chelates in Effective Catalysis”, *Organometallics*, 26(26), 6529-6532, 2007.

[61] C. Argo, S. M. Gillam, & F. Orsini, “Identification of olefin end groups in commercial polybutene oligomers”, *Polymer Bulletin*, 44(1), 71-78, 2000.

[62] P. S. Riehl, & C. S. Schindler, “Lewis Acid-Catalyzed Carbonyl–Olefin Metathesis.” ,*Trends in Chemistry*, 1(2), 272-273, 2019.

[63] J. C. Gee, B. L. Small, & K. D. Hope, “Behavior of protonated cyclopropyl intermediates during polyalphaolefin synthesis: Mechanism and predicted product distribution.”, *Journal of Physical Organic Chemistry*, 25(12), 1409-1417. (2012).

[64] A. Rahbar, N. Bahri-Laleh, & M. Nekoomanesh-Haghighi. “Microstructural study on low viscosity poly-α-olefin oils synthesized via AlCl3/H2O cationic system in the present of xylene and heptane solvents”, *Fuel*, 302, 12111, 2021.

[65] M. A. Bruzzone, “Polyalpha-Olefin Catalysts” In *Advances in Polyolefins* (pp. 99-110). Springer, Boston, MA, 1987.

[66] Y. Gao, J. Chen, Y. Wang, D.B. Pickens, A. Motta, Q. J. Wang & T. J. Marks, “Highly branched polyethylene oligomers via group IV-catalysed polymerization in very nonpolar media”, *Nature Catalysis*, 2(3), 236-242, 2019.

[67] S. Segal, I. Goldberg & M. Kol, “Zirconium and titanium diamine bis (phenolate) catalysts for α-olefin polymerization: From atactic oligo (1-hexene) to ultrahigh-molecular-weight isotactic poly (1-hexene)”, *Organometallics*, 24(2), 200-202, 2005.

[68] Y.U. Xiao-Qiao, S. H. E. N Ben-Xian, S. U. N Hui, Y. A. N. G Lan, L. I. U Lei, & L. I. U. Ji-Chang, “Synthesis of poly alpha olefins used for lubricant base stocks on an AlCl3/TiCl4 catalyst”, *China Petroleum Processing & Petrochemical Technology*, 14(2), 55, 2012.

[69] A. M. Norton, S. Liu, B. Saha, & D.G. Vlachos, “Branched Bio-Lubricant Base Oil Production through Aldol Condensation”, *ChemSusChem*, 12(21), 4780-4785, 2019

[70] B. D. James & C. J. Dain, “Process variables in the manufacture of polyalphaolefins”, *Journal of Synthetic Lubrication*, 5(3), 187-196, 1988.

[71] S. Elomari, R Krug, T. V. Harris, & M. S. Driver, U.S. Patent No. 7,572,943. Washington, DC: U.S. Patent and Trademark Office, 2009.

[72] W. Wang, S. Jiang, Y. Shen, S. Xia, J. Xu, “Synthesis of high viscosity index base stock and study on the lubricating properties”, *Industrial Lubrication and Tribology*, 2016.

[73] G. Biresaw, “Biobased Polyalphaolefin Base Oil: Chemical, Physical, and Tribological Properties”, *Tribology Letters*, 66(2), 1-16. 2018.

[74] J.R. Black, & L. Fenouil, U.S. Patent No. 6,727,399. Washington, DC: U.S. Patent and Trademark Office, 2004.

[75] L. H. Slaugh, L. A. Fenouil, & H. L. H. Fong, (2000). U.S. Patent No. 6,018,089. Washington, DC: U.S. Patent and Trademark Office.

[76] J. C. Perciful, U.S. Patent No. 4,042,488. Washington, DC: U.S. Patent and Trademark Office, 1977.

[77] X.Yu, B. Shen, H. Sun, L. Yang, L. Liu, J. Liu, “Synthesis of Poly Alpha Olefins Using Alpha Olefins Obtained from the Steam Cracking Process of Coal Liquefaction Wax. Energy Sources”, Part A: *Recovery, Utilization, and Environmental Effects*, 37(11), 1195-1201, (2015).

[78] R. Sarin, S.S. Ray, D. K. Tuli, M. M. Rai, S. Ghosh, & A.K. Bhatnagar, U.S. Patent No. 6,184,429. Washington, DC: U.S. Patent and Trademark Office, 2001.

[79] R. Sarin, S.S. Ray, D. K. Tuli, M. M. Rai, S. Ghosh, & A.K. Bhatnagar & M. J. G. Yanjarappa, U.S. Patent No. 6,002,060. Washington, DC: U.S. Patent and Trademark Office, 1999.

[80] M. Hagemeister, A.I. Kramer, P.J Nandapurkar, S. Tirmizi, & M.M.S Wu, U.S. Patent No. 9,469,704. Washington, DC: U.S. Patent and Trademark Office, 2016.

[81] M. C. B Goze, P. Surana, & N. Yang, U.S. Patent No. 8,598,394. Washington, DC: U.S. Patent and Trademark Office, 2013.

[82] W. Song, W.J. & Heilman, U.S. Patent No. 7,129,197. Washington, DC: U.S. Patent and Trademark Office, 2006.

[83] M. M Wu, N. Yang, P. Surana, A. Patil, S.P. Rucker, K. Qian & M.P. Hagemeister, U.S. Patent No. 8,921,291. Washington, DC: U.S. Patent and Trademark Office, 2014.

[84] G. R. Giesbrecht, M.W. Holtcamp, M. Kol, K. Press & G.S. Day, U.S. Patent No. 9,365,661. Washington, DC: U.S. Patent and Trademark Office, 2016.

[85] J.C. Gee, B.L. Small, K.D. Hope, R.C. Coffin & S.M. Bischof, U.S. Patent No. 9,708,549. Washington, DC: U.S. Patent and Trademark Office, 2017.

[86] K. D Hope, D. A Stern, D.W. Twomey & J.B. Collins, U.S. Patent No. 7,615,598. Washington, DC: U.S. Patent and Trademark Office, 2009.

[87] W. Xueqian & W. Huixin, “A Study into Using Olefin Made from Coal to Synthesize Low-viscosity Poly-alpha-olefin Base Oil”, *Sino-Global Energy*, 10, 2013.

[88] L. L. XU, H. S DING, P. P. LIU, & Q. L. LIU, “Synthesis of a medium viscosity PAO”, *Science & Technology in Chemical Industry*, 6, (2010).

[89] G. D. Yadav, & N. S. Doshi, “Development of a green process for poly-α-olefin based lubricants”, *Green Chemistry*, 4(6), 528-540, 2002.

[90] Z. Jia, Z. Wang, C. Liu, L. Zhao, J. Ni, Y. Li & C. Wang, “The synthesis and tribological properties of Ag/polydopamine nanocomposites as additives in poly-alpha-olefin”, *Tribology International*, 114, 2017.

[91] E. Bried, H. F. Kidder, C. M. Murphy, & W. A. Zisman, "Synthetic lubricant fluids from branched-chain diesters physical and chemical properties of pure diesters", *Industrial & Engineering Chemistry*, 39(4), 484-491, 1947.

[92] F. Guo, C. F. Li, J. W. Liu, S. H. Chen & A. W. Yang, "Application of α-olefins in the field of synthetic lubricant", *Chemical Engineer*, 8, 2010.

[93] L. D. A. Kalman, K. J. Voorhees, D. Osborne, & I. N. Einhorn, "Production of a bicyclophosphate neurotoxic agent during pyrolysis of synthetic lubricant oil", *Journal of fire sciences*, 3(5), 322-329, 1985.

[94] H. Fujita & H. A. Spikes, "Study of zinc dialkyldithiophosphate antiwear film formation and removal processes, part II: kinetic model", *Tribology transactions*, 48(4), 567-575, 2005.

[95] Z. Belohlav, P. Zamostny, & T. Herink, "The kinetic model of thermal cracking for olefins production", *Chemical Engineering and Processing: Process Intensification*, 42(6), 461-473, 2003.

[96] D.C. Longstaff, Development of a comprehensive naphtha catalytic cracking kinetic model", *Energy & fuels*, 26(2), 801-809, 2012.

[97] A. Usman, M. A. B. Siddiqui, A. Hussain, A, A. Aitani & S. Al-Khattaf, "Catalytic cracking of crude oil to light olefins and naphtha: experimental and kinetic modelling", *Chemical Engineering Research and Design*, 120, 121-137, 2017.

[98] V. Touloupides, V. Kanellopoulos, P. Pladis, C. Kiparissides, D. Mignon, P. Van-Grambezen, "Modeling and simulation of an industrial slurry-phase catalytic olefin polymerization reactor series", Chem Eng Sci 65:3208–3222, 2010.

[99] R. J. Quann, S. B. Jaffe, "Structure-oriented lumping: describing the chemistry of complex hydrocarbon mixtures", Ind. Eng. Chem. Res. 31 2483–2497, 1992.

[100] A. S. Sarpal, M. I. S. Sastry, G. S. Kapur, V. Bansal, A. K. Mehta, & A. K. Bhatnagar, "Molecular dynamics studies of a lubricant system by NMR spectroscopic techniques", *Lubrication Science*, 16(4), 361-375, 2004.

[101] I. Minami, “Molecular science of lubricant additives”, *Applied sciences,* 7(5), 445, 2017.

[102] Z. Shen, F. Wang, Z. Chen, X. Ruan, H. Zeng, J. Wang & X. Fan, “Numerical simulation of lubrication performance on chevron textured surface under hydrodynamic lubrication”, *Tribology International*, 154, 106704, 2021.

[103] A. A. Mohammed, S. E. K. Fateen, T. S. Ahmed & T. M. Moustafa, “A kinetic model for ethylene oligomerization using zirconium/aluminum-and nickel/zinc-based catalyst systems in a batch reactor”, *Applied Petrochemical Research,* 4(3), 287-295, 2014.

[104] D. Saha & S. Deng, “Adsorption equilibria and kinetics of carbon monoxide on zeolite”, 5A, 13X, MOF-5, and MOF-177. Journal of Chemical & Engineering Data, 54(8), 2245-2250, 2009.

[105] A. A. Mohammed, S. E. K. Fateen, T. S. Ahmed & T. M. Moustafa, “A kinetic model for ethylene oligomerization using zirconium/aluminum-and nickel/zinc-based catalyst systems in a batch reactor”, *Applied Petrochemical Research*, 4(3), 287-295, 2014.

[106] R. J. Quann & S. B. Jaffe, “Structure-oriented lumping: describing the chemistry of complex hydrocarbon mixtures”, *Industrial & engineering chemistry research*, 31(11), 2483-2497, 1992.

[107] Q. Chen, D. Wang, Y. Gu, S. Yang, Z. Tang, Y. Sun & Q. Wu, “Techno-economic evaluation of CO2-rich natural gas dry reforming for linear alpha olefins production” *Energy Conversion and Management,* 205, 112348

[108] Y. Huang, Q. Chu, Q. Yi, W. Y. Li, K. C. Xie, Q. W. Sun, & J. Feng, “Feasibility analysis of high–low temperature Fischer–Tropsch synthesis integration in olefin production”, *Chemical Engineering Research and Design*, 131, 92-103, 2018.

UNIVERSITY OF PETROLEUM & ENERGY STUDIES

PLAGIARISM CERTIFICATE

1. This is to certify that the thesis titled "**Studies on Process Development for production of Synthetic lubes from low value feed stocks"** submitted by Scholar **Mr. Ramachandra Rao Bojja** having SAP ID 500049752, has been run through a Plagiarism Check Software and the Plagiarism Percentage is reported to be about 5 %.

2. Plagiarism Report generated by the Plagiarism Software is attached.

A Panday

Signature of the Internal Guide
(Prof. Ashoutosh Panday)

Signature of the External Supervisor
(Dr. N. V. Choudary, FNAE)

Signature of the Scholar

Ouriginal

Document Information

Analyzed document	Thesis_Ramachandra.pdf (D109299172)
Submitted	6/19/2021 11:15:00 AM
Submitted by	R S Thakur
Submitter email	sinhathakur@yahoo.com
Analysis address	r.s.thakur.upes@analysis.urkund.com

Sources included in the report

W	URL: http://prr.hec.gov.pk/jspui/bitstream/123456789/12322/1/Hussain%20Gulab%20chemistry%202010%20uni%20of%20peshwar%20prr.pdf Fetched: 5/28/2021 6:53:18 AM	7
W	URL: https://www.gminsights.com/industry-analysis/poly-alpha-olefin-pao-market Fetched: 6/19/2021 11:17:00 AM	1
SA	**all.docx** Document all.docx (D31509448)	1
W	URL: https://en.wikipedia.org/wiki/Linear_alpha_olefin Fetched: 6/19/2021 11:17:00 AM	1
J	**Synthesis of Poly Alpha Olefins Using Alpha Olefins Obtained from the Steam Cracking Process of Coal Liquefaction Wax** URL: f69facf1-43cd-4ba8-b3a1-3cfb30038e7e Fetched: 3/13/2019 10:02:51 AM	3
W	URL: https://www.researchgate.net/publication/338820898_Highly_efficient_supported_AlCl3-based_cationic_catalysts_to_produce_polya-olefin_oil_base_stocks Fetched: 5/27/2020 9:55:18 PM	2
SA	**book.pdf** Document book.pdf (D40310423)	2
W	URL: https://www.infineuminsight.com/media/1814/3-lubricant-base-stocks-na.pdf Fetched: 2/17/2021 11:02:16 PM	10
SA	**1530994559_272__Handbook_of_petroleum_refining_processes.pdf** Document 1530994559_272__Handbook_of_petroleum_refining_processes.pdf (D40716888)	6
W	URL: http://www.rsc.org/suppdata/ob/b3/b302016a/b302016a.txt Fetched: 6/19/2021 11:17:00 AM	4
W	URL: ftp://117.239.47.98/Mechnical%20Engineering/Ebooks/Fundamentals%20of%20Petroleum%20Refining.pdf Fetched: 2/22/2021 1:26:11 PM	5
W	URL: https://www.researchgate.net/publication/227247349_Hydrotreating_and_Hydrocracking_Fundamentals	2